Modulation Of Cardiac Inward-Rectifier K^+ Current I_{K1} By Intracellular K^+ And Extracellular K^+

by Oksana Dyachok

Submitted in partial fulfillment of the requirements
for the degree of Doctor of Philosophy

at

Dalhousie University
Halifax, Nova Scotia, Canada
December 2011

DALHOUSIE UNIVERSITY

PHYSIOLOGY AND BIOPHYSICS

The undersigned hereby certify that they have read and recommend to the Faculty of Graduate Studies for acceptance a thesis entitled "Modulation of Inward-Rectifier K^+ Current I_{K1} By Intracellular K^+ And Extracellular K^+" by Oksana Dyachok in partial fulfilment of the requirements for the degree of Doctor of Philosophy.

Dated: December 13, 2011

External Examiner: _____

Research Supervisor: _____

Examining Committee: _____

_____

Departmental Representative: _____

DALHOUSIE UNIVERSITY

DATE: December 13, 2011

AUTHOR: Oksana Dyachok

TITLE: Modulation Of Inward-Rectifier K^+ Current I_{K1} By Intracellular K^+ And Extracellular K^+.

DEPARTMENT OR SCHOOL: Department of Physiology and Biophysics

DEGREE: PhD CONVOCATION: May YEAR: 2012

_____

Signature of Author

TABLE OF CONTENTS

LIST OF TABLES

LIST OF FIGURES

ABSTRACT

The inwardly-rectifying K^+ current (I_{K1}) is important for heart cell function because it sets the resting potential, influences cell excitability, and promotes repolarization of the action potential. My objective was to investigate the modulation of I_{K1} by extracellular K^+ (K^+_o) and intracellular K^+ (K^+_i). I_{K1} was recorded from whole-cell-configured guinea-pig ventricular myocytes that were dialyzed with Na^+-free EGTA-buffered pipette-filling solution and bathed with Na^+ or $NMDG^+$ solution that contained agents that inhibit non-I_{K1} currents.

Lowering K^+_o from standard 5.4 to 2 and 1 mM shifted the reversal potential (E_{rev}) of I_{K1} in accord with calculated K^+ equilibrium potential (E_K), and altered I_{K1} amplitude in accord with conductance (G_{K1})$\propto \sqrt{K^+_o}$. Surprisingly, myocytes bathed with 0-mM K^+ solution had a small outward I_{K1} at holding potential (V_{hold}) −85 mV. This I_{K1} was attributed to channel-activation by T-tubular K^+ (K^+_T) whose concentration is sensitive to the flow of T-tubular I_{K1}. K^+_T in myocytes bathed with 0-mM K^+ solution was ≈ 3.2 mM at V_{hold} −85 mV, but ≈ 0.3 mM following large K^+_T-depleting flows of inward I_{K1} at −160 mV. Results consistent with interplay of I_{K1} and K^+_T were also obtained in experiments on myocytes bathed with 2-, 5.4-, and 15-mM K^+ solution.

Myocytes were dialyzed with pipette solutions that contained 0-140 mM K^+ to investigate modulation by K^+_i. When I_{K1} at V_{hold} was kept small, E_{rev} varied with pipette K^+ in a near-Nernstian manner (i.e., $E_{rev} \approx E_K$); however, when I_{K1} (V_{hold}) was large and inward, E_{rev} was markedly negative to nominal E_K. Findings in experiments that involved shifting V_{hold}, changing K^+_o, and application of Ba^{2+} and Cs^+ suggest that the magnitude/direction of I_{K1} strongly affects the concentration of K^+ in submembrane cytoplasm. Classical G_{K1}-voltage parameters G_{K1}max and $V_{0.5}$ (but not slope factor) were affected by decreases in K^+_i: G_{K1}max declined by ≈ 25% per decade decrease in K^+_i, and $V_{0.5}$ shifted approximately as $0.5 \cdot E_K$-shift. The latter findings are discussed and compared with those of earlier studies on the dependence of inwardly-rectifying K^+ conductance on K^+_i.

LIST OF ABBREVIATIONS AND SYMBOLS USED

A	ampere
Ag^{+}	silver
ATP	adenosine triphosphate
Ba^{2+}	barium
Ba^{2+}_{o}	extracellular barium
C-	carboxy-
ca.	approximately
Ca^{2+}	calcium
Cd^{2+}	cadmium
$chordG_{Kir}$	Kir channel chord conductance
$chordG_{Kir}max$	maximal Kir channel chord conductance
$chordG_{K1}$	K1 channel chord conductance
$chordG_{K1}max$	maximal K1 channel chord conductance
Cl^{-}	chloride
COS-1	cell line derived from kidney cells of the African green monkey
Cs^{+}	cesium
Cs^{+}_{pip}	cesium in pipette filling solution
Ctl	control
DNFB	2,4-dinitrofluorobenzene

DMSO	dimethyl sulfoxide
dV	slope of voltage dependence
ECG	electrocardiogram
EGTA	ethylene glycol-bis(β-aminoethyl ether)-N,N,N',N'-tetraacetic acid
E_K	K^+ equilibrium potential
$E_{K,b}$	K^+ equilibrium potential calculated using bulk external K^+
$E_{K,pip}$	K^+ equilibrium potential calculated using pipette-solution K^+
$E_{K,T}$	K^+ equilibrium potential calculated using T-tubular K^+
E_{rev}	reversal potential
G	conductance
G_{Kir}	non-cardiac inwardly-rectifying K^+ channel conductance
$G_{Kir}max$	maximal G_{Kir}
G_{K1}	K1 channel conductance
$G_{K1}max$	maximal G_{K1}
$G_{K1,T}$	T-tubular membrane K1 channel conductance
G_m	membrane conductance
G_o	specific conductance
G-V	conductance-voltage relationship
G_{Kir}-V	Kir conductance-voltage relationship
G_{K1}-V	K1 conductance-voltage relationship
Glib	glibenclamide

gpvm	guinea-pig ventricular myocyte
HEK293	human embryonic 293 cell line
HEPES	N-2-hydroxyethylpiperazine-N'-2-ethanesulfonic acid
Hz	Hertz (number of cycles per second)
I	current
I-V	current-voltage relationship
I_{K1}-V	I_{K1} current-voltage relationship
$I_{Ca,L}$	L-type Ca^{2+}-channel current
I_{hold}	holding current
$I_{K,ATP}$	K_{ATP}-dependent-channel current
I_{Kir}	non-cardiac inwardly-rectifying K^+ current
I_{K1}	classical cardiac inwardly-rectifying K^+ current
$I_{K1,T}$	I_{K1} across T-tubular membrane
I_{Kr}	rapidly-activating delayed rectifier K^+ current
I_{Ks}	slowly-activating delayed rectifier K^+ current
I_{Na}	sodium current
I_{peak}	maximal amplitude of outward current
I_{to}	classical transient outward current
IC_{50}	concentration that produces 50% inhibition
I/O	inside-out
J_T	diffusion to/from T-tubules

K_{ATP}	ATP-dependent K^+ channel
K^+	potassium
KCNJ	family of genes of inwardly-rectifying potassium channels
K_D	dissociation conctant
kHz	kilohertz
K^+_i	intracellular potassium
Kir	family of inwardly-rectifying K^+ channels
Kir2	subfamily of Kir channels
Kir2.x	a member of Kir2 subfamily (x = 1 to 7)
K^+_o	extracellular potassium
K^+_{pip}	potassium in pipette-filling solution
K_T	T-tubular potassium
K1	classical cardiac inwardly-rectifying K^+ channel
La^{3+}	lanthanum
log	logarithm
LQT	long QT interval
M	mole per litre
Mg^{2+}	magnesium
min	minute
ml	millilitre
mM	millimole per litre
ms	millisecond

mV	millivolt
n	number of experiments (myocytes)
n	Hill coefficient
nA	nanoampere
nm	nanometer
nM	nanomole per litre
nS	nanosiemens
N-	amino-
Na^+	sodium
$NMDG^+$	N-methyl-D-glucamine
P	probability (significance level in statistical test)
P	pore loop
pA	picoampere
pH	negative logarithm of hydrogen ion concentration
pip sol'n	pipette solution
PIP_2	phosphatidylinositol-4,5-bisphosphate
pL	picolitre
PKA	protein kinase A
PKC	protein kinase C
PMA	phorbol 12-myristate 13-acetate
PTK	protein tyrosine kinase
QT	interval between Q and T of the electrocardiogram
QR	interval between Q and R of the electrocardiogram

r	radius
R	steady-state rectification
s	second
S	Siemens
S	slope factor
SEM	standard error of mean
Sim	simulated
SPM	spermine
SQTS	short QT syndrome
slopeG_{Kir}	G_{Kir} from slope of I_{Kir}-V relation
slopeG_{Kir}max	maximal slopeG_{Kir}
slopeG_{K1}	G_{K1} from slope of I_{K1}-V relation
slopeG_{K1}(E_K)	slopeG_{K1} at/near E_K
slopeG_{K1}max	maximal slopeG_{K1}
TM1	transmembrane domain 1
TM2	transmembrane domain 2
µM	micromole per litre
V	volt; voltage
V_{hold}	holding potential
V_m	membrane potential
V_{peak}	voltage at I_{peak}
V_{test}	test potential

$V_{0.5}$	half-voltage of Boltzmann function
Δ	difference (change)
τ	time constant
Ω	Ohm
$M\Omega$	megOhm
°C	degree Celsius
$\surd$	square root
$\propto$	direct proportionality
%	per cent
$\approx$	approximately

ACKNOWLEDGEMENTS

I would like to express my deepest gratitude to my supervisor, Dr. Terence F. McDonald, for his constant support, guidance, advice, and for his patience and encouragement throughout the course of my study at Dalhousie.

I am very grateful to my supervisory committee (Dr. Elizabeth A. Cowley, Dr. Robert A. Rose, and Dr. Roger P. Croll), and to Dr. Younes Anini for their assistance and guidance.

I am indebted to Pavel Zhabyeyev and Sergey Missan for their teaching and guidance in the isolation of myocytes, application of patch-clamp techniques, and analysis of electrophysiological data,

I am thankful to Mrs. Svetlana Zhabeeva, Mrs. Gina Dickie, Mr. Brian Hoyt, Mr. Mark Richard, Ms. Alice Smith, and Ms. Jennifer Graves for their excellent assistance and technical support.

I would like to extend thanks to all my friends for their support and encouragement.

Finally, I am especially grateful to my parents in Ukraine, and to my brother, Oleg Dyachok, for their understanding, encouragement and patience during my Ph.D. work.

CHAPTER 1. INTRODUCTION

1.1. BRIEF OVERVIEW

I_{K1} is the abbreviation commonly used for the classical inwardly-rectifying K^+ current described in studies on cardiac Purkinje fibres and cardiac muscle strands (Hutter & Noble, 1960; Noble, 1965; Dudel *et al.*, 1967; Rougier *et al.*, 1968; Mascher & Peper, 1969) and, later, in early studies on isolated cardiac cells (Isenberg & Klöckner, 1982; Matsuda & Noma, 1984). Since then, I_{K1} has been found in a wide variety of Purkinje fibre cells, ventricular myocytes, and atrial myocytes (Hume & Uehara, 1985; Tourneur *et al.*, 1987; Giles & Imaizumi, 1988; Cohen *et al.*, 1989; Harvey & Ten Eick, 1989; Clark *et al.*, 2001; Bouchard *et al.*, 2004). I_{K1} is constitutively active, and because it is the dominant current at potentials near the resting potential, it is an important determinant of the resting potential in most cardiac cells (Baumgarten & Fozzard, 1992). I_{K1} flows through "K1" channels that are complexes of inwardly-rectifying K^+ (Kir) subunits that belong to a subfamily of Kir subunits, Kir2 (Jan & Jan, 1997). In addition to expression in the heart, Kir2 is expressed in the central nervous system, skeletal muscle, vascular smooth muscle, and elsewhere (for reviews, see Stanfield *et al.*, 2002; Park *et al.*, 2008; de Boer *et al.*, 2010a; Hibino *et al.*, 2010). Aside from the generation of current-voltage (I-V) relations that display strong inward-rectification (i.e., much larger inward current than outward current), hallmark properties of I_{K1} in cardiac cells (and of Kir2 channel current (I_{Kir}) in noncardiac cells) include reversal potential (E_{rev}) that is close to the K^+ equilibrium potential (E_K), activation that is dependent on extracellular K^+, and voltage-dependent block by extracellular Ba^{2+} and Cs^+ (Stanfield *et al.*, 2002). These properties are amongst those investigated in the present study.

The material below begins with a brief account of the objectives of this study (Section 1.2). That is followed by a general background on Kir2 channels, K1 channels, and I_{K1} (Section 1.3) that is organized as follows: structure, gating, and rectification of Kir2 channels (1.3.1); composition, distribution, and localization of K1 channels (1.3.2); regulation of K1 channels (1.3.3); role of I_{K1} in cardiac function (1.3.4); and conditions that affect I_{K1} and cardiac function (1.3.5). This is followed by a 'specific background' section (1.4) that is more closely related to the experimental findings of the study. The areas covered in this section include modulation of I_{K1} by extracellular and intracellular K^+, accumulation and depletion of extracellular K^+, and current flow and possible changes in the concentration of cytoplasmic K^+.

1.2. OBJECTIVES OF THE STUDY

The first objective of this study on guinea-pig ventricular myocytes was to investigate the effects on I_{K1} of lowering the concentration of extracellular K^+ (K^+_o) from standard 5.4 mM to concentrations as low as 0 mM. The parameters of interest included the reversal potential (E_{rev}) of the current, its peak outward amplitude, and the maximal slope of the inward limb of the I-V relation of the current. It turned out that I_{K1} did not completely disappear when K^+_o was lowered to nominally 0 mM. This surprising finding led to investigation of possible accumulation and depletion of K^+ in extracellular restricted-diffusion spaces of myocytes.

A further objective of the study was to investigate the status of I_{K1} in myocytes whose concentration of intracellular K^+ (K^+_i) had been lowered by dialysis with pipette solutions that contained 0-100 mM K^+ (compared to standard 140 mM). The areas of interest in this investigation included (i) E_{rev} and its dependence on the concentration of

K^+ in the pipette solution, and (ii) the relations between E_{rev} ($\approx E_K$) and descriptors of K1 channel conductance (G_{K1}). It turned out that E_{rev} was strongly influenced by holding potential and holding current, and this finding led to an investigation of whether changes in flows of I_{K1} caused changes in the concentration of intracellular K^+.

1.3. GENERAL BACKGROUND

1.3.1 Structure, Gating, And Rectification Of Kir Channels

The basic building block of Kir channels is the Kir subunit. At least sixteen Kir subunit genes have been identified and classified into seven subfamilies, Kir1-7. A number of these genes belong to the Kir2 subfamily, including Kir2.1, Kir2.2, Kir2.3, Kir2.4 (de Boer *et al.*, 2010a; Hibino *et al.*, 2010), and, most recently, Kir2.6 in skeletal muscle (Ryan *et al.*, 2010; Dassau *et al.*, 2011). Four subunits associate in homomeric or heteromeric fashion to form a Kir2 channel. Each subunit has two putative transmembrane domains (TM1 and TM2), a linking pore loop (P), and cytoplasmic amino (N) and carboxy (C) terminal domains (Yang *et al.*, 1995; Raab-Graham & Vandenberg, 1998). The current view of Kir channel architecture, which is based on studies of the structure of mammalian Kir2.1 and Kir3.1 channels, as well as on studies of closely-related bacterial channels (KirBac) (e.g., Kuo *et al.*, 2003; Clarke *et al.*, 2010; Paynter *et al.*, 2010) (for reviews, see Anumonwo & Lopatin, 2010; Hibino *et al.*, 2010; Zhou & Jan, 2010), can be summarized as follows: The four pairs of TM1 (outer helix) and TM2 (inner helix) form the transmembrane pore, and support the four P-helices that span the outer leaflet of the membrane. This scaffolding positions a flexible ion selectivity filter atop the central cavity of the ("upper") pore of the channel. The P-loops contain the GYG

signature sequence important for selectivity of K^+. The bases of the four TM2 helices come together to create a narrow region (bundle crossing) that is situated just above the lower or "cytoplasmic" pore. The walls of the cytoplasmic pore are formed by the N- and C-termini, and residues of these termini are likely involved in the modulation of channel activity by intracellular agents such as PIP_2 (Logothetis *et al.*, 2007). The cytoplasmic pore extends the ion conduction pathway, and may serve as a concentrating region for cytoplasmic K^+ ions (Robertson *et al.*, 2008). The upper region of the cytoplasmic pore has a narrowing called the G-loop (girdle) that may serve as a diffusion barrier (Pegan *et al.*, 2005). Finally, a slide helix at the cytoplasmic end of TM1 is situated outside the TM1 and TM2 helices, lies parallel to the cytoplasmic side of the membrane, and connects the TM1 domain to the N-terminal in the cytoplasmic pore.

Gating of Kir2 channels. Kir2 channel gating occurs at a number of different levels. First, it seems likely that conformational changes in the flexible selectivity filter modulate intra-burst openings and closings observed in single-channel current recordings (for review, see Bichet *et al.*, 2003). Second, Kir2 channels have glycine at a TM2 position analogous to that of the "glycine-hinge" in bacterial Kir channels that exhibit gating. It has been proposed that gating at the glycine-hinge might be involved in activation of Kir channels by PIP_2 (Zhang *et al.*, 1999; Xie *et al.*, 2008)**.** Third, Pegan *et al.* (2005) have suggested that the narrow G-loops are gating elements that may participate in the activation of channels by PIP_2. Fourth, recent studies on KirBac channels suggest that conformational changes in the cytoplasmic domain correlate with conductive configurations of the selectivity filter, and that the slide helix and bundle crossing play an important role in the conformational changes and channel activation (Clarke *et al.*, 2010; Paynter *et al.*, 2010). Finally, Kir2 channels can be considered to be "gated" by the

intracellular polyvalent cations whose voltage-dependent channel blocking is the basis of inward rectification.

Inward rectification. Inward rectification of Kir channels is due to block of channels by cytoplasmic polyvalent cations, including Mg^{2+}, putrescine, spermidine, and spermine (Matsuda *et al.*, 1987; Ficker *et al.*, 1994; Lopatin *et al.*, 1994). The block is voltage-dependent, being stronger at more positive voltages. The degree of the voltage-dependent block is different for different types of Kir channels. The relatively high-affinity block of Kir2.1 secures "strong" inward rectification in these channels. For example, Dhamoon *et al.* (2004) found that Kir2.1 and Kir2.1/Kir2.3 channels underwent "complete" rectification, whereas Kir2.3 channels did not.

Of the polyvalent cations noted above, tetravalent spermine appears to be the most important for inward rectification (Lopatin *et al.*, 2000; Lopatin & Nichols, 2001; Lu, 2004)**.** The channel regions that are critical for spermine action are the negatively-charged regions E224/E229 (in the cytoplasmic pore) and D172 (in the transmembrane pore) (Wible *et al.*, 1994; Yang *et al.*, 1995; Pegan *et al.*, 2005). Mutation of spatially-close E224 and E299 causes a slowing and weakening of block by polyamine (Kubo & Murata, 2001). Likewise, mutation of D172 to neutral D172N weakens rectification in Kir2.1 (Stanfield *et al.*, 1994).

The precise details on block by polyamines remain unclear (Anumonwo & Lopatin, 2010; Clarke *et al.*, 2010). A "deep block" model of rectification (Lopatin *et al.*, 1995; John *et al.*, 2004; Kurata *et al.*, 2006; Kurata *et al.*, 2010) holds that spermine molecules may bind near cytoplasmic-pore region E224/E299 without occluding the pore, and then move towards the selectivity filter and bind between D172 and the GYG sequence of the filter in an occlusive manner. An alternative model, the "shallow block" model, proposes

that the binding of spermine at E229/E299 is occlusive, and that binding at a location between there and D172 stabilizes the block (Guo & Lu, 2003; Shin & Lu, 2005).

In voltage-clamped cardiac cells, the inward rectification of I_{K1} is manifested in the I-V relation as large inward current at voltages negative to E_K, and progressively smaller outward current at voltages progressively more positive than E_K (Noble, 1975). Conversion of I-V data to G_{K1}-V data indicates that inward rectification reflects a strong decline in G_{K1} (i.e., increased block) with membrane depolarization (Saigusa & Matsuda, 1988; Cohen *et al.*, 1989; Anumonwo & Lopatin, 2010). Changes in the extracellular concentration of K^+ change the value of E_K ($= -61 \cdot \log(K^+_i/K^+_o)$ at $\approx 35°C$) and shift G_{K1}-V relations along the voltage axis commensurate with the shift in E_K (Sakmann & Trube, 1984; Saigusa & Matsuda, 1988). The reason for the shift in G_{K1}-V with E_K may be that the I-V region in which there is strong inward flow of K^+ (which effectively knocks intracellular blocking particles off their channel binding sites), shifts along the voltage axis with E_K (Hille, 2001).

An interesting question that can be asked about the relation between the voltage dependence of inward rectification and E_K is whether the voltage dependence shifts with E_K when E_K is shifted via a change in intracellular K^+ rather than extracellular K^+. Studies on I_{K1} and its counterparts in non-cardiac cell types have yielded conflicting answers on the matter (e.g., Hagiwara & Yoshii, 1979; Vandenberg, 1987; Saigusa & Matsuda, 1988), and it is an area of interest in the present study.

1.3.2. Subunit Composition And Localization Of K1 Channels

Kir2.1 is the Kir2 subunit that is most strongly expressed in mammalian ventricular myocytes (Anumonwo & Lopatin, 2010; Hibino *et al.*, 2010); however, Kir2.2 and/or Kir2.3 are also likely to be expressed, perhaps in a species-dependent manner. For

example, both Kir2.1 and Kir2.3 have been detected in dog ventricular myocytes (Melnyk *et al.*, 2002), guinea-pig ventricular myocytes (Warren *et al.*, 2003), fetal mouse ventricular myocytes (Liu *et al.*, 2010), neonatal rat ventricular myocytes (He *et al.*, 2008), and sheep ventricular myocytes (Dhamoon *et al.*, 2004), whereas Kir2.1 and Kir2.2 have been detected in rat ventricular myocytes (Leonoudakis *et al.*, 2001), mouse ventricular myocytes (Panama *et al.*, 2007), and rabbit ventricular myocytes (Zobel *et al.*, 2003; Allah *et al.*, 2011).

The contributions of subunits to the Kir2 channels that carry I_{K1} in guinea-pig ventricular myocytes remain unclear (Hibino *et al.*, 2010). In contrast to the assertion by Liu *et al.* (2001) that Kir2.2 is the strongest contributor to I_{K1} in guinea-pig ventricular myocytes, others have concluded that Kir2.1 subunits make the largest contribution (Warren *et al.*, 2003; Dhamoon *et al.*, 2004; Yan *et al.*, 2005; Caballero *et al.*, 2010). A major contribution of Kir2.1 to I_{K1} appears to be the case in other types of ventricular myocytes as well (Nakamura *et al.*, 1998; Melnyk *et al.*, 2002; McLerie & Lopatin, 2003; Dhamoon *et al.*, 2004; Harrell *et al.*, 2007).

As noted earlier, I_{K1} is found in both ventricular and atrial myocytes, but it has a much larger density in ventricular myocytes of most species (Hume & Uehara, 1985; Bouchard *et al.*, 2004; Dhamoon *et al.*, 2004; Beckmann *et al.*, 2008), with the exception of mouse (Grandy *et al.*, 2007). In general, I_{K1} density and/or Kir2.1 expression in right ventricular myocytes is the same as (Yao *et al.*, 1999; Gaborit *et al.*, 2007) or moderately lower than (Warren *et al.*, 2003; Veeraraghavan & Poelzing, 2008) that in left ventricular myocytes; within the left ventricle, there appears to be little variation in I_{K1} and expression of Kir2.1 (Schram *et al.*, 2002; Szabó *et al.*, 2005; Kondo *et al.*, 2006). In a

study on adult guinea-pig left ventricle, there was no sex-related difference in either the expression level of Kir2.1 or the density of I_{K1} (Brouillette *et al.*, 2007).

Localization. There is a substantial body of evidence indicating that I_{K1}-carrying channels are enriched in the T-tubules of ventricular myocytes. When guinea-pig and rabbit ventricular myocytes are placed in culture, there is a pronounced daily loss of T-tubular membrane (Lipp *et al.*, 1996; Mitcheson *et al.*, 1996; Banyasz *et al.*, 2008) that results in a disproportionately large decline in whole-cell I_{K1} density (Christé, 1999; Banyasz *et al.*, 2008) (but see Beckmann *et al.* (2008) and Vaidyanathan *et al.* (2010)). Immunolocalization and electrophysiological studies on mouse ventricular myocytes have indicated that Kir2.1 channels are predominantly localized in the T-tubules (Clark *et al.*, 2001), and that Kir2.3 channels are exclusively localized to T-tubules (Dyachenko *et al.*, 2009). Furthermore, an immunolocalization study on rat ventricular myocytes indicated that both Kir2.1 and Kir2.2 subunits were localized to T-tubules (Leonoudakis *et al.*, 2001). Using immunocytochemistry and immunohistochemistry techniques, Melnyk *et al*. (2002) found that Kir2.1 was concentrated in the transverse tubules of canine ventricular myocytes, whereas Kir2.3 localized to cell ends. On the other hand, the results of studies on formamide-detubulated rat ventricular myocytes are consistent with uniform density of I_{K1} in T-tubular and surface membrane (Komukai *et al.*, 2002; Swift *et al.*, 2006) (see also Zobel *et al.*, 2003).

1.3.3. Regulation Of I_{K1}

1.3.3.1. Phosphorylation Systems

Since each of the Kir2-subunit contributors to I_{K1} has multiple consensus sites for phosphorylation by protein kinase A (PKA), protein kinase C (PKC), and protein tyrosine kinase (PTK) (NetPhos software (Blom *et al.*, 1999)), it is possible that I_{K1} is directly

regulated by one or more of these kinases. However, information on such regulation is sparse and/or conflicting. Koumi *et al.* (1995) reported that stimulation of PKA activity caused inhibition of I_{K1} in guinea-pig ventricular myocytes, and Vaidyanathan *et al.* (2010) found that stimulation of β_1-adrenoceptors with 1 mM isoproterenal caused a strong inhibition of I_{K1} in cultured adult rat ventricular myocytes. In both of these studies, the inhibition was confined to inward-directed I_{K1}. In contrast to the foregoing, Sonoyama *et al.* (2006) reported that stimulation of PKA had little or no effect on I_{K1} in rat ventricular myocytes. Stimulation of β_3 adrenergic receptors in an expression system caused upregulation of Kir2.1 and Kir2.2, but not Kir2.3 (Scherer *et al.*, 2007), whereas a PKA-stimulating cocktail had moderate mixed effects on Kir2.1 channel current in Cos-1 cells (Vega *et al.*, 2009).

In regard to regulation of I_{K1} by PKC, a low (1 nM) concentration of PKC-activating phorbol ester PMA had no effect on I_{K1} in guinea-pig ventricular myocytes (Tohse *et al.*, 1990), and a 1-μM concentration had no effect on I_{K1} in neonatal rat ventricular myocytes (Puglisi *et al.*, 2011). On the other hand, a 10-nM concentration strongly inhibited I_{K1} in human atrial myocytes (Sato & Koumi, 1995; Karle *et al.*, 2002). PKC activators had little effect on Kir2.1 channel current, but inhibited Kir2.2 and Kir2.3 channel current in expression systems (Zhu *et al.*, 1999; Karle *et al.*, 2002).

In regard to PTK, studies on I_{K1} in guinea-pig ventricular myocytes have concluded that inhibition of the kinase has no effect on the current (Chiang *et al.*, 2002) or decreases its amplitude (Gao *et al.*, 2004). Zhao *et al.* (2008) and Zhang *et al.* (2011) have reported that inhibition of PTK has moderate inhibitory effects on Kir2.1 channel currents in *Xenopus* oocytes and HEK293 cells.

1.3.3.2. Phosphatidylinositol-4,5-Bisphosphate (PIP_2)

Membrane-anchored PIP_2 is an important activator/sustainer of the activity of almost all types of Kir channels (Hilgemann *et al.*, 2001; Xie *et al.*, 2007). Evidence suggests that PIP_2 associates with a number of both positively-charged and neutral residues in the cytoplasmic termini, and thereby affects Kir2 channel activity, perhaps by affecting gating at the glycine-hinge point (Lopes *et al.*, 2002; Xie *et al.*, 2008), the G-loop (Pegan *et al.*, 2005), and/or other putative cytoplasmic gate (Logothetis *et al.*, 2007).

In a recent study, D'Avanzo *et al.* (2010) showed that purified human Kir2.1 and Kir2.2 incorporated in liposomes were directly activated by PIP_2. The activation was highly specific, with little or no activation by other phosphoinositides. The same group has presented evidence indicating that a number of anionic phospholipids may also participate in activation of Kir2.1 and Kir2.2 (Cheng *et al.*, 2011b).

1.3.3.3. Cholesterol

Cholesterol, a major lipid component of the cell, has an inhibitory action on the activity of Kir2 channels (Romanenko *et al.*, 2002). A recent study on Kir2.1 by Rosenhouse-Dantsker *et al.* (2011) suggests that the regulation occurs via cytoplasmic-domain residues that overlap with residues that affect modulation of the channel by PIP_2.

1.3.3.4. Extracellular And Intracellular K^+

With the exception of Kir7.1 (Krapivinsky *et al.*, 1998), all Kir channels respond to changes in K^+_o with changes in channel conductance and the dependence of conductance on voltage (Hibino *et al.*, 2010). However, the degree to which changes in K^+_i affect these parameters is unclear. More detailed overviews of the effects of K^+_o and K^+_i on I_{K1} and K1 channel conductance are provided at later points below (see Sections 1.3.5 and 1.4).

1.3.4. Role Of I_{K1} In Cardiac Function

I_{K1} is the dominant membrane current in resting nonpacemaker cells of the heart, and this ensures that the cell resting potential is almost as negative as E_K (Baumgarten *et al.*, 1981; Isenberg & Klöckner, 1982; Giles & Imaizumi, 1988; Baumgarten & Fozzard, 1992). The negative resting potential plays a key role in cardiac function: it facilitates recovery of Na^+ and Ca^{2+} channels from inactivation induced by action potential depolarization, promotes exchange of extracellular Na^+ for intracellular Ca^{2+}, helps secure rapid conduction of electrical impulses, and antagonizes development of spontaneous electrical activity (Katzung, 1975; Noble, 1986; Bers, 2001; Pogwizd *et al.*, 2001).

I_{K1} plays an important role in the excitation of cardiac cells. Excitation occurs when excitatory depolarizing current is sufficiently strong to attain action potential threshold and trigger regenerative depolarization in a cell. Outward I_{K1} opposes/offsets excitatory depolarizing current, and consequently can influence the level of the threshold potential (Tourneur *et al.*, 1987; Delmar *et al.*, 1989; McDonald *et al.*, 1989; Dhamoon & Jalife, 2005). Positive (depolarizing) shifts in threshold can in turn slow conduction of the action potential (Veeraraghavan & Poelzing, 2008).

I_{K1} also plays an important role in determining the configuration of the action potential. This modulation is almost fully confined to the repolarizing phases of the action potential because the magnitude of I_{K1} is very small at plateau potentials where rectification of the current is near-complete (Hume & Uehara, 1985; Giles & Imaizumi, 1988; Dhamoon *et al.*, 2004; Fink *et al.*, 2006). However, time- and voltage-dependent inactivation of inward current (contributed primarily by L-type Ca^{2+} current ($I_{Ca,L}$)) and activation of outward delayed-rectifier K^+ current promote termination of the plateau and the onset of repolarization (McDonald & Trautwein, 1978; Hume & Uehara, 1985). This

brings the membrane potential to levels (e.g., < −10 mV) that promote removal of rectification. The rate and extent of this removal increase with negative potential, such that I_{K1} becomes a more and more important driver of repolarization as repolarization progresses (Ibarra *et al.*, 1991; Shimoni *et al.*, 1992; Sung *et al.*, 2006; Bányász *et al.*, 2007). This participation of I_{K1} in repolarization affects cardiac function in that the rate of repolarization is a determinant of action potential duration which, in turn, influences Ca^{2+} influx and contraction (Miake *et al.*, 2003; Bouchard *et al.*, 2004; Fink *et al.*, 2006; Romero *et al.*, 2009).

1.3.5. Conditions That Affect I_{K1} And Electrical Activity

1.3.5.1. Changes In Extracellular K^+

Since decreases and increases in extracellular K^+ affect E_K, G_{K1}, and the I-V relation of I_{K1} (see Section 1.4.1 below), they affect electrical activity in the heart. Thus, both hypokalemia and hyperkalemia affect I_{K1} and heart electrical activity.

Hypokalemia refers to plasma K^+ < 3.0 - 3.6 mM (Farber *et al.*, 1951; Weaver & Burchell, 1960; Braunwald, 2001). The condition may be acute or chronic, and lower serum K^+ to ≤ 2 mM in conditions such as primary aldosteronism, familial and non-familial hypokalemic periodic paralysis, chronic diarrhea, and K^+-losing nephritis, as well as secondary to diuretic therapy (Weaver & Burchell, 1960; Cheng *et al.*, 2011a). Hypokalemia increases the amplitude of the U-wave of the ECG (Surawicz & Lepeschkin, 1953), most likely as a consequence of a reduction in I_{K1} (Postema *et al.*, 2009). Hypokalemia also predisposes to generation of afterdepolarizations and promotion of a spectrum of ventricular arrhythmias (Davidson & Surawicz, 1967; Sung *et al.*, 2006). These influences are most likely related to both a lowering of G_{K1} and an overloading of

intracellular Ca^{2+} following low-K^+_o-mediated inhibition of the Na^+-K^+ pump (Eisner & Lederer, 1979; Sung *et al.*, 2006).

It is not only during hyperkalemia (plasma K^+ > 6 mM) that heart cells may experience elevated extracellular K^+. For example, K^+ may accumulate in the clefts between cells and/or in the narrow T-tubules of cells (see Section 1.4.2 below) during ischemia (Kléber, 1983; Wilde *et al.*, 1990) or even during strenuous exercise (Sejersted & Sjøgaard, 2000). Independent of its origin, an increase in extracellular K^+ depolarizes the membrane, increases resting inactivation of voltage-dependent Na^+ channels, and enhances outward I_{K1}. These effects are likely to depress excitability, slow the upstroke of the action potential, and slow conduction (Whalley *et al.*, 1994).

1.3.5.2. Non-K^+_o -Related Conditions That Affect I_{K1} Density

I_{K1} density is likely to be decreased in hypertrophic and failing hearts (Beuckelmann *et al.*, 1993; Kääb *et al.*, 1998; Pogwizd *et al.*, 2001; Domenighetti *et al.*, 2007; Fauconnier *et al.*, 2010). It is inhibited by a variety of clinical pharmacological agents (Tamargo *et al.*, 2004; Rodríguez-Menchaca *et al.*, 2008; Ponce-Balbuena *et al.*, 2009; de Boer *et al.*, 2010b; El Gebeily & Fiset, 2010; López-Izquierdo *et al.*, 2011), and is down-regulated in patients with longQT syndrome LQT7 due to loss-of-function mutations of the *KCNJ2* gene that encodes for the Kir2.1 subunit (Andersen-Tawil syndrome) (Plaster *et al.*, 2001; Donaldson *et al.*, 2004; Lu *et al.*, 2006; Rajakulendran *et al.*, 2010; Tristani-Firouzi & Etheridge, 2010). On the cellular level, a decrease in I_{K1} density can lower the resting potential, lengthen the action potential duration, and slow repolarization. Such changes in cell electrical activity can result in a lengthening of the Q-R and QT intervals, and predispose to arrhythmia (McLerie & Lopatin, 2003; Nattel, 2003; Sung *et al.*, 2006).

I_{K1} density may be increased by gain-of-function mutations in Kir2 channel proteins (Priori *et al.*, 2005) and by the action of pharmacological agents (Caballero *et al.*, 2010). An increase in I_{K1} can speed up repolarization and shorten the action potential (e.g., Miake *et al.*, 2003). Increases in I_{K1} density via increased activity of Kir2.1 are implicated in short QT syndrome (SQT) (Priori *et al.*, 2005; El Harchi *et al.*, 2009) and in both chronic and familial atrial fibrillation (Bosch *et al.*, 1999; Li *et al.*, 2004; Xia *et al.*, 2005; Girmatsion *et al.*, 2009). Over-expression of Kir2.1 in a transgenic mouse model provokes episodes of ventricular fibrillation (Noujaim *et al.*, 2007), and I_{K1}-mediated shortening of the atrial action potential predisposes towards atrial arrhythmogenesis (Zhang *et al.*, 2005; Kharche *et al.*, 2008).

1.4. SPECIFIC BACKGROUND

1.4.1. Effects Of Raising And Lowering K^+_o On I_{K1} And G_{K1}

Effects on I_{K1}. It is well known that raising K^+_o from ca. 5.4 mM to a higher concentration causes a depolarization of the resting membrane of cardiac muscle cells (Gettes *et al.*, 1962; Fozzard & Lee, 1976; Cordeiro *et al.*, 1998), and that the depolarization is primarily related to a positive shift in the E_{rev} of I_{K1} (McDonald & Trautwein, 1978; Boyett *et al.*, 1980; Isenberg & Klöckner, 1982 ; Cordeiro *et al.*, 1998). Conversely, lowering K^+_o from ca. 5.4 mM to, say, 2 or 1 mM causes a marked hyperpolarization of the resting membrane (Gettes *et al.*, 1962; Fozzard & Lee, 1976; Bustamante *et al.*, 1981; Isenberg & Klöckner, 1982; Aronson & Nordin, 1988; Gjini *et al.*, 1996; Akuzawa-Tateyama *et al.*, 1998; Bouchard *et al.*, 2004) that is attributed to a negative shift in the E_{rev} of I_{K1} (Isenberg & Klöckner, 1982; Aronson & Nordin, 1988;

Cordeiro *et al.*, 1998; Spindler *et al.*, 1998; Bouchard *et al.*, 2004). The effects of more drastic lowerings of K^+_o on the resting potential are equivocal. For example, there are studies in which a lowering to nominally 0 mM caused marked depolarization of the resting potential that was attributed to abolition of I_{K1} (Fozzard & Lee, 1976; Isenberg & Klöckner, 1982), and others in which a similar lowering caused marked hyperpolarization (without comment on possible underlying mechanisms) (Fan & Liu, 1996; Akuzawa-Tateyama *et al.*, 1998).

In addition to causing a shift in E_{rev}, increasing K^+_o has distinct effects on I_{K1}-V relations in mammalian cardiac preparations. These include the following: (i) a shift in the entire relation to more positive potentials (Dudel *et al.*, 1967; McDonald & Trautwein, 1978; Isenberg & Klöckner, 1982; Ishihara & Ehara, 1998), (ii) an increase in the slope of the relation near E_{rev} (Dudel *et al.*, 1967; McDonald & Trautwein, 1978; Trautwein & McDonald, 1978; Isenberg & Klöckner, 1982; Sakmann & Trube, 1984), (iii) an increase in the slope of the linear region of the inward limb of the relation (Harvey & Ten Eick, 1988), and (iv) an increase in the amplitude of outward I_{K1} such that the outward limb of the high-K^+_o I-V relation crosses over that of the control-K^+_o relation (Noble, 1975; Trautwein & McDonald, 1978; Boyett *et al.*, 1980; Isenberg & Klöckner, 1982; Sakmann & Trube, 1984; Dhamoon *et al.*, 2004; Gómez *et al.*, 2009).

In contrast to the wealth of quantitative information available on the effects of raising K^+_o on I_{K1}, there is far less available on the effects of lowering K^+_o from ca. 5.4 mM. Isolated observations on ventricular myocytes indicate the following directional effects: (i) a shift in E_{rev} to a more negative potential (Aronson & Nordin, 1988; Harvey & Ten Eick, 1988; Ishihara & Ehara, 1998; Bouchard *et al.*, 2004), (ii) a decrease in the slope of the I-V relation at E_{rev} (Isenberg & Klöckner, 1982; Aronson & Nordin, 1988;

Bouchard *et al.*, 2004), (iii) a decrease in the maximal slope of the inward-current limb of the I-V relation (Harvey & Ten Eick, 1988), (iv) a decrease in the maximal amplitude of outward I_{K1} (Isenberg & Klöckner, 1982; Ishihara & Ehara, 1998; Spindler *et al.*, 1998), and (v) a crossing-over of the outward-current limbs of the low-K^+_o I-V relation and the control-K^+_o I-V relation (Isenberg & Klöckner, 1982; Tseng *et al.*, 1987; Aronson & Nordin, 1988; Shimoni *et al.*, 1992; Spindler *et al.*, 1998; Bouchard *et al.*, 2004).

Effects on G_{K1}. Early studies on cardiac Purkinje fibres indicated that the slope of the I-V relation (slopeG_{K1}) at or near estimated E_K (slope$G_{K1}(E_K)$) increased when K^+_o was raised from ca. 5.4 mM (Hall *et al.*, 1963; Noble, 1965; Dudel *et al.*, 1967). The relation between this G_{K1} parameter and K^+_o was not linear. Indeed, in one of the experiments conducted on sheep Purkinje fibres by Dudel *et al.* (1967), slope$G_{K1}(E_K)$ doubled in magnitude when K^+_o was raised by a factor of four (from 2.7 to 10.8 mM). In retrospect, this response could be taken as an indication that G_{K1} increases approximately as the square root of K^+_o ($\sqrt{K^+_o}$). Subsequent voltage-clamp experiments on guinea-pig and other ventricular muscle preparations indicated that G_{K1}-dominated membrane conductance (G_m) increased when K^+_o was increased from 3 to 10 mM (McDonald & Trautwein, 1978; Trautwein & McDonald, 1978), and that G_m was larger at voltages negative to E_K than at E_K itself (Beeler & Reuter, 1977; Trautwein & McDonald, 1978; Boyett *et al.*, 1980). Later, Daut (1982) reported that apparent slope$G_{K1}(E_K)$ in guinea-pig ventricular muscles increased approximately as $\sqrt{K^+_o}$ when K^+_o was increased between 3 and 6 mM. Sakmann & Trube (1984) measured the effects of K^+_o (5.4 - 43 mM) on slope$G_{K1}(E_K)$ in guinea-pig ventricular myocytes, and found that the relation between log slope$G_{K1}(E_K)$ and log K^+_o was well-described by a straight line with a slope of 0.54 ± 0.04.

The findings of Daut (1982) and Sakmann & Trube (1984) in regard to slope$G_{K1}(E_K)$ and increases in K^+_o were in line with earlier determinations of the conductances of strong inward-rectifiers in noncardiac preparations (G_{Kir}), especially with those of Hagiwara & Takahashi (1974). These investigators measured slope$G_{Kir}(E_K)$ in starfish egg, and found that its magnitude varied approximately with $\sqrt{K^+_o}$. In addition, they determined that the $\sqrt{K^+_o}$ dependence also applied to two other G_{Kir} parameters, slopeG_{Kir}max, and chordG_{Kir}max (where max refers to maximal, and chordG_{Kir} is $I_{Kir}(V)/(V - E_K)$). The equivalent of one of these parameters, slopeG_{K1}max, was measured by Harvey & Ten Eick (1988) in a study on cat ventricular myocytes. They reported that the magnitude of slopeG_{K1}max was approximately dependent on $\sqrt{K^+_o}$.

1.4.2. Effects Of Lowered K^+_i

Heart cells likely experience a lowering of K^+_i during hypoxia (Baumgarten *et al.*, 1981), osmotic swelling (Lado *et al.*, 1984), and ischemia (Case, 1971; Kléber, 1984). The lowering can be pronounced, as judged by the 50% reduction in the intracellular K^+ activity of canine subendocardial Purkinje fibre cells from one-day old infarcts (Dresdner *et al.*, 1987). Intracellular K^+ may also be lowered by chronic hypokalemia. For example, the heart cells of cats subjected to a chronic lowering of plasma K^+ to 3.3 mM had an intracellular K^+ concentration of 92 mM, compared to 154 mM in heart cells from control cats (Harrison *et al.*, 1972).

Heart cells that have lower than normal intracellular K^+ activity have depolarized resting potentials (Baumgarten *et al.*, 1981; Dresdner *et al.*, 1987), but whether the normal close dependencies of resting potential on E_K, and of E_{rev} (I_{K1}) on E_K, remain in force is unclear (Matsuda & Noma, 1984; Dresdner *et al.*, 1987; Baumgarten & Fozzard, 1992; Zhabyeyev *et al.*, 2004). One reason to suspect that the latter dependence is

preserved is that Hagiwara & Yoshii (1979) found that the E_{rev} of I_{Kir} corresponded to calculated E_K when the K^+ concentration of solution perfusing the interior of starfish eggs was lowered from 270 to 125 mM. These investigators also found that in contrast to the effects of raising K^+_o on the G_{Kir}-V relation (i.e., shift along the voltage axis commensurate with the shift in E_K), lowering K^+_i had no apparent effect on the G_{Kir}-V relation. However, the situation in regard to G_{K1} in guinea-pig ventricular myocytes may be quite different because Saigusa & Matsuda (1988) found that a lowering of K^+_i from 150 to 50 mM strongly decreased maximal G_{K1} and shifted the G_{K1}-V relation along the voltage axis to the same degree as the shift in E_K. Saigusa & Matsuda (1988) recorded an increase in maximal outward I_{K1} following a decrease in K^+_i, a result that is the opposite of the response observed in other studies on guinea-pig ventricular myocytes with lowered K^+_i (Matsuda & Noma, 1984; Zhabyeyev *et al.*, 2004).

1.4.3. Accumulation And Depletion Phenomena

1.4.3.1. Accumulation Of Extracellular K^+

It has long been known that large flows of outward K^+ current can cause accumulation of K^+ in restricted-diffusion extracellular spaces of experimental preparations of nerve and muscle tissue (Frankenhaeuser & Hodgkin, 1956; Adrian & Freygang, 1962; Eaton, 1972; Orkand, 1980). Since cardiac cells have a variety of well-developed K^+ current systems (Dudel *et al.*, 1967; McDonald & Trautwein, 1978; Cordeiro *et al.*, 1998; Roden *et al.*, 2002; Nerbonne & Kass, 2005), and multicellular cardiac preparations have restricted-diffusion extracellular spaces that likely include both intercellular clefts and T-tubules (Sommer & Johnson, 1968; Sommer, 1982; Forbes & van Neil, 1988), it is not surprising that both non-voltage-clamp (Kline *et al.*, 1980) and voltage-clamp experiments on cardiac Purkinje fibres (McAllister & Noble, 1966;

Baumgarten *et al.*, 1977), as well as voltage-clamp experiments on frog atrial trabeculae (Noble, 1976), frog ventricular strips (Cleemann & Morad, 1979), and mammalian ventricular trabeculae and papillary muscles (McDonald & Trautwein, 1978; Boyett *et al.*, 1980) have yielded electrophysiological evidence indicating that large outward flows of K^+ through cardiac K^+ channels can cause accumulation of extracellular K^+. For example, Baumgarten *et al.* (1977) measured resting potential immediately after termination of a depolarizing clamp step applied to a cardiac Purkinje fibre and found that the magnitude of the positive shift in the resting potential varied with the magnitude of the preceding flow of outward K^+ current.

A consistent finding in early studies on accumulation of external K^+ due to outward K^+ current in nerve and muscle preparations was that for a given-sized current, the apparent degree of accumulation was inversely related to the concentration of K^+ in the bathing solution (e.g., Frankenhaeuser & Hodgkin, 1956; Orkand, 1980). A similar type of inverse dependence on bathing solution K^+ was also evident in studies of accumulation in multicellular cardiac preparations (e.g., McAllister & Noble, 1966; Baumgarten & Isenberg, 1977; Baumgarten *et al.*, 1977).

It was widely believed that all, or nearly all, of the outward-current-induced accumulation of extracellular K^+ in multicellular cardiac preparations was localized to intercellular clefts whose widths can be as narrow as 20-30 nm (Sommer & Johnson, 1968). Consequently, there was little reason for investigators to believe that the extent of current-induced K^+ accumulation in experiments on (cleftless) isolated cardiomyocytes could be anything other than very small or negligible (e.g., Isenberg & Klöckner, 1982; Matsuura *et al.*, 1987; Mitsuiye & Noma, 1987; Shah *et al.*, 1987; Main *et al.*, 1997). However, voltage-clamp results obtained by Yasui *et al.* (1993) indicated that substantial

accumulation of K^+ could occur under certain circumstances. These investigators activated ATP-dependent K^+ (K_{ATP}) channels in guinea-pig ventricular myocytes by treating the myocytes with nicorandil, a selective opener of this type of K^+ channel (Hiraoka & Fan, 1989). They found that step-depolarizations of nicorandil-treated myocytes elicited large outward currents through K_{ATP} channels ($I_{K,ATP}$), and that repolarizations to a holding potential (−85 mV) that was near E_K (K^+_o 5.4 mM) elicited time-dependent inward tail currents. The amplitude of the inward tail current was related to the amplitude and the duration of flow of the outward $I_{K,ATP}$ on the preceding depolarization, and the decay of the inward tail current (reflecting clearance of the accumulated external K^+) followed a multiexponential time course with a $T_{½} < 100$ ms. Based on morphological considerations, and on the apparent absence of accumulation phenomena in their experiments on nicorandil-activated $I_{K,ATP}$ in guinea-pig atrial myocytes (known to have a paucity of T-tubules (Sommer, 1982)), Yasui *et al.* (1993) concluded that $I_{K,ATP}$-induced accumulation of extracellular K^+ in ventricular myocytes occurs primarily in the T-tubules. Confirmation of key findings of Yasui *et al.* (1993) was obtained by Tourneur *et al.* (1994) who used a non-nicorandil channel-opener to activate K_{ATP} channels in guinea-pig ventricular myocytes. Knopp *et al.* (1999) also obtained a number of results similar to those reported by Yasui *et al.* (1993). They treated guinea-pig ventricular myocytes with 2,4-dinitrophenol and other metabolic inhibitors that lower intracellular ATP and open K_{ATP} channels. They found that large flows of outward $I_{K,ATP}$ elicited by depolarizations were followed by inward tail currents on repolarizations to −80 mV, and concluded that the inward tails were related to shifts in E_K to potentials positive to −80 mV as a result of accumulation of K^+ in T-tubules.

A further important study on accumulation of extracellular K^+ in ventricular myocytes was that conducted by Clark *et al*. (2001) on murine ventricular myocytes. In contrast to the $I_{K,ATP}$-related protocol of increasing K^+ outflow used by Yasui *et al*. (1993) and Knopp *et al.* (1999), Clark and colleagues secured large outflow of K^+ into restricted-diffusion extracellular spaces by activating transient outward K^+ current (I_{to}). They found that large surges of outward K^+ current elicited by strong depolarizations from holding potential −80 mV were followed by large Ba^{2+}-sensitive inward tail currents on repolarizations. They attributed the inward tail currents to I_{K1} flowing as a consequence of accumulations of K^+ that shifted E_{rev} to voltages positive to the holding potential of −80 mV. Clark *et al*. (2001) also reported that accumulation-related inward tails were not observed in experiments on mouse atrial myocytes (which have a low density of T-tubules) (see also Fiset *et al.*, 1997).

1.4.3.2. Depletion Of Extracellular K^+

Given that large *outward* K^+ current can lead to accumulation of K^+ in restricted-diffusion extracellular spaces (see above), it is plausible that large *inward* K^+ current can cause *depletion* of K^+ from these same spaces. Amongst the first to consider K^+-current-induced depletion of extracellular K^+ were Adrian, Almers, and colleagues (e.g., Adrian & Freygang, 1962; Adrian *et al.*, 1970; Almers, 1972; Barry & Adrian, 1973). These investigators recorded inwardly-rectifying K^+ current (I_{Kir}) from frog skeletal muscle fibres, and found that hyperpolarizing steps to voltages more negative that E_K elicited large inward I_{Kir} that decayed with time during the steps. They attributed much of the decay of the current to a time-dependent depletion of K^+ in the T-tubules. Reasons for this view included observations that hyperpolarizing pulses caused the E_{rev} of I_{Kir} to shift to more negative potentials, and that both the degree of the negative shift and the degree

of decay of I_{Kir} were much smaller after elevation of the concentration of K^+ in the bathing solution.

Results suggesting that depletion of extracellular K^+ can also occur in multicellular cardiac preparations were reported by Maughan *et al.* (1973), Baumgarten & Isenberg (1977), Baumgarten *et al.* (1977), and McDonald & Trautwein (1978). They found that hyperpolarizing steps applied from holding potentials near E_{rev} elicited inward-going I_{K1} that decayed during the steps. The decays of the currents were concomitant with negative shifts in E_{rev}, and attenuated by increases in external K^+.

The findings in the aforementioned studies on multicellular cardiac preparations offer little guidance on whether the depletion of K^+ occurred in intercellular clefts and/or in T-tubules. However, there have been a number of studies on isolated myocytes that suggest that strong hyperpolarizing pulses can cause depletion of T-tubular K^+. For example, Harvey & Ten Eick (1988) observed that 70-ms hyperpolarizations to –170 mV shifted the E_{rev} of I_{K1} in cat ventricular myocytes by -7.1 ± 1.4 mV. They also found that inward I_{K1} elicited by hyperpolarizing pulses decayed markedly during the pulses. They attributed part of the decay phases to declines in T-tubular K^+ (and, therefore, declines in K^+ inward driving force and K^+_o-dependent G_{K1}), and part to an "inactivation" of I_{K1} related to the presence of Na^+ in the bathing solution. In their study on human ventricular myocytes, Bailly *et al.* (1998) reported that inward I_{K1} elicited by 200-ms hyperpolarizations to voltages ≤ -140 mV underwent substantial decay during the pulses**.** They attributed the decay of I_{K1} to time-dependent block of K1 channels by external Na^+, as well as to depletion of K^+ in restricted-diffusion extracellular spaces. They suggested that the depletion likely occurred in the T-tubules, and that the finding of strong

attenuation of decay by elevation of K^+_o from 4 to 20 mM offered strong support for the depletion hypothesis.

Pásek *et al.* (2003) developed a computer model that is based on a quantitative description of electrical activity in the guinea-pig ventricular myocyte formulated by Luo & Rudy (1994). One purpose of the model was to separate ionic transport systems in "surface" membrane from those in T-tubular membrane to evaluate responses related to events occurring in the T-tubules. Model cylindrical myocytes of 100-μm length and 10-μm radius had T-tubular morphology that was based on the microscopic analysis of rat ventricular myocytes conducted by Soeller & Cannell (1999). The average radius of the tubules was 127 nm, the average length 10 μm, and the fractional volume 3.12%; the tubular membrane represented 69% of the total membrane area (which is considerably larger than estimated for guinea-pig ventricular myocytes, 52.6% (Amsellem *et al.*, 1995)). One set of simulations performed by Pásek *et al.* (2003) was of electrical activity in a myocyte bathed with 5.4-mM K^+ solution and externally stimulated at 1 Hz. These indicated that the K^+ concentration in T-tubules increased by ≈ 4.7% during each action potential, and then gradually returned to bulk concentration during the next several hundred milliseconds. They speculated that such accumulation could enhance T-tubular G_{K1} and thereby have a stabilizing effect on the diastolic resting potential of the myocyte; on the other hand, it could have a proarrhythmic influence due to a diminished difference between diastolic resting potential and threshold potential. Subsequent simulations focused on a guinea-pig ventricular model suggested that the increase in T-tubular K^+ was ≈ 4% during each action potential (Pásek *et al.*, 2008).

Pásek *et al.* (2003) also simulated membrane currents in response to voltage-clamp steps. They found that progressively larger inward I_{K1} elicited by progressively stronger

hyperpolarizing pulses to voltages between −100 and −160 mV induced progressively larger depletions of T-tubular K^+. At steady-state at −160 mV, for example, the concentration of K^+ in the tubules was just 2 mM. The time-dependent lowering of T-tubular K^+ early during a pulse was concomitant with marked time-dependent decay of tubular-membrane inward I_{K1}. Simulated whole-myocyte inward I_{K1} displayed less marked decay than tubular I_{K1} due to the contribution of non-decaying inward I_{K1} in the surface membrane.

1.4.3.3. Current Flow And Possible Changes In Cytoplasmic K^+

Frankenhaeuser (1962) may have been the first investigator to have speculated on an effect of K^+ current flow on intracellular K^+ in a voltage-clamped preparation. He recorded delayed-rectifier K^+ current from myelinated nerve fibres, and raised the possibility that flows of outward current might cause depletions of K^+ at the inner edge of the nodal membrane. Other investigators of nerve electrical activity recognized that influxes of Na^+ during high-frequency stimulation could shift the Na^+ equilibrium potential by tens of millivolts, and surmised that it might be due to accumulation of the ion in a submembrane space from which it only slowly diffuses to the bulk axoplasm (Nakajima & Onodera, 1969; Bergman, 1970). More recently, the concept that Na^+ may accumulate within a layer of cytoplasm just below the sarcolemma ("restricted" or "fuzzy space") of heart cells (Lederer *et al.*, 1990) has become widely accepted. Electron probe X-ray microanalysis studies on guinea-pig and rabbit ventricular myocytes suggest that the restricted-diffusion subsarcolemmal space for Na^+ may extend 50 to 200 nm below the sarcolemma (Wendt-Gallitelli *et al.*, 1993; Silverman *et al.*, 2003). Estimates of the volume of the fuzzy space for Na^+ range from < 1% to 10-14% of cell volume (for review, see Török, 2007). However, these estimates may only apply in relation to transmembrane movements of Na^+ of a particular order of magnitude. For example,

Carmeliet (1992b) has made the point that large influxes of Na^+ likely fill up any fuzzy space and spill over into the bulk cytoplasm, and Despa *et al.* (2004) have shown that it is possible to establish large Na^+ gradients in the bulk cytoplasm of rat ventricular myocytes.

Carmeliet (1992b) expressed the view that microheterogeneity of intracellular ions was more likely the rule rather than the exception. In that regard, Hwang *et al.* (1992) noted the possibility that outward Cl^- current elicited by holding the membrane at a depolarized level might lead to accumulation of Cl^- in the submembrane cytoplasm of a ventricular myocyte, and thereby engender a Cl^- equilibrium potential (E_{Cl}) different than that calculated from external Cl^- and the Cl^- concentration in the pipette solution.

Despite the foregoing studies and concepts, there has been little attention paid to the possibility that K^+ current flow could affect the concentration of K^+ in the cytoplasm of myocytes. The most likely reason for this is that studies on K^+ currents in whole-cell configured myocytes are almost always conducted using pipettes that are filled with solutions that contain ca. 140 mM K^+, i.e., this concentration of K^+ in the cytoplasm, along with diffusion of K^+ to and from the pipette, should be able to buffer gains and losses of cytoplasmic K^+ related to "typical flows" of outward- and inward-directed K^+ current. However, a more careful examination may be warranted when the myocyte is dialyzed with a solution that contains, say, 10 mM K^+. The buffering capacity is now very much smaller, and large K^+ current flows are likely to create K^+ concentration gradients between submembrane cytoplasmic regions where K^+ ions have entered or exited, and cytoplasmic regions near the tip of the pipette. The larger and the longer-lasting the current flow, the greater the expected accumulation or depletion of K^+ in submembrane cytoplasmic regions, and, consequently, the greater the expected

discrepancy between measured E_{rev} ($\approx E_K$) and E_K calculated as $-61 \cdot \log(K^+_{pip}/K^+_o)$ where K^+_{pip} is the concentration of K^+ in the pipette-filling solution. A moderating factor in any scenario of accumulation/depletion of K^+ is the diffusion of K^+ into/out of the patch-pipette. For the case of a typical ventricular myocyte under typical whole-cell voltage-clamp conditions, Mathias *et al.* (1990) have calculated that the time constant of exchange of pipette K^+ and cytoplasmic K^+ is close to 100 s.

CHAPTER 2. METHODS

All of the experimental data reported in this study were obtained from experiments on guinea-pig ventricular myocytes that were isolated using an enzymatic method, and investigated using a whole-cell voltage-clamp method. Simulated data on the dependence of I_{K1} on voltage and external K^+ were obtained using an equation (see below).

2.1. ISOLATION OF MYOCYTES

Guinea pigs weighing 250 - 350 g were sacrificed in accord with national and local regulations on animal experimentation. The animals were anesthetized using isofluorane in 100% oxygen. Hearts were quickly excised, and attached to the base of an 80-cm Langendorff column. The hearts were then retrogradely perfused with normal Tyrode's solution (see below) for ≈ 1 min. Thereafter, they were sequentially perfused with Ca^{2+}-free supplemented-Tyrode's solution for 7 - 9 min, Ca^{2+}-free supplemented-Tyrode's solution containing collagenase (0.1 - 0.15 mg/ml; Yakult Pharmaceutical Ind. Co., Ltd., Tokyo, Japan) for 10 - 12 min, and a high-K^+ storage solution for 6 min. The Ca^{2+}-free supplemented-Tyrode's solution contained (in mM) NaCl 125, KCl 4.6, $MgCl_2$ 1.16, taurine 20, glucose 20, and N-2-hydroxyethylpiperazine-N'-2-ethanesulfonic acid (HEPES) 5 (pH 7.4 with NaOH). The high-K^+ storage solution contained (in mM) KCl 30, KOH 80, KH_2PO_4 30, glutamic acid 50, $MgSO_4$ 3, taurine 20, glucose 10, ethylene glycol-bis(β-aminoethyl ether)-N,N,N',N'-tetraacetic acid (EGTA) 0.5, and HEPES 10 (pH 7.4 with KOH). All solutions were oxygenated with 100% O_2 and maintained at 37 °C.

Following the final period of heart perfusion, the ventricles were cut into chunks, and myocytes were dispersed by gentle mechanical agitation. The myocyte suspension was filtered through 220-μm polyethylene mesh, and the filtrate was kept in storage solution at room temperature.

2.2. ELECTROPHYSIOLOGICAL RECORDING AND ANALYSIS

An aliquot of myocyte-containing storage solution was dropped into the 0.3-ml main chamber of a plastic and glass bath (Sarstedt, Inc., Newton, NC, USA) positioned on top of the stage of an inverted microscope (Nikon Diaphot, Tokyo, Japan). After the myocytes had settled on the glass bottom of the chamber, the chamber was perfused with a bathing solution (see below) at a rate of 2-3 ml/min.

Single myocytes were voltage clamped using the conventional whole-cell configuration of the patch-clamp technique (Hamill *et al.*, 1981). Pipettes were pulled from thick-walled borosilicate glass capillaries (H15/10/137, Jencons Scientific, Leighton Buzzard, UK) by using the usual two-step process. Pipettes had an inside diameter of 2 - 3 μm, and a resistance of 2 - 3 MΩ when filled with pipette solution and immersed in normal Tyrode's solution. After establishing a gigaohm seal between the pipette tip and the myocyte surface, a brief surge of suction was applied to rupture the patch of membrane under the pipette tip. Myocytes were lifted off the bottom of the bath to ensure satisfactory superfusion of all myocyte surfaces.

The voltage clamp amplifier used was an EPC-9 (HEKA Electronics, Mahone Bay, NS, Canada). The reference electrode was an Ag-AgCl wire or a DRIREF-2SH electrode (World Precision Instruments, Inc., Sarasota, FL, USA). Series resistance was 4 - 6 MΩ, and compensated by 60 - 70%. Cell capacitance generally ranged from 80 to 140

pF. Membrane currents were filtered at 3 kHz by the amplifier, and digitized at 12 kHz with Pulse software (HEKA Electronics). Data files were converted from Pulse to Axon (Union City, CA, USA) data format, and analyzed with Axon Clampfit software (version 6).

Myocytes that were dialyzed with 140-mM K^+ pipette-filling solution (see below) were usually held at –85 mV or at potentials that were near calculated E_K, whereas myocytes that were dialyzed with low-K^+ pipette-filling solution (see below), were held at predetermined potentials between –10 and –105 mV. Current-voltage (I-V) relations were obtained by using either voltage-ramp or voltage-step protocols. In the voltage-ramp protocols, myocytes were hyperpolarized to a negative potential (e.g., –120 mV) for 2-200 ms and then depolarized at 0.05-0.1 V/s to a selected more positive potential, or were depolarized to a selected ramp-start potential and then hyperpolarized to a selected more negative potential at 0.05-0.1 V/s. In general, voltage ramps were applied every 15-30 s. In voltage-step protocols, myocytes were pulsed from the holding potential to one or more test potentials for 200-1000 ms every 5-30 s. Current amplitudes measured at the ends of pulses were used to construct quasi-steady-state I-V relations. Conductance data were obtained from measurements of the slopes of the linear regions of the inward limbs of I-V relations, or by other procedures detailed in the Results (Chapter 3). Pipette offsets were nulled prior to patch formation and liquid junction potentials (≈ –11 mV for $NMDG^+$-Tyrode's solution-K^+ pipette solution combination) were compensated for (–10 mV) during analysis.

2.3. EXPERIMENTAL SOLUTIONS

2.3.1 Bathing Solutions

Myocytes were bathed with a Na^+ Tyrode's solution that contained (in mM) NaCl 140, KCl 5.4, $CaCl_2$ 1.8, $MgCl_2$ 1, glucose 10, and HEPES 5 (pH 7.4 with NaOH), a Na^+ Tyrode's solution that contained 0 mM K^+ (KCl omitted), or a Na^+ Tyrode's solution that contained either higher or lower K^+ than 5.4 mM (higher or lower KCl than 5.4 mM, with suitable adjustment of NaCl to maintain normal osmolarity). Alternatively, myocytes were bathed with a Tyrode's solution similar to the above except that NaCl was replaced by N-methyl-D-glucamine ($NMDG^+$) chloride, and the pH was brought to 7.4 with HCl. Glibenclamide (3-5 μM) was added to all bathing solutions except for those in experiments which involved activation of $I_{K,ATP}$ (see Chapter 3); other ion channel blockers (Cd^{2+}, E4031, and chromanol 293B) were frequently added as well (see below and Chapter 3). The temperature of the bathing solutions was 35-36°C.

A number of the experiments involved application of strong hyperpolarizing pulses. Since these can trigger irregular inward currents through hyperpolarization-induced electropores, solutions were sometimes supplemented with 0.1-0.2 mM La^{3+} to minimize their occurrence and magnitude (Akuzawa-Tateyama *et al.*, 1998; Song & Ochi, 2002; Dyachok *et al.*, 2010). These concentrations of La^{3+} have little effect on I_{K1} in rabbit ventricular myocytes (Akuzawa-Tateyama *et al.*, 1998).

2.3.2 Pipette-Filling Solutions

The standard 140-mM K^+ pipette-filling solution contained (in mM): KCl 30, K^+ aspartic acid 110, Mg-ATP 5, EGTA 5, and HEPES 5 (pH 7.2 with KOH). Pipette

solution that had a concentration of K^+ that ranged from 100 mM to 0 mM was made by replacing K^+ with Cs^+, or, in some experiments, with $NMDG^+$.

2.4. CHEMICALS

All chemicals used to prepare bathing solutions and pipette-filling solutions were purchased from Sigma-Aldrich (Oakville, ON, Canada) and TOCRIS bioscience (Ellisville, MO, USA).

2.5. DRUGS

In general, drugs were dissolved in vehicle and stored in stock solutions. Stock solutions were kept in the dark at –20 °C, and drugs were added to experimental solutions just prior to experiments.

Organic channel blockers were used as required in order to minimize currents that might overlap with I_{K1}. These agents included the rapidly-activating delayed-rectifier (Kr) channel blocker E4031, the slowly-activating delayed-rectifier (Ks) channel blocker chromanol 293B, and the ATP-dependent K^+ (K_{ATP}) channel blocker glibenclamide. E4031 (Eisai, Tokyo, Japan) was dissolved in distilled water, stored as a 10-mM stock solution, and added to bathing solution. Chromanol 293B (Aventis, Strasbourg, France), cromakalim (Sigma-Aldrich), and glibenclamide (TOCRIS bioscience) were dissolved in dimethyl sulfoxide (DMSO) (Sigma-Aldrich), stored as 10- to 100-mM stock solutions, and added to bathing solution.

Other compounds used in the study included spermine (Sigma-Aldrich), 2,4-dinitrofluorobenzene (DNFB) (Sigma-Aldrich), daidzein (Calbiochem, La Jolla, CA, USA), and 17β-estradiol (Sigma-Aldrich). Spermine was dissolved in distilled water, stored as a 10- or 100-mM stock solution, and added to pipette-filling solution. DNFB, daidzein, and 17β-estradiol were freshly prepared in DMSO just before experiments, and added to bathing solutions. The final concentration of DMSO in external solutions was ≤ 0.1%.

2.6. SIMULATION OF I_{K1}-V

I_{K1}-V relations were simulated in accord with the following assumptions:

1. I_{K1} is a function of G_{K1} and driving force ($V - E_K$): $I_{K1} = G_{K1}(V - E_K)$.
2. $G_{K1}max$ is dependent on square root of K^+_o: $G_{K1}max = G_o \sqrt{K^+_o}$, where G_o = 43.03 nS/mM$^{-1/2}$, and $G_{K1}max$ for 5.4 mM K^+_o is 100 nS.
3. Steady-state rectification is described by a Boltzmann function as follows:

$$R = \frac{1}{1 + \exp\left(\frac{V - V_{0.5}}{dV}\right)},$$

   where V is membrane voltage, $V_{0.5}$ is half-voltage of rectification, and dV is slope of rectification. $V_{0.5}$ and dV for 5.4 mM K^+_o are –70 mV and –17 mV, respectively.
4. Steady-state rectification shifts with the reversal potential of I_{K1} (E_{rev}). That is accomplished by (i) assuming that dV is constant and independent of K^+_o, and (ii) expressing $V_{0.5}$ as a linear function of E_K: $V_{0.5} = E_K + 15$.

After combining the foregoing assumptions into a single formula, I_{K1} depends on voltage (V) and K^+_o (E_K set by K^+_o and K^+_i) as follows:

$$I_{K1} = \frac{G_o \sqrt{K_o}(V - E_K)}{1 + \exp\left(\frac{V - (E_K + 15)}{dV}\right)}.$$

I_{K1}-V relations were plotted using data analysis software (OriginPro 7; OriginLab, MA, USA) as function graphs with voltage as an independent variable with increment of 0.5 mV, and current as a dependent variable.

2.7. STATISTICS

Results are expressed as means ± SEM, with n indicating the number of experiments. Single comparisons were made using Student's paired or unpaired *t* test, and multiple comparisons were made using one-way analysis of variance (ANOVA) followed by the Tukey-Kramer multiple comparison test. Differences were considered significant when $P < 0.05$.

CHAPTER 3. RESULTS

3.1. FEATURES OF I_{K1} IN GUINEA-PIG VENTRICULAR MYOCYTES

Material presented in this section provides a brief overview of features of I_{K1} in guinea-pig ventricular myocytes. This facilitates the presentation of data at later points in this chapter. The section begins with a figure that shows records of currents elicited by clamp steps to voltages between −170 and +80 mV, and continues by illustrating that the current is sensitive to inhibition by external Ba^{2+} and Cs^{+}, and that the current is modulated by external K^{+}. The section closes with data that illustrate the stability of the current in these myocytes. All of the experiments reported in this section were performed on myocytes that were dialyzed with standard 140-mM K^{+} pipette solution.

3.1.1. K^{+} Currents Elicited By Voltage-Clamp Pulses

Figure 1A shows records of membrane currents obtained in an experiment on a myocyte that was bathed with 5.4-mM K^{+} Na^{+} solution that contained 0.2 mM Cd^{2+} to block L-type Ca^{2+} current ($I_{Ca,L}$) (McDonald *et al.*, 1994), partially block voltage-dependent Na^{+} current (I_{Na}) (Visentin *et al.*, 1990), and suppress fast-activating I_{Kr} (Sanguinetti & Jurkiewicz, 1990). The myocyte was held at −40 mV, and pulsed to potentials between −100 and +80 mV for 500 ms every 10 s. The traces indicate that the current was near the zero-current level on the pulse to −85 mV, large and inward-directed on the pulse to −100 mV, moderately large and outward-directed on the pulse to −55 mV, and very small and outward-directed on the pulse to −10 mV. The currents were increasingly large and outward-directed on the pulses to potentials between +10 and +80

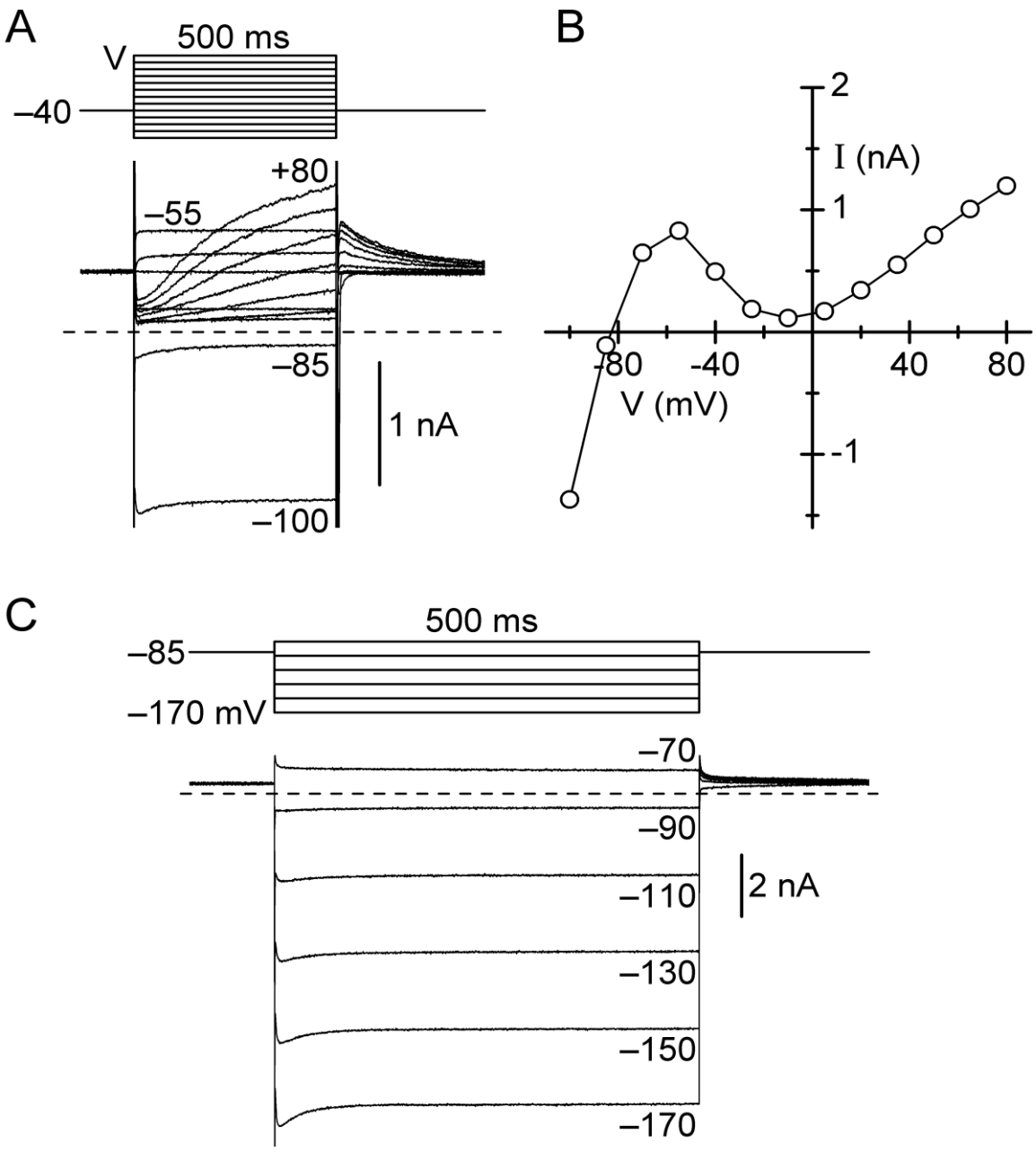

Figure 1. Membrane currents recorded from representative guinea-pig ventricular myocytes. The myocytes were superfused with 5.4-mM K^+ Na^+ solution that contained 0.2 mM Cd^{2+}, and pulsed from the holding potential to other potentials for 500 ms every 10 s. **A,B.** Panel A: note the relatively flat shape of currents between –100 and –10 mV (indicative of I_{K1}), and the time dependence of current at more positive potentials (indicative of I_{Ks}). Panel B: the I-V relation obtained from measurements of current amplitudes at the ends of the pulses shown in A. **C.** Records of inward I_{K1} elicited at potentials down to –170 mV in a different myocyte. The dashed lines on the records indicate the zero-current levels.

mV, and had a very different character than the currents on the pulses to potentials between −100 and −10 mV. The latter were relatively flat (time-independent) after completion of early transients, whereas the outward currents at positive potentials increased with time during the pulses. The dependence of these currents on time ("delayed rectification"), the dependence of their activation on voltage, and the outward tail currents that followed them on the repolarizations to –40 mV, identify them as slowly-activating delayed-rectifying K^+ currents, i.e., I_{Ks} (Sanguinetti & Jurkiewicz, 1990; Jones *et al.*, 1998). When end-of-pulse current amplitude is plotted against pulse voltage, it is I_{Ks} amplitude that forms the rightmost ascending limb of the I-V relation in Figure 1B. Aside from the ascending limb contributed by I_{Ks}, the relation has a pronounced inwardly-rectifying shape that is contributed almost exclusively by I_{K1} between −10 mV and −100 mV (as in Figure 1B), as well as by I_{K1} at more negative potentials (see Figure 1C). The major reason for the predominance of I_{K1} at negative potentials in guinea-pig ventricular myocytes is that it is a relatively large current; by comparison, the amplitudes of basal Cl^- current (I_{Cl}) and background Na^+ current are negligible (e.g., Matsuda & Noma, 1984).

3.1.2. Effects Of Classical I_{K1} Blockers Ba^{2+} And Cs^+

As noted above, in the absence of I_{Na} and $I_{Ca,L}$ the predominant current at potentials negative to −10 mV in guinea-pig ventricular myocytes is I_{K1}. One way of showing this is to record currents at such potentials, and then apply I_{K1}-blocker Ba^{2+}. In an experiment on a representative myocyte, 1 mM Cd^{2+} was used to block I_{Na} and $I_{Ca,L}$, 3 μM E4031 to block I_{Kr}, and 30 μM chromanol 293B to inhibit any I_{Ks}. The myocyte was held at −85 mV and pulsed for 500 ms to more positive and negative potentials at 0.1 Hz. The families of currents in Figure 2A were elicited by pulses to potentials between −100 and

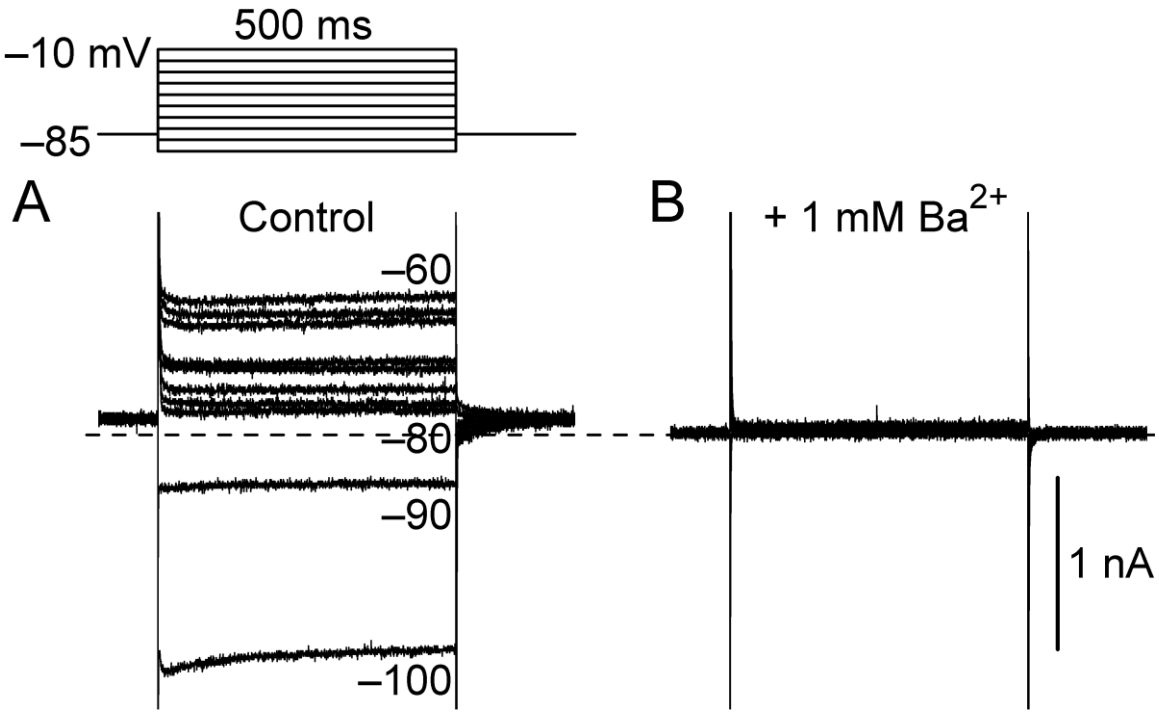

Figure 2. Effects of 1 mM Ba^{2+} on membrane currents. The myocyte was bathed with 5.4-mM K^+ Na^+ solution that contained 1 mM Cd^{2+}, 3 μM E4031, and 30 μM chromanol 293B, and pulsed from −85 mV to other potentials at 0.1 Hz. **A,B.** Records obtained before (Control) (A) and 5 min after addition of 1 mM Ba^{2+} (B). The dashed line indicates the zero-current level.

−10 mV before (control) and 5 min after application of 1 mM Ba^{2+}. The records indicate that Ba^{2+} inhibited almost all of the control current.

Like Ba^{2+}, external Cs^+ is a classical blocker of I_{K1} in cardiac ventricular preparations (Trautwein & McDonald 1978; Harwey & Ten Eick, 1988). To evaluate its action on I_{K1} in guinea-pig ventricular myocytes, myocytes superfused with 5.4-mM K^+ $NMDG^+$ solution were held at −85 mV and pulsed with 500-ms steps at 0.1 Hz for determination of end-of-pulse I-V relations just before and 6-8 min after switching to solution that contained Cs^+ (equimolar replacement of $NMDG^+$). The I-V relations obtained in representative experiments with 2 and 10 mM Cs^+ indicate that the inhibition of I_{K1} was dependent on the concentration of the blocker, and that the degree of inhibition increased with negative test potential (Figure 3A,B). For reasons that will be apparent at a later point in relation to myocytes dialyzed with low-K^+ pipette solution, it was of value to determine the IC_{50} at −60 mV in myocytes dialyzed with standard pipette solution. Earlier findings of interest include the following (i) 5 mM Cs^+ had no significant effect on I_{K1} at −60 mV in guinea-pig (Tourneur *et al.*, 1987) and cat (Harvey & Ten Eick, 1988) myocytes, and (ii) 10 mM Cs^+ reduced I_{K1} at −60 mV by ≈ 55% in bovine papillary muscle (Trautwein & McDonald, 1978). Myocytes were treated with a single concentration of Cs^+ ranging from 0.1 to 100 mM, and the amplitude of current at −60 mV during steady-state Cs^+ action was expressed as a percentage of pre-Cs^+ control amplitude. As indicated by the curve in Figure 3C, the data are well described by the Hill equation with an IC_{50} of 7.5 ± 0.3 mM and a coefficient of 1.13 ± 0.04.

3.1.3. Modulation By External K^+

A hallmark property of I_{K1} in cardiac preparations is that it is modulated by external K^+ (K^+_o). An increase in K^+_o not only shifts the reversal potential (E_{rev}) of I_{K1} to a more

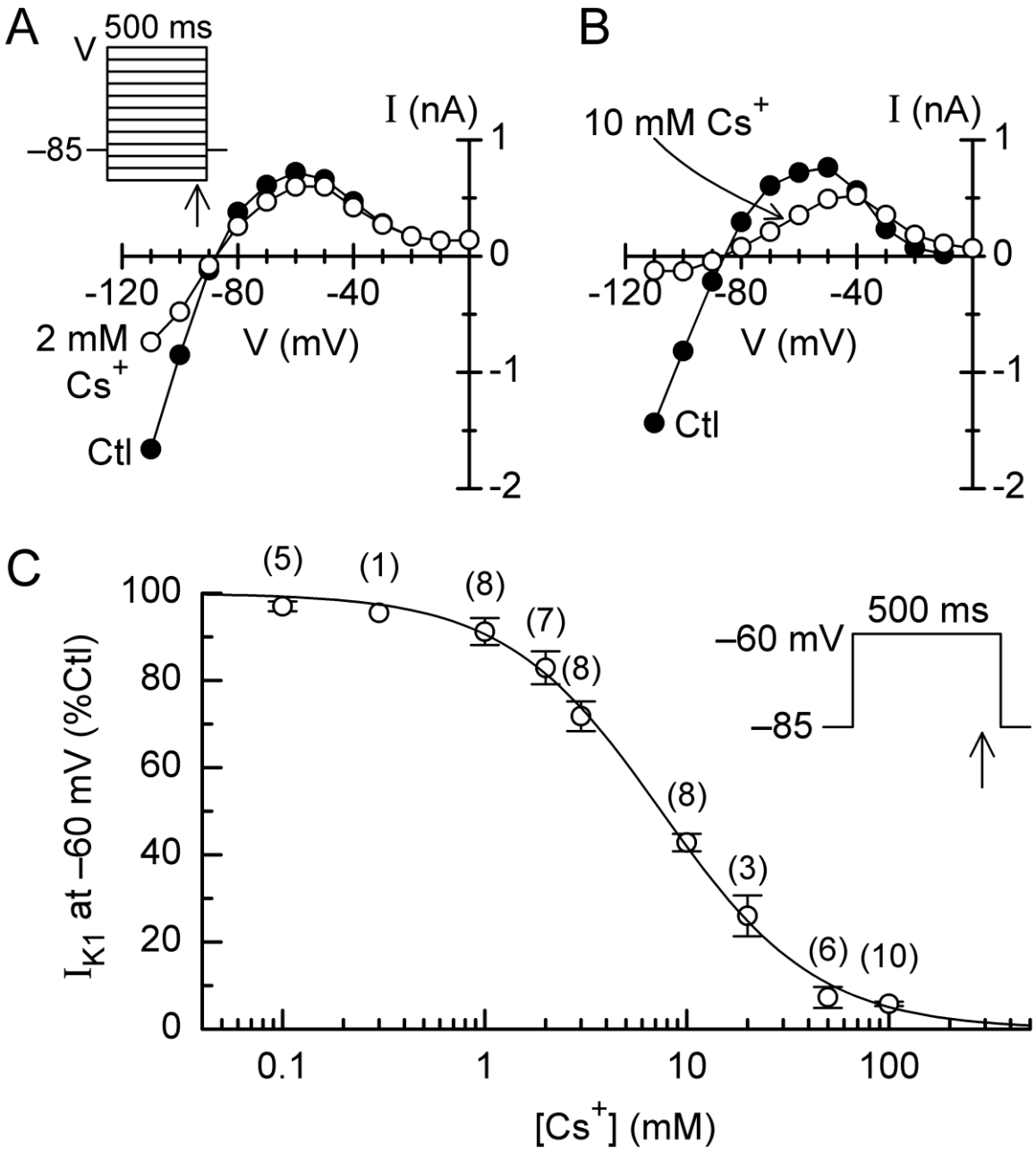

Figure 3. Inhibition of I_{K1} by Cs^+. Myocytes superfused with 5.4-mM K^+ $NMDG^+$ solution that contained 1 mM Cd^{2+} and 5 μM E4031 were held at −85 mV and pulsed to other potentials for 500 ms at 0.1 Hz before (Ctl) and ≈ 7 min after switching to ($NMDG^+$-substituted) Cs^+ solution. **A,B.** Inhibition in myocytes treated with 2 mM Cs^+ (A) and 10 mM Cs^+ (B). **C.** Dependence of inhibition at −60 mV on the concentration of Cs^+. Current amplitudes measured at the ends of Cs^+ treatments were expressed as percentages of amplitudes before treatments (Ctl). The Hill equation fitting the data has an IC_{50} of 7.5 ± 0.3 mM and a coefficient of 1.13 ± 0.04. Number of myocytes in parentheses.

positive potential, it also increases the amplitude of current at given driving forces negative to and positive to E_{rev} (e.g., Dudel *et al.*, 1967; Trautwein & McDonald, 1978). A decrease in K^+_o has the opposite effects of an increase (e.g., Isenberg & Klöckner, 1982), and full removal of K^+_o more or less completely shuts off the current (e.g., Matsuda & Noma, 1984; Backx & Marban, 1993).

The foregoing features of modulation of I_{K1} by K^+_o were observed in the guinea-pig ventricular myocytes investigated in the present study, and two examples of modulation are illustrated in Figure 4. In the first of these, the I-V relation obtained after raising K^+_o to 17.1 mM from 5.4 mM had an E_{rev} that is shifted to a more positive potential, as well as an increased inward and outward current (Figure 4A). The shift in E_{rev} was +30 mV in the example experiment, and +32 mV in an additional one (not shown). Thus, the shift in E_{rev} was close to that expected for a purely-K^+ current (which, based on calculations using the Nernst equation, is $-61 \log (5.4/17.1)$, or + 30.5 mV).

The second example of modulation of I_{K1} by K^+_o is provided by the effect of removing external K^+ in a representative experiment. The myocyte was held at –85 mV and pulsed to –50 mV for measurement of the amplitude of outward I_{K1} at that potential before, during, and after replacement of 5.4-mM K^+ bathing solution by 0-mM K^+ solution. As indicated by the time course of I_{K1} amplitude in Figure 4B, the admission of 0-mM K^+ solution rapidly reduced the amplitude of the current from ≈ 580 pA to ≈ 20 pA, and re-admission of 5.4-mM K^+ solution restored it to its original level.

3.1.4. Stability Of I_{K1}

The full recovery of the current in the experiment with 0-mM K^+ bathing solution (Figure 4B) provides an example of the stability of I_{K1} in the myocytes investigated in the present study. An examination of the stability was conducted by measuring the amplitude

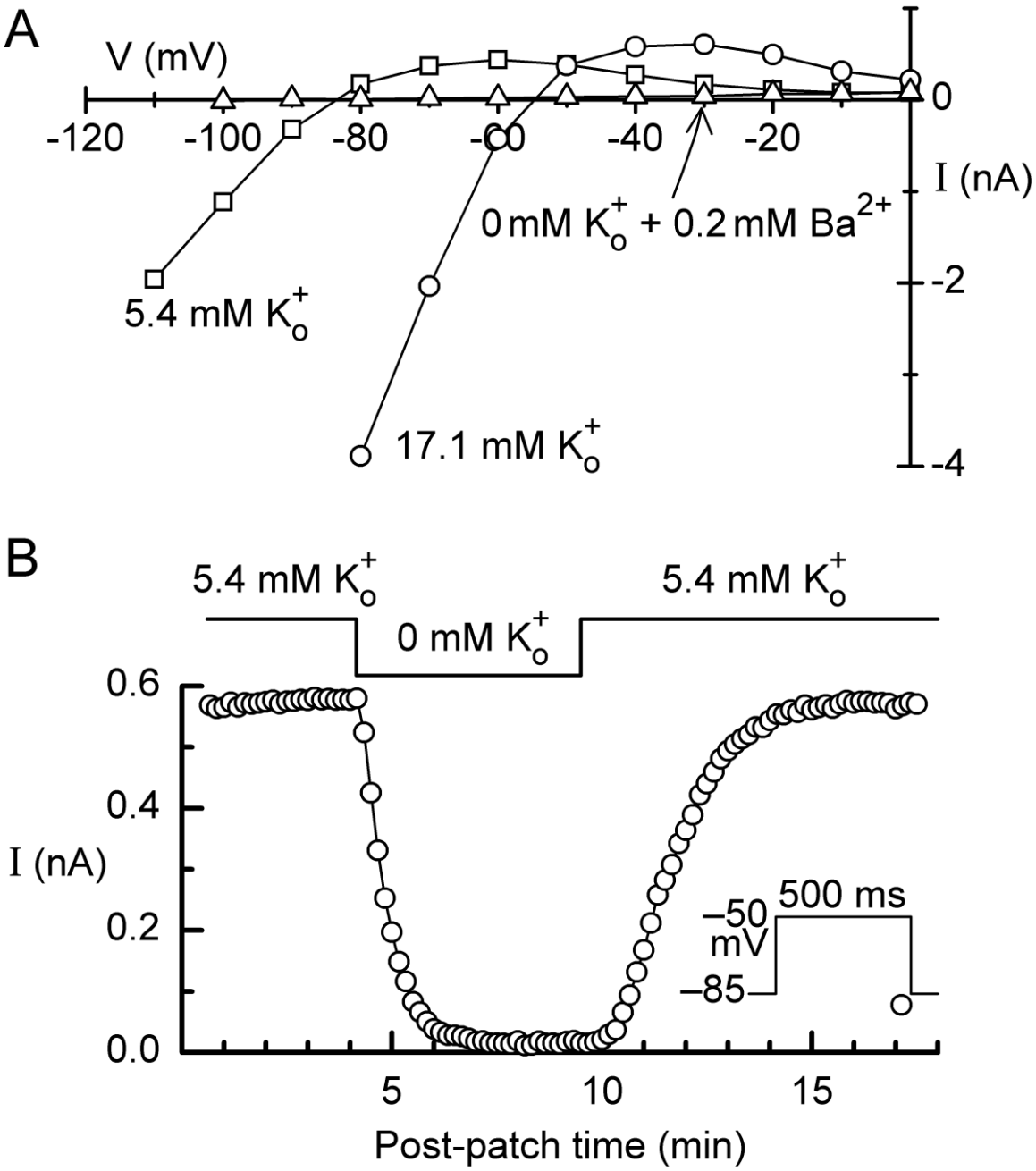

Figure 4. Modulation of I_{K1} by external K^+. The myocytes were bathed with $NMDG^+$ solution that contained 1 mM Cd^{2+}, 3 μM E 4031, and 30 μM chromanol 293B. **A**. Effects of increasing external K^+ (K^+_o) from 5.4 to 17.1 mM. The myocyte was held at −85 mV for the 5.4-mM determination, and then at −55 mV for the 17.1-mM determination ≈ 5 min later. Data points indicate the end-of-pulse amplitudes of currents elicited by 500-ms pulses applied at 0.1 Hz. **B.** Shut-down of I_{K1} (−50 mV) upon replacement of 5.4-mM K^+ solution by 0-mM K^+ solution.

of outward I_{K1} at −50 mV in control experiments that lasted for at least 30 min. The myocytes were bathed with 5.4-mM K^+ $NMDG^+$ solution that contained 1 mM Cd^{2+} and 3 μM E4031, held at −85 mV, and pulsed to −50 mV. The result obtained in one such experiment is shown in the time plot of Figure 5A, and the overall result from twenty-two experiments conducted over a period of several months is shown in Figure 5B. In the latter experiments, the amplitude of the current measured 30 min after patch-breakthrough was 97 ± 2% of the amplitude measured 1 min after patch breakthrough.

The data in Figure 5 notwithstanding, there were experiments in which there were marked rundowns in I_{K1}. This behaviour was generally evident during the first five minutes after patch-breakthrough, and these experiments were terminated.

3.2. MODULATION OF I_{K1} BY LOWERING EXTERNAL K^+

An objective of the present study was to quantify the effects of lowering K^+_o from 5.4 to 2, 1, and 0 mM on parameters that characterize I_{K1}-V relations in myocytes dialyzed with 140-mM K^+ pipette solution. These parameters included E_{rev}, maximal slope of the inward limb of the relation (slopeG_{K1}max), maximal amplitude of outward $I_{K1,}$ and voltage of maximal (peak) outward I_{K1}. The results of experiments related to this objective are detailed in Section 3.2.1 below. It turned out that the configurations of currents elicited by hyperpolarizing pulses applied to myocytes bathed with 0-mM K^+ $NMDG^+$ solution were both novel and unusual. It also turned out that steady-state I_{K1} was distinctly outward over a wide voltage range when myocytes were superfused with 0-mM K^+ $NMDG^+$ solution. As a first step in the investigation of the latter findings, it was important to evaluate the degree to which they were reversible. This evaluation is described in Section 3.2.2 below.

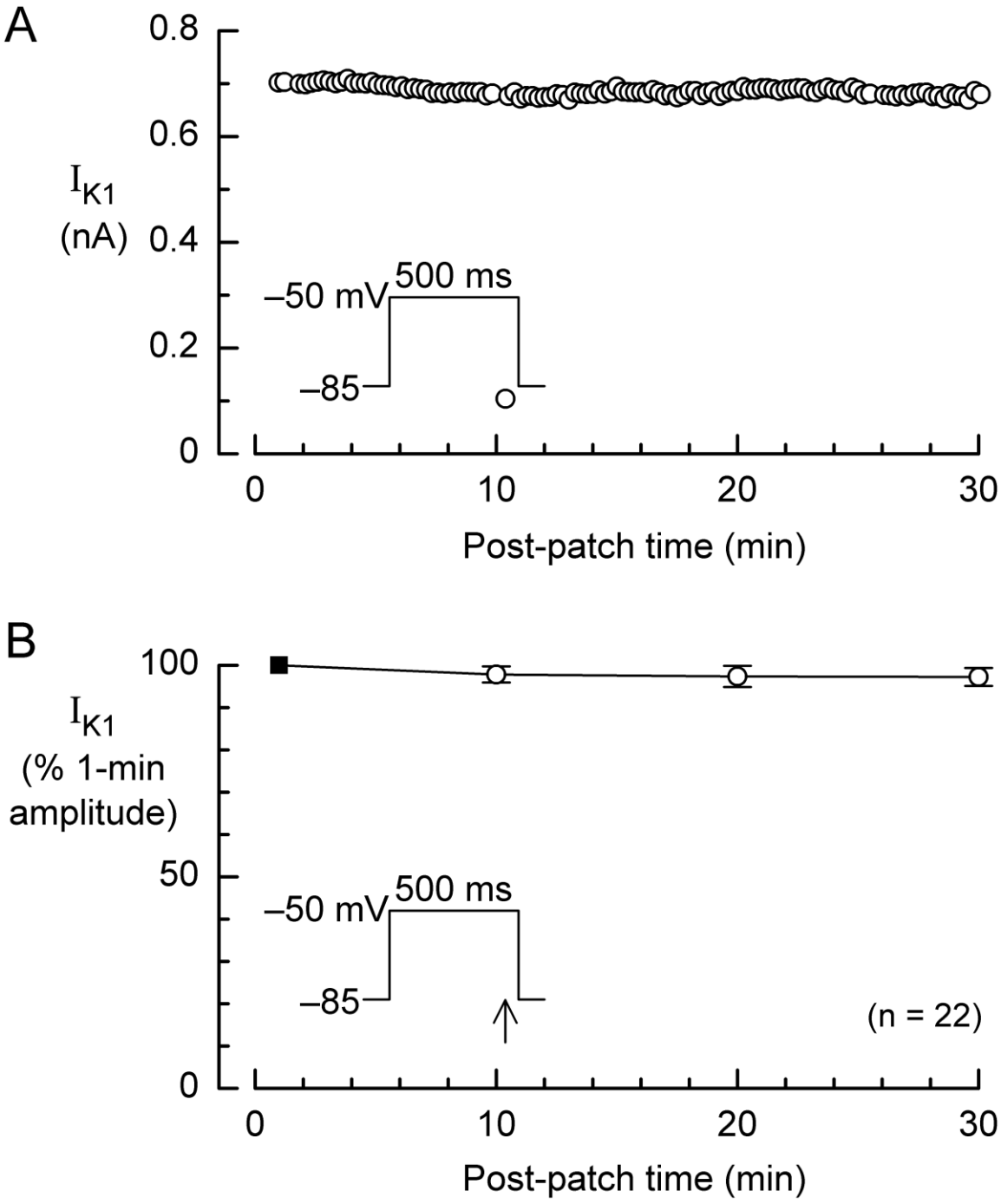

Figure 5. Stability of outward I_{K1} elicited at −50 mV. The myocytes were bathed with 5.4-mM K^+ $NMDG^+$ solution that contained 1 mM Cd^{2+} and 3 μM E4031. **A.** Data from a representative experiment. **B.** Data from experiments on twenty-two myocytes.

3.2.1. Effects Of Lowering K^+_o From Standard 5.4 mM

In these experiments, myocytes were equilibrated with 5.4-mM K^+ solution for ≈ 10 min, and end-of-pulse I-V relations were determined using 500-ms pulses from holding potential −85 mV to other potentials. Thereafter, K^+_o was lowered from 5.4 mM to 2, 1, or 0 mM, and the test I-V relation determined 5-10 min later. In general, a further I-V relation was determined after subsequent addition of Ba^{2+} to null I_{K1}. The principal external cation was $NMDG^+$ except where otherwise noted.

Lowering K^+_o to 2 mM. I-V relations obtained from a myocyte sequentially superfused with 5.4-mM K^+ solution, 2-mM K^+ solution, and 2-mM K^+ solution that contained 3 mM Ba^{2+} are shown in Figure 6A. Compared to the I-V relation obtained during superfusion with 5.4-mM K^+ solution, the one obtained during superfusion with 2-mM K^+ solution was shifted by ≈ −25 mV, and slopeG_{K1}max was reduced by 32%. The maximum amplitude of outward I_{K1} was smaller than that in the 5.4-mM K^+ relation, and occurred at a voltage that was 25-30 mV negative to that in the 5.4-mM K^+ relation.

A summary of the results obtained from seven myocytes is provided in Figure 6B. As expected from the high K^+ selectivity of K1 channels, lowering K^+_o from 5.4 mM to 2 mM had a marked effect on the E_{rev} of I_{K1}. The E_{rev} was −85.4 ± 1.3 mV during superfusion with 5.4-mM K^+ solution, and −111.4 ± 1.9 mV during superfusion with 2-mM K^+ solution ($P < 0.001$). These E_{rev} values are similar to the E_K values of −86 and −112.6 mV for 5.4 and 2 mM K^+_o, respectively, calculated on the basis that the concentration of K^+ in the cytoplasm was the same as that in the pipette solution. The negative shift in E_{rev} was accompanied by a negative shift in the voltage at which outward I_{K1} reached maximal amplitude; the latter was −54.9 ± 2.0 mV in 5.4-mM K^+ solution, and −83.3 ± 2.8 mV in 2-mM K^+ solution ($P < 0.001$). SlopeG_{K1}max declined to 68.2 ± 3.5 % of that determined during superfusion with 5.4-mM K^+ solution ($P < 0.001$),

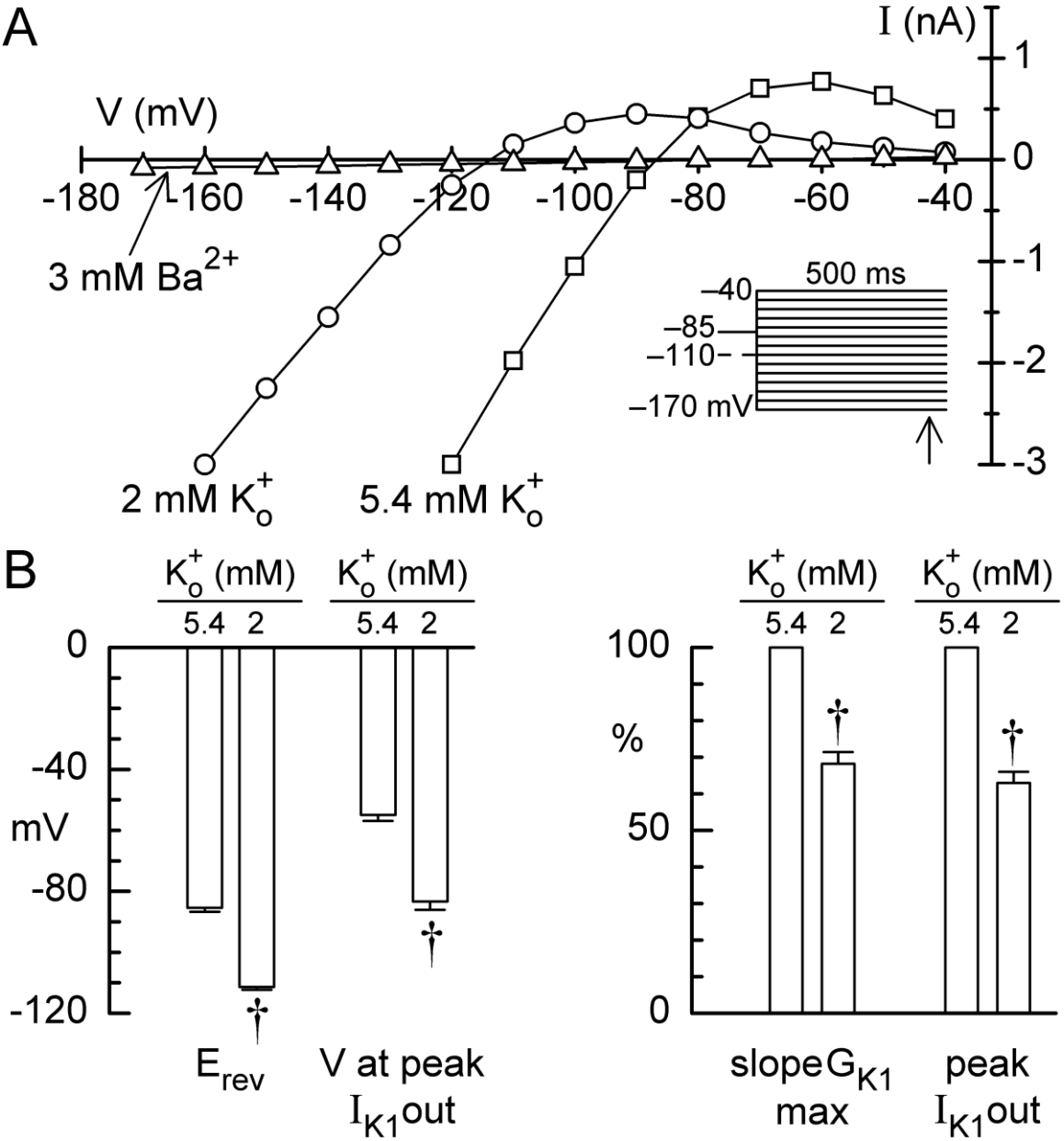

Figure 6. Effects of lowering K^+_o from 5.4 to 2 mM on steady-state I_{K1} parameters. The myocytes were sequentially bathed with $NMDG^+$ solutions that contained 5.4 mM K^+, 2 mM K^+, and 2 mM K^+ + 3 mM Ba^{2+}. I-V relations were determined at the end of each 7-min superfusion by using 500-ms pulses applied at 0.1 Hz from holding potential –85 mV (5.4 mM K^+) or –105 mV (2 mM K^+, Ba^{2+}). **A.** I-V relations from one of the experiments. **B.** Summary of data from seven experiments. Values in each experiment were determined after subtraction of Ba^{2+} data from 5.4-mM K^+ and 2-mM K^+ data. Left: effects of K^+_o on E_{rev} and the voltage at peak outward I_{K1}. Right: relative magnitudes of slopeG_{K1}max and peak outward I_{K1}. † $P < 0.001$, paired *t* test.

a degree of decline close to that predicted by a dependence of slopeG_{K1}max on the square root of external K^+ concentration (61%). In the outward current region of the I-V, the maximal amplitude of I_{K1} during superfusion of 2-mM K^+ solution was 63.0 ± 3.1% of that measured in the presence of 5.4-mM K^+ solution ($P < 0.001$).

Lowering K^+_o to 1 mM. I-V relations obtained from a myocyte sequentially superfused with 5.4-mM K^+ solution, 1-mM K^+ solution, and 1-mM K^+ solution that contained 3 mM Ba^{2+} are shown in Figure 7A. Compared to the I-V relation determined during the superfusion with 5.4-mM K^+ solution, the relation determined during the superfusion with 1-mM K^+ solution was shifted by about –45 mV and diminished in amplitude both below and above the zero-current voltage level. The lowering of K^+_o reduced slopeG_{K1}max by about two-thirds, and reduced the maximal amplitude of the outward current by about the same extent.

A summary of the results obtained from seven myocytes is shown in Figure 7B. Decreasing K^+_o from 5.4 to 1 mM shifted E_{rev} from –84.1 ± 1.1 mV to –129.1 ± 0.9 mV ($P < 0.001$). The latter value is close to the calculated E_K value of –130.9 mV. The negative shift in E_{rev} was accompanied by a negative shift in the voltage at which outward I_{K1} reached its maximal amplitude. The voltages at maximal amplitude were –58.3 ± 1.9 mV (5.4 mM K^+_o) and –98.3± 2.8 mV (1 mM K^+_o) ($P < 0.001$).

Lowering K^+_o to 1 mM decreased slopeG_{K1}max to 42.7 ± 5.7% of that measured in control 5.4-mM K^+ solution ($P < 0.001$) (Figure 7B). Although the extent of this decline was very close to the 43% decline predicted by a dependence of slopeG_{K1}max on the square root of external K^+ concentration, it is possible that it was overestimated to some degree because the 1-mM K^+_o slope may have been steeper over a more negative voltage range than over the one that was actually used (–150 to –140 mV). In line with the

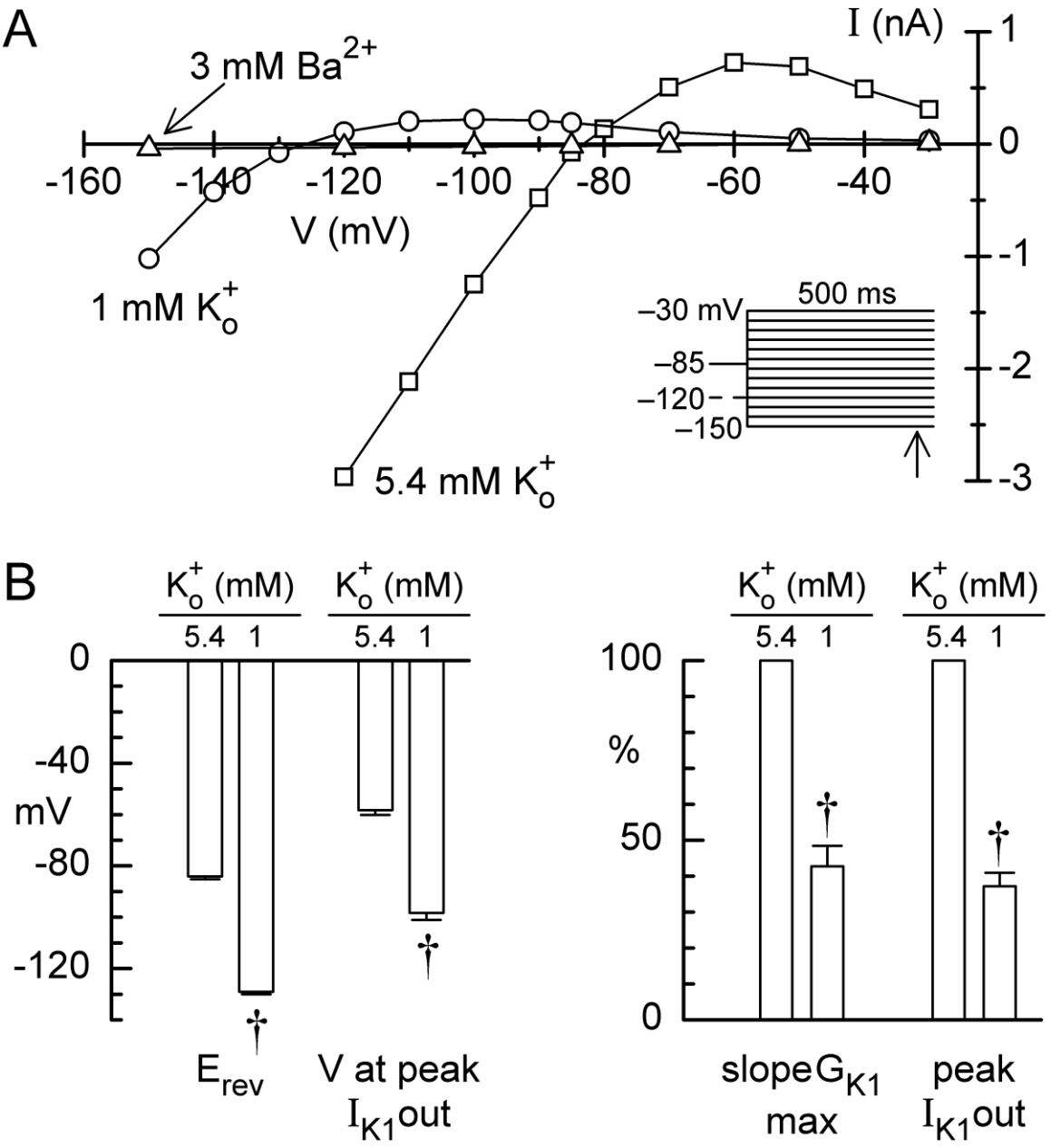

Figure 7. Effects of lowering K^+_o from 5.4 to 1 mM on steady-state I_{K1} parameters. The myocytes were sequentially bathed with $NMDG^+$ solutions that contained 5.4 mM K^+, 1 mM K^+, and 1 mM K^+ + 3 mM Ba^{2+}, and I-V relations were determined at the end of each 7-min superfusion using 500-ms pulses applied at 0.1 Hz from holding potential −85 mV (5.4 mM K^+_o) or −120 mV (1 mM K^+_o, 1 mM K^+_o + Ba^{2+}). **A.** I-V relations from one of the experiments. **B.** Summary of data from seven experiments. Values in each experiment were determined after subtraction of Ba^{2+} data from 5.4-mM K^+_o and 1-mM K^+_o data. Left: effect of K^+_o on E_{rev} and the voltage at peak outward I_{K1}. Right: relative magnitudes of slopeG_{K1}max and peak outward I_{K1}. † $P < 0.001$, paired *t* test.

decline in slopeG_{K1}max, the maximal amplitude of the outward current was reduced to 37.2 ± 3.7% of its 5.4-mM K^+ amplitude ($P < 0.001$) (Figure 7B).

Inter-relationships and dependencies. It was of interest to take the data collected in the experiments on lowering K^+_o to 2 and 1 mM and examine how certain parameters might relate to others, and how certain parameters varied with K^+_o. Figure 8 shows plots of E_{rev} versus log K^+_o, V_{peak} versus E_{rev}, slopeG_{K1}max versus log K^+_o, and maximal amplitude of outward current versus log K^+_o. The slope of the straight line describing the dependence of E_{rev} on K^+_o has a near-Nernstian value of 61.3 ± 5.1 mV (Figure 8A), and the slope of the straight line fitted to the relation between V_{peak} and E_{rev} has a value of 0.95 ± 0.06 (Figure 8B). The relation between log slopeG_{K1}max and log K^+_o is well-fitted by a straight line with slope 0.47 ± 0.07 (Figure 8C), whereas the relation between the log of the maximal amplitude of outward current (I_{peak}) and log K^+_o is well-fitted by a straight line with slope 0.54 ± 0.07 (Figure 8D).

Lowering K^+_o to 0 mM. A large number of experiments was conducted on myocytes that were superfused with 5.4-mM K^+ $NMDG^+$ solution and then with 0-mM K^+ $NMDG^+$ solution. The effects of lowering K^+_o from 5.4 to 0 mM were surprising. In particular, hyperpolarizing pulses from holding potential −85 mV elicited large inward currents that declined in a time-dependent manner such that end-of-pulse levels were typically small and outward in direction. A detailed investigation of these phenomena is presented in Section 3.3 below.

3.2.2. Reversibility Of Effects Of Lowering K^+_o To 0 mM

Prior to starting on a more detailed investigation of membrane currents in myocytes bathed with K^+-free solution, it was important to examine whether removal of external K^+ has deleterious effects on K1 channels that, for example, could be caused by rapid

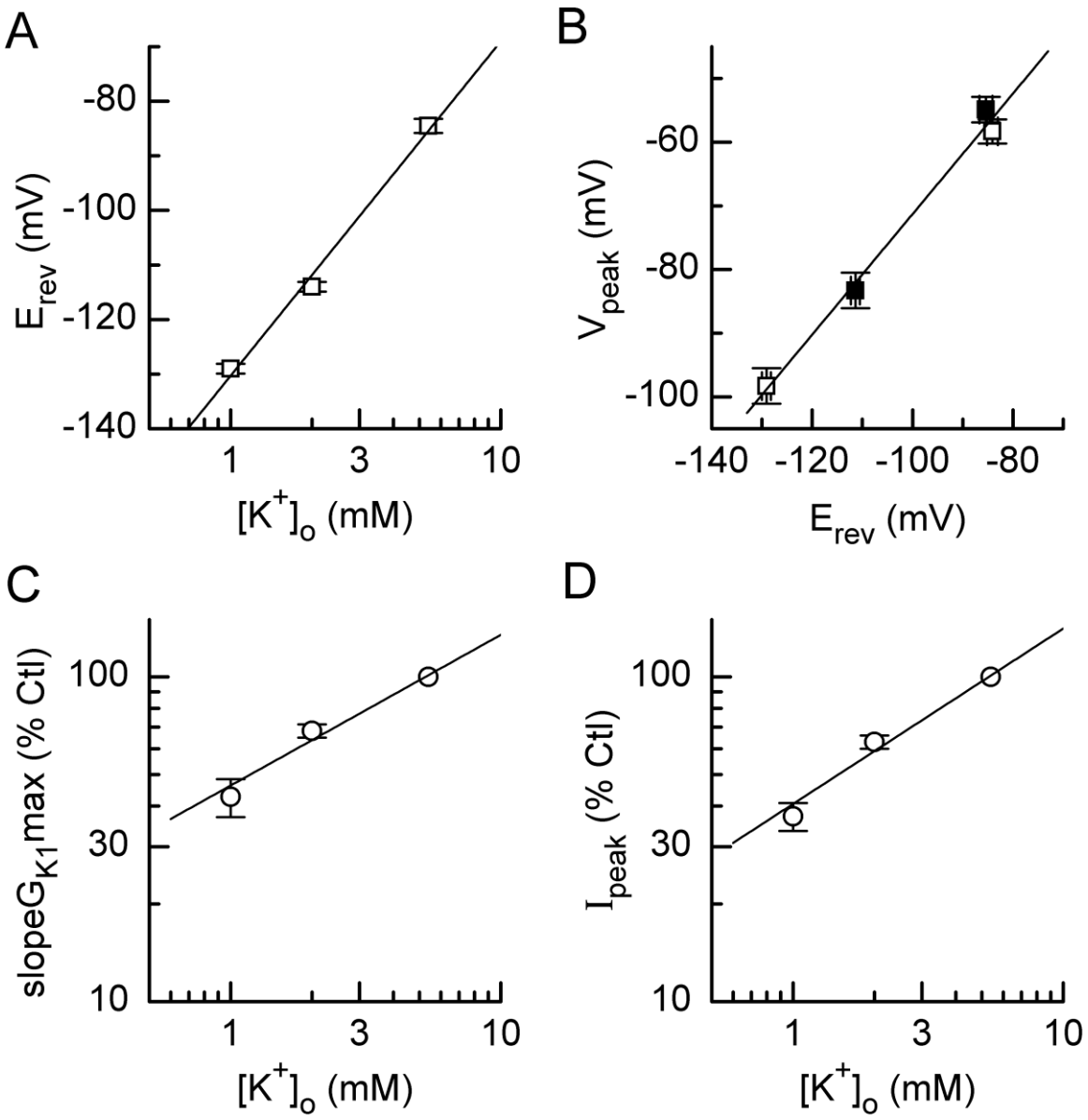

Figure 8. Dependencies of I_{K1} parameters on K^+_o. Same myocytes as in Figures 6 and 7. **A**. E_{rev} versus log K^+_o. The best-fit straight line ($r^2 = 0.986$) is drawn in accord with $E_{rev} = A + B \bullet \log K^+_o$ where A = –130.3 ± 2.4 mV and B is 61.3 ± 5.1 mV. **B.** Voltage at maximum outward current (V_{peak}) versus E_{rev}. The best-fit straight line follows the equation $V_{peak} = A + B \bullet E_{rev}$ where A = 23.4 ± 6.4 mV and B = 0.95 ± 0.06. **C.** Log slopeG_{K1}max versus log K^+_o. The best-fit straight line ($r^2 = 0.980$) follows the equation slopeG_{K1}max (% 5.4-mM control) = $A \bullet (K^+_o)^b$ where A = 46.3 ± 4.5 and slope b = 0.47 ± 0.07. **D.** Log I_{peak} (maximal outward current) versus log K^+_o. The best-fit straight line follows the equation I_{peak} (% 5.4-mM control) = $A \bullet (K^+_o)^b$ where A = 40.6 ± 4.1 and slope b = 0.54 ± 0.07.

deterioration of myocyte health in K^+-free solutions (see Spindler *et al.*, 1998) or by changes in the properties of K1 pores (as observed in some voltage-dependent K^+ channels (Melishchuk *et al.*, 1998; Loboda *et al.*, 2001; Wang *et al.*, 2009)). This examination was performed by measuring the responsiveness of I_{K1} to elevations of K^+_o following prolonged exposures of myocytes to K^+-free solution.

Elevation of K^+_o to 0.1 and 1 mM. Five myocytes were superfused with K^+-free solution for ≈ 15 min, and then superfused with 0.1-mM K^+ solution for ≈ 7 min. The myocytes were held at −85 mV and pulsed with 500-ms steps to more positive and negative potentials near the ends of the two superfusion periods. The amplitudes of the end-of-pulse currents recorded from one of these myocytes are shown in Figure 9. They indicate that the introduction of the K^+-containing solution resulted in perceptible increases in outward current amplitude at voltages between −100 and −150 mV, but had little or no effect on outward current amplitude at voltages between −90 and −20 mV. In the five experiments of this type, the 0.1-mM K^+ solution increased the amplitude of the current at −130 mV by 22 ± 8 pA, but only increased that at −85 mV by 4 ± 3 pA.

Four myocytes were bathed with K^+-free solution for 15 min and then bathed with 1-mM K^+ solution for 5 min. The myocytes were held at −85 mV and pulsed to −140 mV at 0.05 Hz. The amplitudes of the currents at these two potentials at the end of the K^+-free exposures were +59 ± 18 and +73 ± 23 pA, respectively, whereas the amplitudes at the end of the reactivation period with 1 mM K^+ were +234 ± 33 and −489 ± 59 pA, respectively. The latter values are similar to those measured in experiments in which K^+_o was lowered from 5.4 to 1 mM (see Figure 7A above).

Elevation of K^+_o to 5.4 mM. Myocytes were exposed to K^+-free solution for a lengthy period, and tested for response to elevation of K^+_o. Examples of time courses of

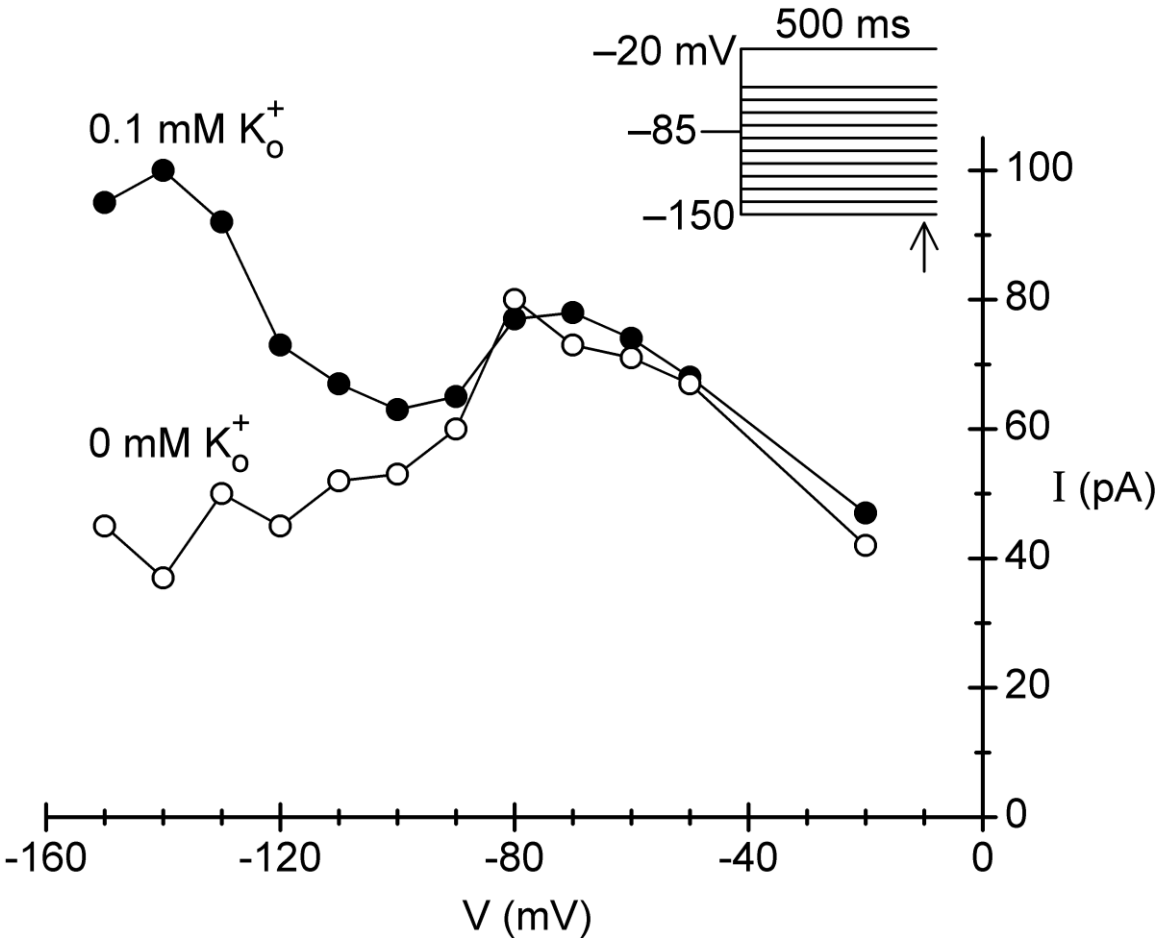

Figure 9. Effects of raising K^+_o from 0 mM to 0.1 mM. The myocyte was bathed with K^+-free $NMDG^+$ solution for ≈ 15 min, and then with 0.1-mM K^+ $NMDG^+$ solution for ≈ 7 min. The holding potential was –85 mV, and pulses to other potentials were applied for 500 ms at 0.1 Hz just before and at the end of the superfusion with 0.1-mM K^+ solution.

current amplitudes monitored at various potentials in myocytes undergoing this protocol are shown in Figure 10. In the first example, currents monitored at –55, –85, and –100 mV responded to admission of 5.4-mM K^+ solution after ≈ 30 min exposure to K^+-free solution with large increases in outward and inward current at –55 and –100 mV, respectively, and a small increase in outward current at –85 mV (Figure 10A). These changes, which were fully reversible (Figure 10A), indicate that the test solution caused a robust reactivation of I_{K1}. In the second example, current monitored at –90 mV was small (≈ 50 pA) and outward in direction after a 55-min exposure to K^+-free solution (Figure 10B). It responded to admission of test 5.4-mM K^+ solution with a marked inward-directed excursion.

The degree of recovery of I_{K1} was evaluated by performing I-V determinations on myocytes that were superfused with 5.4-mM K^+ solution for 5-7 min (control), exposed to K^+-free solution for 32.8 ± 1.6 min (n = 5) or 58.8 ± 5.4 min (n = 5), and then superfused with 5.4-mM K^+ solution once again. In all cases, the myocytes responded to the addition of K^+ with a reactivation of I_{K1} such that the test steady-state I-V relation resembled the control steady-state relation. A quantitative measure of the degree of reactivation was obtained by comparing test slopeG_{K1}max with control slopeG_{K1}max. The test value was 91.0 ± 4.1% of the control value in the myocytes exposed to K^+-free solution for ≈ 33 min, and 85.2 ± 10.8% of the control in myocytes exposed for ≈ 59 min. These results, together with those on elevation of K^+_o to 0.1 and 1 mM, suggest that K1 channel function was not unduly affected by relatively long exposures to K^+-free solution.

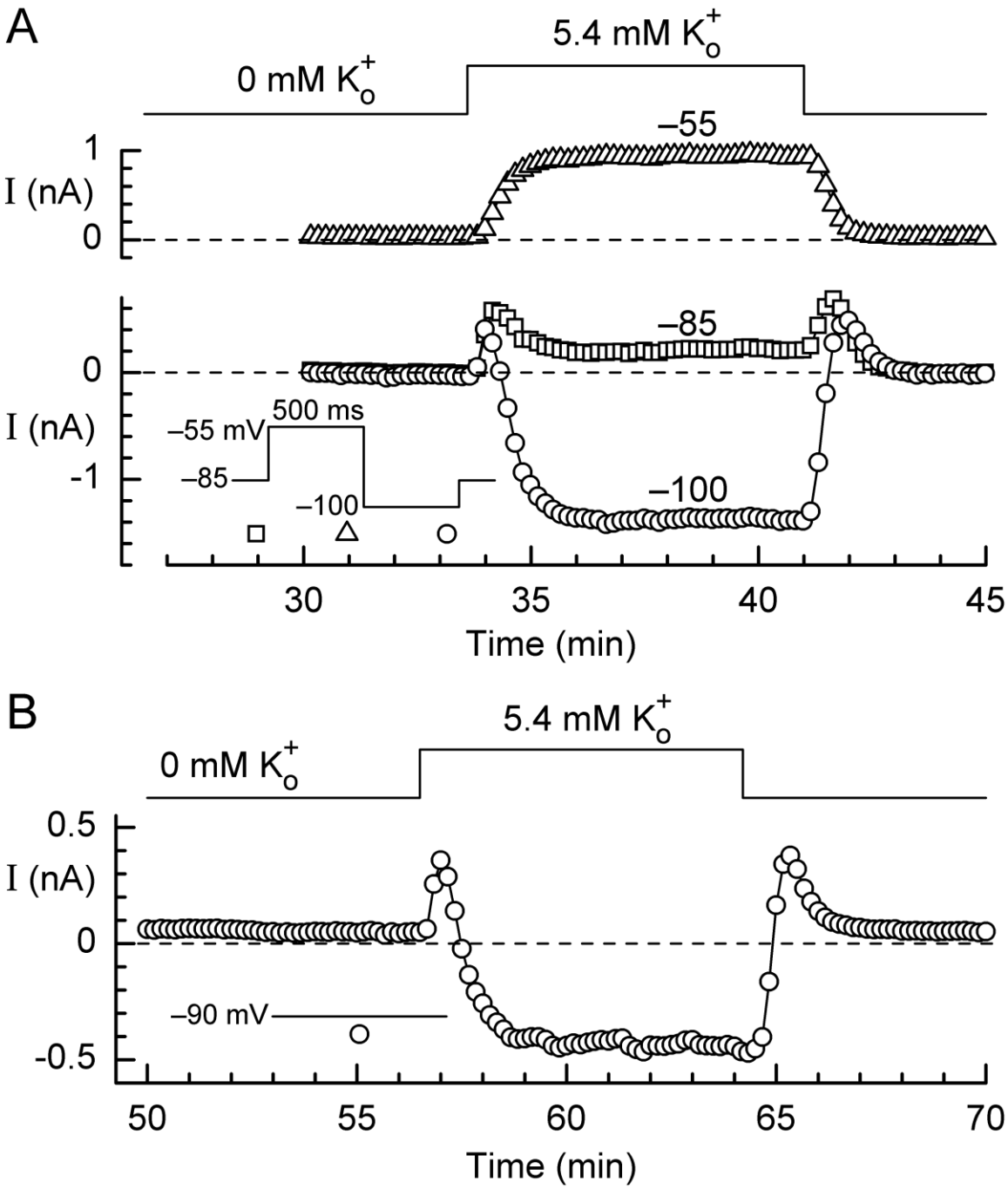

Figure 10. Reactivation of I_{K1} following prolonged superfusions with K^+-free solution. **A,B.** Myocytes were superfused with 0-mM K^+ $NMDG^+$ solution for ≈ 34 min (A) and ≈ 57 min (B), and then superfused with 5.4-mM K^+ $NMDG^+$ solution for ≈ 7 min. The time plots indicate the amplitudes of currents monitored at –55, –85, and –100 mV (A) (see voltage schematic), and at holding potential –90 mV (B).

3.3. I_{K1} IN MYOCYTES BATHED WITH K^+-FREE SOLUTION

A wide range of experiments was performed on myocytes bathed with K^+-free solution to evaluate the contributions of a number of ionic pathways to steady-state outward current at negative potentials and to transient inward currents elicited by hyperpolarizations. The initial task was to determine the extent of possible contributions by non-I_{K1} currents. This was accomplished by conducting experiments on (i) myocytes that were bathed with K^+-free solution in which Na^+ was the principal cation, and (ii) myocytes that were dialyzed with Cs^+ pipette solution instead of standard K^+ pipette solution (Section 3.3.1 below). The results of these experiments led to the hypothesis that both the steady-state outward current and the time-dependent (transient) inward current reflect K^+ movement through K1 channels; more specifically, that the currents reflect the effects of accumulation and depletion of T-tubular K^+ (K^+_T) on the flow of I_{K1} across T-tubular membrane ($I_{K1,T}$). The hypothesis was tested by examining the voltage dependence of the inward transient, the effects of external Ba^{2+}, the dependence of tail current configuration on the preceding hyperpolarization, and the effects of low external Cs^+ (Section 3.3.2 below).

3.3.1. Investigation Of Contributions By Non-I_{K1} Currents

3.3.1.1. Findings On Involvement Of Na^+ Channel Current

There were two reasons for performing experiments aimed at evaluating the possible involvement of Na^+ channel current in the steady-state outward current and time-dependent inward current of myocytes bathed with K^+-free solution. The first was connected with the possibility that a fraction of voltage-dependent Na^+ channels in ventricular myocytes may be constitutively active at hyperpolarized potentials (Zilberter

et al., 1994), and the second with the possibility that withdrawal of external K^+ from myocytes may affect channel selectivity (Wang *et al.*, 2009).

Lack of involvement in steady-state outward current. The first series of experiments was conducted to evaluate the possibility that a major part of the steady-state outward current at negative potentials was due to outward movement of K^+ through Na^+ channels. If there were such outward K^+-carried current, bathing myocytes in K^+-free Na^+ solution rather than K^+-free $NMDG^+$ solution should promote large inward Na^+-carried current that would more than offset outward K^+-carried current. Myocytes were bathed with 5.4-mM K^+ Na^+ solution for ≈ 10 min, and then bathed with K^+-free Na^+ solution for an additional 7 min. The myocytes were held at −80 mV and pulsed to potentials between −110 and 0 mV for 300 ms at 0.1 Hz for determination of quasi-steady-state (end-of-pulse) I-V relations near the ends of the two superfusions. The results obtained in one of these experiments are shown in Figure 11A. Neither the 5.4-mM K^+ Na^+ I-V relation nor the K^+-free Na^+ I-V relation was distinguishable from relations determined in experiments with K^+-free $NMDG^+$ solution.

Average quasi-steady-state relations from five experiments with Na^+ solution (Figure 11B) indicate that the effects of removal of external K^+ on myocytes bathed with Na^+ solution were not very different than those observed on myocytes that were bathed with $NMDG^+$ solution. For example, the quasi-steady-state amplitude of the current at −100 mV was +25 ± 38 pA in the Na^+ series (Figure 11B) versus +51 ± 22 pA (n = 6) in a parallel $NMDG^+$ series.

The protocol used in the second series of experiments with Na^+ solution involved patching myocytes coincident with a switch from 5.4-mM K^+ solution to K^+-free solution, and monitoring current amplitude at constant potential −90 mV. The amplitudes

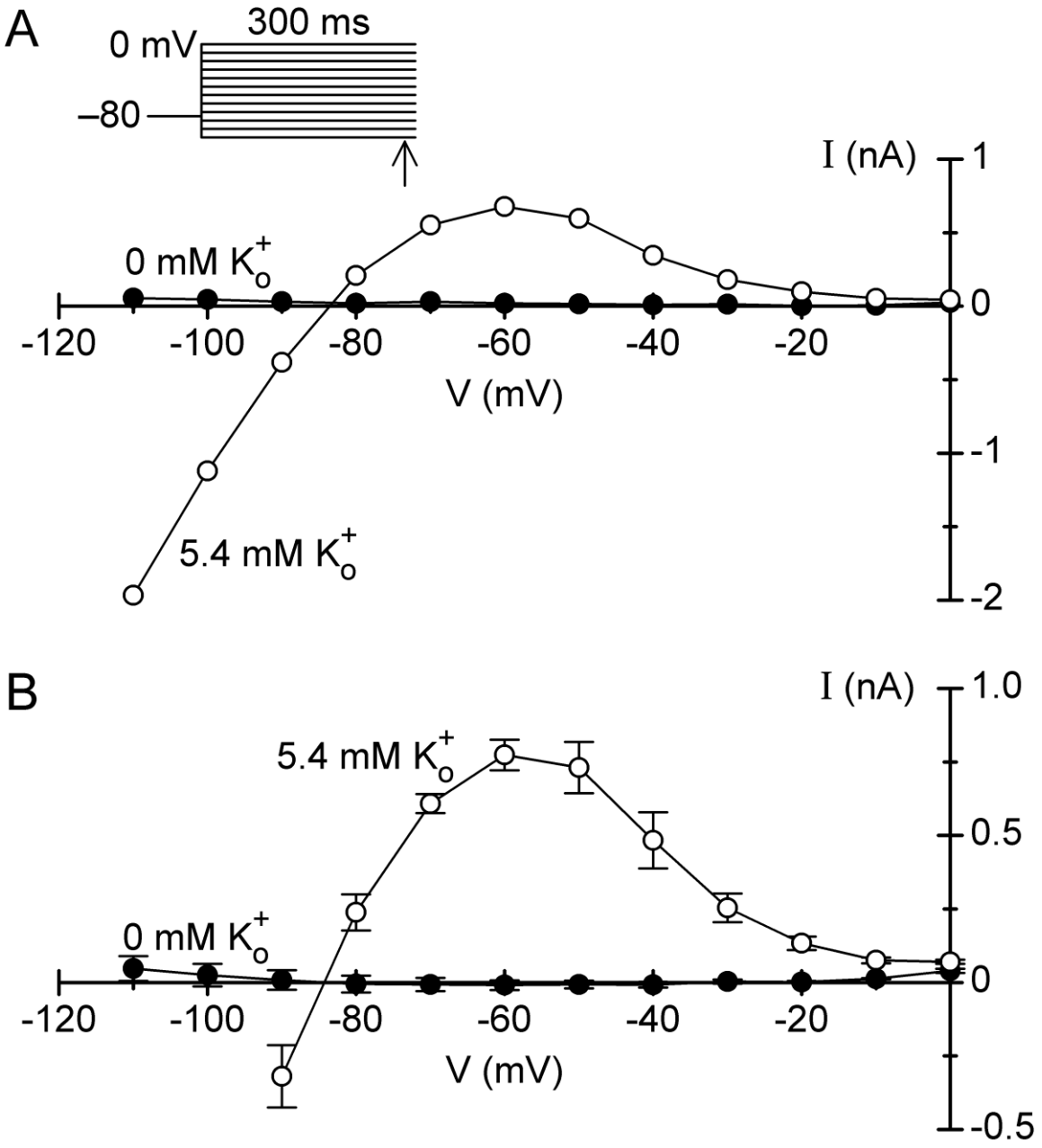

Figure 11. I-V relations obtained from myocytes bathed with K^+-free Na^+ solution. The myocytes were bathed with 5.4-mM K^+ Na^+ solution for ≈ 10 min, and then with 0-mM K^+ Na^+ solution for ≈ 7 min. **A.** I-V relations from an example experiment. **B.** Average of I-V relations from five experiments. Note that the current amplitude scale is different than that in A.

were generally small and stable over prolonged periods of time. When measured at 10 min post-patch-breakthrough, they were between –25 and +25 pA in 26 of the 42 myocytes investigated. In the remaining 16 myocytes, the currents were larger and more often outward than inward. The overall amplitude of the current at –90 mV was +16 ± 5 pA (n = 42) (data not depicted).

Lack of involvement in inward transients. An additional observation in the experiments with K^+-free Na^+ solution was that hyperpolarizing steps to voltages below –90 mV elicited time-dependent inward currents that were similar to those observed in experiments with K^+-free $NMDG^+$ solution. Records of inward transients elicited in a representive myocyte bathed with Na^+ solution are shown in Figure 12A. Both the amplitude and rate of decay of the transient increased with increasing negative voltage in a manner similar to that observed in experiments with $NMDG^+$ solution (see below).

The presence of Na^+ rather than $NMDG^+$ in the bathing solution had little effect on the amplitude of the inward transient. This information was obtained from experiments in which myocytes were bathed in K^+-free $NMDG^+$ solution for 10 min, and then in K^+-free Na^+ solution for another 10 min. The myocytes were hyperpolarized from –85 to –130 mV for 300 ms near the end of each superfusion, and the difference in current amplitude at 15 ms and 290 ms into the pulse was taken as an estimate of the amplitude of the transient. In eleven experiments, the amplitude of the transient during superfusion with Na^+ solution was 99.3 ± 5.6% of that measured during the preceding superfusion with $NMDG^+$ solution (Figure 12B).

3.3.1.2. Lack Of Major Involvement Of Any Non-K^+ Current

As explained below, the results of experiments in which K^+_i was replaced with Cs^+ allow conclusions to be drawn concerning possible contributions by various current types to steady-state outward currents and to hyperpolarization-induced inward transients.

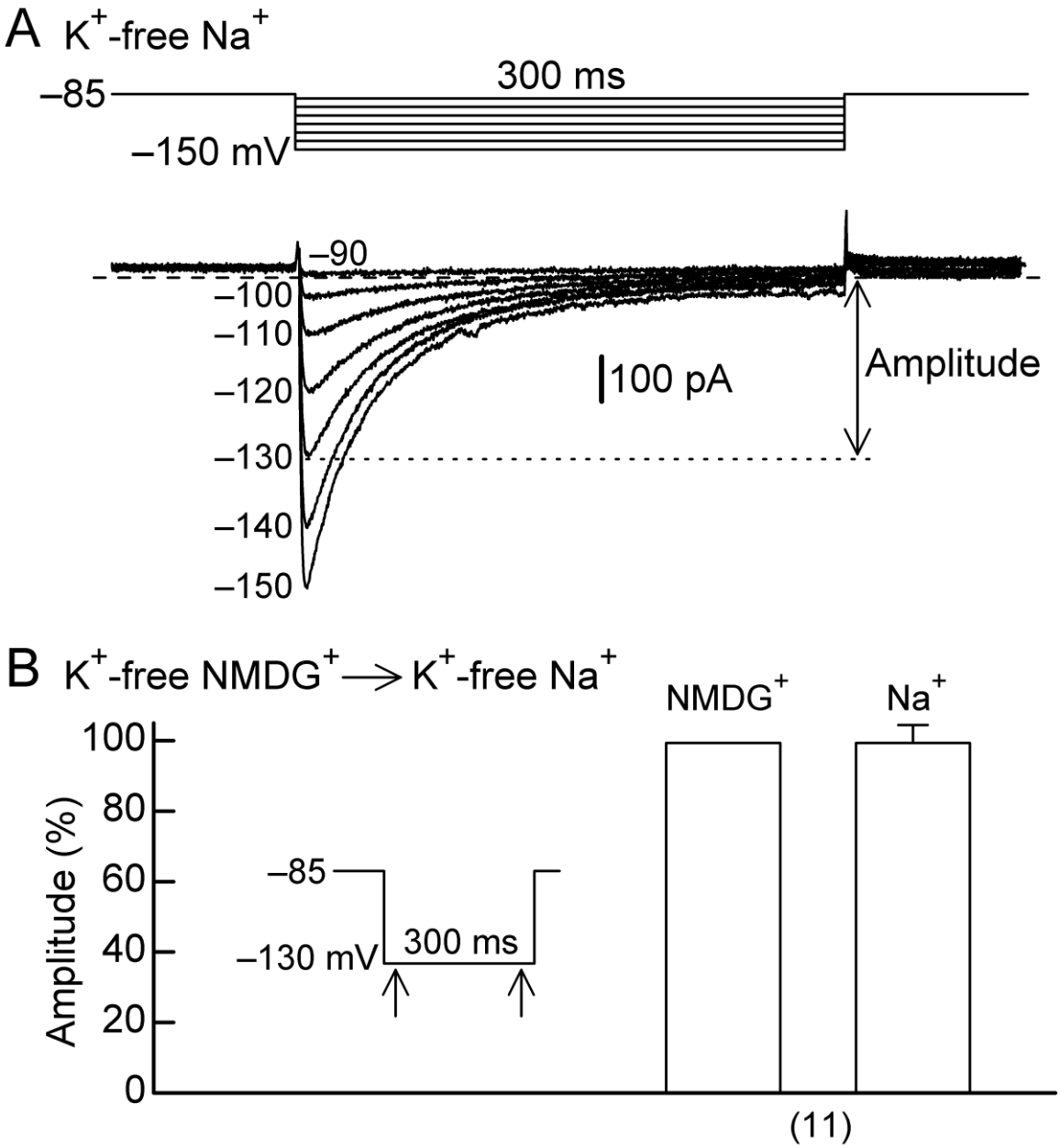

Figure 12. External Na^+ and inward transients in experiments with K^+-free solution. **A**. Records obtained in a representative experiment. The upper dashed line indicates the zero-current level. **B.** Lack of effect of switching from K^+-free $NMDG^+$ solution to K^+-free Na^+ solution on the amplitudes of the inward transients elicited by 300-ms pulses to −130 mV (see panel A and schematic). Number of experiments in parentheses.

Effects of replacement of K^+_i by Cs^+. Myocytes were dialyzed with K^+-free Cs^+ pipette solution to evaluate the effects of replacement of K^+_i by Cs^+. In practice, the results obtained in experiments with Cs^+ pipette solution were compared with those obtained in experiments with K^+ pipette solution. The most obvious difference between them was that hyperpolarizations elicited inward transients in K^+-dialyzed myocytes, but not in Cs^+-dialyzed myocytes (e.g., Figure 13A,B). A second important difference emerged from analysis of currents elicited by 1000-ms pulses to test potentials between −110 and −10 mV. As indicated by the data shown in Figure 13C, the average end-of-pulse I-V relation determined in twenty experiments with Cs^+ pipette solution was more inward-directed than that determined in fifteen experiments with K^+ pipette solution. The difference between the two relations was (i) significant at all voltages between −110 and −30 mV ($P < 0.001$, Tukey-Kramer multiple comparison test), and (ii) larger at voltages below −90 mV than at voltages above it. As a point of reference, the amplitude of the current at −90 mV was −19 ± 3 pA (n = 20) in myocytes dialyzed with Cs^+ pipette solution, and +59 ± 8 pA (n = 15) in those dialyzed with K^+ solution.

The inward shift caused by replacement of K^+_i by Cs^+ appears to rule out the possibility that steady-state outward current was *entirely* due to outward K^+ current through nonselective cation channels because intracellular Cs^+ ions should have moved as easily as intracellular K^+ ions through these channels (Isenberg, 1993; Kiyosue *et al.*, 1993) (see also Section 3.3.2.2 below). Rather, the shift suggests that the steady-state outward current in myocytes dialyzed with K^+ solution was primarily due to outward movement of K^+ through K^+-selective channels. Further, the voltage dependence of the shift indicates that the K^+ channels had inwardly-rectifying I-V relations.

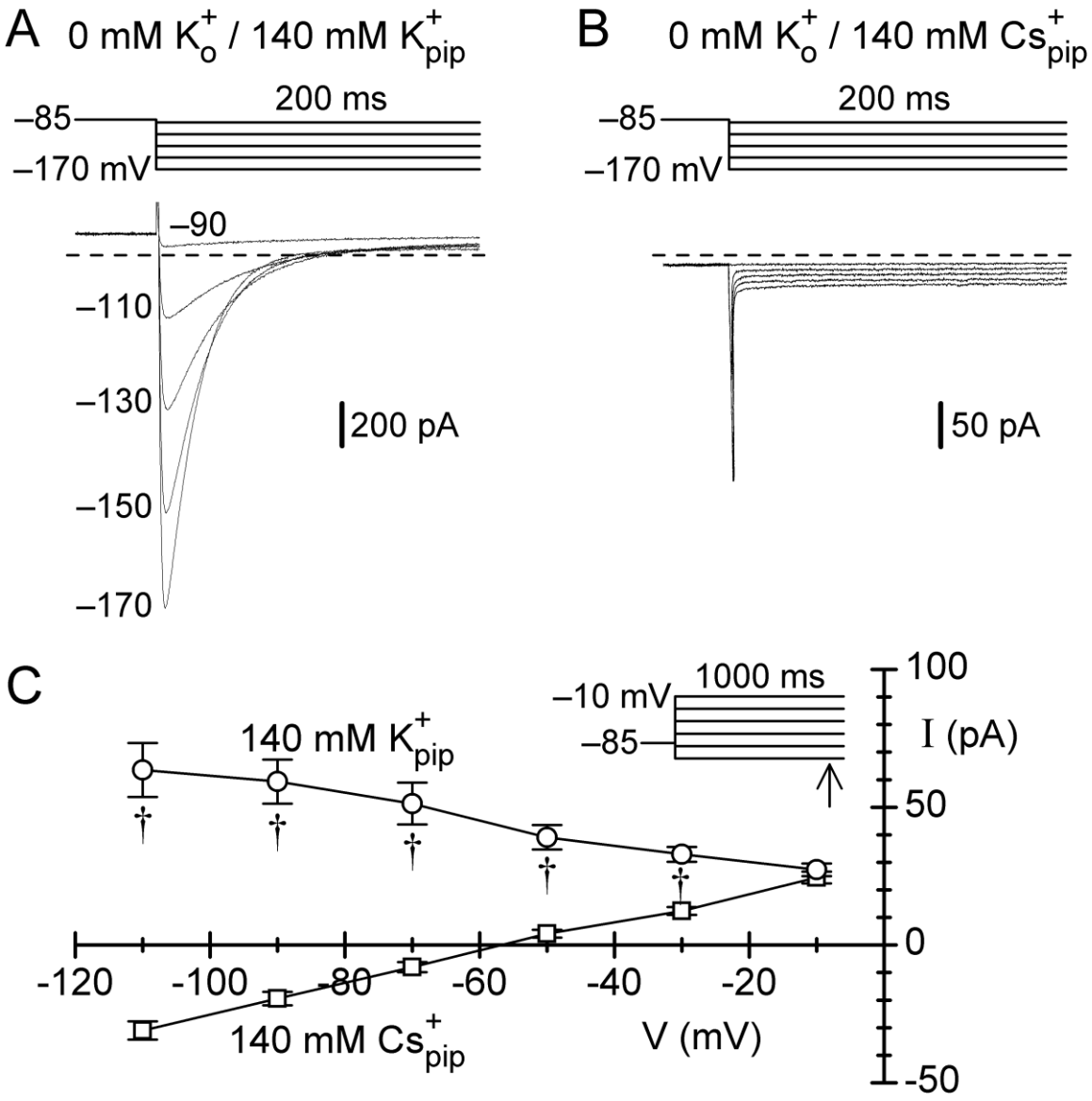

Figure 13. Effects of Cs^+ pipette solution on membrane currents and I-V relations in myocytes bathed with 0-mM K^+ $NMDG^+$ solution. **A,B.** Records of membrane currents elicited by hyperpolarizing steps in representative myocytes dialyzed with K^+ pipette solution (K^+_{pip}) (A) and Cs^+ pipette solution (Cs^+_{pip}) (B). Note the absence of inward transients in B. The dashed lines indicate the zero-current levels. **C.** Average I-V relations obtained from myocytes dialyzed with K^+ solution (n = 15) and myocytes dialyzed with Cs^+ solution (n = 20). Current amplitudes were measured at the ends of 1000-ms pulses applied at 0.1 Hz to potentials between –110 and –10 mV. † $P < 0.001$ (ANOVA, Tukey-Kramer multiple comparison test).

Replacement of K^+_i by Cs^+ eliminated inward transients. This finding rules out participation of Ca^{2+} channel currents in the transients elicited in K^+-dialyzed myocytes. Likewise, it rules out possible contributions by inward currents through non-selective cation channels, and by inward currents through anion channels. In brief, this process of elimination leads to the view that the channel type most likely to be central to the generation of the inward transient is an inwardly-rectifying K^+ channel.

3.3.2. Investigation Of Contributions By I_{K1}

The results of the experiments with external Na^+ solution and internal Cs^+ solutions suggested that steady-state outward current at negative potentials was due to outward movement of K^+ through inwardly-rectifying K^+ channels. It seemed highly likely that these were K1 channels rather than inwardly-rectifying K_{ATP} channels because the latter should have been (i) inactive due to the high concentration of ATP in the pipette solution, and (ii) blocked by the glibenclamide (3-5 μM) present in all bathing solutions. To examine the contributions of I_{K1} to steady-state currents, inward transients, and tail currents, experiments were conducted using external Ba^{2+} and external Cs^+ to block K1 channels.

3.3.2.1. Contribution Of I_{K1} To Holding Current At –85 mV

The level of current in myocytes dialyzed with K^+ pipette solution, bathed with K^+-free $NMDG^+$ solution, and held at −85 mV was measured just before and 5 min after the addition of Ba^{2+} (1-3 mM). Current records from representative experiments indicate that Ba^{2+} abolished the outward holding current (Figure 14). In twenty-two experiments, the level of the current before addition of Ba^{2+} was +53.5 ± 6.8 pA, and the level after addition was −13 ± 2 pA ($P < 0.001$) (Figure 14). It is noteworthy that the magnitude of the current inhibited by Ba^{2+} in these experiments (67 ± 6 pA) is in good agreement with

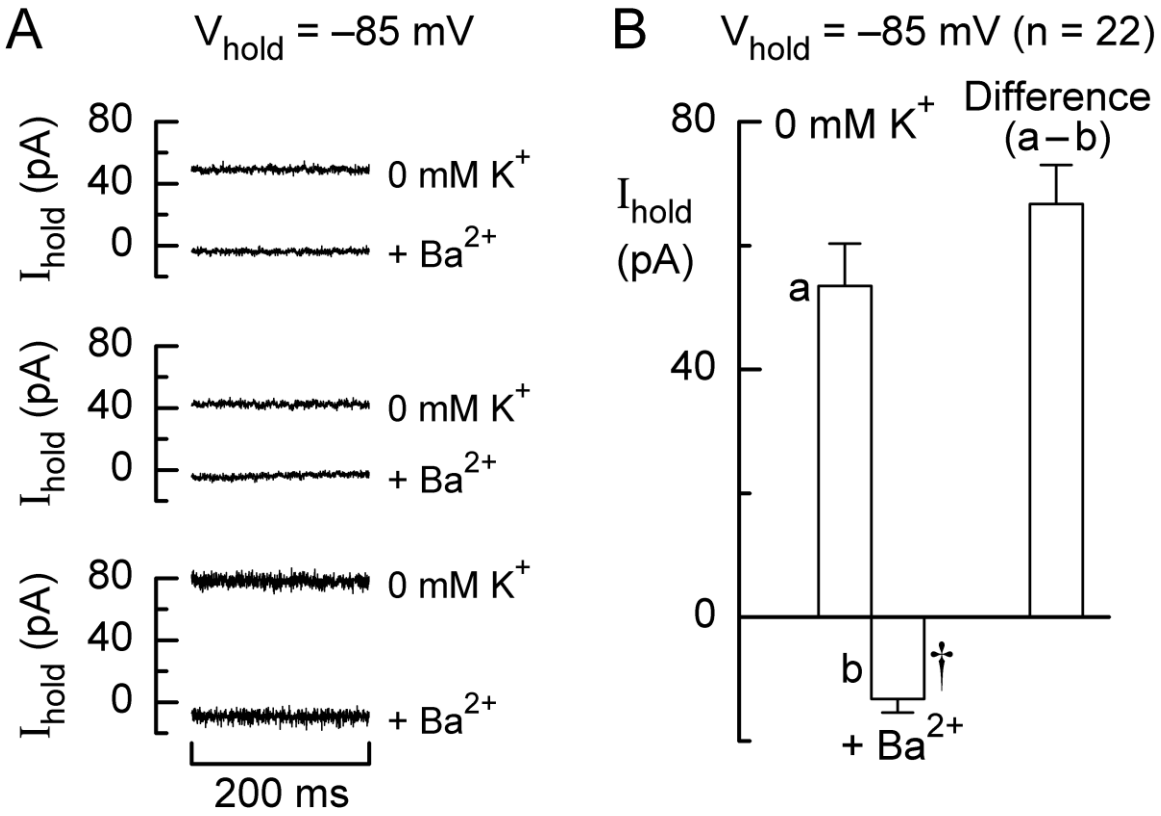

Figure 14. Effect of Ba^{2+} on holding current in myocytes bathed with K^+-free $NMDG^+$ solution. Myocytes dialyzed with K^+ pipette solution and bathed with 0-mM K^+ $NMDG^+$ solution for ≈ 10 min were treated with 1-3 mM Ba^{2+} for 5 min. **A.** Superimposed traces of segments of holding currents (I_{hold}) recorded at the holding potential (V_{hold}) of –85 mV in three representative experiments**. B.** Summary of I_{hold} data obtained from 22 experiments (including the 15 K^+_{pip} experiments of Figure 13). † $P < 0.001$, paired *t* test. "Difference" data were obtained by subtracting Ba^{2+} data (column b) from corresponding 0-mM K^+ data (column a).

the magnitude of the difference in current amplitude at –90 mV between myocytes dialyzed with K^+ pipette solution and myocytes dialyzed with Cs^+ pipette solution (average 79 pA, see above).

In a further series of experiments, myocytes bathed with K^+-free Na^+ solution were held at –85 mV and treated for 5 min with 1 mM Ba^{2+}. The level of the current at –85 mV was +23 ± 11 pA before the addition of the blocker, and –47 ± 8 pA afterwards (n = 10) ($P < 0.001$) (data not depicted).

3.3.2.2. Contribution Of I_{K1} To End-Of-Pulse Currents

Myocytes superfused with K^+-free $NMDG^+$ solution for 10-15 min were treated with a relatively low concentration of Ba^{2+} for 10 min. I-V relations were determined just before and at the end of the treatment using 500-ms pulses from holding potential –85 mV. The results obtained in two representative experiments are shown in Figure 15. In the first of these, a very low (0.01 mM) concentration of Ba^{2+} markedly reduced the amplitude of the steady-state outward current at all potentials between –140 and –20 mV (Figure 15A). In the second, addition of 0.1 mM Ba^{2+} abolished the inward transient and shifted the end-of-pulse current in the inward direction (Figure 15B).

The main series of experiments was conducted using 1 mM Ba^{2+}. I-V relations were determined by applying 1000-ms pulses from holding potential –85 mV to voltages between –110 and –30 mV just before and ≈ 7 min after addition of the blocker. The results obtained from fifteen myocytes were averaged, and these values are shown in Figure 16. Ba^{2+} shifted the end-of-pulse current in the inward direction over the entire voltage range, and these shifts were highly significant ($P < 0.001$) at all potentials negative to –40 mV. The Ba^{2+}-sensitive (difference) current (nominally I_{K1}) had a strong inwardly-rectifying I-V relationship, with mean current amplitude declining from near 80 pA at –110 mV, to 55 and 20 pA at –70 and –40 mV, respectively.

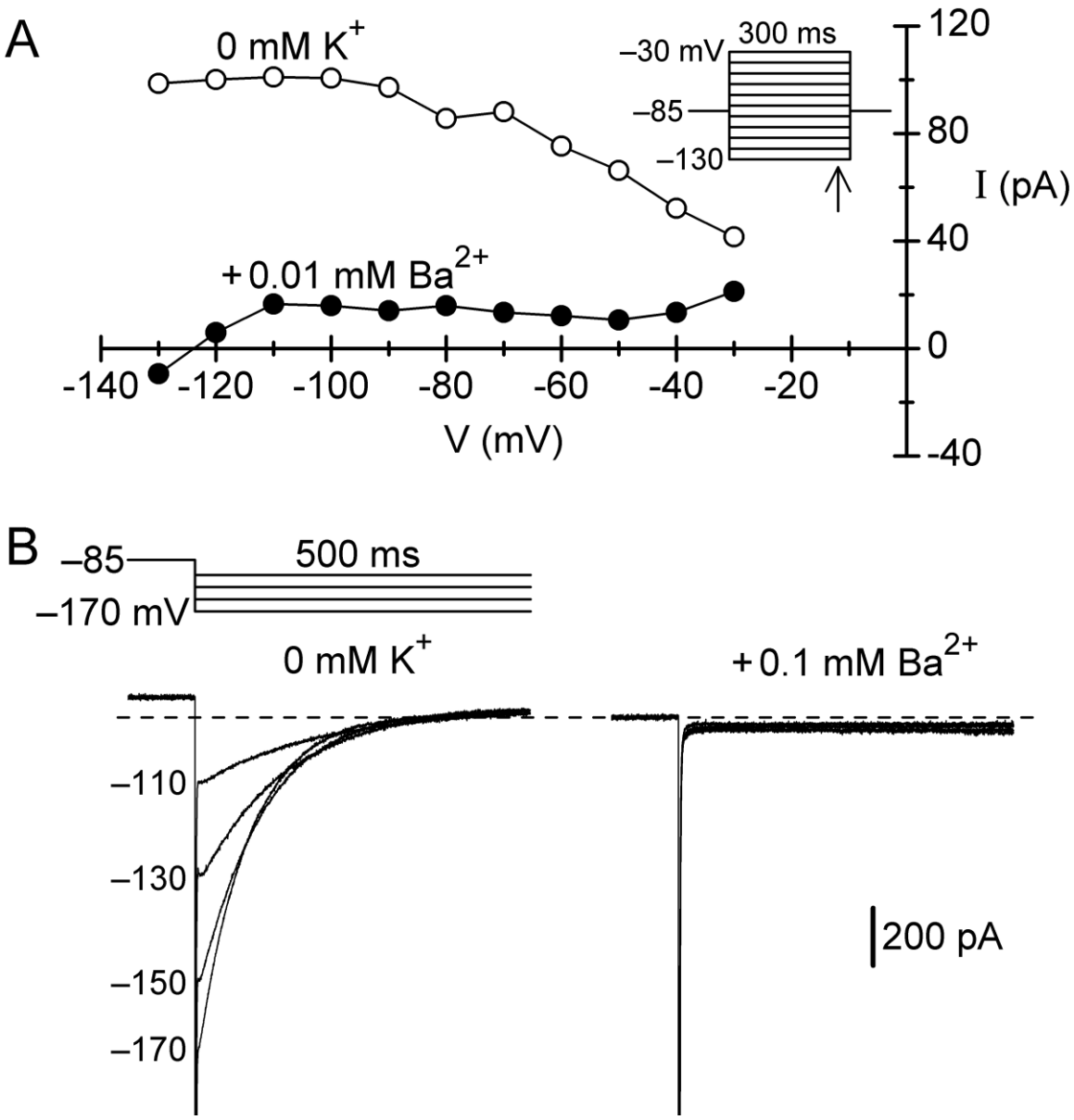

Figure 15. Effects of low concentrations of Ba^{2+} on membrane currents in myocytes bathed with 0-mM K^+ $NMDG^+$ solution. The myocytes were held at −85 mV and pulsed with a series of 300- or 500-ms steps at 0.1 Hz before and 10 min after addition of Ba^{2+}**.** **A.** End-of-step current amplitudes measured in an experiment with 0.01 mM Ba^{2+}. **B.** Records obtained before and after addition of 0.1 mM Ba^{2+}.The dashed line indicates the zero-current level.

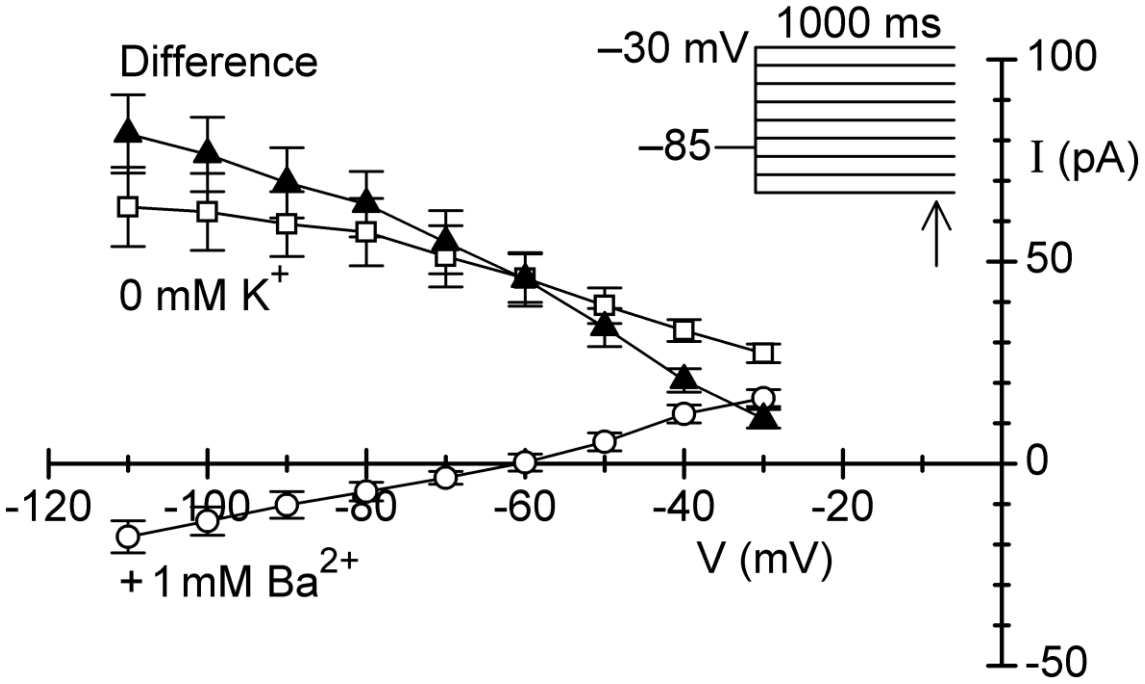

Figure 16. Effects of 1 mM Ba^{2+} on the steady-state I-V relations of myocytes bathed with 0-mM K^+ $NMDG^+$ solution. The myocytes were held at –85 mV and pulsed to other potentials for 1000 ms at 0.1 Hz just before (0 mM K^+) and 7 min after addition of Ba^{2+}. The data obtained under these two conditions are significantly different ($P < 0.001$) at all potentials below –40 mV (ANOVA, Tukey-Kramer multiple comparison test). "Difference" data were obtained by subtracting Ba^{2+} data from corresponding 0-mM K^+ data. The myocytes (n = 15) are the same as those in Figure 13 (K^+_{pip}).

It was of value to compare steady-state I-V relations in myocytes dialyzed with K^+ pipette solution and treated with Ba^{2+}, with steady-state relations in myocytes dialyzed with Cs^+ pipette solution and treated with Ba^{2+}. The K^+-pipette data were already in hand (Figure 16), and the Cs^+-pipette data were obtained from sixteen myocytes that were bathed with K^+-free NMDG solution and treated with 1 mM Ba^{2+} for ≈ 5 min. As indicated by the I-V plot of Figure 17, there is little difference between the two sets of data. This result suggests that the magnitude of one component of the steady-state I-V relation under these experimental conditions, outward-directed nonselective cation current, was similar in K^+-dialyzed and Cs^+-dialyzed myocytes. Thus, it seems highly likely that in the case of non-Ba^+-treated myocytes, the more inward I-V relation in Cs^+-dialyzed myocytes than in K^+-dialyzed ones (see Figure 13 above) was entirely or almost entirely related to absence of outward I_{K1} in Cs^+-dialyzed myocytes.

3.3.2.3. Contribution Of I_{K1} To Inward Transients

The absence of inward transients on hyperpolarizations of myocytes dialyzed with Cs^+ solution provides an indirect indication of the involvement of I_{K1} in the transients. A more direct indication is provided by the finding that application of 0.1 mM Ba^{2+} abolished the transient (Figure 15). Supporting evidence was obtained in experiments with I_{K1}-blocker Cs^+. Myocytes bathed with K^+-free $NMDG^+$ solution were held at −85 mV and hyperpolarized to −120 mV for 200 ms every 10 s before and during application of 0.3 mM Cs^+. After 3-min application of the blocker, the amplitude of the hyperpolarization-induced transient (difference in current levels at 15 and 190 ms post-pulse-onset) was reduced to 37 ± 4% of its pre-Cs^+ value (n =10 myocytes) ($P < 0.001$) (Figure 18). The inhibition was reversible, i.e., 3-min washouts of Cs^+ from four test myocytes produced recoveries of transients to 94 ± 5% of pre-Cs^+ amplitudes.

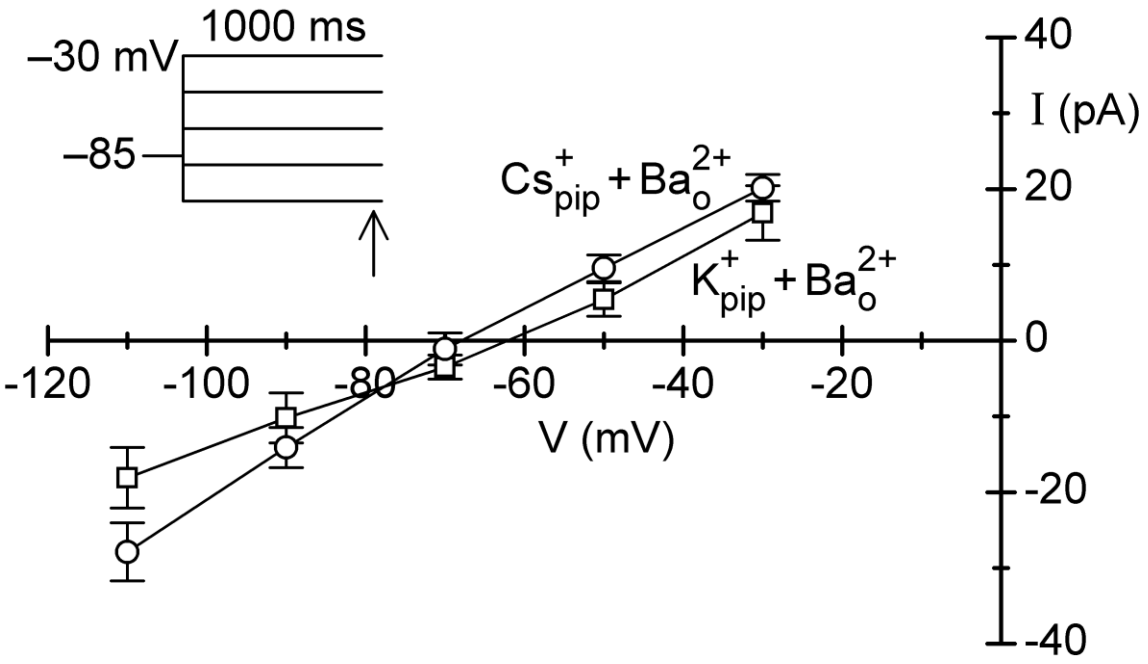

Figure 17. Steady-state I-V relations obtained from Ba^{2+}-treated myocytes dialyzed with K^+ and Cs^+ pipette solutions. The myocytes were bathed with K^+-free $NMDG^+$ solution and treated with 1 mM Ba^{2+} for 5-7 min. The K^+-dialyzed-myocyte data ($K^+_{pip} + Ba^{2+}_o$; n = 15) (from Figure 16) are not significantly different than the Cs^+-dialyzed-myocyte data ($Cs^+_{pip} + Ba^{2+}_o$; n = 16).

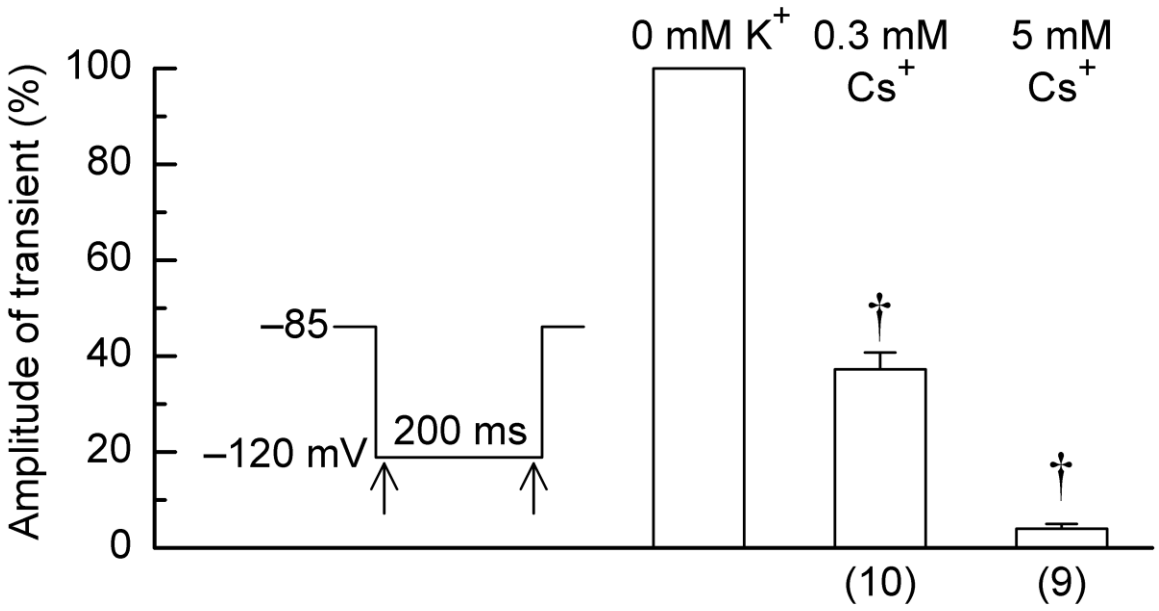

Figure 18. Reduction of the amplitude of the inward transient by external Cs^+. Myocytes were superfused with 0-mM K^+ $NMDG^+$ solution for 10-15 min and then with similar solution that contained 0.3 mM or 5 mM Cs^+ for an additional 3 min. The myocytes were held at −85 mV and pulsed to −120 mV for 200 ms at 0.1 Hz. The amplitudes of the transients were measured as the difference in current levels at 15 and 190 ms post-pulse-onset, and expressed as percentages of pre-Cs^+ (0 mM K^+) values. † $P < 0.001$, paired *t* test.

Additional experiments were conducted using 5 mM Cs^+. This concentration reduced the amplitude of the transient to 4 ± 1% of its pre-Cs^+ amplitude (n = 9 myocytes) ($P < 0.001$) (Figure 18). In brief, the effects of Cs^+ on the amplitude of the transient were similar to those of Ba^{2+}.

3.3.2.4. Contribution Of I_{K1} To Tail Currents At –85 mV

Tails following small-amplitude pulses. The traces shown in Figure 19 illustrate the configurations of the tail currents that followed small-amplitude voltage steps. These particular tails were recorded in an experiment on a myocyte that was bathed in K^+-free $NMDG^+$ solution, held at −85 mV, and pulsed to −110, −100, −90, −80, and −70 mV for 500 ms at 0.1 Hz before and after addition of 0.1 mM Ba^{2+}. The tail currents that followed the hyperpolarizing pulses were outward in relation to the holding current level, and they decayed by > 70% within 100-ms of their onsets (Figure 19A). By contrast, the tail current that followed the depolarizing pulse to −70 mV was markedly inward in relation to the holding current level (Figure 19A). Although not shown in the figure, the tail current that followed the depolarization from −85 to −80 mV was also inward, but smaller in amplitude than the tail that followed the −70-mV pulse. Both outward- and inward-directed tail currents were abolished by addition of 0.1 mM Ba^{2+} (Figure 19B), leading to the conclusion that they were carried by K1 channels. That being the case, the outward-directed tail currents in question must have been caused by hyperpolarization-induced increases in G_{K1} and/or hyperpolarization-induced increases in outward driving force on K^+ ions. Since these increases likely declined with time after termination of the hyperpolarizing pulses, they likely account for the time dependencies of the tails. In regard to whether the tail was induced by an increase in G_{K1} and/or an increase in driving force, the following may be noted: (i) it was difficult to discern whether or not G_{K1}

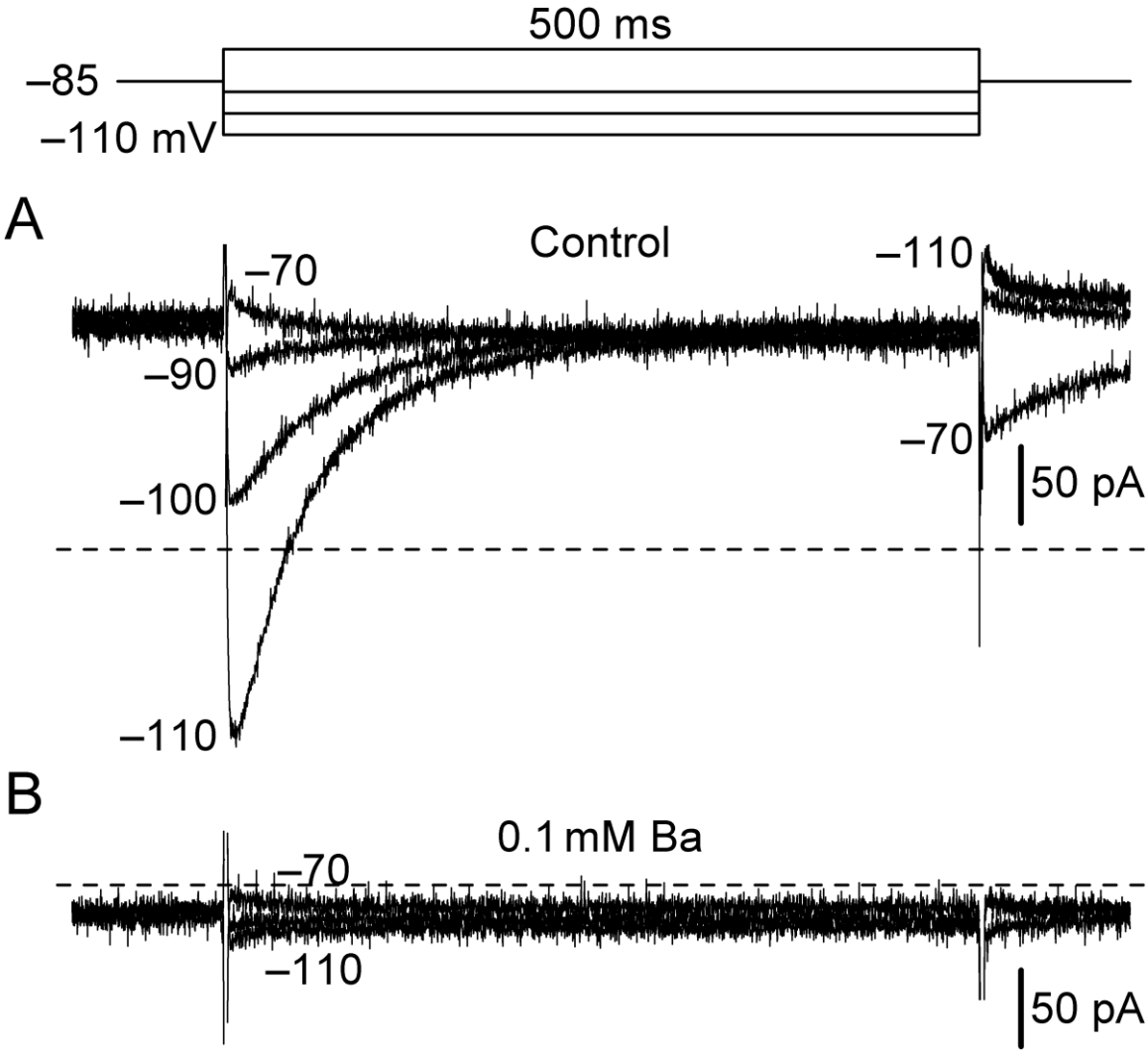

Figure 19. Tail currents elicited after small-amplitude hyperpolarizing and depolarizing pulses. The myocyte was bathed with K^+-free $NMDG^+$ solution for 15 min, and then with K^+-free solution that contained 0.1 mM Ba^{2+} for an additional 7 min. The dashed lines indicate the zero-current level. **A.** Records obtained at the end of the superfusion with K^+-free solution. Note that the tail current after the pulse to –70 mV was inward-directed, whereas the tail currents after pulses to more negative potentials were outward-directed. **B.** Records obtained at the end of the superfusion with 0.1 mM Ba^{2+} solution.

increased during hyperpolarizing pulses; and (ii) by contrast, it is highly likely that hyperpolarization (inward current)-induced depletion of K^+_T (see below) resulted in transient increases in post-hyperpolarization outward driving force.

The traces in Figure 19A indicate that with respect to the holding current, the tail current was outward after the pulse to –90 mV and inward after the pulse to –70 mV. Scrutiny of the configurations of the currents recorded *during* the pulses to these potentials provides little reason for the change in tail current direction, i.e., the currents almost superimpose on each other, with the exception of oppositely-directed small transients at early times. It may be that the decaying inward tail current after the pulse to –70 mV reflects a clearance of K^+ accumulated during the pulse, as well as a time-dependent recovery of I_{K1} from the rectification that occurred during the pulse.

Tails following large-amplitude hyperpolarizations. Tail currents following hyperpolarizing steps from –85 mV to –90, –100, and –110 mV were always similar to the ones shown in Figure 19A, i.e., they were time-dependent and outward with respect to the level of the holding current at –85 mV. Tail currents following hyperpolarizing steps to more negative voltages such as –140 mV were different; they were always *inward* with respect to the holding current level. An example of this dependence of tail direction on pulse voltage is provided by the traces shown in Figure 20. They were obtained by subtracting records obtained during treatment of a myocyte with 0.1 mM Ba^{2+} from those obtained before treatment. The I_{K1} tail on termination of the hyperpolarizing pulse to –150 mV was inward with respect to the steady-state holding current; it was largest just after the termination, and declined to near-zero over the next 500 ms. A plausible explanation for this behaviour is that the depletion of K^+_T during the pulse resulted in a

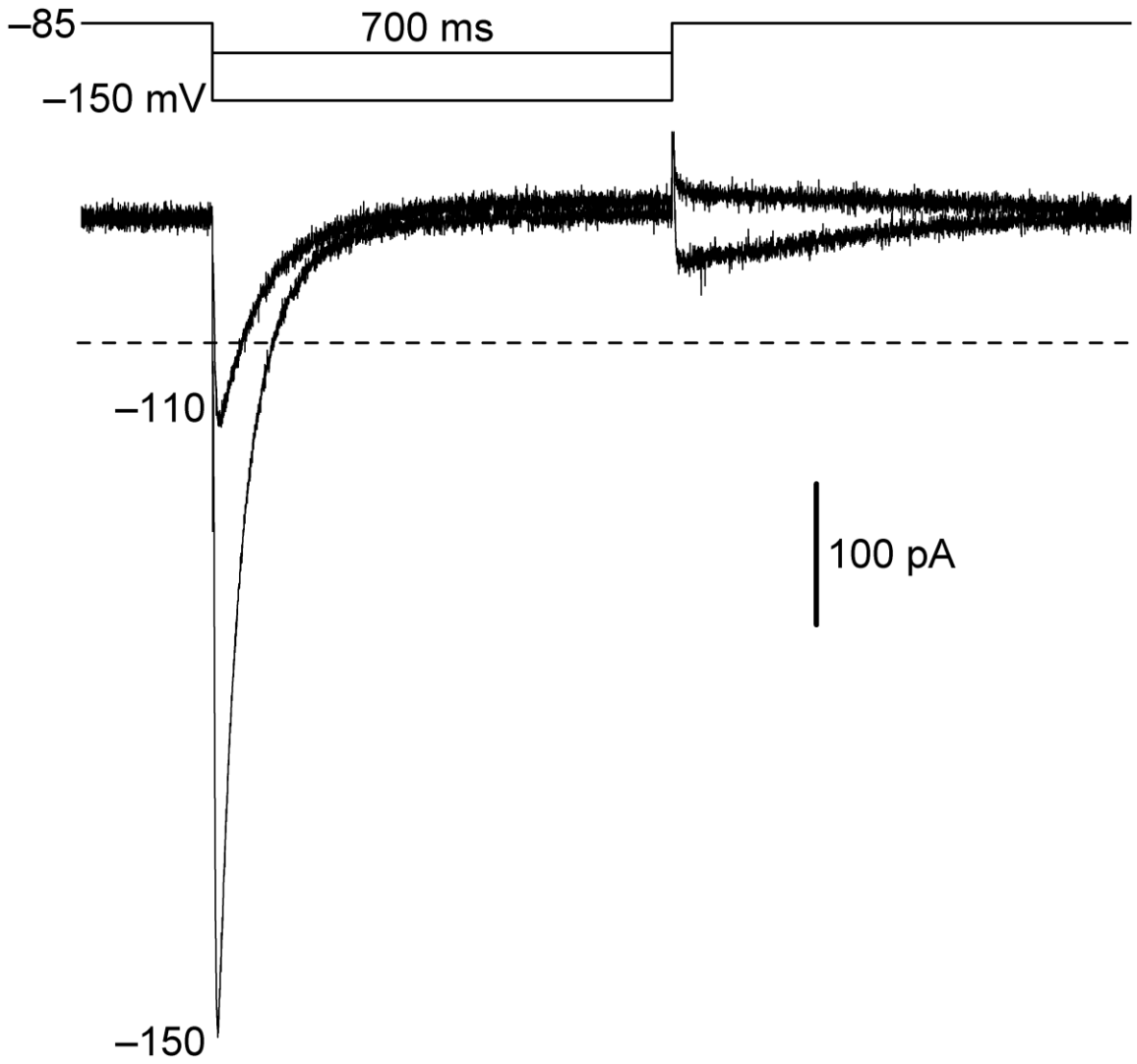

Figure 20. Dependence of I_{K1} tail configuration on the amplitude of the preceding hyperpolarization. The myocyte was bathed with 0-mM K^+ $NMDG^+$ solution for 10 min, and then treated with 0.1 mM Ba^{2+} for 5 min. The currents shown are difference currents (pre-Ba^{2+} minus Ba^{2+}). The dashed line indicates zero difference current.

lowering of $G_{K1,T}$ and a subsequent dampening effect on tail current amplitude that more than offset the stimulatory effect of increased outward driving force.

3.4. OUTWARD I_{K1} AND ACCUMULATION OF EXTRACELLULAR K^+

Findings presented in Section 3.3 suggest that outward I_{K1} can cause accumulation of K^+ in restricted-diffusion extracellular spaces of myocytes that are bathed with 0-mM K^+ solution. The purpose of experiments described below was to evaluate whether outward I_{K1} can cause accumulation of K^+ in myocytes bathed with 5.4-mM K^+ solution. The first step in this investigation was to follow earlier findings by others in regard to accumulation elicited by large outward $I_{K,ATP}$.

3.4.1. Accumulation Mediated By Outward Flow Of $I_{K,ATP}$

In the seminal study on K^+-current-induced accumulation of K^+ in restricted extracellular spaces of guinea-pig ventricular myocytes, the prerequisite large flow of outward K^+ current that engendered the hallmark inward tail current on repolarization was attained by activating K_{ATP} channels with nicorandil (Yasui *et al.*, 1993). In the present study, we used the K_{ATP}-activation approach to evoke accumulation as a prelude to investigation of accumulation mediated by I_{K1}. Figure 21A shows results obtained from a myocyte that was treated with creatine kinase inhibitor DNFB (1 mM) to activate $I_{K,ATP}$ (Lawrence *et al.*, 2002; Ryu *et al.*, 2005). The myocyte was bathed with 5.4-mM K^+ Na^+ solution, held at –80 mV, and pulsed to potentials up to +20 mV for 500 ms at 0.1 Hz. The current records obtained after activation of $I_{K,ATP}$ featured inward tail currents whose amplitudes increased with those of the preceding outward $I_{K,ATP}$ and whose time courses could be described by monoexponential functions with τ's that

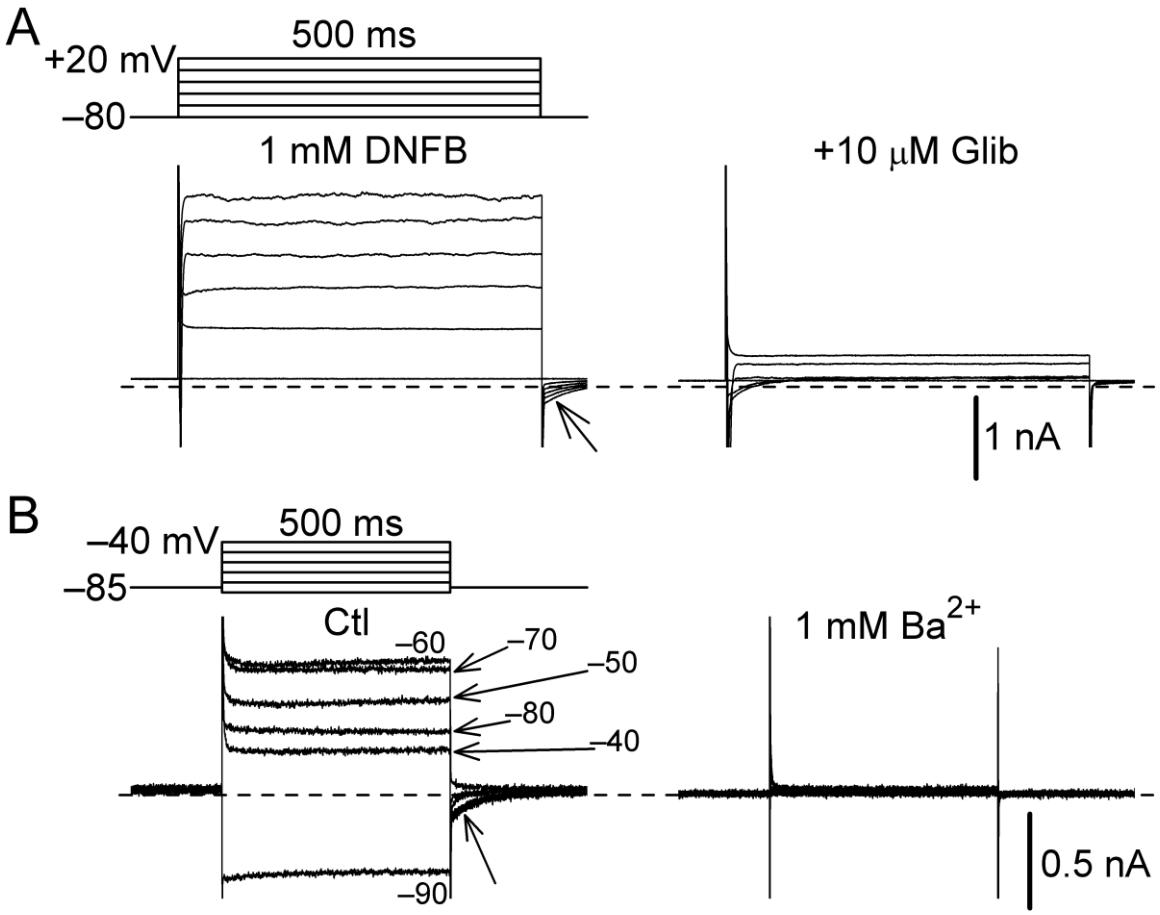

Figure 21. Inward tail currents associated with flows of outward $I_{K,ATP}$ and I_{K1}. **A**. Current records obtained from a myocyte that was bathed in 5.4-mM K^+ Na^+ solution and treated with 1 mM DNFB for ≈ 15 min to activate $I_{K,ATP}$. Left: records showing outward $I_{K,ATP}$ elicited by depolarizations, and associated inward tail currents elicited by repolarizations (arrow). Right: records indicating marked inhibition of both outward $I_{K,ATP}$ and inward tail current shortly after application of 10 μM glibenclamide (Glib). **B.** Current records obtained in an experiment on a myocyte that was bathed with 5.4-mM K^+ $NMDG^+$-blocker solution, held at –85 mV, and pulsed to voltages between –90 and –40 mV for 500 ms at 0.1 Hz. The records were obtained just before (Ctl) and 5 min after addition of 1 mM Ba^{2+}. The lower diagonal arrow on the left points to tails associated with the pulses to –70, –60, and –50 mV. The dashed lines on records indicate zero-current levels.

ranged from 77 to 91 ms. Both outward $I_{K,ATP}$ and inward tail current were strongly diminished by $I_{K,ATP}$ blocker glibenclamide (10 μM) (Figure 21A, right). Similar glibenclamide-sensitive inward tail currents were recorded on repolarizations to −80 mV in other experiments with DNFB (n = 6) and K_{ATP}-activator cromakalim (50 μM) (n = 5).

In marked contrast to the foregoing, but in agreement with Yasui *et al.* (1993), inward tail currents were absent in myocytes bathed and dialyzed with K^+-free solution and treated with K_{ATP} channel opener (n = 5) (data not depicted). Thus, these results point to the following relation between K^+ outflow on depolarization and inward tail current on repolarization (cf. Yasui *et al.*, 1993): (i) large outward $I_{K,ATP}$ during a depolarizing pulse causes an accumulation of K^+ in narrow restricted-diffusion T-tubules, (ii) this elevation of T-tubular K^+ (K^+_T) shifts the applicable E_K ($E_{K,T}$) to a voltage above holding potential −80 mV, and (iii) repolarization to −80 mV elicits inward K^+ current that decays in concert with the clearance of accumulated K^+ via diffusion to bulk extracellular space and K^+-channel passage to the cytoplasm.

3.4.2. Accumulation Mediated By Outward Flow Of I_{K1}

To investigate the possibility that an outward flow of I_{K1} on depolarization can cause an accumulation of K^+ that evokes an inward tail current on repolarization, experiments were conducted on myocytes in which $I_{K,ATP}$ was suppressed by inclusion of 5 mM MgATP in the pipette solution and 5 μM glibenclamide in the bathing solution. Non-I_{K1} current components were minimized by using $NMDG^+$ bathing solution that contained channel blockers Cd^{2+} (1 mM) and E4031 (3 μM) in addition to glibenclamide ($NMDG^+$-blocker solution). Current records obtained from a representative myocyte bathed with 5.4-mM K^+ $NMDG^+$-blocker solution are shown in Figure 21B. The myocyte was held at −85 mV and pulsed to more positive and negative potentials for 500 ms at 0.1

Hz just before (control) and 5 min after addition of I_{K1}-blocker Ba^{2+} (1 mM). The control records indicate that the end-of-pulse amplitude of the current varied with the amplitude of the pulse in a manner characteristic of inwardly-rectifying I_{K1}. Flows of outward current were followed by inward tail currents, and both of these current components were almost completely abolished by the addition of Ba^{2+}. In six experiments of this type, the amplitude of the tail current (obtained by extrapolation of monoexponential tail-fits to zero-time) following pulses to −50 mV was −169 ± 46 pA. In a larger group of myocytes (n = 35), the ratio of the amplitude of the inward tail current to that of the outward current at −50 mV was −0.19 ± 0.02. The time constants of decay of tail currents ranged from 40 to 95 ms.

Effects of I_{K1}-blocker Cs^+ on outward I_{K1} and inward tail current are shown in Figure 22A. The records in the figure were obtained from a myocyte that was held at −85 mV and pulsed to −75 and −80 mV for 500 ms at 0.1 Hz before and during 5-min superfusions with 2- and 10-mM Cs^+ solutions. The pulses elicited outward I_{K1}, and the repolarizations to −85 mV elicited inward tail currents that decayed with time constants near 45 ms. The amplitudes of the tails were roughly proportional to those of the preceding outward I_{K1}, and Cs^+ decreased both components in a concentration-dependent manner. Similar results were obtained in five other experiments of this type.

Another approach that was used to establish a linkage between outward I_{K1} and inward tail current was to determine the effects of certain I_{K1}-inhibitory organic compounds on the tail current. Amongst these compounds were daidzein, 17β-estradiol, and spermine. Each of these agents decreased the amplitude of outward I_{K1} and concomitantly decreased the amplitude of the inward tail current. I_{K1}-inhibitor daidzein ($IC_{50} \approx 62$ μM (Chiang *et al.*, 2002)) was applied at a concentration of 100 μM for ≈ 7

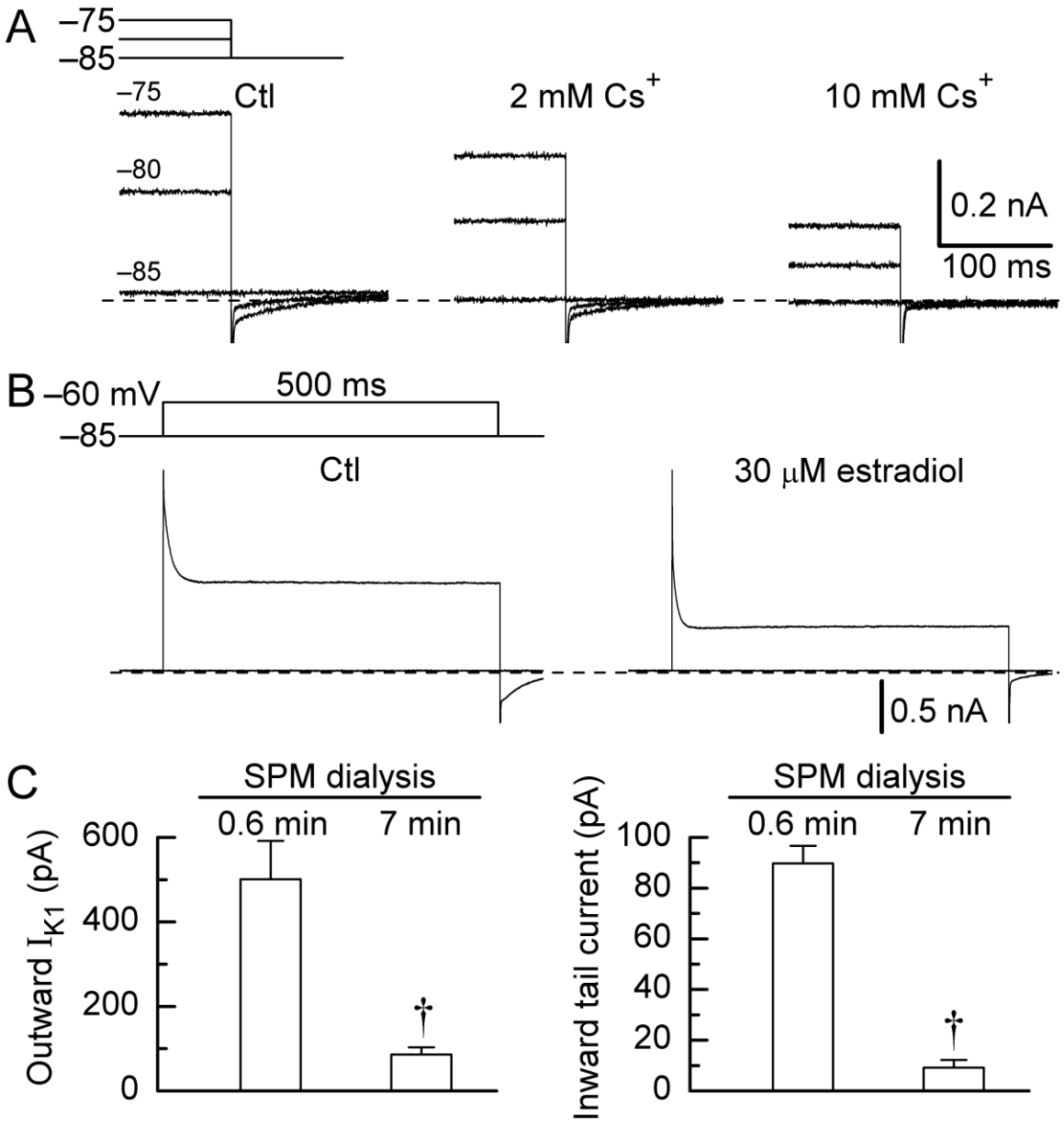

Figure 22. Inhibitory effects of I_{K1} blockers on outward I_{K1} on depolarization and inward tail current on repolarization. The myocytes were bathed with 5.4-mM K^+ $NMDG^+$-blocker solution, held at −85 mV, and pulsed to other potentials for 500 ms at 0.1 Hz. Dashed lines on records indicate zero-current levels. **A.** Inward tail currents recorded before (Ctl) and during sequential superfusions with 2- and 10-mM Cs^+ solution. **B.** Records obtained before (Ctl) and after 20-min treatment with 30 μM 17β-estradiol. **C.** Comparison of the amplitudes of outward I_{K1} (−60 mV) (left hand panel) and associated inward tail current (−85 mV) (right hand panel) in myocytes that were dialyzed with pipette solution that contained 0.3 mM spermine (SPM). Measurements were made at post-patch breakthrough times of 0.6 min (quasi-control) and 7 min (spermine action). † $P < 0.001$ versus 0.6-min amplitude (paired *t* test) (n = 5).

min. It reduced the amplitudes of the outward current (–50 mV) and associated tail current by 55.1 ± 3.8 and 51.3 ± 6.1% (n = 7), respectively (data not depicted). Twenty-min applications of inhibitor 17β-estradiol (30 μM) (Berger *et al.*, 1997) had similar effects (n = 3) (e.g., Figure 22B).

The data obtained from the myocytes that were dialyzed with 0.3-mM spermine solution are shown in Figure 22C. The dialysate depressed the amplitude of outward I_{K1} and concomitantly depressed the amplitude of the inward tail current. To quantify the effects, the amplitudes of outward I_{K1} on depolarization to –60 mV and inward tail current on repolarization to –85 mV were measured at 0.6 and 7 min post-patch-breakthrough, and taken as quasi-control and quasi-steady-state-spermine values, respectively. Spermine dialysate decreased ($P < 0.001$) the amplitudes of both outward I_{K1} and inward tail current by more than 80% (n = 5).

3.4.3. Effects Of Raising And Lowering K^+_o On The Inward Tail Current

Findings in previous studies on K^+ accumulation in ventricular myocytes indicate that raising K^+_o from 5.4 to 20 or 30 mM greatly diminishes the degree of accumulation induced by large outward K^+ current (Yasui *et al.*, 1993; Clark *et al.*, 2001). In the present study, the modulatory effects of K^+_o on inward tail current were investigated by raising K^+_o from 5.4 to 15 mM and by lowering K^+_o from 5.4 to 2 mM.

Effects of raising K^+_o. Myocytes were held at a potential just negative to E_{rev}, and pulsed to a series of more positive potentials for 500 ms at 0.1 Hz just before and 5 min after switching from 5.4- to 15-mM K^+ $NMDG^+$-blocker solution. Comparison of data obtained under the two K^+ conditions was performed by selecting a current on a pulse to near the peak of the 5.4-mM-K^+ I-V relation, finding a similar-sized current in the 15-mM K^+ series, and measuring the amplitudes of the associated inward tail currents.

Traces of inward tail currents that followed "matched" steady-state outward currents of 1.07 nA (5.4 mM K^+, −55 mV) and 1.19 nA (15 mM K^+, −35 mV) are shown in Figure 23A. The amplitude of the tail current was much smaller during the superfusion with 15-mM K^+ solution (−35 pA) than with 5.4-mM K^+ solution (−160 pA), and its time course of decay was somewhat slower (τ 104 ms versus 78 ms). Current amplitude data from seven experiments were normalized by expressing the amplitudes obtained during the superfusion with 15-mM K^+ solution as percentages of those obtained during the superfusions with 5.4-mM K^+ solution. As depicted in Figure 23B, the relative amplitudes of the (matched) outward currents were similar (98.6 ± 6.8% versus 100%), but those of the inward tails were very much smaller (26.1 ± 2.1% versus 100%).

Effects of lowering K^+_o. Myocytes were held at a potential just negative to E_{rev}, and pulsed to a series of more positive potentials for 500 ms at 0.1 Hz just before and ≈ 7 min after switching from 5.4- to 2-mM K^+ solution. Figure 24A shows representative records of currents elicited by pulses to potentials ≈ 30 mV positive to E_{rev}. As expected from a near-square-root dependence of K1 channel conductance (G_{K1}) on K^+_o, the amplitude of the outward current was ≈ 40% smaller under the lower-K^+_o condition. Despite this reduction, the amplitude of the inward tail current was little affected (Figure 24B). In four experiments of this type, the amplitude of the outward current at −80 mV with 2 mM K^+_o was 57.5 ± 4.1% of that at −50 mV with 5.4 mM K^+_o, whereas the amplitude of the associated inward tail current near E_{rev} (−110 mV) was 113.9 ± 12.7% of that near E_{rev} (−85 mV) with 5.4 mM K^+_o. A matching of outward current amplitudes at other pulse potentials, and evaluation of associated inward tail current amplitudes, yielded 2-mM K^+_o (relative to 5.4-mM K^+_o) percentage values of 81.9 ± 5.4 and 167.4 ± 14.1% for outward current and inward tail current, respectively. Thus, when pro-rated to the amplitude of the

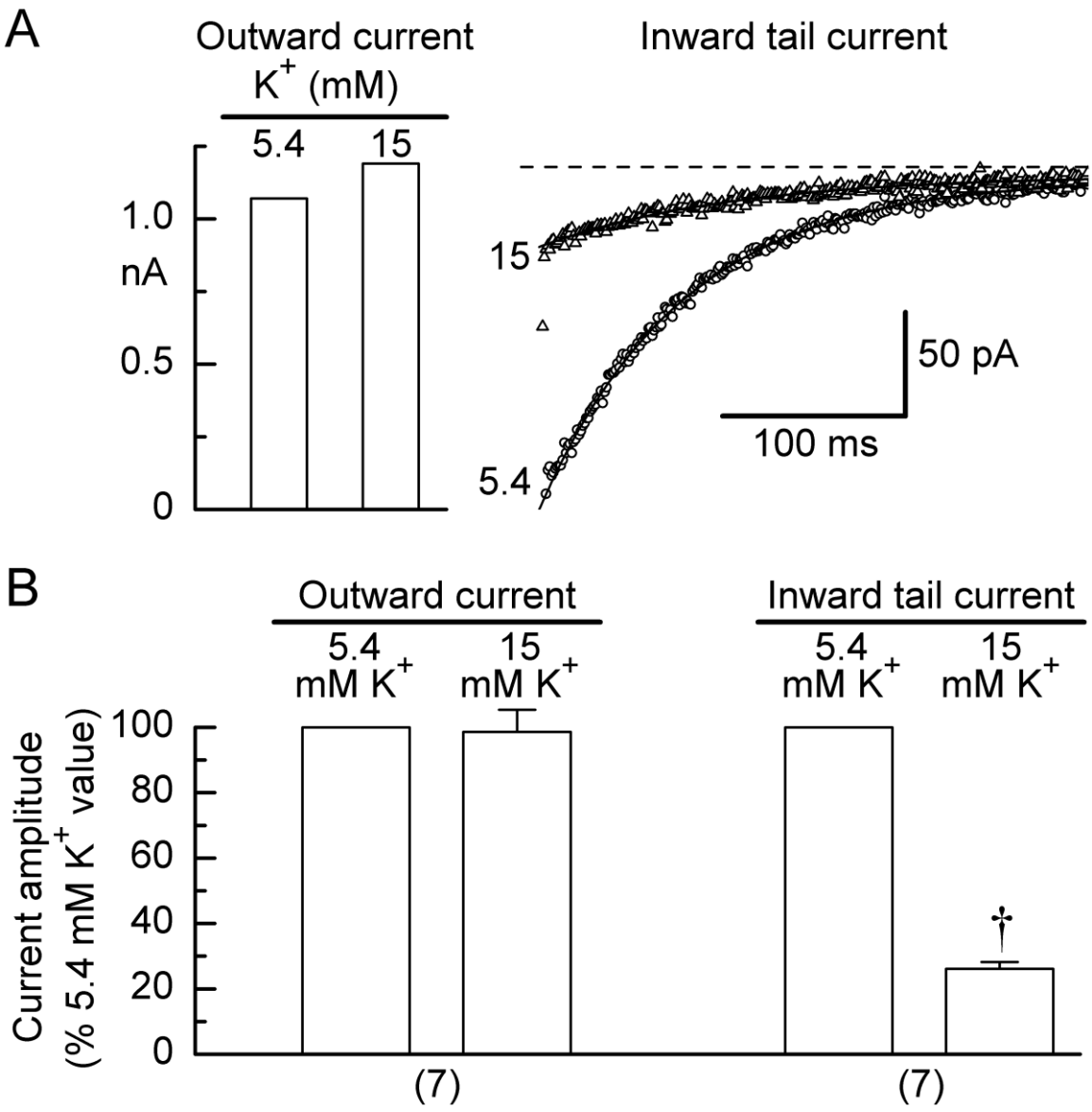

Figure 23. Effects of raising external K^+ on the relative amplitude of the inward tail current. Myocytes sequentially bathed with 5.4-mM K^+ and 15-mM K^+ $NMDG^+$-blocker solutions were held at −85 mV and pulsed (500 ms, 0.1 Hz) to potentials between −60 and −50 mV (5.4 mM K^+), and then held at −60 mV and pulsed to potentials between −45 and −30 mV (15 mM K^+) for measurement of the amplitudes of end-of-pulse outward currents and associated inward tail currents. In each experiment, an outward current (15 mM K^+) was amplitude-matched with an outward current (5.4 mM K^+) for comparison of the amplitudes of the associated tail currents. **A**. Results obtained in a representative experiment. Left: the amplitudes of matched outward currents; right: the associated inward tail currents fitted with monoexponential curves. The dashed line indicates the steady-state holding current level. **B.** Relative amplitudes of the 15-mM-K^+ currents (5.4 mM K^+ = 100%). † $P < 0.001$, paired *t* test, n = 7.

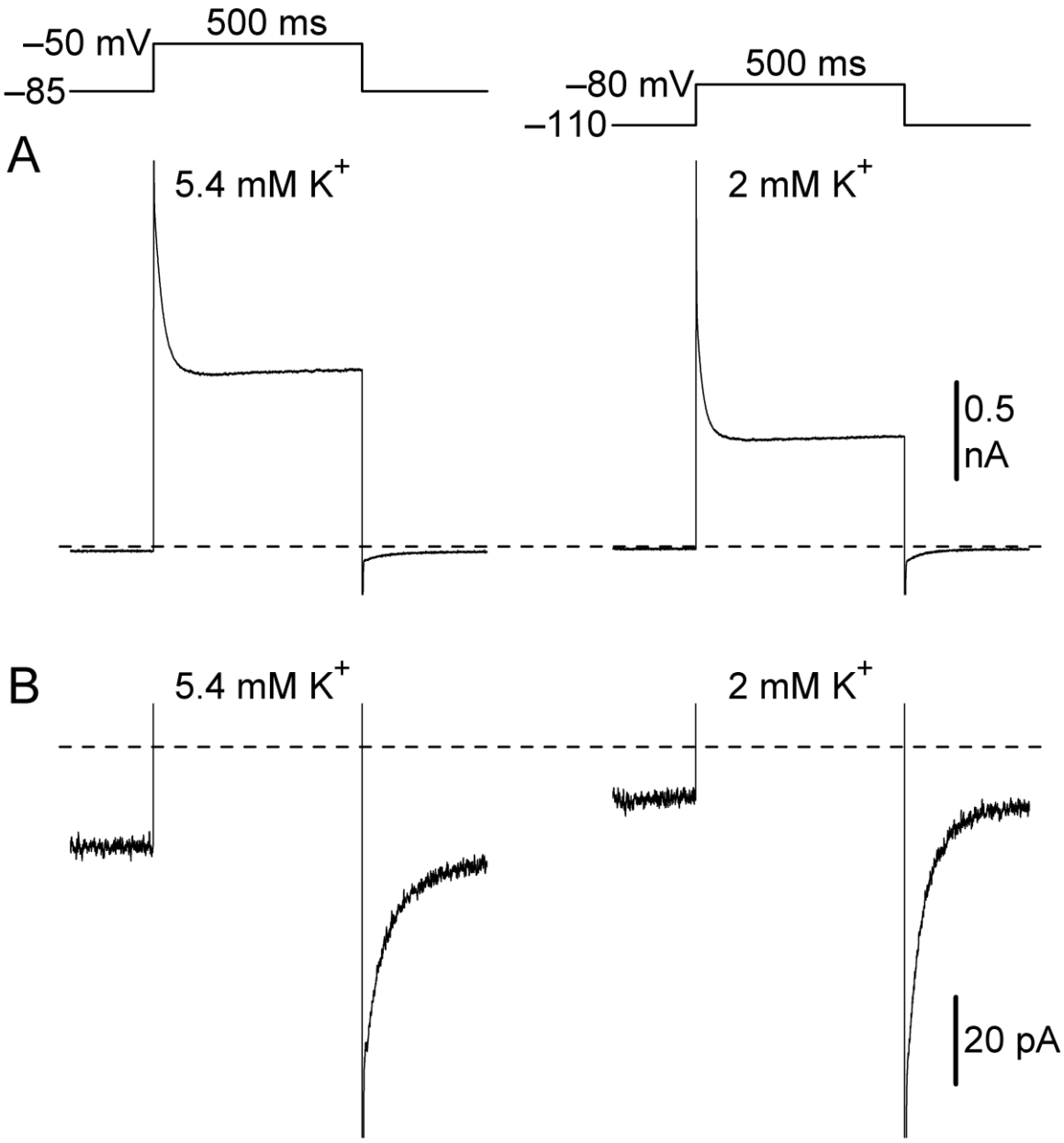

Figure 24. Effects of lowering external K^+ on the relative amplitude of the inward tail current. Myocytes were first bathed with 5.4-mM K^+ $NMDG^+$-blocker solution and held at –85 mV, and then bathed with 2-mM K^+ $NMDG^+$-blocker solution and held at –110 mV. **A,B**. Records obtained in a representative experiment. The full records are shown in A, and higher gains around the zero-current level (dashed lines) are shown in B.

outward current, the amplitude of the inward tail current in 2-mM K^+ solution was approximately twice as large as that in 5.4-mM K^+ solution.

3.5. I_{K1} IN MYOCYTES WITH LOWERED INTRACELLULAR K^+

The findings below were obtained from myocytes that were bathed with solutions that contained 1 mM Cd^{2+} and 3 μM E4031. The concentration of K^+ in the cytoplasm was lowered by dialyzing myocytes with pipette solution that contained a concentration of K^+ lower than 140 mM. Unless otherwise specified, the osmolarity was maintained by using Cs^+ as an equimolar replacement for K^+.

The first section below focuses on the changes in I_{K1} that occurred during the early stages of dialysis with pipette solution that contained 10-20 mM K^+. The second section is concerned with the steady-state effects of holding potential on I_{K1}, and with the reversal potential (E_{rev}) of I_{K1} in myocytes dialyzed with 0-20 mM K^+ pipette solution. The third section details the dependence of E_{rev} on the concentration of K^+ in the pipette solution, and the fourth examines the interplay between I_{K1}-mediated K^+ flux and the concentration of K^+ in the cytoplasm.

3.5.1. I_{K1} During The Lowering Of Intracellular K^+

Myocytes bathed in 5.4-mM K^+ Na^+ solution were dialyzed with 10-mM K^+ pipette solution to lower intracellular K^+. Changes in I_{K1} occurring during this lowering were monitored by recording membrane currents in response to voltage-ramp commands, and the results obtained in a representative experiment are shown in Figure 25. The myocyte was held at −50 mV, hyperpolarized to −120 mV for 5 ms, and depolarized from there to +20 mV with 1.2-s-long voltage ramps to record I-V relations. The first ramp was applied

at 25 s post-patch-breakthrough, and subsequent ramps were applied at 15 s intervals. Records of the membrane currents elicited by a number of these ramps are superimposed on the I-V plot of Figure 25. They indicate that the I-V relation had an inwardly-rectifying shape throughout the observation period. However, there was a flattening-down of the outward-current region over this time, as well as a marked shift of the relation to more positive voltages. In addition, it was evident that shifted I-V relations "crossed over" the initial (25 s) I-V relation. Similar changes were evident in myocytes that were dialyzed with low-K^+ $NMDG^+$ pipette solution (data not shown).

The records in Figure 25 indicate that E_{rev} shifted to more positive potentials as dialysis progressed. The E_{rev} was −79 mV after 25 s of dialysis and −45 mV after 265 s. On the assumption that nearly all of the recorded current was contributed by I_{K1} (see below), and on the additional assumption that $E_{rev} \approx E_K = -61\log(K^+_i/5.4)$, the E_{rev} values of −79 and −45 mV suggest that the concentration of K^+ in the cytoplasm declined from ≈ 140 mM just before patch-breakthrough, to ≈ 110 mM after 25 s dialysis, and ≈ 30 mM within a short time thereafter.

3.5.2. Effects Of Holding Potential On E_{rev}

The effects of holding potential on I_{K1} and E_{rev} in low-K^+_i myocytes are illustrated by the two sets of current traces shown in Figure 26. The upper set was recorded from a myocyte that was dialyzed with 20-mM K^+ pipette solution and held at −80 mV, while the lower set was from a myocyte that was similarly dialyzed but held at −10 mV. The myocytes were pulsed to 0 mV for 200 ms at 0.1 Hz, and pulsing was interrupted at selected times for a series of 200-ms pulses to more positive and/or negative potentials.

Figure 26A shows records of currents elicited by pulses at 7 and 27 min post-patch-breakthrough in the myocyte held at −80 mV. The records indicate that there was little

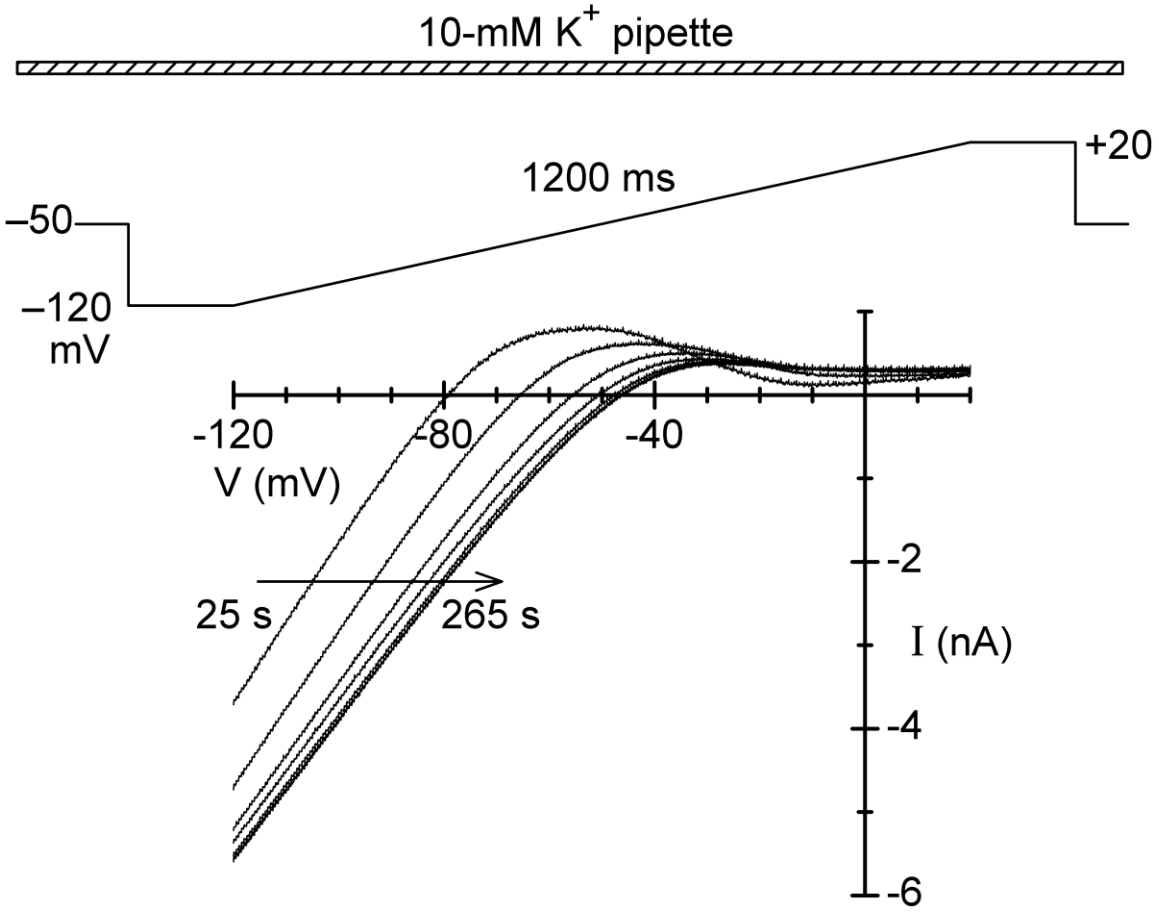

Figure 25. Membrane current during the early stages of dialysis of a myocyte with 10-mM K^+ pipette solution. The myocyte was superfused with 5.4-mM K^+ Na^+ solution, held at –50 mV, and probed with 1.2-s-long voltage ramps from –120 to +20 mV every 15 s. The I-V plot shows the currents elicited by selected ramps, beginning with the initial one at 25 s post-patch-breakthrough. With time after patch breakthrough, there was a slight decline in the steepness of the linear region of the inward-current limb of the I-V relation, a positive shift in the zero-current potential (E_{rev}), and a flattening of the outward-current limb.

change in the amplitudes and configurations of currents during the observation period. The currents were large and inward in direction at −100 and −80 mV, nearly zero at −60 mV, and relatively small and outward in direction at more positive potentials. The latter outward currents featured early relaxation phases, and currents elicited by repolarizations from those test potentials (i.e., tail currents) featured early phases of increasing inward current. These types of early phases have been attributed to time-dependent development of rectification and time-dependent removal of rectification ("activation"), respectively (Matsuda & Noma, 1984; Zhang *et al.*, 2009).

Traces of currents recorded at 11 and 62 min post-breakthrough from the myocyte held at −10 mV are shown in Figure 26B. They indicate that the amplitudes and configurations of the currents were stable over this time. The currents at −10 and −20 mV were relatively small and outward in direction, whereas the currents at −40 mV were larger and inward in direction. Thus, E_{rev} was near −30 mV, or about 30 mV more positive than the E_{rev} determined in the myocyte held at −80 mV.

To evaluate the extent of the modulation of E_{rev} by the holding potential, myocytes were dialyzed with 0-mM or 10-mM K^+ pipette solution, and the holding potential was fixed at a level between −105 and −25 mV. After ≥ 10 min dialysis, the myocytes were pulsed with 500-ms steps to potentials above and below apparent E_{rev} before and 3-5 min after addition of 1-3 mM Ba^{2+}. Actual E_{rev} values were determined using difference (raw minus Ba^{2+}) currents. The data on the plot of E_{rev} versus holding potential (V_{hold}) shown in Figure 27 indicate that E_{rev} was slightly more negative in the myocytes dialyzed with 10-mM K^+ pipette solution (open squares) than in those dialyzed with 0-mM K^+ pipette solution (filled squares), and little affected by use of $NMDG^+$-based pipette solution (triangles) instead of standard Cs^+-based pipette solution. However, independent of the

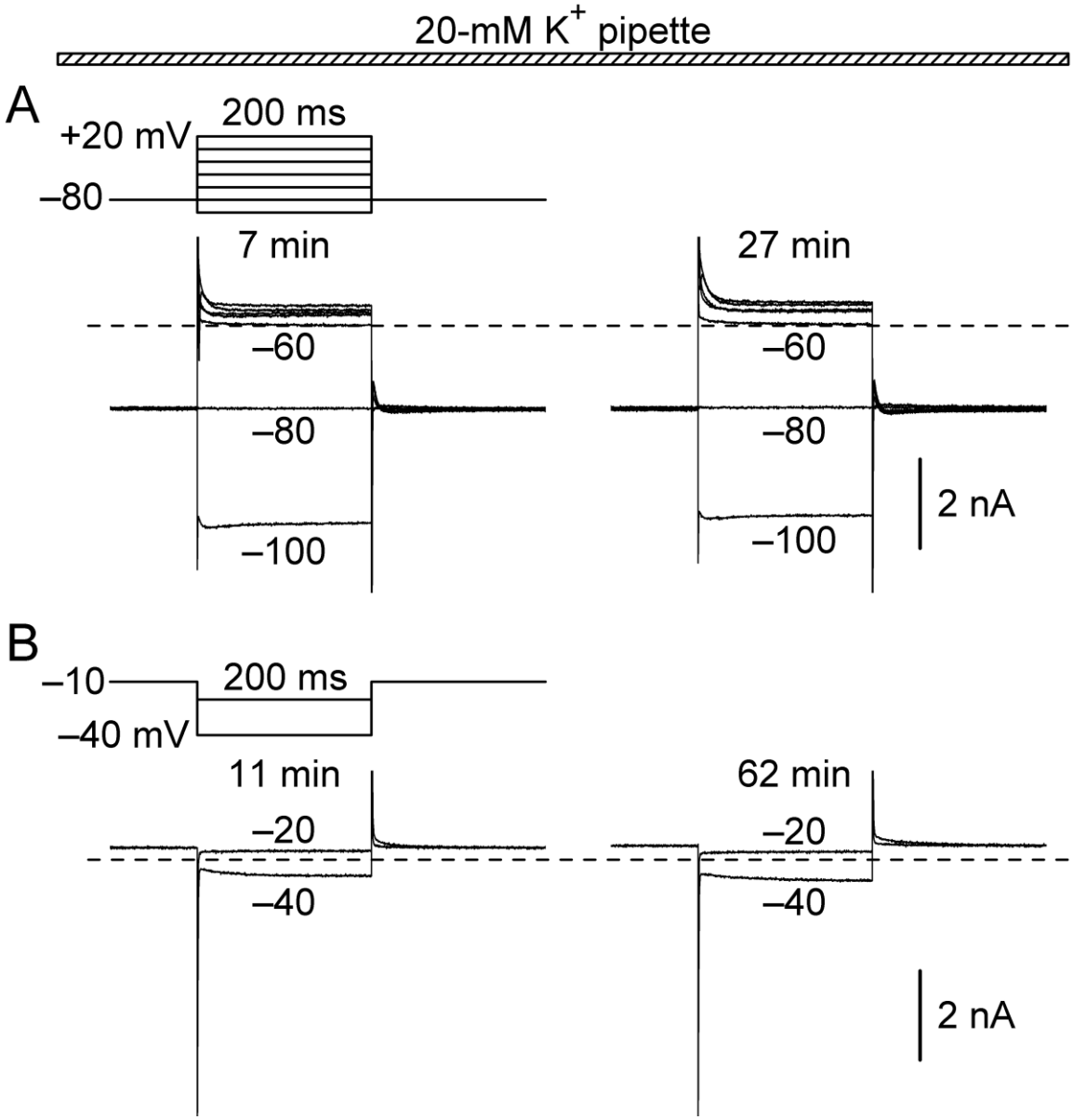

Figure 26. Membrane currents recorded from myocytes dialyzed with 20-mM K^+ pipette solution for prolonged periods of time. The myocytes were bathed in 5.4-mM K^+ $NMDG^+$ solution, held at either –80 or –10 mV, and pulsed with 200-ms steps at 0.1 Hz. The dashed lines indicate zero-current levels, and times above records refer to post-patch times. **A.** Currents recorded from the myocyte held at –80 mV. Note that E_{rev} was near –60 mV. **B.** Currents recorded from the myocyte held at –10 mV. Note that E_{rev} was positive to –40 mV.

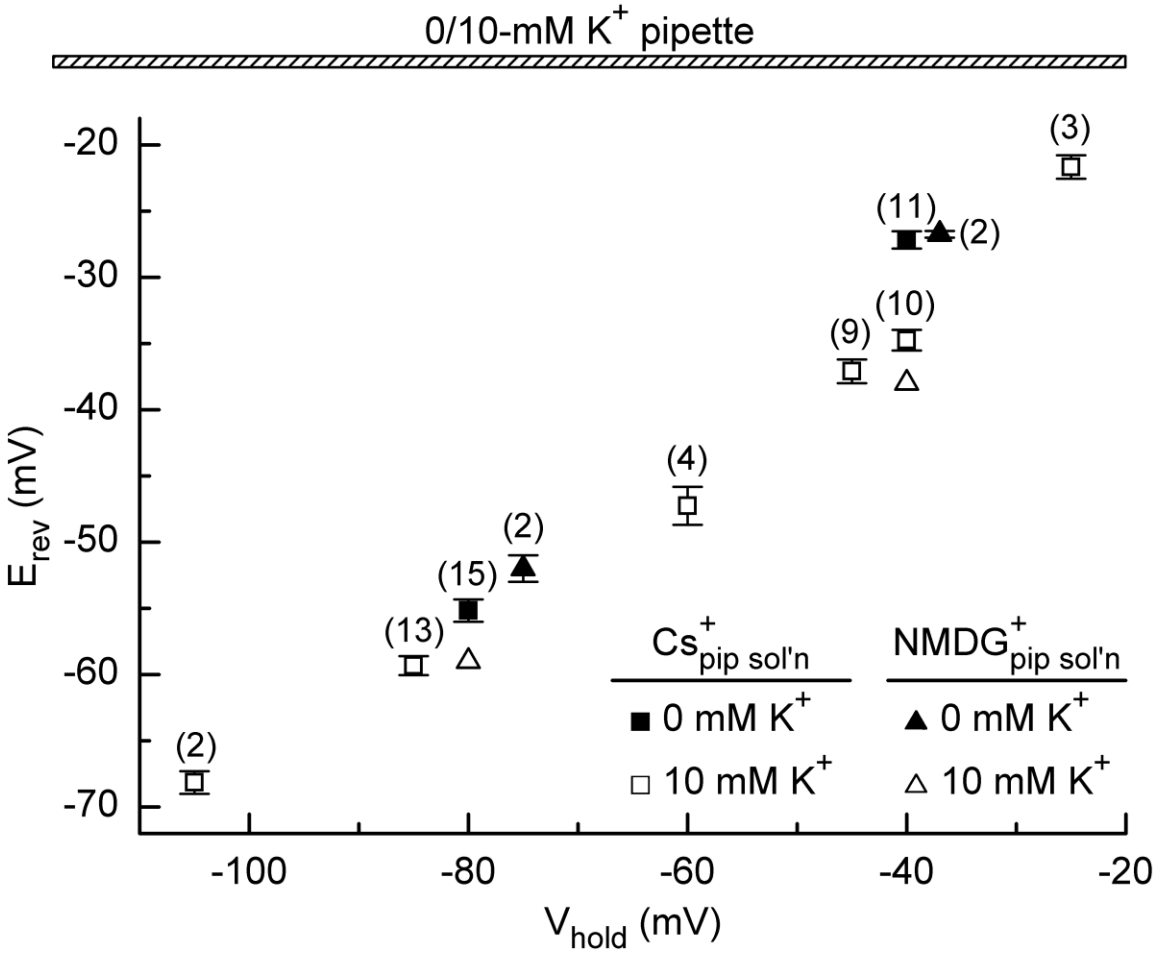

Figure 27. Dependence of the E_{rev} of I_{K1} on holding potential in low-K^+_i myocytes. Myocytes bathed with 5.4-mM K^+ Na^+ solution were dialyzed with 0- or 10-mM K^+ Cs^+ pipette solution (pip sol'n) or with 0- or 10-mM K^+ $NMDG^+$ pipette solution. The holding potential (V_{hold}) was constant during any given experiment, and a sequence of 500-ms steps to more negative and positive potentials was applied at ≈ 10 min post-patch-breakthrough and once more at the end of a subsequent 5-min application of 1-3 mM Ba^{2+}. E_{rev} values were obtained from the end-of-step I-V relations of difference (pre-Ba^{2+} minus Ba^{2+}) currents. Number of myocytes in parentheses.

dialysate used in this series of experiments, the salient feature of the data is that the more negative the holding potential, the more negative the E_{rev}.

The current traces in Figure 26 indicate that small outward currents are required to hold low-K^+_i myocytes at −10 mV (and thereby secure E_{rev} near −30 mV), and that large inward currents are required to hold them at −80 mV (and thereby secure E_{rev} near −60 mV). It seemed probable that these holding currents played a role in determining E_{rev}, most likely by affecting the concentrations of K^+ across the cell membrane. A prerequisite for investigation of the role of current flow in determining E_{rev} in low-K^+_i myocytes was an evaluation of the dependence of E_{rev} on K^+_i in the absence or near-absence of either outward or inward holding current.

3.5.3. Effect Of Pipette K^+ On The E_{rev} Of I_{K1}

The E_{rev} of I_{K1} was determined in experiments on myocytes that were bathed with 5.4-mM K^+ $NMDG^+$ solution and dialyzed with pipette solution whose concentration of K^+ ranged from 10 to 140 mM. In order to ensure equilibration of pipette K^+ and cytoplasmic K^+, myocytes were dialyzed for at least 15 min prior to determination of E_{rev}, and the magnitude of the holding current was minimized by adjustment of the holding potential.

The actual determinations of E_{rev} were performed by using I-V relations generated by step commands to voltages that ranged from just below to just above zero-current voltages. The E_{rev} values were as follows: −85.3 ± 1.1 mV (n = 5) (140-mM K^+ pipette), −76.6 ± 1.4 mV (n = 5) (100-mM K^+ pipette), −67.2 ± 2.6 mV (n = 4) (70-mM K^+ pipette), −49.1 ± 0.9 mV (n = 4) (33-mM K^+ pipette), −33.2 ± 3.3 mV (n = 7) (20-mM K^+ pipette), and −17.3 ± 1.5 mV (n = 8) (10-mM K^+ pipette). As shown in the plot of E_{rev}

versus the logarithm of pipette K^+ concentration, the data are well-fitted by an expression with slope −59.7 ± 1.4 mV per decade pipette K^+ (Figure 28, solid line).

3.5.4. I_{K1} And The Concentration Of Subsarcolemmal K^+

The pronounced dependence of the E_{rev} of I_{K1} on holding potential (V_{hold}) in low-K^+_i myocytes (Figure 27) appeared to be related to the direction and magnitude of I_{K1} at the holding potential. It seemed likely that this involved interplay between the flow of I_{K1} and the concentration of K^+ in a submembrane cytoplasmic space of undetermined size ('subsarcolemmal space'). Conceptually, small *outward* holding I_{K1} mediates an efflux of K^+ that slightly decreases the concentration of K^+ in the subsarcolemmal space. Conversely, *inward* holding I_{K1} driven, for example, by $V_{hold} << E_{rev}$, generates large resting K^+ influx that markedly increases subsarcolemmal K^+ concentration. In turn, the elevation of subsarcolemmal K^+ is moderated by diffusion of K^+ to the bulk cytoplasmic space and the pipette, as well as by a negative feedback on driving force due to the postulated negative shift in E_K. The results of experiments designed to investigate whether this scheme is broadly valid are described in the subsections below.

3.5.4.1. Effects Of Increasing K^+ Influx By Increasing Inward Holding I_{K1}

Inward holding I_{K1} was increased by increasing the inward driving force on K^+. The first method of doing this was to shift the holding potential from a voltage near E_{rev} to one much more negative; the second was to set the holding potential just below E_{rev} and then increase K^+_o from 5.4 to 20 mM.

Negative shift in holding potential. Myocytes superfused with 5.4-mM K^+ Na^+ solution and dialyzed with 10-mM K^+ pipette solution were held at –45 mV for 10-12 min and then held at –85 mV for 5 min. I-V relations were determined just before and at the end of the latter period by using a series of 500-ms steps applied at 0.1 Hz. The

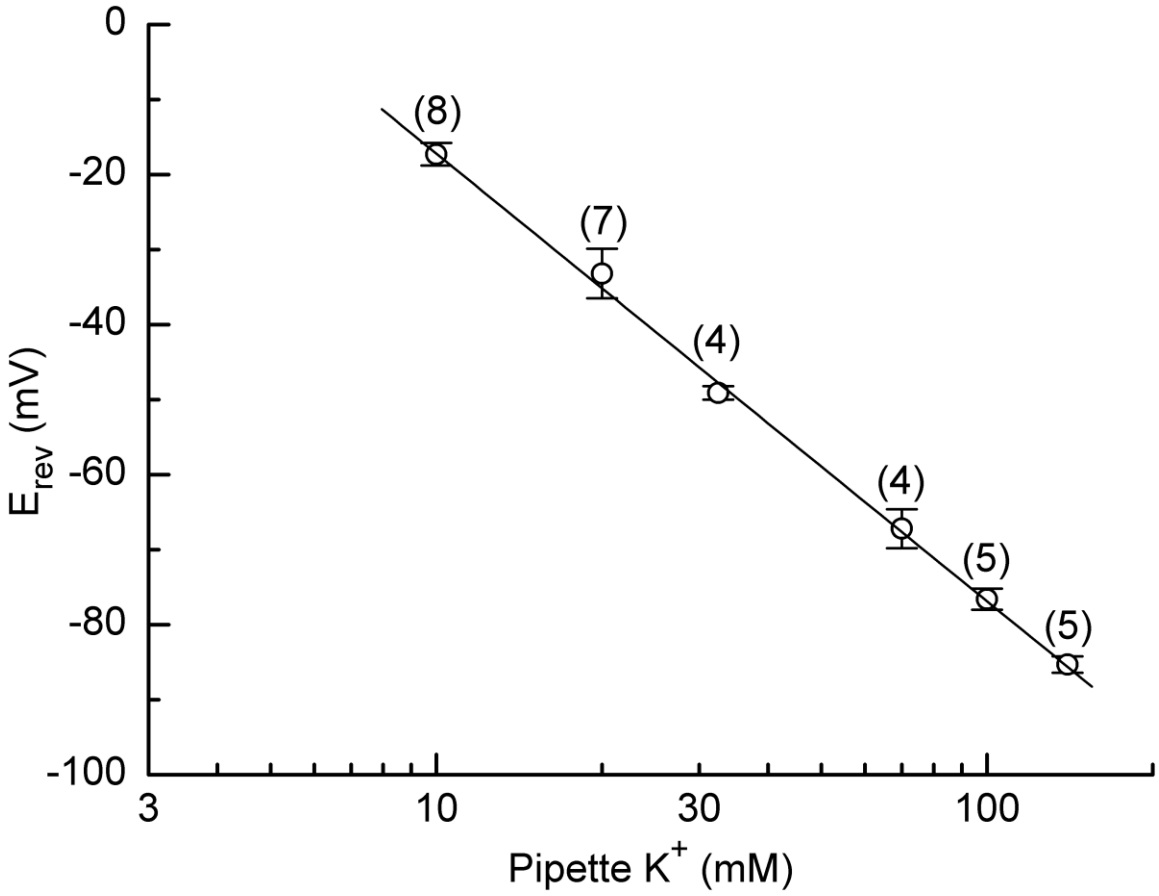

Figure 28. Dependence of E_{rev} on the K^+ concentration of the pipette solution. Myocytes superfused with 5.4-mM K^+ Na^+ solution were dialyzed with pipette solution that contained a specified concentration of K^+ (pipette K^+) (K^+ + Cs^+ constant at 140 mM). The holding potential was kept close to the zero-current potential, and E_{rev} values were determined from end-of-step (200 ms) I-V relations. The best-fit straight line to the E_{rev} data (E_{rev} = A + B (log K^+_{pip})) has slope B of –59.7 ± 1.4 mV per decade pipette K^+) (solid line). Number of myocytes in parentheses.

change in holding potential from −45 to −85 mV shifted E_{rev} from −37.7 ± 1.9 mV to −60.6 ± 3.6 mV (n = 7) ($P < 0.001$) (Figure 29A).

In a second group of experiments, the holding potential of myocytes superfused with 5.4-mM K^+ Na^+ solution and dialyzed with 20-mM K^+ pipette solution was set at −10 mV for 10-15 min, and then shifted to −80 mV for ≈ 5 min. I-V relations were determined by using sequences of 200-ms pulses applied just before and at the end of the latter period. In sixteen experiments, E_{rev} was −31.4 ± 1.2 mV when the holding potential was −10 mV, and −61.0 ± 0.8 mV ($P < 0.001$) after it had been shifted to −80 mV (Figure 29B). Calculations based on the assumptions that K^+_o was 5.4 mM and $E_{rev} \approx E_K$ suggest that the concentration of intracellular K^+ pertinent to E_{rev} was several millimolar lower than that in the pipette solution (20 mM) when the holding potential was −10 mV, and a three-times-higher 54 mM when the holding potential was −80 mV. It is possible that the inward holding current caused a depletion of K^+_T that affected E_{rev}. However, it is important to note that even if K^+_T had been lowered to, say, an implausibly-low 2 mM, mean K^+_o would have been 3.7 mM, and calculated $K^+_i \approx 37$ mM or nearly 100% larger than calculated K^+_i when the holding potential was −10 mV. (The "implausible" term here is based on simulations by Pásek *et al.* (2003) suggesting that lowering of K^+_T to 2 mM in guinea-pig ventricular myocytes requires pulses to ≈ 80 mV negative to E_{rev}).

Increase in K^+_o. When myocytes bathed in 5.4-mM K^+ solution and dialyzed with 10-mM K^+ pipette solution were held at −40 mV for 10 min after patch-breakthrough, E_{rev} was near −30 mV (e.g., Figure 27). It seemed likely that K^+ influx (at −40 mV) in such myocytes would be enhanced by raising K^+_o from 5.4 to 20 mM because this ought to increase both inward driving force and K1 channel conductance (see Figure 4A).

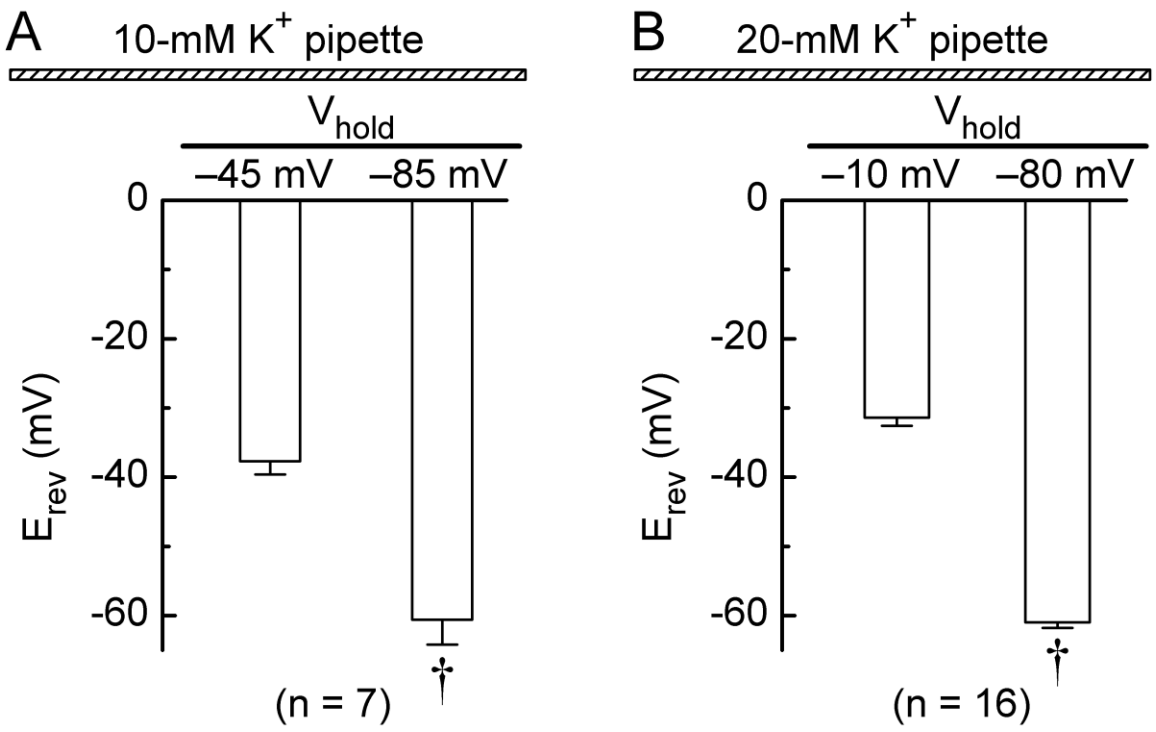

Figure 29. Effects of negative shifts in holding potential on E_{rev} in low-K^+_i myocytes. **A,B**. Myocytes were dialyzed with 10- or 20-mM K^+ pipette solution and superfused with 5.4-mM K^+ Na^+ solution. The holding potential (V_{hold}) was set at –45 mV (A) or –10 mV (B) for 10-12 min and then shifted to –85/–80 mV (with the objective of increasing inward I_{K1}). E_{rev} values were determined from I-V relations obtained using 500-ms steps applied from V_{hold} just before and 5 min after the shifts in holding potential. † $P < 0.001$, paired *t* test. Number of myocytes in parentheses.

Myocytes dialyzed with 10-mM K^+ pipette solution and held at –40 mV were superfused with 5.4-mM K^+ $NMDG^+$ solution for ≈ 15 min, and then with 20-mM K^+ $NMDG^+$ solution for an additional 5 min. I-V relations were obtained using 2.4-s ramps from –160 to +20 mV every 20 s. Raising K^+_o caused a shift in holding current of –1025 ± 44 pA, and a shift in ramp-determined E_{rev} (ΔE_{rev}) of +13.5 ± 0.9 mV (n = 7) ($P < 0.001$) (data not depicted). This ΔE_{rev} is considerably smaller than the ΔE_{rev} expected on the basis of $E_{rev} \approx E_K$ where E_K is calculated on the assumption that subsarcolemmal K^+ in the test myocytes is unaffected by the increase in K^+_o (i.e., in the latter case, $\Delta E_{rev} \approx \Delta E_K$=–61(log 5.4/20), or +35 mV). Since it seems unlikely that there was any substantial depletion of K^+_T related to large inward holding current/ramp current during the superfusions with 20 mM K^+ solution, the most straightforward explanation for the observed ΔE_{rev} of just +13.5 mV is that the increase in K^+ influx increased subsarcolemmal K^+ concentration by at least 100 %.

3.5.4.2. Effects Of Decreasing K^+ Influx By Decreasing Inward Holding I_{K1}

A number of experimental protocols were used to decrease inward holding I_{K1} in myocytes held at a potential negative to E_{rev}. These included removal of external K^+, application of a low concentration of Ba^{2+}, and application of low concentrations of Cs^+.

Removal of external K^+. Myocytes dialyzed with 0-mM K^+ pipette solution were superfused with 5.4-mM K^+ Na^+ solution for 12-15 min, 0-mM K^+ Na^+ solution for ≈ 10 min, and 5.4-mM K^+ Na^+ solution once again. During these superfusions, the myocytes were held at –80 mV and pulsed to –40 mV except for periodic sequences of 500-ms prepulses to –40 mV followed by 500-ms test pulses to voltages between –85 and –25 mV. The current records obtained near the end of the initial 5.4-mM K^+ superfusion indicated that E_{rev} was ≈ –55 mV (not shown). The current traces in Figure 30A indicate that there was little current elicited by test pulses after the switch from 5.4-mM to 0-mM

K^+ solution, and robust currents after the subsequent switch to 5.4-mM K^+ solution. The records also indicate that E_{rev} was near –55 mV after the latter switch.

An evaluation of whether E_{rev} was shifted to a more positive value as a consequence of inhibiting the inward holding current that was present during the initial superfusion with 5.4-mM K^+ solution can be made by considering the amplitudes and directions of the currents at –80 and –40 mV during the restoration of that inward I_{K1} following the switch from 0-mM to 5.4-mM K^+ solution (Figure 30B). Within 1 min of the switch to 5.4-mM K^+ solution, the holding current at –80 mV had increased from approximately zero to –1.6 nA; during the same time, the test current at –40 mV had increased from approximately zero to –0.24 nA. An extrapolation of these values on an I-V plot suggests that E_{rev} at this juncture was near –25 mV. Taking $E_{rev} \approx E_K = -25$ mV, the subsarcolemmal concentration of K^+ was ≈ 14 mM provided that K^+_o had reached 5.4 mM. If K^+_o had not yet reached that level, and/or K^+_T was lower than bulk K^+_o, the subsarcolemmal K^+ was lower than 14 mM. Approximately 1 min later, the current at –80 mV was ≈ –1.8 nA, and the current at –40 mV was ≈ zero. Thus, E_{rev} was now ≈ –40 mV, and calculated subsarcolemmal K^+ was ≈ 25 mM assuming that mean K^+_o was 5.4 mM. At steady-state several minutes later, E_{rev} was ≈ –55 mV (Figure 30B, right). On the assumption that mean K^+_o = 5.4 mM at that time, calculated subsarcolemmal K^+ concentration was ≈ 43 mM. In other words, the termination of K^+ influx at the holding potential following the switch from initial 5.4-mM to 0-mM K^+ solution resulted in a ca. 70% decrease (from 43 to 14 mM) in the concentration of subsarcolemmal K^+. Similar results were obtained in five other experiments of this type.

It is important to consider whether the foregoing conclusion holds up, at least qualitatively, in the event that mean K^+_o was lower than 5.4 mM as a consequence of K^+_T

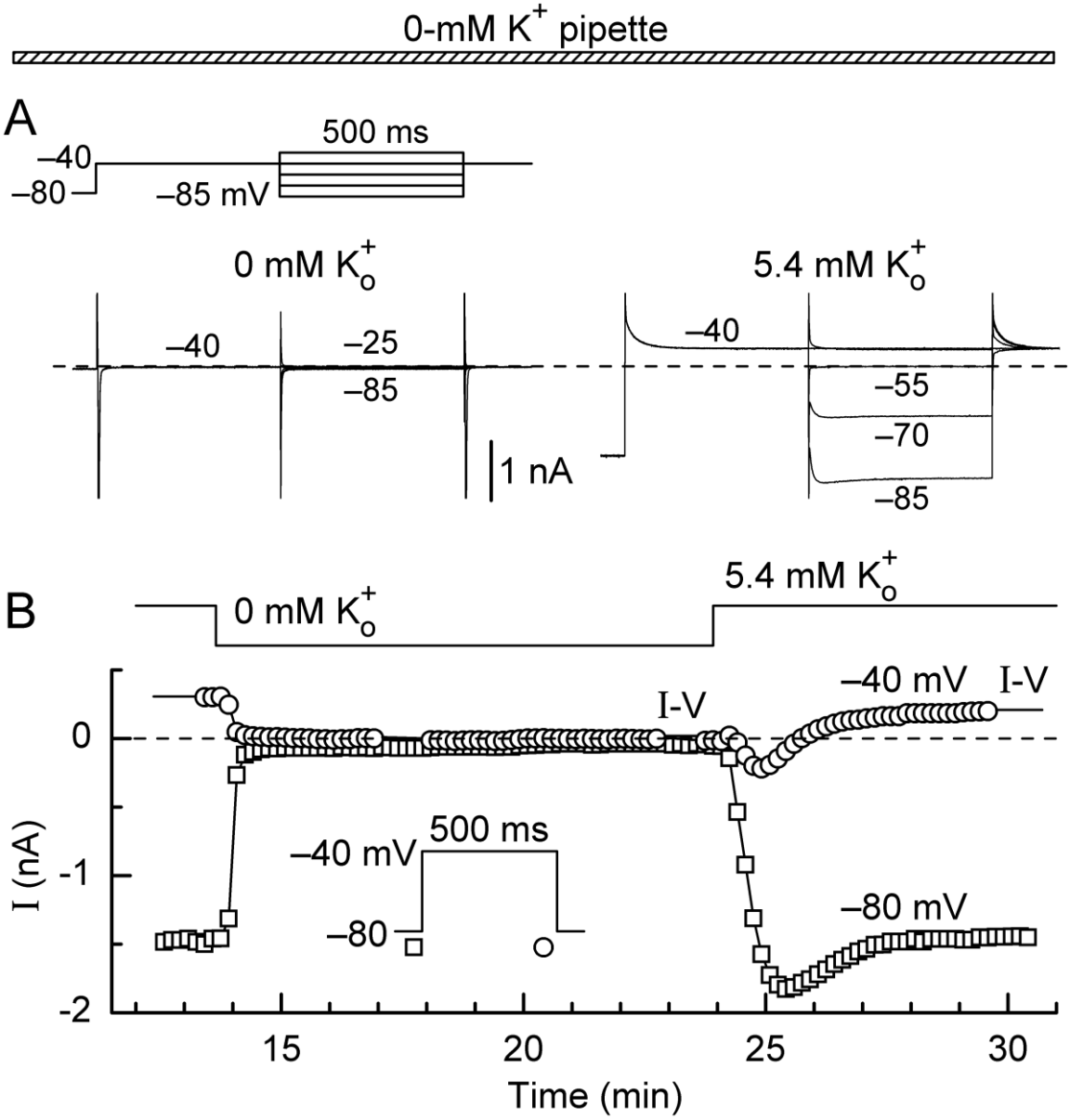

Figure 30. Effects of removal of external K^+ on inward holding I_{K1} and E_{rev} in a low-K^+_i myocyte. The myocyte was dialyzed with 0-mM K^+ pipette solution and sequentially bathed with 5.4-mM K^+ (not shown), 0-mM K^+, and 5.4-mM K^+ Na^+ solutions for ≈ 10 min each. During this time, the myocyte was pulsed from –80 to –40 mV for 500 ms at 0.1 Hz except for determinations of I-V relations using sequences of 500-ms test pulses**. A.** Records obtained on I-V runs at the times marked "I-V" in panel B. The dashed line indicates the zero-current level. **B.** Time plot of the amplitudes of currents at –80 and –40 mV.

< 5.4 mM due to depletion (inward holding I_{K1}) at −80 mV and lack of full repletion during the prepulse to −40 mV and during the test pulse to −55 mV (see Figure 30A). Even if K^+_T had been 2.6 mM (i.e., mean K^+_o 4 mM), calculated K^+_i at steady state was 32 mM, or more than twice the ≤ 14 mM at 1 min.

Application of 30 μM Ba^{2+}. Two low-K^+_i myocytes were exposed to low Ba^{2+} for 4 min to partially block K1 channels and thereby decrease inward I_{K1} at a holding potential negative to E_{rev}. The results obtained in one of these experiments are shown in Figure 31. The myocyte was dialyzed with 10-mM K^+ pipette solution, pulsed from holding potential −60 mV to test potential −30 mV every 15 s, and superfused with 0-mM K^+ solution. After 10 min, the superfusate was changed to 5.4-mM K^+ solution until currents had stabilized. At that point, the 5.4-mM K^+ solution was supplemented with 30 μM Ba^{2+} for 4 min. The Ba^{2+} reduced the inward holding current at −60 mV by about 75%, and reduced the outward current at test potential −30 mV by an even greater amount (Figure 31A). A plausible explanation for this seemingly anomalous action by Ba^{2+} (stronger block at a more positive voltage) is that in addition to blocking K1 channels at −30 mV, it caused a lowering of outward K^+ driving force at that potential. This view is supported by the configurations of the ramp currents recorded during the experiment (Figure 31B). The introduction of Ba^{2+} shifted E_{rev} from −51 mV to −33 mV. A similar result (shift of +16 mV) was obtained in the other experiment of this type, suggesting that inhibition of inward holding I_{K1} by Ba^{2+} can result in a lowering of subsarcolemmal K^+ via restriction of K^+ inflow and resultant dissipation of the intracellular K^+ gradient.

Application of Cs^+. The objective of these experiments was to determine whether there is a relation between the degree of reduction of inward holding I_{K1} by I_{K1}-blocker Cs^+, and the degree of shift of E_{rev} in low-K^+_i myocytes. In preparation for this

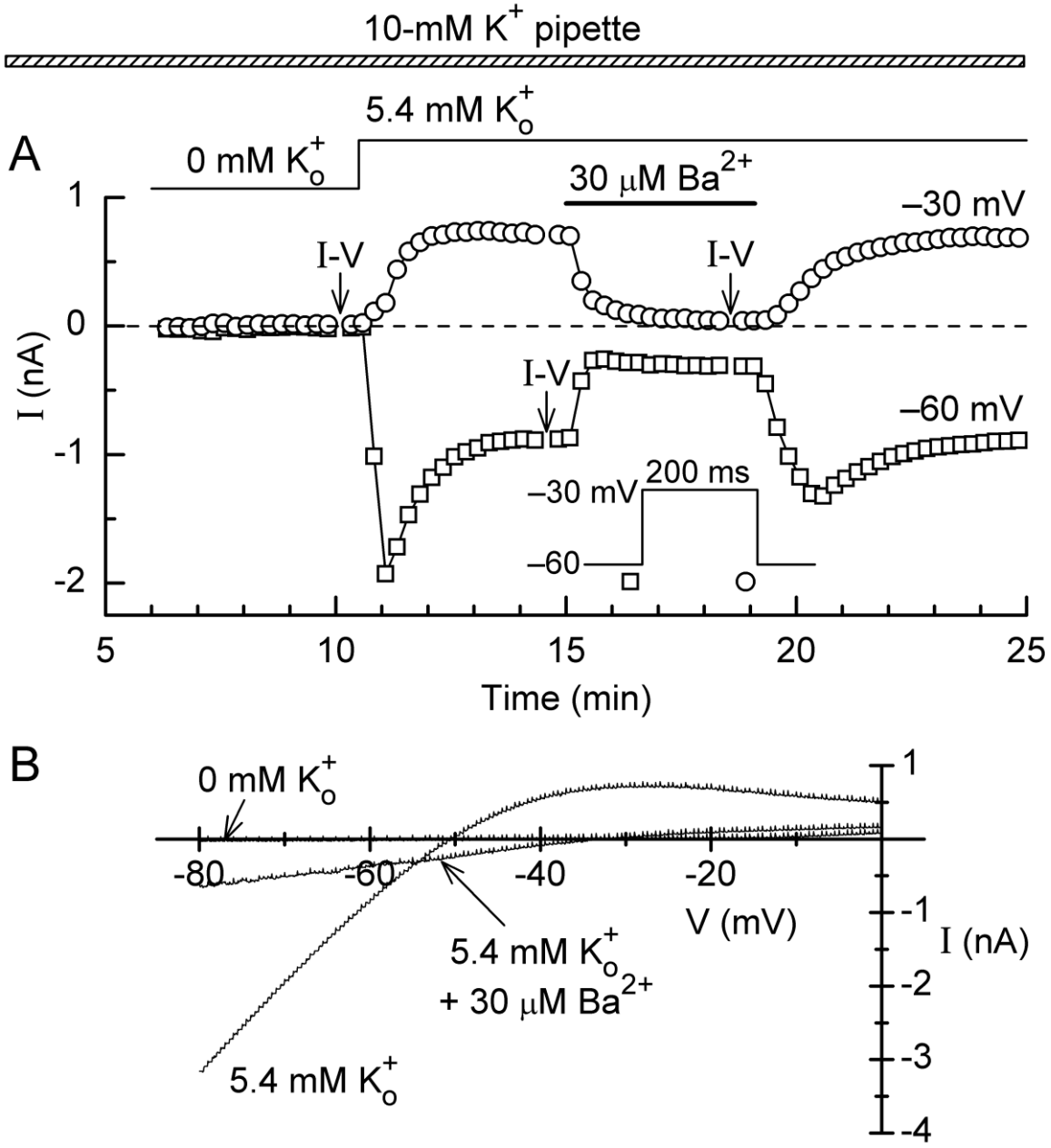

Figure 31. Effects of Ba^{2+}-induced reduction of inward holding I_{K1} on E_{rev} in a low-K^+_i myocyte. The myocyte was dialyzed with 10-mM K^+ pipette solution and sequentially superfused with 0-mM K^+ Na^+ solution , 5.4-mM K^+ Na^+ solution, 5.4-mM K^+ Na^+ solution that contained 30 μM Ba^{2+}, and 5.4-mM K^+ Na^+ solution once again. **A.** Time plot of the amplitudes of currents at holding potential –60 and test potential –30 mV. **B.** Ramp I-V relations obtained at the times indicated in panel A. The Ba^{2+}-induced reduction of resting inward I_{K1} at –60 mV (see A) contributed to an 18-mV shift in E_{rev}.

determination, experiments were conducted to assess the Cs^+ sensitivity of I_{K1} in myocytes dialyzed with 20-mM K^+ pipette solution and bathed with 5.4-mM K^+ solution. Myocytes were held at −10 mV and hyperpolarized to −60 mV for 200 ms at 0.1 Hz to elicit inward I_{K1} before and during application of Cs^+ for 5-7 min and subsequent application of 1 mM Ba^{2+} to null the current. Evaluations on eight myocytes established that (i) 1 mM Cs^+ had no effect on I_{K1} at holding potential −10 mV, and (ii) inhibition of I_{K1} at −60 mV was well-described by a Hill equation, I_{K1} (% Ctl) = 100/ (1 + $([Cs^+]/IC_{50})^n$), with IC_{50} = 0.20 ± 0.02 mM and Hill coefficient n = 1.02 ± 0.10 (data not depicted). This IC_{50} is nearly forty times lower than that determined in normal-K^+_i myocytes (see Section 3.1.2 above). With this information in hand, test myocytes were dialyzed with 20-mM K^+ pipette solution, bathed with 5.4-mM K^+ solution, and held at −80 mV. After a 30-min equilibration period, the myocytes were treated with either 0.03, 0.1, 0.3, or 1 mM Cs^+ for 10-12 min, and then with 5 mM Ba^{2+} to null I_{K1}. I-V relations were determined using 1.6-s voltage ramps from +20 mV down to −140 mV every 30 s.

The difference (Cs^+ minus Ba^{2+}) ramp I-V relations shown in Figure 32A illustrate that (i) the I-V relations in low-K^+_i myocytes exposed to low concentrations of Cs^+ had inverted-bell shapes, and (ii) the voltage at maximum inward I_{K1} was more positive the higher the concentration of Cs^+. In regard to interplay between inward holding I_{K1} and subsarcolemmal K^+, the pertinent finding was that Cs^+ inhibited inward holding I_{K1} and shifted E_{rev} to a more positive potential. E_{rev} was −50, −46, −38, and −35 mV in the myocytes treated with 0.03, 0.1, 0.3, and 1 mM Cs^+, respectively (Figure 32A).

The I-V relations in Figure 32A indicate that the Cs^+-induced rightward shift in E_{rev} was coincident with a marked reduction in the amplitude of the inward holding current at −80 mV. Figure 32B shows a plot of E_{rev} versus inward holding I_{K1}.The results from the

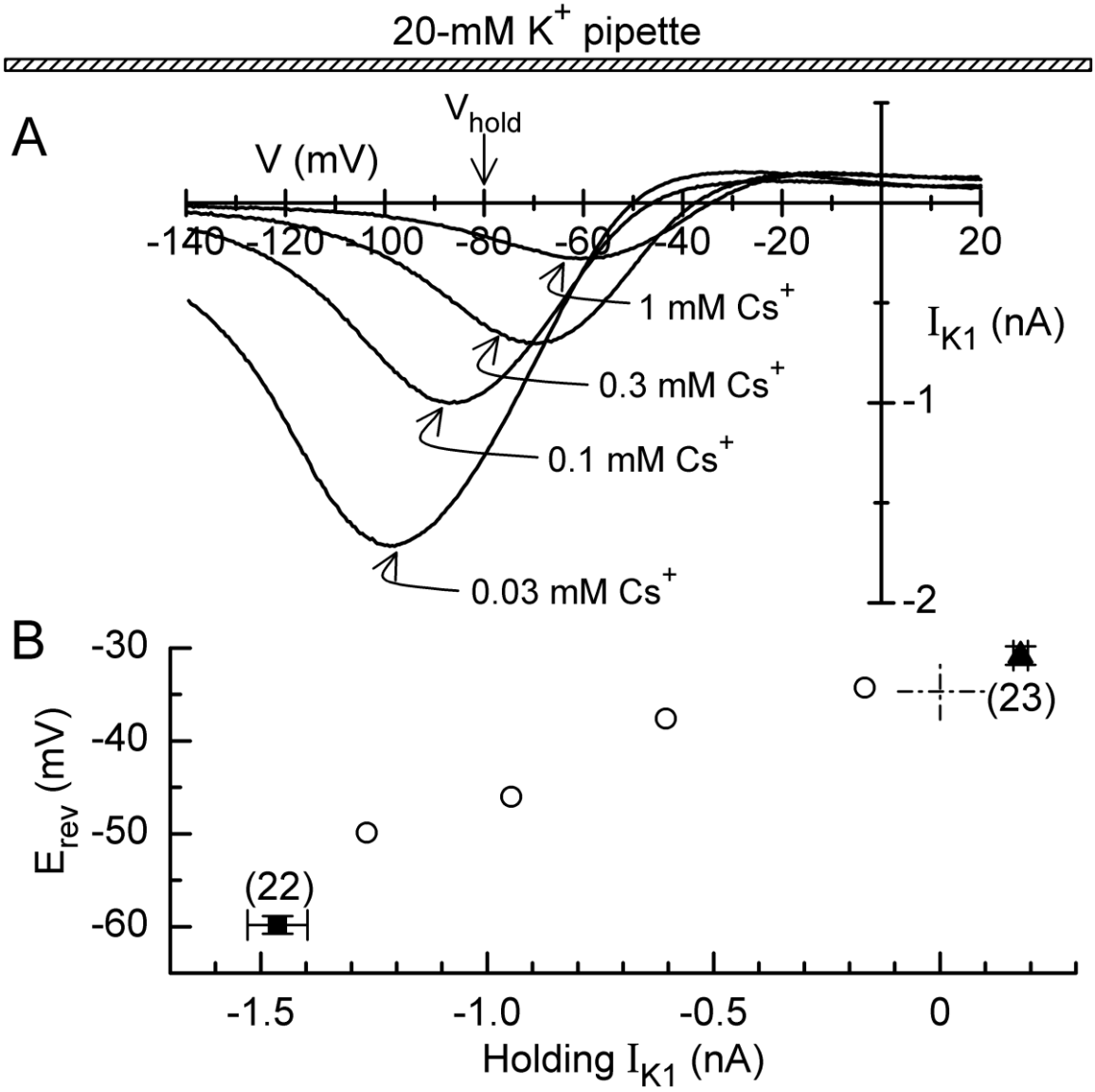

Figure 32. Effects of Cs^+-induced reduction of inward holding I_{K1} on E_{rev} in low-K^+_i myocytes. Myocytes were bathed with 5.4-mM K^+ Na^+ solution and dialyzed with 20-mM K^+ pipette solution. **A.** I_{K1} and E_{rev} in four myocytes held at −80 mV, probed with 1.6-s voltage ramps from +20 to −140 mV every 30 s, treated with Cs^+ for 10-12 min, and then treated with 5 mM Ba^{2+}. The Cs^+ – Ba^{2+} difference currents reveal that treatment with Cs^+ caused positive shifts in E_{rev}. **B.** Plot of E_{rev} versus amplitude of holding I_{K1}. Open circles: Cs^+ data from panel A. Filled symbols: reference data from (non-Cs^+) experiments at holding potential −80 mV (square) and −10 mV (triangle). Includes data from experiments related to Figure 29B. Crosshairs: reference intersection of $E_{rev} \approx E_K$ (K^+_i = 20 mM) and zero I_{K1}. Number of myocytes in parentheses.

Cs^+ experiments are represented by the open circles, and average E_{rev} and holding current amplitudes from experiments in which the holding potential was −80 mV (n = 22) or −10 mV (n = 23) are represented by the filled symbols. The overall pattern is one of a dependence of E_{rev} on the amplitude of inward holding I_{K1}.

3.5.4.3. Loss Of K^+ From Subsarcolemmal Space

Many of the experiments described above concerned inward holding I_{K1} and putative accumulation of K^+ in subsarcolemmal space. A question that arises is what happens to the accumulated K^+ when the K^+ inflow stops or is replaced by an outflow. To address this, experiments were performed in which myocytes dialyzed with 10-mM K^+ pipette solution were held at −85 mV for ≈ 5 min to promote K^+ inflow, and −45 mV to shut off the inflow. During this time, the current at −45 mV was monitored as test current at the end of 200-ms step depolarizations from holding potential −85 mV, and then as holding current.

The results obtained from one of these experiments are depicted in Figure 33. At the moment before the shift of the holding potential to −45 mV, the amplitude of the inward holding I_{K1} at −85 mV was approximately −2 nA (not shown) and E_{rev} was likely to have been near −60 mV (e.g., see Figure 27). Within seconds after the shift, the large K^+ inflow at the holding potential had been replaced by a small outflow (Figure 33, open circle at ≈ 16 min) that waned over the next 30 s in a manner that most likely reflected a dissipation of the outward driving force on K^+. The fact that the current did not simply decline in amplitude with time, but actually turned inward in direction, provides a strong indication that "extra" K^+ in the subsarcolemmal space is drawn down not only via I_{K1}-mediated diffusion to the extracellular space, but also via diffusion to the pipette. The time course of the process was a relatively slow one; in eight experiments of this type, the halftime was 44 ± 2 s.

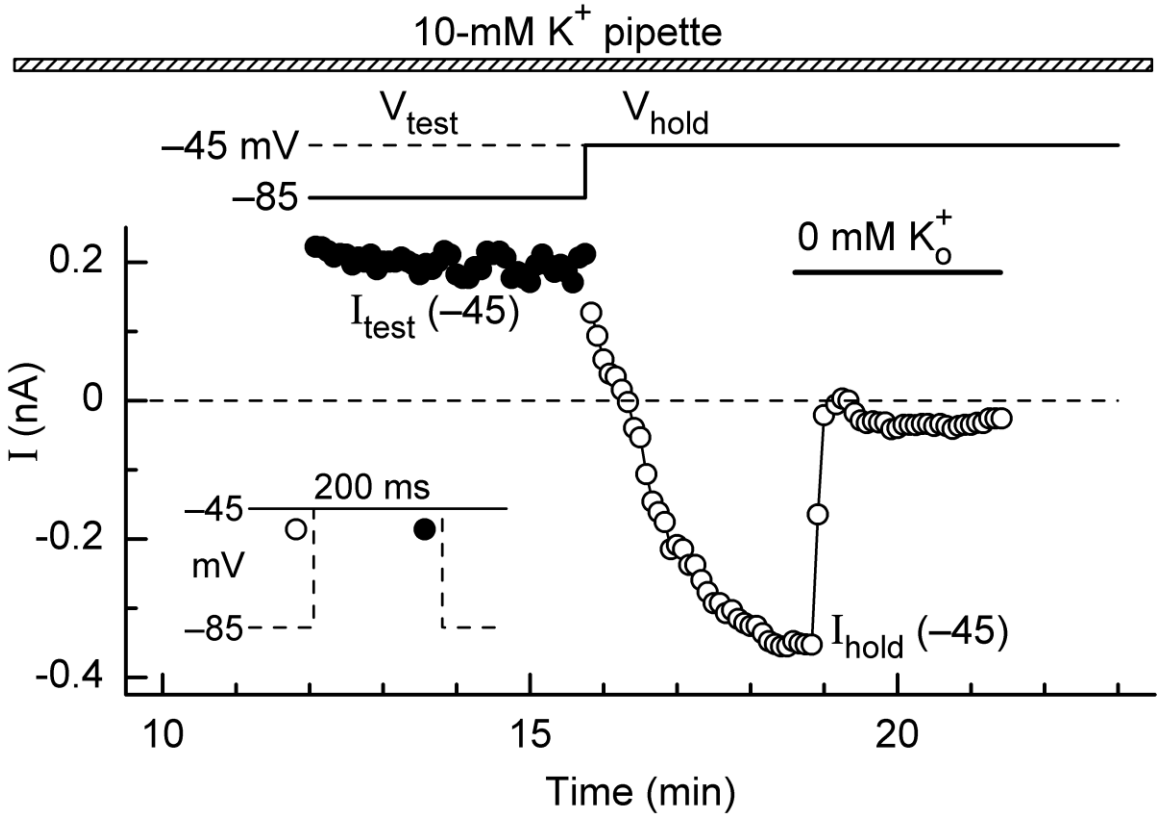

Figure 33. Slow equilibration and change in direction of I_{K1} (–45 mV) following a 40-mV shift in holding potential. The myocyte was dialyzed with 10-mM K^+ pipette solution, superfused with 5.4-mM K^+ Na^+ solution, and sequentially held at –85 and –45 mV. The current at –45 mV (circles) was monitored as test current elicited by 200-ms steps from –85 mV or as holding current. The shift in holding potential to –45 mV terminated large K^+ influx via large inward holding I_{K1} at –85 mV (≈ –2.4 nA, not shown); thereafter, outward I_{K1} at –45 mV did not simply get smaller with time (as would be expected for outward-I_{K1}-mediated loss of accumulated K^+_i), but actually turned inward in direction.

3.6. DEPENDENCE OF G_{K1} ON K^+_i

3.6.1. ChordG_{K1} Parameters During Lowerings Of K^+_i

Chord conductance parameters of macroscopic K1-channel conductance (chordG_{K1}) (see Noble, 1965; Boyett *et al.*, 1980; Tourneur *et al.*, 1987) were calculated from I-V relations obtained from myocytes that were dialyzed with 10-mM K^+ pipette solution and held at –40 mV to promote a decline in intracellular K^+ and a positive shift in the E_{rev} of I_{K1}. Ramps from –110 to +20 mV were applied every 15 s, with the first one at 15-30 s post-patch-breakthrough and the last one at 150-165 s post-patch-breakthrough. The amplitudes of the currents elicited by the ramps were measured at 2-mV intervals and converted to chordG_{K1} data by dividing them by $V–E_{rev}$. The chordG_{K1} data were then fitted with the Boltzmann function, chordG_{K1} = chordG_{K1}max/(1 + exp (($V_{0.5}$ – V)/S)), where chordG_{K1}max is maximal chordG_{K1}, $V_{0.5}$ is the voltage at which chordG_{K1} is one-half of chordG_{K1}max, and S is a slope factor (cf. Cohen *et al.*, 1989; Missan *et al.*, 2004).

Figure 34 shows results from an experiment in which the first ramp was applied at 20 s and the tenth one at 155 s. The chordG_{K1}-V data derived from the ramp I-V relation at 155 s are shifted to the right of the data at 20 s; however, each set of data is well-described by a non-linear least-square fit of the Boltzmann function (Figure 34A). The values of the parameters obtained from fits to data from each of the ten ramps are plotted against E_{rev} in Figure 34B and C. ChordG_{K1}max declined from 92 to 75 nS, and $V_{0.5}$ from –63 to –44 mV, as E_{rev} declined from –80 to –50 mV. However, slope factor S was almost unchanged at ≈ –15.5 mV (Figure 34C).

Fourteen myocytes were investigated in the manner described above. In these myocytes, E_{rev} declined from –79.3 ± 0.9 mV on the first ramp, to –45.9 ± 1.7 mV (calculated K^+_i ≈ 30 mM) on the tenth ramp ($P < 0.001$). ChordG_{K1}max declined from

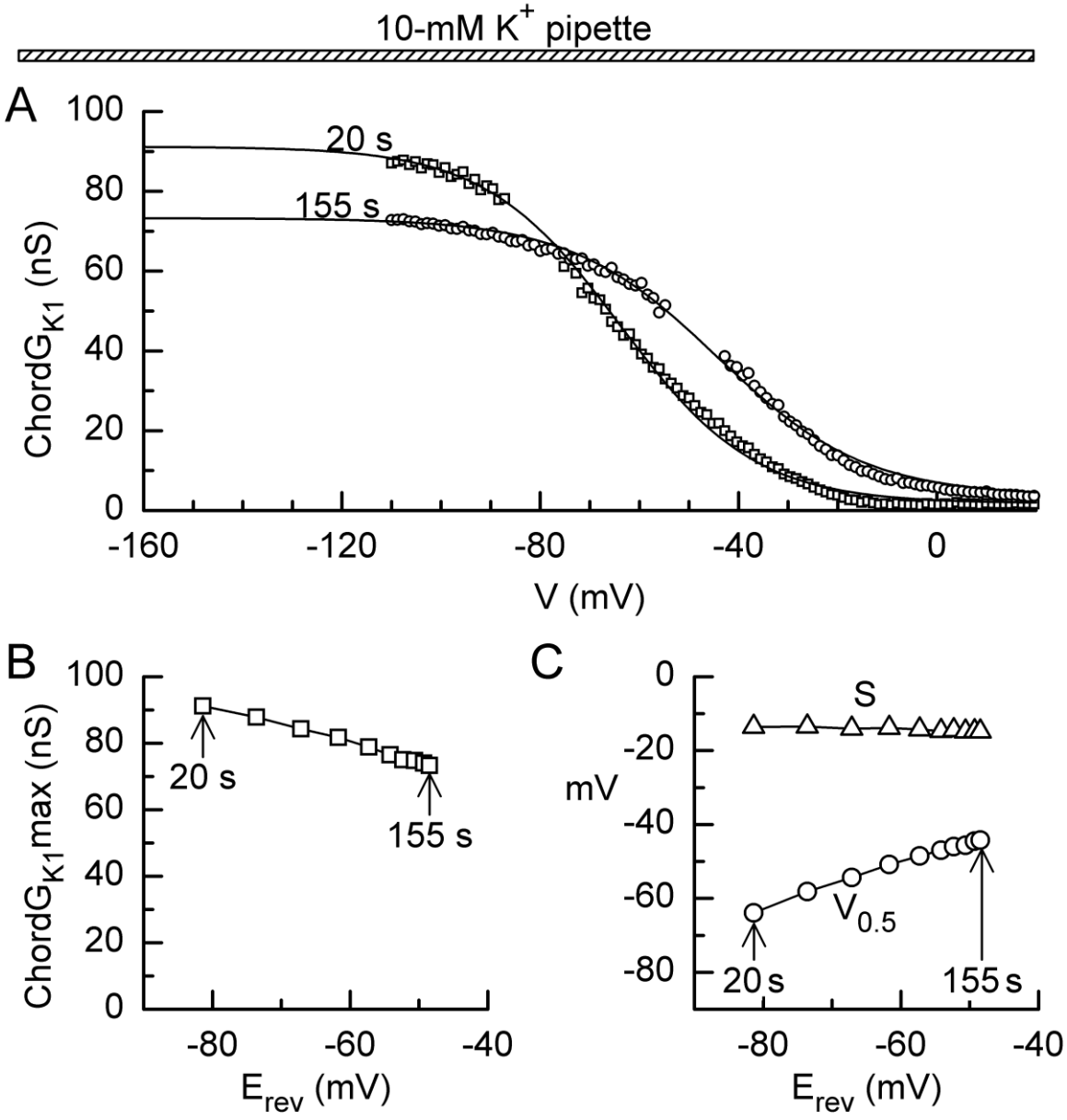

Figure 34. $ChordG_{K1}$ parameters during the early stages of dialysis of a myocyte with 10-mM K^+ pipette solution. The myocyte was superfused with 5.4-mM K^+ $NMDG^+$ solution, held at –40 mV, and probed with 1.5-s voltage ramps at 20 s post-patch-breakthrough and every 15 s thereafter. $ChordG_{K1}$ data obtained by dividing ramp I-V data by $V–E_{rev}$ were fitted with the Boltzmann function. **A.** Boltzmann fits (solid lines) to $chordG_{K1}$ data calculated from the 20-s and 155-s ramp I-V data. **B,C.** Dependence of $G_{K1}max$, S, and $V_{0.5}$ on E_{rev}.

102.5 ± 5.1 nS on the first ramp, to 87.5 ± 3.8 nS on the tenth ramp ($P < 0.001$) (Figure 35A), and there was a slight change in the steepness of the chordG_{K1}-V relation ($P < 0.01$) (Figure 35B). $V_{0.5}$ shifted from −63.6 ± 1.9 mV on the first ramp, to −44.7 ± 1.8 mV on the tenth ramp ($P < 0.001$) (Figure 35B). Importantly, shifts in $V_{0.5}$ with time were not observed in experiments on normal-K^+_i myocytes (0.5 min: −66.4 ± 2.1 mV; 10 min: −68.2 ± 2.4 mV (n = 11)).

3.6.2. ChordG_{K1} And Holding Potential In Low-K^+_i Myocytes

To obtain further information on the relationship between G_{K1} and E_{rev} in low-K^+_i myocytes, chordG_{K1} parameters were determined in experiments in which E_{rev} was quickly shifted by ≈ −30 mV. The myocytes were dialyzed with 20-mM K^+ pipette solution and superfused with 5.4-mM K^+ solution, and the shifts in E_{rev} were achieved by moving the holding potential from −10 mV to −80 mV. I-V relations were determined just before and 5 min after the move in holding potential by using a series of 200-ms voltage steps. E_{rev} values were obtained from polynomial interpolations of I-V data near apparent zero-current crossings, and chordG_{K1} data were calculated from I-V and E_{rev} data and fitted with the Boltzmann function.

In sixteen experiments, the shift in holding potential increased E_{rev} from −31.4 ± 1.2 mV to −61.0 ± 0.8 mV ($P < 0.001$), increased chordG_{K1}max from 80.9 ± 3.5 to 90.9 ± 4.1 nS ($P < 0.001$), and shifted $V_{0.5}$ from −46.1 ± 1.1 mV to −57.8 ± 1.5 mV ($P < 0.001$) (data not depicted; same myocytes as in Figure 29B).

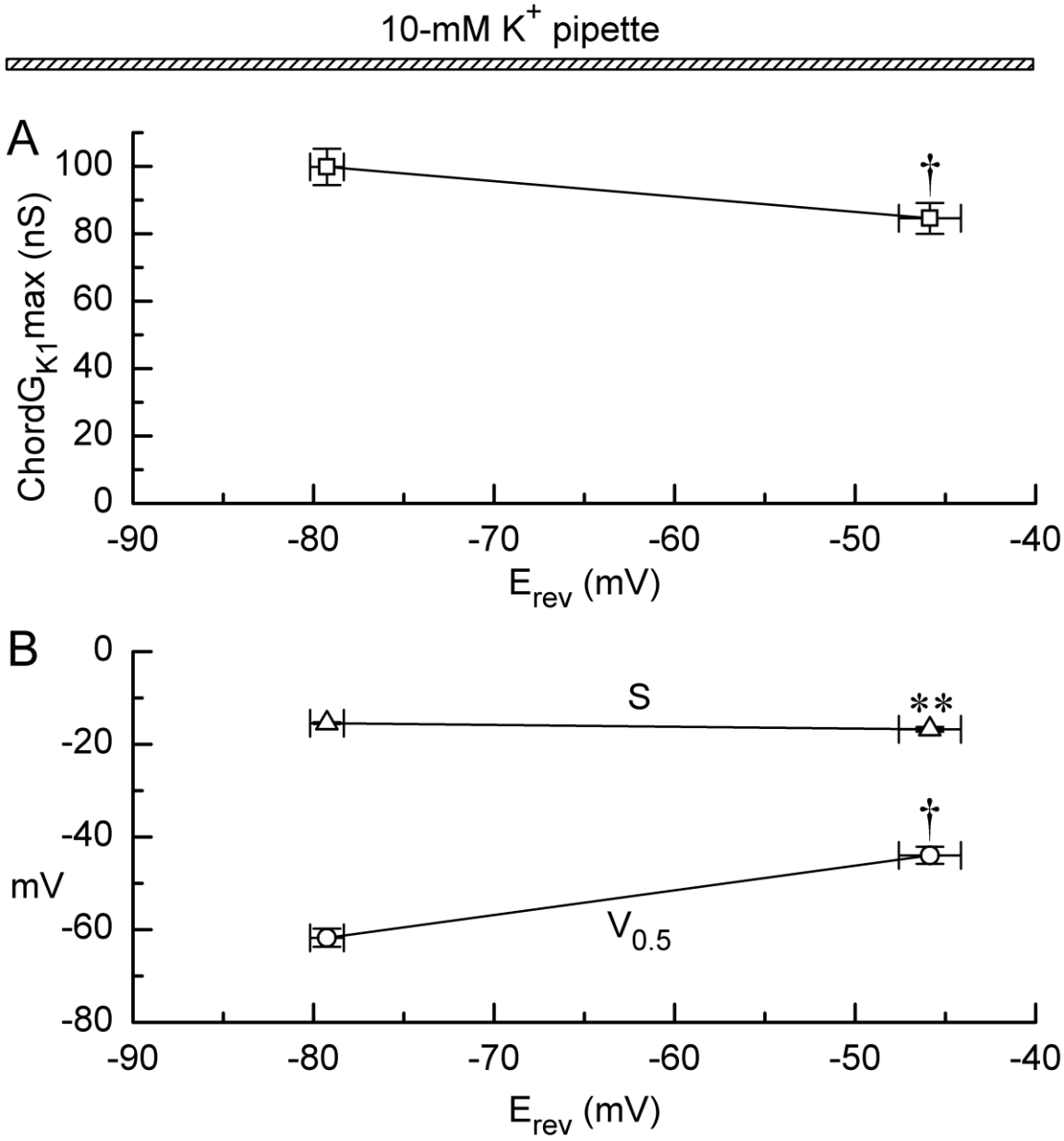

Figure 35. Summary of changes in chordG_{K1} parameters during the early stages of dialysis of myocytes with 10-mM K^+ pipette solution**.** Same experimental conditions and analysis as in Figure 34. **A,B.** The symbols in line with E_{rev} −80 mV and E_{rev} −45 mV indicate data obtained from first and tenth ramps, respectively, applied every 15 s (n = 14 myocytes). ** $P < 0.01$ and †$P < 0.001$ compared to first ramp, paired *t* test.

3.6.3. Dependence Of SlopeG_{K1}max On E_{rev} And Calculated K^+_i

Figure 36 shows the values of slopeG_{K1}max, E_{rev}, and calculated K_i obtained from experiments on 37 normal-K^+_i myocytes and 83 lowered-K^+_i myocytes bathed with 5.4-mM K^+ Na^+ or 5.4-mM K^+ $NMDG^+$ solution. The slopeG_{K1}max values are plotted against corresponding E_{rev} values in the scattergram of Figure 36A, and against the corresponding calculated-K^+_i values in the scattergram of Figure 36B. The regression line in Figure 36A has slopeG_{K1}max of ≈ 118 nS at E_{rev} of −86 mV, ≈ 109 nS at E_{rev} of −66 mV, ≈ 104 nS at E_{rev} of −56 mV, and ≈ 94 nS at E_{rev} of −36 mV. Thus, these results and those in Figure 36B point to moderate declines in slopeG_{K1}max with reductions in $K^+_{i..}$

3.6.4. Response To Elevation Of K^+_o

An additional finding in regard to G_{K1} in low-K^+_i myocytes comes from experiments in which myocytes dialyzed with 10-mM K^+ pipette solution were held at −40 mV, bathed with 5.4-mM K^+ solution for ≈ 15 min, and then bathed with 20-mM K^+ solution for ≈5 min. In seven experiments (see also Section 3.5.4.1), slopeG_{K1}max increased from 89.3 ± 8.3 to 158.9 ± 15.1 nS (n = 7) ($P < 0.001$) (data not depicted). This 1.8-fold increase in average slopeG_{K1}max is close to the ≈ 1.92-fold increase expected on the basis of a dependence of maximal G_{K1} in mammalian ventricular myocytes on the square root of external K^+ concentration (Sakmann & Trube, 1984; Harvey & Ten Eick, 1988), suggesting that the dependence of G_{K1} on K^+_o is little affected by a lowering of K^+_i.

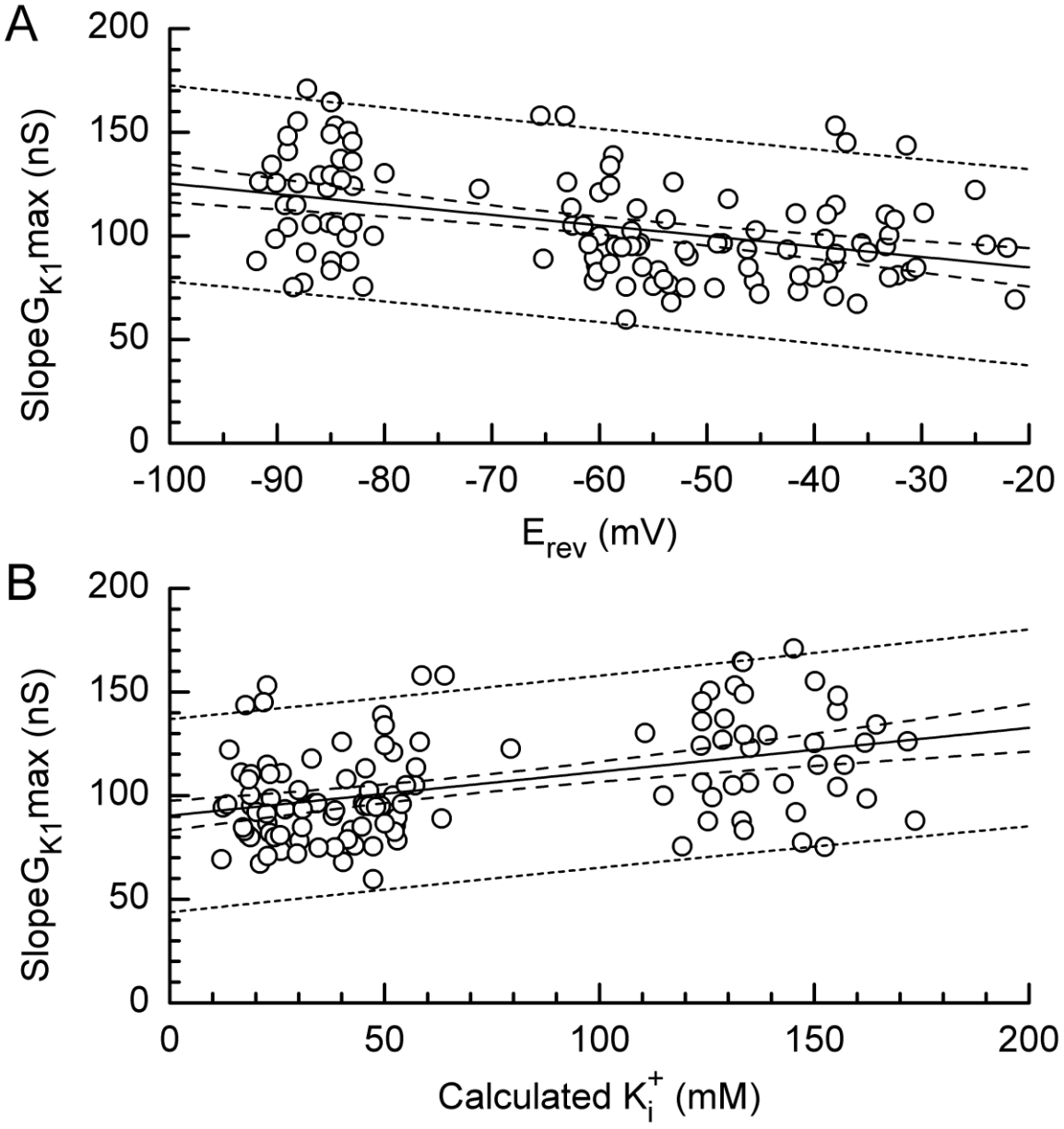

Figure 36. SlopeG$_{K1}$max values determined in experiments on 37 normal-K^+_i myocytes and 83 lowered-K^+_i myocytes. **A.** Scattergram of slopeG$_{K1}$max versus E_{rev}. Linear fit: Y = A + B·X, where A = 74.7 and B = –0.51. **B.** Scattergram of slopeG$_{K1}$max versus K^+_i calculated on the basis $E_{rev} \approx E_K$. Same myocytes as in A. Linear fit: Y = A + B·X, where A = 90.3 and B = 0.21. Solid lines: linear fits of data points; long-dashed lines: 95% confidence limits of the means; short-dashed lines: 95% prediction bands.

CHAPTER 4. DISCUSSION

The results obtained in the study are discussed under five main headings: effects of lowering external K^+ (Section 4.1), accumulation of K^+ in restricted extracellular space (Section 4.2), effects of K^+-free bathing solution (Section 4.3), inward transients (Section 4.4), and I_{K1} in myocytes dialyzed with low-K^+ pipette solution (Section 4.5).

4.1. EFFECTS OF LOWERING EXTERNAL K^+

An objective of the present study was to quantify the effects of lowering K^+_o on parameters that characterize I_{K1}-V relations. These included E_{rev}, voltage at maximal amplitude of the outward limb of the relation, maximal slope of the inward limb of the relation (i.e., slopeG_{K1}max), and maximal amplitude of the outward limb of the relation. The effects of lowering K^+_o from 5.4 to 2 and 1 mM on these parameters are detailed below, and compared with data provided (or estimated from figures) in earlier studies.

4.1.1. Negative Shift In E_{rev}

In the experiments that examined the effects of lowering K^+_o from 5.4 mM to 2 mM, the E_{rev} determined just before the lowering was −85.4 ± 1.3 mV (n = 7). This E_{rev} is in good agreement with values determined in earlier studies on guinea-pig ventricular myocytes bathed with 5.4-mM K^+ solution (e.g., Sakmann & Trube, 1984; Matsuura *et al.*, 1987; Aronson & Nordin, 1988; Martin *et al.*, 1995; Warren *et al.*, 2003). The effect of lowering K^+_o to 2 mM was to shift E_{rev} to −111.4 ± 1.9 mV (n = 7). This E_{rev} can be compared with values obtained in earlier studies on the following types of ventricular

myocytes: −105 mV (guinea-pig, n = 1) (Aronson & Nordin, 1988), −109 mV (bovine, n = 1) (Isenberg & Klöckner, 1982), and (estimated) −109 ± 4 mV (cat, n = 8) (Harvey & Ten Eick, 1988). Thus, the present results on guinea-pig ventricular myocytes are in good agreement with results obtained in the earlier studies, especially those on bovine and cat ventricular myocytes.

A lowering of K^+_o from 5.4 mM to 1 mM shifted E_{rev} by nearly −45 mV to −129 ± 0.9 mV (n = 7). This E_{rev} can be compared with two 1-mM-K^+_o E_{rev} values determined in earlier studies, −101 mV (n = 1) in a sheep Purkinje fibre (Dudel *et al.*, 1967) and −127 mV (n = 1) in a rabbit ventricular myocyte (Bouchard *et al.*, 2004) (estimated: their figure 1). Clearly, the latter value and the present one are in good agreement. Furthermore, the present one (−129 ± 0.9 mV) is indistinguishable from the E_K (−130.9 mV) calculated for these myocytes. Although the E_{rev} of I_{K1} in guinea-pig ventricular myocytes bathed in 1-mM K^+ solution may be considered to be at an extremely negative voltage, it is worth noting that there are examples of even more negative ones in the literature. Current records shown by Akuzawa-Tateyama *et al.* (1998) indicate that E_{rev} in a rabbit ventricular myocyte superfused with 0.3-mM K^+ solution was ≈ −145 mV (estimated; their figure 6), and E_{rev} in a rabbit ventricular myocyte superfused with 0.1-mM K^+ solution was ≈ −155 mV (estimated; their figures 6 and 7).

4.1.2. Negative Shift In Voltage At Maximal Amplitude Of Outward I_{K1}

Scrutiny of figures in earlier studies on guinea-pig ventricular myocytes bathed with 5.4-mM K^+ solution (Sakmann & Trube, 1984; Ibarra *et al.*, 1991; Stadnicka *et al.*, 1997; Ishihara *et al.*, 2002; Warren *et al.*, 2003; Dhamoon *et al.*, 2004; Brouillette *et al.*, 2007) indicates that the voltage at which the amplitude of steady-state outward I_{K1} reached its maximum (termed V_{peak} here) was typically between −50 and −65 mV. Thus, the

"control" (5.4-mM K^+) values of V_{peak} determined in experiments on the two groups of myocytes that were subjected to superfusion with lowered-K^+ solution in the present study (–54.9 ± 2.0 mV (n = 7), and –58.3 ± 1.9 mV (n = 7)) are in line with those found in earlier studies.

Lowering K_o from 5.4 mM to 2 or 1 mM shifted V_{peak} to a more negative potential. After a lowering to 2 mM, V_{peak} was –83.3 ± 2.8 mV (n = 7). Although this value is considerably more negative than that indicated in the I-V relation (2 mM K^+_o) obtained from a guinea-pig ventricular myocyte by Spindler *et al.* (1998) (estimated –70 mV, their figure 4A), it is in good agreement with a relation obtained from a rabbit ventricular myocyte by Shimoni *et al.* (1992) (estimated –84 mV, their figure 8), as well as with those obtained from guinea-pig ventricular myocytes by Aronson & Nordin (1988) (estimated –80 mV, their figure 6) and Koumi *et al.* (1995) (estimated –85 mV, their figure 2).

In the present study, a lowering of K^+_o from 5.4 mM to 1 mM shifted V_{peak} from –58.3 ± 1.9 to –98.3 ± 2.8 mV (n = 7). This 1-mM-K^+_o value is more negative than that indicated in the I-V relation (1 mM K^+_o) obtained from a guinea-pig ventricular myocyte by Spindler *et al.* (1998) (estimated –90 mV, their figure 4A), and more negative than that obtained from a rat ventricular myocyte by Bouchard *et al.* (2004) (estimated –92 mV, their figure 1C). However, it is less negative than that indicated in an I-V relation obtained from a rabbit ventricular myocyte by Bouchard *et al.* (2004) (estimated –108 mV, their figure 2).

The results obtained in the present study indicate that both V_{peak} and E_{rev} (see above) shift to more negative potentials when K^+_o is lowered from 5.4 mM. In fact, the plot of V_{peak} versus E_{rev} data in Figure 8B indicates that the two parameters change in

concert (slope 0.95 ± 0.06). Basically, this signifies that the $V_{0.5}$ of the underlying G_{K1}-V relation shifts with E_K as K^+_o is lowered from 5.4 mM, with little change in the slope of the relation. A complementary conclusion, that the $V_{0.5}$ of the G_{Kir}-V relation shifts with E_K as K^+_o is elevated, has been drawn from findings on strong inward-rectifier K^+ systems in frog skeletal muscle fibres (Hestrin, 1981) and bovine pulmonary artery endothelial cells (Silver *et al.*, 1994).

4.1.3. Decrease In G_{K1}

In the present study, the magnitude of slopeG_{K1}max declined to 68.2 ± 3.5% (n = 7) of its control 5.4-mM-K^+_o magnitude when K^+_o was lowered to 2 mM, and to 42.7 ± 5.7% (n = 7) of its control magnitude when K^+_o was lowered to 1 mM. The only comparable data come from a study on cat ventricular myocytes by Harvey & Ten Eick (1988). In that study, slopeG_{K1}max in a myocyte declined to an estimated 61% of the control 5-mM-K^+_o value when K^+_o was lowered to 2 mM (their figure 4B).

When the slopeG_{K1}max data obtained in the present study are positioned on a double-logarithmic plot of slopeG_{K1}max versus K^+_o, they are well-described by a straight line generated by the equation slopeG_{K1}max = A•$(K^+_o)^b$, where *b* (slope of the line) is 0.47 ± 0.07 (Figure 8C). Thus, the dependence of slopeG_{K1}max on K^+_o over the range 5.4 to 1 mM K^+_o is close to that of a square root one (*b* = 0.50). This finding on guinea-pig ventricular myocytes complements an earlier finding by Harvey & Ten Eick (1988). In experiments on cat ventricular myocytes, these investigators observed that the slope of the line fitting log-slopeG_{K1}max versus log-K^+_o data for K^+_o between 2 and 20 mM was 0.56.

It is of interest to compare the present conductance data from guinea-pig ventricular myocytes with data from studies on strong inward-rectifier K^+ pathways in noncardiac

cells. Straight-line fits of log-slopeG_{Kir}max versus log-K^+_o data had slopes between 0.46 and 0.55 in studies on bovine pigmented ciliary epithelial cells probed with K^+_o 0.5 to 50 mM (Stelling & Jacob, 1992), RBL-1 cells probed with K^+_o 5.4 to 100 mM (Wischmeyer *et al.*, 1995), rat coronary artery smooth muscle cells probed with K^+_o 6 to 140 mM (Bradley *et al.*, 1999), bovine pulmonary artery epithelial cells probed with K^+_o 6 to 120 mM (Voets *et al.*, 1996), and Kir2.1-expressing oocytes probed with K^+_o 4 to 20 mM (Kubo *et al.*, 1993). It is also of interest that the elementary conductance of strong inward-rectifier K^+ channels at voltages negative to E_K varies approximately with $\sqrt{K^+_o}$ for K^+_o above ≈ 10 mM. This is indicated by the results of studies on cell-attached patches of rabbit (Kameyama *et al.*, 1983) and guinea-pig (Sakmann & Trube, 1984; Vandenberg, 1987) ventricular myocytes, as well as by the results of studies on cell-attached patches of cultured murine macrophages (McKinney & Gallin, 1988), rabbit osteoclasts (Kelly *et al.*, 1992), and Kir2.1-expressing host cells (Klein *et al.*, 1999; D'Avanzo *et al.*, 2005).

The actual mechanism whereby K^+_o modulates G_{K1} (and G_{Kir} in noncardiac cells) remains as unclear as it was three decades ago (for example, see Leech & Stanfield, 1981; Chang *et al.*, 2010). One proposal is that external K^+ ions have direct activatory action on the K^+ channels, most likely by occupying extracellular sites (e.g., Kubo, 1996; Murata *et al.*, 2002) that potentially lie within the selectivity filter (Claydon *et al.*, 2004). The other major hypothesis concerns the blocking-particle model. It holds that external K^+ ions bind to a high-affinity site in the channel pore, and that increases (decreases) in K^+_o weaken (strengthen) pore blockade by intracellular polyvalent cations (e.g., Pennefather *et al.*, 1992; Lopatin & Nichols, 1996; Matsuda *et al.*, 2010).

4.1.4. Decrease In Maximal Amplitude Of Outward I_{K1}

It has long been observed that a several-fold lowering of K^+_o from a control concentration near 5.4 mM causes a reduction in the maximal amplitude of steady-state outward I_{K1} in cardiac preparations (Dudel *et al.*, 1967; Isenberg & Klöckner, 1982; Tseng *et al.*, 1987; Ishihara & Ehara, 1998). In the present study, a lowering of K^+_o to 2 mM reduced the maximal amplitude of the outward current to 63.0 ± 3.1% (n = 7) of the control 5.4-mM maximal amplitude. This percentage is somewhat larger than the 51% value indicated by I-V relations obtained from a guinea-pig ventricular myocyte by Spindler *et al.* (1998) (their figure 4A), and somewhat smaller than that indicated by relations obtained from guinea-pig ventricular myocytes by Koumi *et al.* (1995) (their figure 2). However, it is close to the 60 - 68% indicated by I-V relations obtained from rabbit ventricular myocytes by Shimoni *et al.* (1992) (their figure 8) and Cordeiro *et al.* (1998) (their figure 3). In the present series of experiments in which K^+_o was lowered to 1 mM, the maximal amplitude of outward I_{K1} was reduced to 37.2 ± 3.7% (n = 7) of its control 5.4-mM K^+ amplitude. This value is close to the 41% value estimated from data that Spindler *et al.* (1998) obtained in an experiment on a guinea-pig ventricular myocyte (their figure 4A). Measurements on I-V data published by Bouchard *et al.* (2004) indicate that reduction of K^+_o from 5 to 1 mM reduced the amplitude of maximal outward I_{K1} to ≈ 54% control in a rabbit ventricular myocyte (their figure 1), and to ≈ 41% control in a rat ventricular myocyte (their figure 1), a value close to that found in the guinea-pig ventricular myocytes studied here.

In summary, lowering K^+_o from 5.4 mM to 2 and 1 mM reduced the amplitude of maximal outward I_{K1} to 63.0 ± 3.1 and 37.2 ± 3.7% control, respectively. When the logarithms of these values are plotted against log K^+_o, they are well-fitted by a straight-line function with a slope of 0.54 ± 0.07 (Figure 9D). This near-$\sqrt{K^+_o}$ dependence of

maximal outward current is likely to be related to the near-$\sqrt{K^+_o}$ dependence of slopeG_{K1}max and to a voltage dependence of steady-state rectification of I_{K1} whose $V_{0.5}$ shifts with E_K. In a recent study on outward currents through Kir2.1 channels, Liu *et al.* (2011) suggested that external K^+ regulates the amplitude of outward currents by regulating single-channel conductance independent of changes in channel-opening probability or spermine-binding kinetics.

4.2. ACCUMULATION OF K^+ IN RESTRICTED EXTRACELLULAR SPACE

Yasui *et al.* (1993) used channel-opener nicorandil to activate K_{ATP} channels in guinea pig ventricular myocytes, and found that large flows of outward $I_{K,ATP}$ were followed by inward tail currents on the repolarizations to holding potential −85 mV. They proposed that a depolarization-induced flow of outward $I_{K,ATP}$ causes an accumulation of K^+ in the T-tubules, that this accumulation shifts $E_{K,T}$ to a voltage positive to −85 mV, and that repolarization to −85 mV elicits an inward K^+ tail current that is likely carried by K_{ATP} and K1 channels. Two central findings of Yasui *et al.* (1993), that flows of outward $I_{K,ATP}$ on depolarization evoke inward tail currents on repolarization, and that glibenclamide largely abolishes both of these current components, were confirmed in the present study.

Although there is good evidence that flows of outward I_{K1} can cause substantial accumulations of extracellular K^+ in multicellular cardiac preparations (Baumgarten & Isenberg, 1977; Baumgarten *et al.*, 1977; Boyett *et al.*, 1980), there is seemingly no mention in the literature that they cause accumulations and evoke inward tail currents in experiments on isolated ventricular myocytes. Accumulation-related phenomena may well have been observed and judged to have been peripheral to the topic under

investigation, or not have been observed due to the use of ramps and/or repolarizations to holding potentials well below or well above the E_{rev}.

In the present study, myocytes were held at potentials near the E_{rev} of I_{K1}, and repolarizations that followed depolarization-induced flows of outward I_{K1} elicited inward tail currents. Both of these current components were abolished by Ba^{2+}. Given the experimental solutions that were used (Na^{+}-free EGTA-buffered MgATP dialysate; Na^{+}-free, glibenclamide, Cd^{2+}, E4031 supefusate), and the relatively low amplitude depolarizations that were applied, it is difficult to ascribe the Ba^{2+}-sensitive components to anything other that I_{K1}. A similar argument can be made in regard to concomitant reduction of outward current and inward tail current by Cs^{+}, spermine, and other K1 channel blockers.

It is important to acknowledge that while the inward tail currents are attributed to the consequences of I_{K1}-mediated accumulation of K^{+} in T-tubules, there is no hard evidence that the accumulation is not occurring elsewhere. However, the following suggest that most, if not all, the accumulation occurs in the T-tubules. (i) The character of the outward-I_{K1}-induced inward tails resembled the character of the inward tail currents that were previously observed in ventricular myocytes, but were absent in T-tubule-sparse atrial myocytes (Yasui *et al.*, 1993; Clark *et al.*, 2001). (ii) Rapid-solution-change experiments on guinea-pig and other types of ventricular myocytes indicate that there is relatively slow diffusion of monovalent and divalent cations between exracellular bulk solution and extracellular solution in the T-tubules (Yao *et al.*, 1997; Shepherd & McDonough, 1998). (iii) Mathematical simulations suggest that T-tubules should be viewed as a functional extracellular compartment in which K^{+} can accumulate (Yasui *et al.*, 1993; Swift *et al.*, 2006). Finally, (iv) studies on (T-tubule-less) HEK293 cells

indicate that there is little, if any, accumulation of K^+ after large flows of outward K^+ current (Kiss *et al.*, 1999; Frazier *et al.*, 2000)).

Yao *et al.* (1997) suggested that in addition to T-tubules, physical factors such as sarcolemmal folds, caveolae, and sarcolemmal-surface negatively-charged proteins might contribute to slowed diffusion of extracellular K^+ in heart cells. A major role for surface-sarcolemmal caveolae in the accumulation that engenders inward tail current in ventricular myocytes seems unlikely on the basis that such currents are not observed in atrial myocytes and HEK293 cells (see above). Whether caveolae in T-tubular sarcolemmal are critical for development of inward tail currents is less clear. Singer & Walsh (1980) performed calculations to evaluate whether the K^+ concentration of solution in caveolae is likely to differ from that in bulk solution due to K^+ current flow. They calculated that there would be negligible difference, primarily due to the small length of the neck of the flask-shaped caveolae (even when calculations were performed for necks elongated to an unlikely 60 nm). It could be that the situation is more complex when the caveolae are present in chainlike configurations as in the T-tubular sarcolemma of mouse ventricular myocytes; however, caveolae in the T-tubular sarcolemma of guinea-pig ventricular myocytes are almost always found as single entities (Forbes *et al.*, 1984; Forbes & van Neil, 1988)

A consistent finding in early studies on current-flow-induced accumulation of K^+ in nerve and muscle preparations was that for a given-sized outward K^+ current, the apparent degree of accumulation was reduced by raising the concentration of K^+ in the bathing solution (e.g., Frankenhaeuser & Hodgkin, 1956; Orkand, 1980). A similar modulation by external K^+ was observed in the case of accumulation in multicellular cardiac preparations (e.g., McAllister & Noble, 1966; Baumgarten & Isenberg, 1977;

Baumgarten *et al.*, 1977). In their study on accumulation caused by outward $I_{K,ATP}$ in guinea-pig ventricular myocytes, Yasui *et al.* (1993) found that accumulation-related inward tail currents near E_{rev} were no longer evident when 5.4-mM K^+ bathing solution was replaced by 30-mM K^+ solution. Likewise, Clark *et al.* (2001) observed that there was a marked reduction in the amplitude of inward tail currents induced by large K^+ current in mouse ventricular myocytes when external K^+ was raised from 5.4 to 20 mM. The results reported here are in good accord with the foregoing observations, i.e., the amplitudes of inward tails evoked after equi-sized flows of outward I_{K1} were reduced by a factor of four upon replacement of 5.4-mM K^+ solution with 15-mM K^+ solution. An additional finding was that the amplitude of the tail increased by a factor or approximately two when 5.4-mM K^+ solution was replaced by 2-mM K^+ solution. The simplest explanation for the modulation of tail amplitude by K^+_o is that outward $I_{K1,T}$ can elevate K^+_T to a larger degree when "resting" K^+_T ($\approx K^+_o$) is low rather than high.

An estimate of the increase in K^+_T (ΔK^+_T) induced by a 500-ms flow of outward $I_{K1,T}$ at a potential near V_{peak} can be obtained by using the mean amplitude of the tail current that followed pulses to −50 mV in six experiments, −169 pA, and making the following assumptions: (i) ΔK^+_T-induced changes in rectification and conductance near $E_{K,T}$ were relatively small and can be disregarded, (ii) holding potential was very close to $E_{K,b}$ (the E_K determined by bathing solution K^+), and (iii) 50% of myocyte membrane is T-tubular membrane (Amsellem *et al.*, 1995), and 50% of myocyte G_{K1} is $G_{K1,T}$ (cf. Swift *et al.*, 2006). Then, it can be shown that $E_{K,b} - E_{K,T}$ (or ΔE_K) equals −169 pA/$G_{K1,T}$ (where $G_{K1,T}$ is taken as 50% of the slopeG_{K1} of 69.5 nS at E_{rev} measured in the six experiments). This gives ΔE_K = –4.86 mV, and ΔK^+_T = 1.09 mM.

4.3. EFFECTS OF K^+-FREE BATHING SOLUTION

It has long been appreciated that switching from K^+-containing bathing solution to K^+-free bathing solution dramatically lowers or even nulls I_{K1} in heart cells (e.g., Dudel *et al.*, 1967). For this reason, steady-state I-V relations determined during superfusion with K^+-free solution have often been subtracted from those determined during superfusion with K^+-containing solution to arrive at an improved estimate of the true I-V relation of I_{K1} at that particular K^+_o (e.g., Dudel *et al.*, 1967; Backx & Marban, 1993; Zaza *et al.*, 1998; Yan *et al.*, 2005). Statements concerning whether K^+-free solution abolished all I_{K1} (versus "most of it") are virtually absent in the literature. However, Backx & Marban (1993) contended that superfusion of guinea-pig ventricular myocytes with K^+-free solution resulted in the complete elimination of I_{K1} between −100 and −30 mV. In support of this view, they reported that there was no difference in the I-V relations determined in K^+-free solution and those determined in the presence of 1-2 mM Ba^{2+}**.** In regard to this issue, it is worth noting that Zhang *et al.* (2009) stated that K^+-free solution abolished all current carried by Kir2.1 channels in HEK293 cells.

If one takes the position that superfusion of a ventricular myocyte with K^+-free solution completely abolishes I_{K1}, it is reasonable to suppose that the steady-state I-V relation determined during the superfusion with K^+-free solution will be more or less inward at negative voltages due to various inward leak current components that include "background" nonselective cationic current. In fact, this is the configuration of the I-V relation most commonly presented in the literature for the K^+-free condition at voltages between −30 and ≈ −100 mV. Examples of this configuration of I-V for guinea-pig ventricular myocytes can be found in Ishihara *et al.* (1989), Backx & Marban (1993), Zaza *et al.* (1998), Ishihara & Ehara (1998), and Song & Ochi (2002).

In the present study, the steady-state current in guinea-pig ventricular myocytes superfused with K^+-free $NMDG^+$ solution was invariably outward at voltages as negative as −130 mV, and was frequently outward at voltages as negative as −170 mV. This was a most unexpected finding, and a thorough search of the literature suggested that it was a novel one but for mention in an *abstract* by Carmeliet (1992a) that the steady-state I-V relation in guinea-pig ventricular myocytes bathed in K^+-free Na^+-free solution (Na^+ substitute not stated) and voltage-clamped using a two-suction-pipette method, was outward over the range −30 to −120 mV. Neither figures nor further details were provided. The steady-state outward current in the myocytes investigated here was due to outward K^+ movement through K1 channels because it was absent in myocytes dialyzed with Cs^+ pipette solution rather than K^+ pipette solution**,** had an inwardly-rectifying I-V relation, and was sensitive to inhibition by concentrations of Ba^{2+} as low as 10 μM.

An issue that arises with the finding that the (K^+-free) steady-state I-V relation for I_{K1} is outward over a wide potential range is the level of "trace" K^+ in the K^+-free $NMDG^+$ solution. Mass spectroscopy analysis of the solution indicated levels of K^+ that were below the detection limit (60 μM) of the system that was used (analysis performed by QE II Environmental Services, Halifax). The only reference data found in the literature concerning trace K^+ in K^+-free solution come from Wang *et al.* (2009). They reported that $NMDG^+$ (same supplier as used here) contributed trace K^+ to K^+-free bath solution similar to that used here, such that 140-mM $NMDG^+$ K^+-free bath solution contained ≈ 33 μM K^+ (as measured using inductively coupled plasma optical emission spectroscopy).

For additional insight into the matter of trace K^+ and steady-state outward I_{K1} in myocytes bathed with K^+-free solution, it is useful to turn to simulations of I_{K1}-V

relations for K^+_o concentrations ranging from 5.4 mM down to 0.01 mM. The simulated relations, which are based on $E_{rev} = E_K$ and a dependence of G_{K1} on $\sqrt{K^+_o}$, are shown in the log I_{K1} amplitude *versus* voltage plot of Figure 37A. The next step in the process is to focus on the current amplitude at −85 mV (the standard holding potential used in the experiments with K^+-free solution). This is facilitated by referring to a plot of (simulated) log I_{K1} amplitude at −85 mV, versus log K^+_o for K^+_o ranging from 0.008 mM to 1 mM (Figure 37B). In the figure, the amplitude of I_{K1} at 1 mM K^+_o (filled circle) is in line with that measured in the experiments in which bathing solution K^+ was elevated from nominally 0 to 1 mM (234 ± 33 pA), and the diagonal line extending from there down to the K^+_o axis at 0.008 mM is in accord with the simulated I-V relations of Figure 37A. In the absence of additional information, the concentration of trace K^+ in K^+-free solution is designated as 0.03 mM. The first point to be made is that the amplitude of outward I_{K1} that would be activated by the designated trace K^+ is ≈ 0.7 pA in this scenario (Figure 37B, lower left), or almost two orders smaller than the experimentally measured amplitude (Figure 37B, filled diamond). Thus, according to this scenario, it is highly unlikely that trace K^+ in K^+-free bathing solution is responsible for activation of steady-state I_{K1} at −85 mV in actual experiments.

A further item of interest in the plot of Figure 37B is the effect of addition of 0.1 mM K^+ on the amplitude of I_{K1} at −85 mV. In the case of simulated I_{K1}, the addition increases the amplitude by ≈ 9 pA (Figure 37B, Sim Δ); in actual experiments (e.g., Figure 9), the increase in amplitude was approximately the same (4 ± 3 pA (n = 5)) (especially since it seems likely that the increase observed in experiments was primarily due to elevation of K^+ at (shell) surface membrane, rather than at T-tubular membrane (where external K^+ was most likely >> 0.1 mM (see below))). In summary, these findings

offer no support for the notion that the source of the K^+ that activates steady-state I_{K1} (–85 mV) in myocytes bathed with K^+-free solution is the trace K^+ in that solution. The only other K^+ in the experimental setting was the K^+ in the cytoplasm of the myocyte, and the only way that it could have activated I_{K1} was to pass from the cytoplasm into an extracellular location from which it was not immediately washed away. In other words, it needed to pass into an extracellular restricted-diffusion space in which it could accumulate to a concentration much higher than that in the bathing solution. Hypothesizing that this space is that in the T-tubules appears to be reasonable in view of the evidence suggesting that K^+ outflow via K1 channels can accumulate there (see Chapter 3.4 and Section 4.2 above).

The situation can be visualized by reference to the diagram in Figure 38A. It shows a T-tubule, K1 channels in T-tubular membrane, and a dashed line indicating restricted diffusion of K^+ from T-tubular solution to bulk solution. When the myocyte is superfused with 5.4-mM K^+ solution and held at $V_m = –85$ mV ($\approx E_K$), the concentration of K^+ in the T-tubules (K^+_T) is ≈ 5.4 mM, and E_K pertinent to T-tubular membrane ($E_{K,T}$) is the same as E_K pertinent to surface membrane. When the 5.4-mM K^+ superfusate is exchanged for 0-mM K^+ superfusate, K^+_T declines from 5.4 mM towards 0 mM due to diffusion of K^+ (J_T) down its concentration gradient. The decline in K^+_T shifts $E_{K,T}$ negative to V_m; consequently, there is an outflow of K^+ ($I_{K1,T}$) from the cytoplasm to the T-tubules. As long as the cytoplasm is supplied with K^+ from the pipette, K^+_T remains higher than bulk 0-mM K^+. At equilibrium, the average concentration of K^+ in the T-tubules can be estimated by applying a series of step hyperpolarizations from –85 mV and determining the E_{rev} of the "instantaneous" current. In the example shown in Figure 38B, E_{rev} ($\approx E_{K,T} = –61 \log (140/K^+_T)$) was near –100 mV. Overall, E_{rev} was –99.8 ± 0.9 mV (n = 27), and

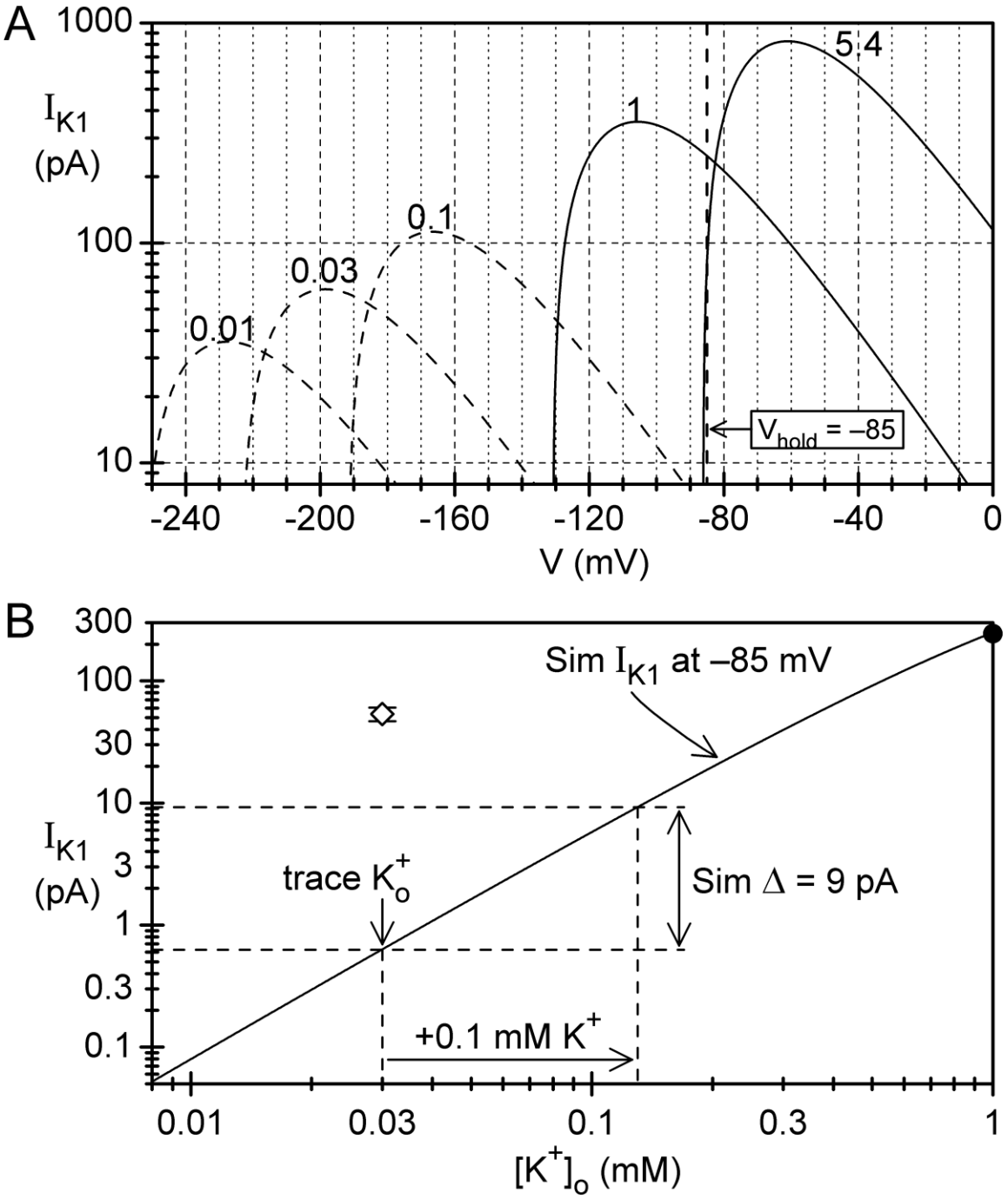

Figure 37. Simulated I_{K1}-V relations. **A.** Plot of I_{K1} amplitude *versus* voltage for $K^+_o \leq$ 5.4 mM. **B.** Log-log plot of I_{K1} amplitude (–85 mV) versus K^+_o. Filled circle: experimental mean value. Solid line: amplitude of simulated (Sim) I_{K1}. Vertical and horizontal dashed lines (lower left): putative trace K^+ (0.03 mM) in 0-mM K^+ solution activates simulated I_{K1} of ≈ 0.7 pA. Horizontal arrow (bottom): addition of 0.1 mM K^+ increases simulated I_{K1} by ≈ 9 pA (Sim Δ). Open diamond: observed I_{K1} in myocytes bathed with 0-mM K^+ solution.

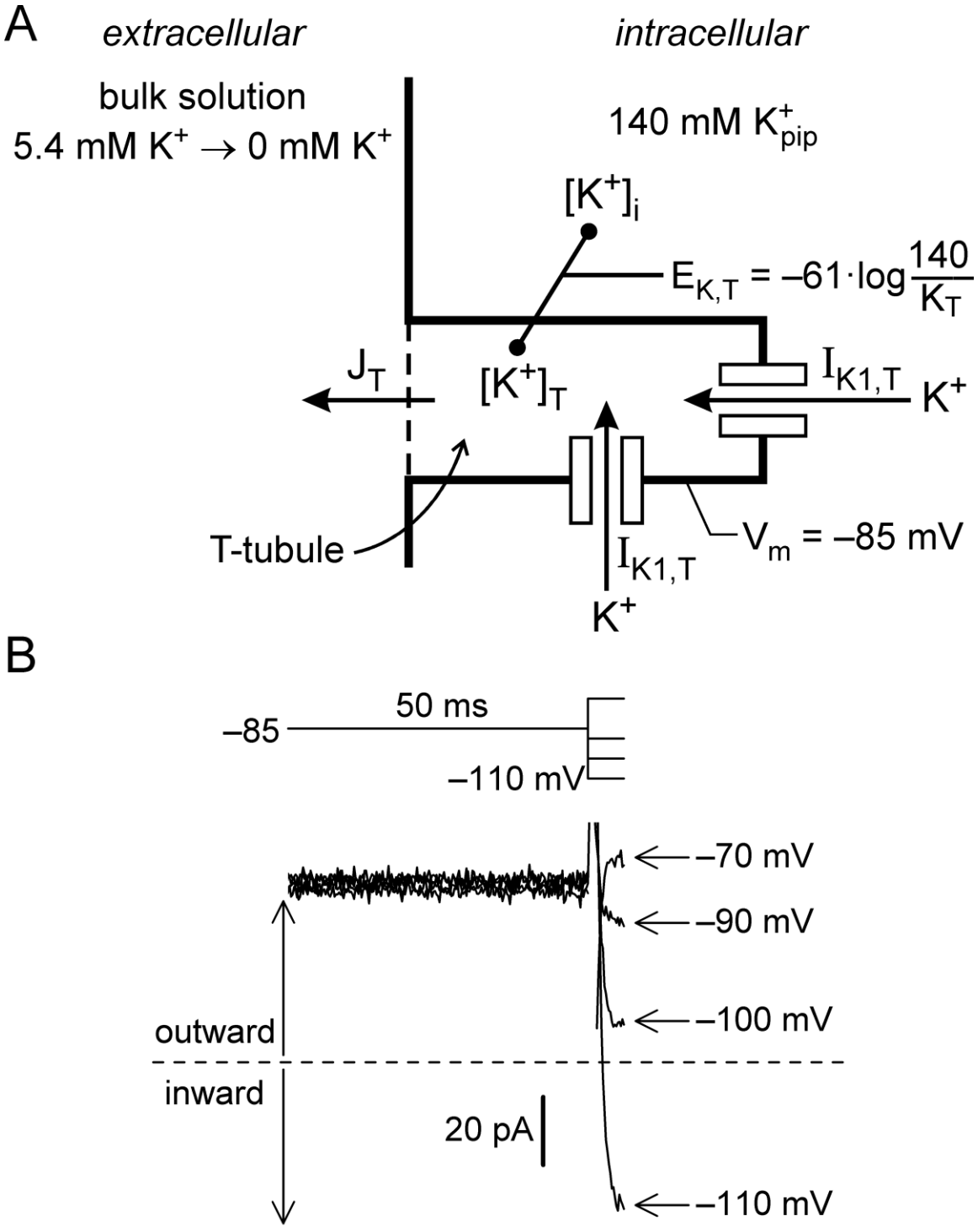

Figure 38. K^+_T in myocytes bathed with 0-mM K^+ solution and held at −85 mV. **A.** Cartoon that depicts K^+-related events in T-tubules when 5.4-mM K^+ bathing solution is replaced by 0-mM K^+ bathing solution. **B**. Determination of E_{rev} in a myocyte bathed with 0-mM K^+ solution. The dashed line indicates the zero-current level.

calculated K^+_T was near 3.2 mM. This K^+_T only applies in the steady-state at $V_m = -85$ mV; it will be lower at more negative potentials. For example, hyperpolarizing pulses to −160 mV can elicit currents that turn outward in direction following initial inward phases; therefore, E_{rev} at the time of the change in direction is < −160 mV, and calculated $E_{K,T}$ is < 0.32 mM. These matters are considered in more detail below.

4.4. INWARD TRANSIENTS

Hyperpolarizing pulses applied from holding potential −85 mV to voltages negative to ≈ −100 mV elicited inward transients in myocytes bathed with K^+-free solution, i.e., the currents reached an inward peak shortly after the onset of the pulse, decayed in a monotonic fashion over the next several hundred milliseconds, crossed over the zero current level, and stabilized at a slightly outward level. The amplitude of the transient was dependent on the hyperpolarizing pulse that was applied: the more negative-going the pulse, the larger the amplitude of the inward peak.

The inward transient was identified as I_{K1} based on the finding that it was abolished by concentrations of Ba^{2+} as low as 10 μM. That being the case, the charge-carrier for the inward segment of the transient was external K^+. A second important finding regarding the inward transient was that it was absent in myocytes that were dialyzed with Cs^+ pipette solution rather than standard K^+ pipette solution. That absence is consistent with charge-carrier K^+ being localized in the T-tubules, i.e., because there was no K^+ flowing out across the T-tubular membrane in the Cs^+-dialyzed myocytes, K^+_T was fully equilibrated with bulk 0-mM K^+, or near 0 mM. Note that if charge-carrier K^+ were actually in the bulk solution, its inward movement via K1 channels would not have been

prevented by the presence of high Cs^+ in the cytoplasm (see Stelling & Jacob, 1992; Matsuda, 1996).

Two additional possibilities concerning the decay phase of the inward transient deserve consideration. The first is that the decay was due to time-dependent block of inward I_{K1} by external monovalent cations. Such block (see Biermans *et al.*, 1987; Harvey & Ten Eick, 1989) has sometimes been held responsible for decay of large inward I_{K1} to near-zero within several hundred milliseconds of application of a hyperpolarizing step (e.g., Ranjan *et al.*, 1998). Since the aforementioned studies (and numerous others) indicate that external Na^+ (rather than $NMDG^+$) is the culprit, monovalent cation block is an unlikely cause in the present case. The second possibility is that the decay phase of the inward transient might have been caused by time-dependent block of K1 channels by trace Ba^{2+} in the bathing solution (see Choe *et al.*, 1999; So *et al.*, 2001). However, this appears to be an unlikely explanation for the decay phase because there was little evidence of decay phases in traces of inward I_{K1} in experiments on myocytes bathed with solution that contained 3 to 5.4 mM K^+ (e.g., Figure 1C). In other words, any trace Ba^{2+} present in solutions was not an effective blocker of inward I_{K1} in myocytes exposed to an external K^+ concentration similar to that (≈ 3.2 mM) proposed to be activating I_{K1} in myocytes bathed with K^+-free solution.

A scheme that can explain the inward transient is shown in Figure 39. The solid lines in the figure depict the effects of a hyperpolarizing pulse (from a V_m of −85 mV to a V_m of −160 mv) on $E_{K,T}$, on the driving force on K^+, and on $I_{K1,T}$. Just before the pulse, V_m (−85 mV) is positive to $E_{K,T}$ (≈ −100 mV) and this drives outward $I_{K1,T}$. Early on during the pulse, V_m (−160 mV) is negative to $E_{K,T}$ (≈ −100 mV) and this drives inward $I_{K,T}$. With time, the inward flow of $I_{K1,T}$ causes depletion of K^+_T; this reduces driving

force and attenuates inward $I_{K1,T}$. The change in direction of current occurs because concomitant diffusion of K^+ to the bulk solution further depletes K_T and pushes $E_{K,T}$ negative to the V_m of −160 mV. Though not shown in the figure, post-pulse return of V_m to −85 mV should markedly increase outward driving force on K^+ and promote outward $I_{K1,T}$ that gradually restores K^+_T and $I_{K1,T}$ to prepulse steady-state levels.

A question that arises in connection with the inward transients is whether other investigators have shown (or mentioned) them in earlier studies on ventricular myocytes.

A thorough search of the literature suggests that the answer is in the negative. Surprisingly, for all the studies that have used K^+-free solution as a protocol, there appears to be not one that shows records of membrane currents on hyperpolarizing pulses to potentials negative to −100 mV. On the other hand, there are records of membrane currents elicited by such hyperpolarizations in studies on inwardly-rectifying currents in non-cardiac cells bathed in K^+-free solution. Jow & Numann (1998) showed records from experiments on inwardly-rectifying K^+ currents in human capillary endothelial cells, and Zhang *et al*. (2009) showed records from experiments on inwardly-rectifying K^+ currents carried by Kir2.1 channels expressed HEK293 cells. In both cases, the hyperpolarizing pulses were to potentials as negative as −120 mV, and there were no indications of inward transients on the current records from these T-tubule-less cells.

A rough estimate of the percentage of myocyte membrane that contributes to holding $I_{K1,T}$ in myocytes bathed with K^+-free solution can be obtained by reference to Figure 11 where the average outward current at 15 mV positive to E_{rev} is ≈ 600 pA under 5.4 mM K^+_o conditions, or ≈ 460 pA at E_{rev} + 15 mV (i.e., at −85 mV) when it is scaled down (in a K^+_o-dependent manner) to the estimated K^+_T value of 3.2 mM. At −85 mV, the average amplitude of $I_{K1,T}$ was ≈ 60 pA, or about 13% of estimated 3.2-mM whole-

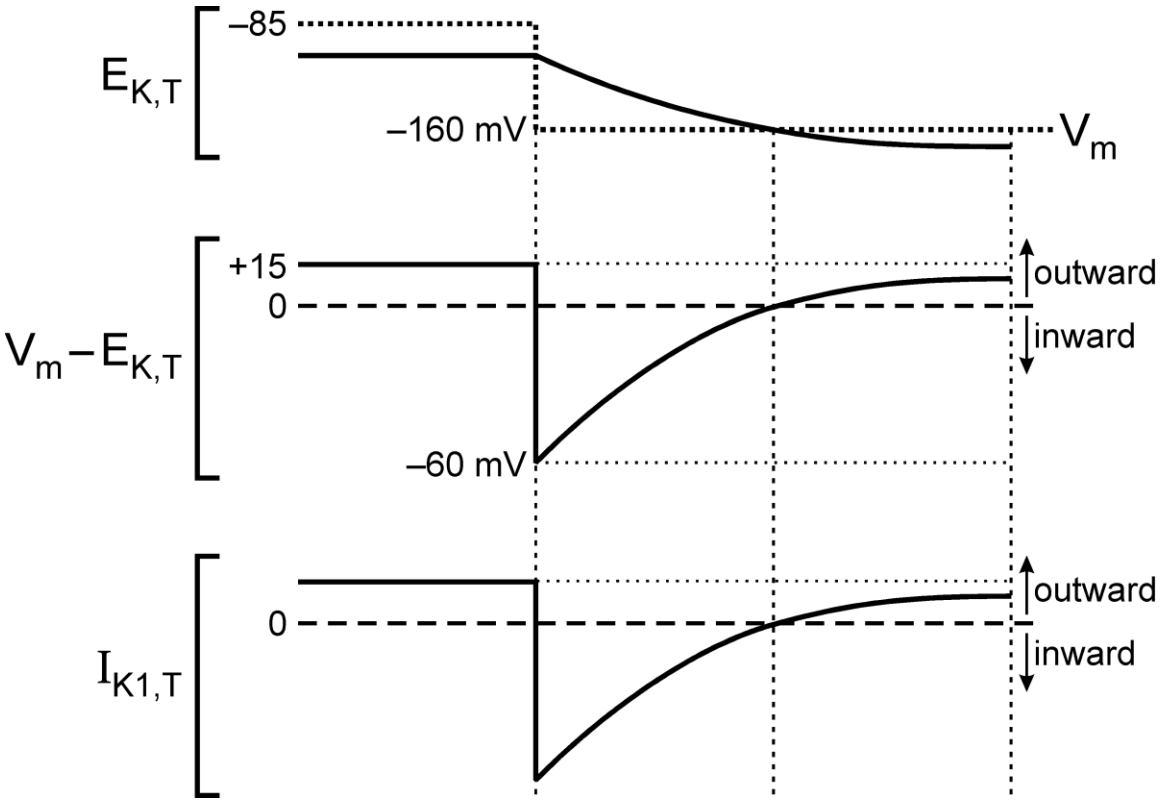

Figure 39. Depiction of the effects of a ca. 300-ms hyperpolarization from –85 to –160 mV on determinants of $I_{K1,T}$.

cell I_{K1}. This suggests that holding I_{K1} was contributed by ≈ 25% of T-tubular membrane.

Ramifications of findings with K^+-free solution. There are a number of ramifications of the findings obtained on myocytes bathed with K^+-free solution. One is that whole-myocyte I_{K1} should be viewed as a composite of I_{K1} flowing across surface membrane ($I_{K1,S}$), and I_{K1} flowing across T-tubular membrane ($I_{K1,T}$). A second arises from the fact that the flow of $I_{K1,T}$ either augments or depletes K^+ in the restrictive confines of the T-tubules. As a consequence, step changes in membrane potential that affect the amplitude/direction of $I_{K1,T}$ will invariably affect K^+ concentration in the T-tubules, and introduce extra time-dependent components into voltage-clamp recordings of whole-myocyte I_{K1}. These time-dependent components are likely to be at their largest in experiments on myocytes bathed in K^+-free solution, and at their smallest in myocytes bathed with high-K^+ (e.g., 30 mM) solution. They will clearly complicate analysis of time-dependent features of whole-cell I_{K1} such as rectification, removal of rectification, and "inactivation". A third ramification is that the use of K^+-free solution to remove interference from I_{K1} in experiments on, say, delayed-rectifier I_{Ks}, non-selective cationic current, Na^+-pump current, or Na^+-Ca^+ exchanger current could lead to erroneous conclusions. A simple example in the case of I_{Ks} is the use of (post-I_{Ks}-activation) hyperpolarizing pulses to a series of potentials negative to −100 mV in K^+-free solution for the purpose of determining the potential at which the I_{Ks} tail reverses direction in order to evaluate the relative selectivity of the Ks channel (e.g., Hadley & Hume, 1990; Sanguinetti & Jurkiewicz, 1992); clearly, the (masked) inward transient will offset decaying outward I_{Ks} tails, and make determination of the E_{rev} of the I_{Ks} tail seemingly impossible using this protocol.

4.5. I_{K1} IN MYOCYTES DIALYZED WITH LOW-K^+ PIPETTE SOLUTION

A large number of experiments were conducted on myocytes that were dialyzed with pipette solution that contained K^+ at a concentration lower than that in the standard 140-mM K^+ pipette solution. As evaluated by measurements of E_{rev}, the myocytes dialyzed with low-K^+ pipette solution had low concentrations of intracellular K^+ and are referred to as low-K^+_i myocytes (versus normal-K^+_i myocytes). The findings in experiments with low-K^+ pipette solution are discussed below under headings on features of I_{K1} in low-K^+_i myocytes, current-flow-induced changes in K^+_i, and conductance and lowered K^+_i.

4.5.1. Features Of I_{K1} In Low-K^+_i Myocytes

4.5.1.1. Dependence Of E_{rev} On Pipette K^+

It is well established from studies on normal-K^+_i ventricular preparations that raising external K^+ from control ca. 5 mM to a distinctly higher concentration causes a positive shift in the E_{rev} of I_{K1}, and that the degree of the shift in E_{rev} is very close to that of the shift in E_K calculated on the assumption that K^+_i is unaffected by elevation of K^+_o (McDonald & Trautwein, 1978; Isenberg & Klöckner, 1982; Saigusa & Matsuda, 1988). However, there is little evidence that lowering K^+_i from ca. 140 mM induces commensurate positive shifts in E_{rev} and calculated E_K. Nevertheless, it is the expected outcome based on results obtained by Hagiwara & Yoshii (1979) on inward-rectifier K^+ current in starfish eggs. They found that the E_{rev} of the current corresponded to E_K calculated on the basis that K^+_i = pipette K^+, or $E_{K,pip}$, when the eggs were dialyzed with pipette solutions that contained 50, 125, 200, and 300 mM K^+. Vandenberg (1987) found that the E_{rev} of average single channel current in a cell-attached patch of a guinea-pig ventricular myocyte was ≈ 10 mV more negative than $E_{K,pip}$ when she dialyzed the

myocyte with a 25-mM K^+ internal solution via a saponin-permeabilized distal cell end. Thereafter, Saigusa & Matsuda (1988) used a patch-pipette-perfusion arrangement to exchange a 150-mM K^+ pipette solution for a low-K^+ one while the patch-pipette was sealed to a guinea-pig ventricular myocyte. They found that E_{rev} deviated considerably from calculated $E_{K,pip}$. For example, the ΔE_{rev} values on switching from 150-mM K^+ pipette solution to 75- or 50-mM ones were < 60% of the magnitudes expected on the basis of calculated $E_{K,pip}$. They suggested that the deviation might have been due to poor exchange of dialysates in the patch-pipette.

In the present study, myocytes were dialyzed with pipette solution whose concentration of K^+ ranged from 10 to 140 mM, and E_{rev} was determined after allowing at least 15 min for equilibration of pipette solution K^+ and cytoplasmic K^+. The overall finding was that E_{rev} varied in a near-Nernstian manner with pipette K^+ (slope of -59.7 ± 1.4 mV per decade pipette K^+). It seems reasonable to conclude that E_{rev} has a near-Nernstian dependence on K^+_i.

4.5.1.2. Block By External Cs^+

Open-channel block by external Cs^+ is a signature property of Kir channels (Hille, 2001; Stanfield *et al.*, 2002). The blocking action is quasi-instantaneous (Gay & Stanfield, 1977; Klein *et al.*, 1999), and the degree of block increases steeply with negative potential (Hagiwara *et al.*, 1976; Harvey & Ten Eick, 1989). An indication of the voltage dependence of block of I_{K1} by Cs^+ is provided by the I-V relations obtained from a representative normal-K^+_i myocyte before and during the application of 10 mM Cs^+ (Figure 3), i.e., the cation blocked ≈ 90% of the current at −100 mV, but only ≈ 50% at −60 mV. Overall, the K_D of block at −60 mV in normal-K^+_i myocytes was 7.5 ± 0.3 mM, a value in good agreement with isolated observations in an earlier study on I_{K1} in cardiac muscle preparations (Trautwein & McDonald, 1978). The surprising finding was

that the K_D for block at the same potential in low-K^+_i myocytes was a near-40-times lower 0.20 ± 0.02 mM. Another way of viewing the Cs^+ sensitivity of I_{K1} in low-K^+_i myocytes compared to that in normal-K^+_i myocytes is in terms of a shift in voltage dependency. In that regard, interpolation of voltage-dependent block data for 0.1 and 0.5 mM Cs^+ reported by Harvey & Ten Eick (1989) (their figure 3) in their study on I_{K1} in normal-K^+_i cat ventricular myocytes suggests that 0.2 mM was the approximate K_D at −130 mV. In other words, the effect of lowering K^+_i from ≈ 140 mM to ≈ 20 mM was to shift the voltage sensitivity to Cs^+ by ≈ +70 mV.

The reason why Cs^+ is a much more potent blocker of I_{K1} in low-K^+_i myocytes than in normal-K^+_i myocytes is not apparent. One possibility (cf.,Yellen, 1984) is that the *trans* "knock-off" of Cs^+ from its binding site in the pore is severely attenuated by a decrease in K^+_i. In that regard, Chang *et al.* (2009) found that the "off" rate of Ba^{2+} from the selectivity filter of the Kir2.1 channel can decline by a factor of ≈ 40 when the concentration of K^+ in solution bathing the intracellular side of excised membrane patches is lowered from 200 to 20 mM.

4.5.2. Current-Flow-Induced Changes In K^+_i

As noted in Chapter 1, there has been considerable attention paid to intracellular accumulation (and depletion) of Na^+ in cardiomyocytes (for reviews, see Barry, 2006; Török, 2007), but little attention to intracellular accumulation (or depletion) of K^+. The most likely reason for this is that studies on K^+ currents in whole-cell configured myocytes are almost always conducted using pipettes that are filled with solutions that contain ca. 140 mM K^+, i.e., this concentration of K^+ in the cytoplasm, along with diffusion of K^+ to and from the patch-pipette, should be able to buffer gains and losses of cytoplasmic K^+ related to outward- and inward-directed K^+ current. However, the

situation is different when the myocyte is dialyzed with a solution that contains, say, 10 mM K^+. The "buffering" of K^+ flux is now very much weaker, and large flows of K^+ current are likely to create K^+ concentration gradients between submembrane cytoplasmic regions and the tip of the pipette. In regard to I_{K1}, the larger and the longer-lasting the current flow, the greater the putative accumulation or depletion of K^+ in submembrane cytoplasmic regions, and, consequently, the greater the likely discrepancy between measured E_{rev} ($\approx E_K$) and calculated $E_{K,pip}$. In particular, the larger the inward flow of I_{K1} generated by the driving force on K^+, the larger the expected discrepancy between E_{rev} and $E_{K,pip}$.

In essence, this type of dependency on driving force can explain the influence of holding potential on E_{rev} shown in Figure 27, i.e., the more negative the V_{hold}, the more negative the E_{rev}. A similar relationship was evident when V_{hold} was changed for several minutes during the course of an experiment. Conversely, experimental manipulations (e.g., Ba^{2+}, Cs^+) that decreased K^+ influx by decreasing inward I_{K1} at negative V_{hold} shifted E_{rev} to more positive potentials. In fact, there appeared to be a link between magnitude of the reduction in inward holding current and reduction of the difference between E_{rev} and $E_{K,pip}$ (e.g., Figure 32).

E_{rev} values in the experiments on inward holding K^+ current, E_{rev}, and $E_{K,pip}$ were used to estimate the degrees to which inward holding currents likely increased the concentration of subsarcolemmal K^+ above the concentration of K^+ in the pipette-filling solution. A complexity with these estimations was that bathing solution K^+ was taken as K^+_o in the calculations when, in fact, effective (mean) K^+_o may have been lower due to lowering of K^+_T induced by the flow of inward holding current. However, as explained in connection with results obtained with a number of pertinent protocols in Chapter 3.5.4,

increases in subsarcolemmal K^+ of 100% and more were calculated even when due account was taken of possible reductions in K^+_T. It is worthwhile evaluating whether the magnitudes of inward holding currents were large enough to cause large increases in subsarcolemmal K^+. The E_{rev} versus holding I_{K1} data obtained from myocytes dialyzed with 20 mM K^+ pipette solution (Figure 32) indicates that E_{rev} was ≈ −60 mVwhen the amplitude of the holding current was ≈ −1.5 nA. Thus, the amount of K^+ that passed into a myocyte during a 120-s period was

$$1{,}500 \text{ pA} \cdot 120 \text{ s} / 96{,}485 \text{ A} \cdot \text{s/mol} = 1.87 \text{ pmol}$$

In the case of a 20-pL myocyte (Satoh *et al.*, 1996) with osmotically-active volume-fraction of 0.67, this amount is sufficient to increase cytoplasmic K^+ by 144 mM. Most of the K^+ influx is likely to be counterbalanced by diffusion of K^+ into the pipette. The time constant for the latter process can be estimated from the 150-165 s it takes K^+_i to fall from ≈ 140 mM at patch-breakthrough time to ≈ 30 mM (calculated from E_{rev} on tenth ramp) (Figure 34). Interpolation gives a mean τ of 103 s (which is very close to the value (≈ 100 s) calculated by Mathias *et al.* (1990) for the case of a 4-MΩ pipette and a 20-pL ventricular myocyte).

4.5.3. Conductance And Lowered K^+_i

Hagiwara & Yoshii (1979) were the first to evaluate the effects of lowering K^+_i on the conductance of strong inwardly-rectifying K^+ channels (G_{Kir}). That study was conducted on starfish eggs whose interiors were dialyzed using a pipette "cell-perfusion" system. In regard to chordG_{Kir}, these investigators found that positive shifts in E_{rev} of +24 and +53 mV induced by lowerings of K^+_i resulted in pronounced decreases in maximal conductance values. However, the shifts in E_{rev} were not accompanied by comparable

shifts in the G_{Kir}-V relation along the voltage axis. In fact, the relation did not shift at all in response to changes in calculated E_K induced by changes in K^+_i, whereas it shifted in good accord with calculated E_K when the latter was changed by changing K^+_o.

Following the work by Hagiwara & Yoshii (1979), studies on the effects of lowering K^+_i on G_{Kir} have been conducted on preparations as diverse as frog skeletal muscle fibres, excised *Xenopus* oocyte membrane patches containing expressed Kir2.1 channels, cell-attached patches of guinea-pig ventricular myocytes, guinea-pig ventricular myocytes, and canine Purkinje fibre myocytes. The findings obtained on the starfish eggs and the other preparations are summarized in Table 1. Also shown in the table are pertinent experimental details that include the degree of the shift in calculated E_K elicited by the lowering of K^+_i, the method used to achieve the lowering, the external K^+ that was used, and the temperature at which determinations were made. Aside from the large +53-mV and +43-mV shifts achieved by Hagiwara & Yoshii (1979) and Vandenberg (1987), respectively, the E_K shifts in the cited studies were relatively small (range +8.7 to +27 mV).

Effects on maximal conductance. Five of the eight studies reported on the effects of E_K shifts on G_{Kir}max. Aside from Hagiwara & Yoshii (1979) (who registered decreases of 53 and 77%), the only other study that noted decreases was that conducted on guinea-pig ventricular myocytes by Saigusa & Matsuda (1988). They reported that G_{K1}max declined by 31 and 57% for shifts in calculated E_K of +8.7 and +15.4 mV, respectively.

The experimental conditions used in the present study on the effects of lowering K^+_i on G_{K1} differed from those in the studies cited above in that both external K^+ and temperature were kept at near-physiological levels. SlopeG_{K1}max was measured in experiments on 120 myocytes in which E_{rev} ranged from ≈ –90 mV to ≈ –20 mV (see

Figure 36). A synopsis of the results is that slopeG_{K1}max was ≈ 118 nS at E_{rev} of –86 mV, ≈109 nS at E_{rev} of –66 mV, ≈ 104 nS at E_{rev} of –56 mV, and ≈ 94 nS at E_{rev} of –36 mV. Importantly, a negative shift in holding potential that shifted E_{rev} by an average –30 mV (n = 16 myocytes) resulted in a significant 12% increase in chordG_{K1}max. All in all, these results point to moderate declines in G_{K1}max with reductions in K^+_i. In that regard, they are in good agreement with the findings of Matsuda (1991), but not with those of Saigusa & Matsuda (1988).

Precisely why a lowering of K^+_i may have caused a moderate lowering of G_{K1}max remains to be clarified. One possibility is that a lowering of K^+_i affects the blocking of K1 channels by intracellular polyvalent cations. Thus, intracellular K^+ ions appear to compete with channel-blocking polyvalent cations for binding sites in the pore (Lopatin & Nichols, 1996; Guo *et al.*, 2003)**,** and a decrease in K^+_i might tip the balance in favour of blocking particles.

Amongst the experimental factors that may have contributed to the decrease in chordG_{K1}max and slopeG_{K1}max in myocytes with lowered K^+_i was the use of Cs^+ as replacement cation for intracellular K^+, i.e., intracellular Cs^+ ions may have exerted an inhibitory influence on inward I_{K1}. In that regard, Matsuda (1996) has reported that 150-mM intracellular Cs^+ induced flickering in K1 single-channel inward current carried by K^+. On the other hand, block by intracellular Cs^+ that affects G_{K1}max is likely to be voltage-dependent and consequently would be expected to induce distortions in the shape of the G_{K1}-V relation. Such distortions in the relation were not evident here (e.g., Figure 34). A second experimental factor that may have contributed to the decrease in slopeG_{K1}max is related to the linear section of the inward limb of the I-V relation in low-K^+_i myocytes. Relative to E_{rev}, the linear section occurred at more negative voltages in

low-K^+_i myocytes than in normal-K^+_i myocytes, and this may have promoted a reduction of inward current related to depletion of K^+ in the T-tubules.

Effects on the position of the G_{Kir}-V relation. The notations and data in the G_{Kir}-V column of Table 1 indicate that the only studies in which shifts along the voltage axis occurred were in those conducted on guinea-pig ventricular myocytes (Saigusa & Matsuda, 1988) and canine Purkinje fibre myocytes (Cohen *et al.*, 1989). In each of these, the $V_{0.5}$ of chordG_{K1} shifted in the same direction as E_K shifted when K^+_i was lowered. The ratios of the shifts were ≈ 8/8.7 and 15/15.4 in the Saigusa & Matsuda (1988) study, and ≈ 5/23 and 8/20 in the Cohen *et al.* (1989) study. The results obtained in the present study, whether for smaller or larger shifts in E_K (see Figures 34C, 35B), indicate that the ratios of the shifts (e.g., 17.8/35, or ≈ 0.5 (Figure 35B)) were more like those in the Cohen *et al.* (1989) study. A consequence of a positive shift in $V_{0.5}$ with a lowering of K^+_i is that the outward-current limb of the I-V relation in a low-K^+_i myocyte crosses over that of a normal-K^+_i myocyte. Even so, the amplitude of the outward current in the former is much smaller than that in the latter at equivalent driving forces. It may be that lowering K^+_i reduces the rate of entry of intracellular K^+ ions into the pore, lowers the K^+ occupancy of the selectivity filter, and reduces K^+ exit to the extracellular solution (see Morais-Cabral *et al.*, 2001). Inward I_{K1} is far less affected by low K^+_i, most likely because the entry of extracellular K^+ ions into the filter and on into the vestibule is little affected, especially at sub-E_K membrane potentials where K^+-K^+ interaction in the pore promotes efficient throughput of K^+ (see Yeh *et al.*, 2005; Fujiwara & Kubo, 2006).

Table 1. Survey of effects of lowering K^+_i on conductance parameters of strong inwardly-rectifying K^+ (Kir) channels.

Study	K^+_o	Shift in $E_{rev}(E_K)$ via lowering of K^+_i*			Temp
		Degree of shift in E_K	Effects of shift in E_K on G_{Kir} parameters		
			G_{Kir} max	G_{Kir}-V	
Hagiwara & Yoshii (1979). *Starfish egg*	25 mM 25 mM	+24 mV +53 mV	↓53% ↓ 77%	No shift No shift	22°C 22°C
Leech & Stanfield (1981). *Skeletal muscle*	40 mM	+23 mV	No change	No shift	3°C
Hestrin (1981). *Skeletal muscle*	50 mM	+26 mV	—	No shift	5°C
Lopatin & Nichols (1996). *Kir2.1 I/O patch*	150 mM	+28 mV	—	No shift	22°C
Vandenberg (1987). *Gpvm patch***	150 mM	+43 mV	No change	—	19°C
Matsuda (1991). *Gpvm patch***	150 mM	+27 mV	↓7%	—	24°C
Cohen et al. (1989). *Purkinje fibre myocyte*	12 mM 42 mM	+23 mV +20 mV	—	Shift of +5 mV +8 mV	9°C
Saigusa & Matsuda (1988). *Gpvm*	40 mM 40 mM	+8.7 mV +15.4 mV	↓31% ↓57%	Shift of ≈ +8 mV ≈ +15 mV	15°C

* Lowering of K^+_i. Row 1, 3, 5, 6, 7, 8: via dialysis with low-K^+ solution.
Row 2: via osmotic swelling.
Row 4: via low-K^+ bath (internal) solution.

** Cell-attached patch on a permeabilized myocyte.

Gpvm – guinea-pig ventricular myocyte

Dashed line: data not provided.

Downward arrow: decrease of.

4.6. CONCLUDING REMARKS

Areas of the study that deserve further comment include I_{K1} in relation to T-tubules, and I_{K1} in myocytes with lowered cytoplasmic K^+ concentration.

Results obtained in the present study indicate that flows of outward I_{K1} elicited by step depolarizations can cause accumulation of K^+ in the T-tubules of guinea-pig ventricular myocytes. The accumulation introduces extra time-dependent components into voltage-clamp recordings of whole-myocyte I_{K1}. These time-dependent components are more pronounced under low-K^+_o than high-K^+_o conditions, and are likely to complicate analysis of time-dependent features of I_{K1} such as rectification and removal of rectification, as well as analysis of other membrane currents recorded in the presence of I_{K1}. During cardiac electrical activity, accumulation related to $I_{K1,T}$ flowing during the latter phases of repolarization may well persist into early diastole and influence cell excitability. In turn, accumulation and its influence on excitability are likely to be affected by a wide range of physiological and pathophysiological factors, including heart rate, extracellular K^+ concentration, and status of K1-channel conductance, not to mention T-tubule remodelling/dysfunction (Louch et al., 2010; Ibrahim et al., 2011).

Bearing in mind the likely central physiological role of T-tubules in myocyte K^+ movement and cardiac electrical activity, it will be important to extend this area of study in two directions. The first of these would address the question of whether membrane currents in guinea-pig ventricular myocytes subjected to detubulation procedures behaved in a manner consistent with signature findings in the present work. The second would be to develop a theoretical model to evaluate the importance of T-tubular geometry and T-tubular K^+ currents on myocyte electrical activity.

In regard to I_{K1} in myocytes with lowered cytoplasmic K^+ concentration, results obtained on myocytes dialyzed with < 140-mM K^+ pipette solution indicate that the dependence of E_{rev} on log pipette K^+ could be well-fitted by a straight line with slope -59.7 ± 1.4 mV per decade of pipette K^+ concentration. It seems reasonable to conclude that E_{rev} has a near-Nernstian dependence on K^+_i. A ramification of this result is that provided G_{K1} near E_K remains relatively strong, and resting inward cationic and anionic conductances relatively small, K^+_i is almost certainly a major determinant of the resting potential of ventricular myocytes as previously suggested by Baumgarten & Fozzard (1992).

REFERENCES

Adrian R. H., Chandler W. K. & Hodgkin A. L. (1970). Slow changes in potassium permeability in skeletal muscle. *J Physiol* **208,** 645-668.

Adrian R. H. & Freygang W. H. (1962). The potassium and chloride conductance of frog muscle membrane. *J Physiol* **163,** 61-103.

Akuzawa-Tateyama M., Tateyama M. & Ochi R. (1998). Low K^+-induced hyperpolarizations trigger transient depolarizations and action potentials in rabbit ventricular myocytes. *J Physiol* **513,** 775-786.

Allah E. A., Tellez J. O., Yanni J., Nelson T., Monfredi O., Boyett M. R. & Dobrzynski H. (2011). Changes in the expression of ion channels, connexins and Ca^{2+}-handling proteins in the sino-atrial node during postnatal development. *Exp Physiol* **96,** 426-438.

Almers W. (1972). Potassium conductance changes in skeletal muscle and the potassium concentration in the transverse tubules. *J Physiol* **225,** 33-56.

Amsellem J., Delorme R., Souchier C. & Ojeda C. (1995). Transverse-axial tubular system in guinea pig ventricular cardiomyocyte: 3D reconstruction, quantification and its possible role in K^+ accumulation-depletion phenomenon in single cells. *Biol Cell* **85,** 43-54.

Anumonwo J. M. & Lopatin A. N. (2010). Cardiac strong inward rectifier potassium channels. *J Mol Cell Cardiol* **48,** 45-54.

Aronson R. S. & Nordin C. (1988). Arrhythmogenic interaction between low potassium and ouabain in isolated guinea-pig ventricular myocytes. *J Physiol* **400,** 113-134.

Backx P. H. & Marban E. (1993). Background potassium current active during the plateau of the action potential in guinea pig ventricular myocytes. *Circ Res* **72,** 890-900.

Bailly P., Mouchonière M., Bénitah J. P., Camilleri L., Vassort G. & Lorente P. (1998). Extracellular K^+ dependence of inward rectification kinetics in human left ventricular cardiomyocytes. *Circulation* **98,** 2753-2759.

Banyasz T., Lozinskiy I., Payne C. E., Edelmann S., Norton B., Chen B., Chen-Izu Y., Izu L. T. & Balke C. W. (2008). Transformation of adult rat cardiac myocytes in primary culture. *Exp Physiol* **93,** 370-382.

Bányász T., Magyar J., Szentandrássy N., Horváth B., Birinyi P., Szentmiklósi J. & Nánási P. P. (2007). Action potential clamp fingerprints of K^+ currents in canine cardiomyocytes: their role in ventricular repolarization. *Acta Physiol (Oxf)* **190,** 189-198.

Barry P. H. & Adrian R. H. (1973). Slow conductance changes due to potassium depletion in the transverse tubules of frog muscle fibers during hyperpolarizing pulses. *J Membr Biol* **14,** 243-292.

Barry W. H. (2006). Na^+ "Fuzzy space": does it exist, and is it important in ischemic injury? *J Cardiovasc Electrophysiol* **17 Suppl 1,** S43-S46.

Baumgarten C. M., Cohen C. J. & McDonald T. F. (1981). Heterogeneity of intracellular potassium activity and membrane potential in hypoxic guinea pig ventricle. *Circ Res* **49,** 1181-1189.

Baumgarten C. M. & Fozzard H. A. (1992). Cardiac Resting and Pacemaker Potential. In *The Heart and Cardiovascular System - Scientific Foundations*, ed. Fozzard HA, Haber E, Jennings RB, Katz AM & Morgan HE, pp. 963-1001Raven Press, New York.
.

Baumgarten C. M. & Isenberg G. (1977). Depletion and accumulation of potassium in the extracellular clefts of cardiac Purkinje fibers during voltage clamp hyperpolarization and depolarization. *Pflügers Arch* **368,** 19-31.

Baumgarten C. M., Isenberg G., McDonald T. F. & Ten Eick R. E. (1977). Depletion and accumulation of potassium in the extracellular clefts of cardiac Purkinje fibers during voltage clamp hyperpolarization and depolarization: experiments in sodium-free bathing media. *J Gen Physiol* **70,** 149-169.

Beckmann C., Rinne A., Littwitz C., Mintert E., Bosche L. I., Kienitz M. C., Pott L. & Bender K. (2008). G protein-activated (GIRK) current in rat ventricular myocytes is masked by constitutive inward rectifier current (I_{K1}). *Cell Physiol Biochem* **21,** 259-268.

Beeler G. W. & Reuter H. (1977). Reconstruction of the action potential of ventricular myocardial fibres. *J Physiol* **268,** 177-210.

Berger F., Borchard U., Hafner D., Pütz I. & Weis T. M. (1997). Effects of 17beta-estradiol on action potentials and ionic currents in male rat ventricular myocytes. *Naunyn Schmiedebergs Arch Pharmacol* **356,** 788-796.

Bergman C. (1970). Increase of sodium concentration near the inner surface of the nodal membrane. *Pflügers Arch* **317,** 287-302.

Bers D. M. (2001). *Excitation-Contraction Coupling and Cardiac Contractile Force*, vol. 1. Kluwer Academic Publishers, Dordrecht.

Beuckelmann D. J., Näbauer M. & Erdmann E. (1993). Alterations of K^+ currents in isolated human ventricular myocytes from patients with terminal heart failure. *Circ Res* **73,** 379-385.

Bichet D., Haass F. A. & Jan L. Y. (2003). Merging functional studies with structures of inward-rectifier K^+ channels. *Nat Rev Neurosci* **4,** 957-967.

Biermans G., Vereecke J. & Carmeliet E. (1987). The mechanism of the inactivation of the inward-rectifying K current during hyperpolarizing steps in guinea-pig ventricular myocytes. *Pflügers Arch* **410,** 604-613.

Blom N., Gammeltoft S. & Brunak S. (1999). Sequence and structure-based prediction of eukaryotic protein phosphorylation sites. *J Mol Biol* **294,** 1351-1362.

Bosch R. F., Zeng X., Grammer J. B., Popovic K., Mewis C. & Kühlkamp V. (1999). Ionic mechanisms of electrical remodeling in human atrial fibrillation. *Cardiovasc Res* **44,** 121-131.

Bouchard R., Clark R. B., Juhasz A. E. & Giles W. R. (2004). Changes in extracellular K^+ concentration modulate contractility of rat and rabbit cardiac myocytes via the inward rectifier K^+ current I_{K1}. *J Physiol* **556,** 773-790.

Boyett M. R., Coray A. & McGuigan J. A. (1980). Cow ventricular muscle. I. The effect of the extracellular potassium concentration on the current-voltage relationship. II. Evidence for a time-dependent outward current. *Pflügers Arch* **389,** 37-44.

Bradley K. K., Jaggar J. H., Bonev A. D., Heppner T. J., Flynn E. R., Nelson M. T. & Horowitz B. (1999). Kir2.1 encodes the inward rectifier potassium channel in rat arterial smooth muscle cells. *J Physiol* **515** 639-651.

Braunwald E., Fauci A.S., Kasper D.L., Hauser S.L., Longo D.L., Jameson J.L. (2001). *Harrison's principles of internal medicine*. McGraw Hill, New York.

Brouillette J., Lupien M. A., St-Michel C. & Fiset C. (2007). Characterization of ventricular repolarization in male and female guinea pigs. *J Mol Cell Cardiol* **42,** 357-366.

Bustamante J. O., Watanabe T. & McDonald T. F. (1981). Single cells from adult mammalian heart: isolation procedure and preliminary electrophysiological studies. *Can J Physiol Pharmacol* **59,** 907-910.

Caballero R., Dolz-Gaitón P., Gómez R., Amorós I., Barana A., González de la Fuente M., Osuna L., Duarte J., López-Izquierdo A., Moraleda I., Gálvez E., Sánchez-Chapula J. A., Tamargo J. & Delpón E. (2010). Flecainide increases Kir2.1 currents by interacting with cysteine 311, decreasing the polyamine-induced rectification. *Proc Natl Acad Sci U S A* **107,** 15631-15636.

Carmeliet E. (1992a). Extracellular Cs^+ ions block but also activate K^+ current in cardiac myocytes. *Biophys J* **61,** A251.

Carmeliet E. (1992b). A fuzzy subsarcolemmal space for intracellular Na^+ in cardiac cells? *Cardiovasc Res* **26,** 433-442.

Case R. B. (1971). Ion alterations during myocardial ischemia. *Cardiology* **56,** 245-262.

Chang H. K., Lee J. R., Liu T. A., Suen C. S., Arreola J. & Shieh R. C. (2010). The extracellular K^+ concentration dependence of outward currents through Kir2.1 channels is regulated by extracellular Na^+ and Ca^{2+}. *J Biol Chem* **285,** 23115-23125.

Chang H. K., Marton L. J., Liang K. K. & Shieh R. C. (2009). K^+ binding in the G-loop and water cavity facilitates Ba^{2+} movement in the Kir2.1 channel. *Biochim Biophys Acta* **1788,** 500-506.

Cheng C. J., Lin S. H., Lo Y. F., Yang S. S., Hsu Y. J., Cannon S. C. & Huang C. L. (2011a). Identification and functional characterization of Kir2.6 mutations associated with non-familial hypokalemic periodic paralysis. *J Biol Chem* **286,** 27425-27435.

Cheng W. W., D'Avanzo N., Doyle D. A. & Nichols C. G. (2011b). Dual-mode phospholipid regulation of human inward rectifying potassium channels. *Biophys J* **100,** 620-628.

Chiang C. E., Luk H. N., Chen L. L., Wang T. M. & Ding P. Y. (2002). Genistein inhibits the inward rectifying potassium current in guinea pig ventricular myocytes. *J Biomed Sci* **9,** 321-326.

Choe H., Palmer L. G. & Sackin H. (1999). Structural determinants of gating in inward-rectifier K^+ channels. *Biophys J* **76,** 1988-2003.

Christé G. (1999). Localization of K^+ channels in the tubules of cardiomyocytes as suggested by the parallel decay of membrane capacitance, IK_1 and IK_{ATP} during culture and by delayed IK_1 response to barium. *J Mol Cell Cardiol* **31,** 2207-2213.

Clark R. B., Tremblay A., Melnyk P., Allen B. G., Giles W. R. & Fiset C. (2001). T-tubule localization of the inward-rectifier K^+ channel in mouse ventricular myocytes: a role in K^+ accumulation. *J Physiol* **537,** 979-992.

Clarke O. B., Caputo A. T., Hill A. P., Vandenberg J. I., Smith B. J. & Gulbis J. M. (2010). Domain reorientation and rotation of an intracellular assembly regulate conduction in Kir potassium channels. *Cell* **141,** 1018-1029.

Claydon T. W., Makary S. Y., Dibb K. M. & Boyett M. R. (2004). K^+ activation of Kir3.1/Kir3.4 and Kv1.4 K^+ channels is regulated by extracellular charges. *Biophys J* **87,** 2407-2418.

Cleemann L. & Morad M. (1979). Potassium currents in frog ventricular muscle: evidence from voltage clamp currents and extracellular K accumulation. *J Physiol* **286,** 113-143.

Cohen I. S., DiFrancesco D., Mulrine N. K. & Pennefather P. (1989). Internal and external K^+ help gate the inward rectifier. *Biophys J* **55,** 197-202.

Cordeiro J. M., Spitzer K. W. & Giles W. R. (1998). Repolarizing K^+ currents in rabbit heart Purkinje cells. *J Physiol* **508** 811-823.

D'Avanzo N., Cheng W. W., Doyle D. A. & Nichols C. G. (2010). Direct and specific activation of human inward rectifier K^+ channels by membrane phosphatidylinositol 4,5-bisphosphate. *J Biol Chem* **285,** 37129-37132.

D'Avanzo N., Cho H. C., Tolokh I., Pekhletski R., Tolokh I., Gray C., Goldman S. & Backx P. H. (2005). Conduction through the inward rectifier potassium channel, Kir2.1, is increased by negatively charged extracellular residues. *J Gen Physiol* **125,** 493-503.

Dassau L., Conti L. R., Radeke C. M., Ptáček L. J. & Vandenberg C. A. (2011). Kir2.6 regulates the surface expression of Kir2.x inward rectifier potassium channels. *J Biol Chem* **286,** 9526-9541.

Daut J. (1982). The passive electrical properties of guinea-pig ventricular muscle as examined with a voltage-clamp technique. *J Physiol* **330,** 221-242.

Davidson S. & Surawicz B. (1967). Ectopic beats and atrioventricular conduction disturbances. In patients with hypopotassemia. *Arch Intern Med* **120,** 280-285.

de Boer T. P., Houtman M. J., Compier M. & van der Heyden M. A. (2010a). The mammalian K_{IR}2.x inward rectifier ion channel family: expression pattern and pathophysiology. *Acta Physiol (Oxf)* **199,** 243-256.

de Boer T. P., Nalos L., Stary A., Kok B., Houtman M. J., Antoons G., van Veen T. A., Beekman J. D., de Groot B. L., Opthof T., Rook M. B., Vos M. A. & van der Heyden M. A. (2010b). The anti-protozoal drug pentamidine blocks K_{IR}2.x-mediated inward rectifier current by entering the cytoplasmic pore region of the channel. *Br J Pharmacol* **159,** 1532-1541.

Delmar M., Michaels D. C. & Jalife J. (1989). Slow recovery of excitability and the Wenckebach phenomenon in the single guinea pig ventricular myocyte. *Circ Res* **65,** 761-774.

Despa S., Kockskämper J., Blatter L. A. & Bers D. M. (2004). Na/K pump-induced $[Na]_i$ gradients in rat ventricular myocytes measured with two-photon microscopy. *Biophys J* **87,** 1360-1368.

Dhamoon A. S. & Jalife J. (2005). The inward rectifier current (I_{K1}) controls cardiac excitability and is involved in arrhythmogenesis. *Heart Rhythm* **2,** 316-324.

Dhamoon A. S., Pandit S. V., Sarmast F., Parisian K. R., Guha P., Li Y., Bagwe S., Taffet S. M. & Anumonwo J. M. (2004). Unique Kir2.x properties determine regional and species differences in the cardiac inward rectifier K^+ current. *Circ Res* **94,** 1332-1339.

Domenighetti A. A., Boixel C., Cefai D., Abriel H. & Pedrazzini T. (2007). Chronic angiotensin II stimulation in the heart produces an acquired long QT syndrome associated with I_{K1} potassium current downregulation. *J Mol Cell Cardiol* **42,** 63-70.

Donaldson M. R., Yoon G., Fu Y. H. & Ptacek L. J. (2004). Andersen-Tawil syndrome: a model of clinical variability, pleiotropy, and genetic heterogeneity. *Ann Med* **36 Suppl 1,** 92-97.

Dresdner K. P., Kline R. P. & Wit A. L. (1987). Intracellular K^+ activity, intracellular Na^+ activity and maximum diastolic potential of canine subendocardial Purkinje cells from one-day-old infarcts. *Circ Res* **60,** 122-132.

Dudel J., Peper K., Rüdel R. & Trautwein W. (1967). The potassium component of membrane current in Purkinje fibers. *Pflügers Arch Gesamte Physiol Menschen Tiere* **296,** 308-327.

Dyachenko V., Husse B., Rueckschloss U. & Isenberg G. (2009). Mechanical deformation of ventricular myocytes modulates both TRPC6 and Kir2.3 channels. *Cell Calcium* **45,** 38-54.

Dyachok O., Zhabyeyev P. & McDonald T. F. (2010). Electroporation-induced inward current in voltage-clamped guinea pig ventricular myocytes. *J Membr Biol* **238,** 69-80.

Eaton D. C. (1972). Potassium ion accumulation near a pace-making cell of *Aplysia*. *J Physiol* **224,** 421-440.

Eisner D. A. & Lederer W. J. (1979). Inotropic and arrhythmogenic effects of potassium-depleted solutions on mammalian cardiac muscle. *J Physiol* **294,** 255-277.

El Gebeily G. & Fiset C. (2010). 4-Hydroxytamoxifen inhibits K^+ currents in mouse ventricular myocytes. *Eur J Pharmacol* **629,** 96-103.

El Harchi A., McPate M. J., Zhang Y., Zhang H. & Hancox J. C. (2009). Action potential clamp and chloroquine sensitivity of mutant Kir2.1 channels responsible for variant 3 short QT syndrome. *J Mol Cell Cardiol* **47,** 743-747.

Fan J. S. & Liu T. F. (1996). Role of inward and delayed rectifier currents in generation of early afterdepolarization in guinea pig ventricular myocytes under K^+-free or low K^+ superfusion. *Methods Find Exp Clin Pharmacol* **18,** 25-32.

Farber S. J., Pellegrino E. D., Conan N. J. & Earle D. P. (1951). Observations on the plasma potassium level of man. *Am J Med Sci* **221,** 678-687.

Fauconnier J., Pasquié J. L., Bideaux P., Lacampagne A. & Richard S. (2010). Cardiomyocytes hypertrophic status after myocardial infarction determines distinct types of arrhythmia: role of the ryanodine receptor. *Prog Biophys Mol Biol* **103,** 71-80.

Ficker E., Taglialatela M., Wible B. A., Henley C. M. & Brown A. M. (1994). Spermine and spermidine as gating molecules for inward rectifier K^+ channels. *Science* **266,** 1068-1072.

Fink M., Giles W. R. & Noble D. (2006). Contributions of inwardly rectifying K^+ currents to repolarization assessed using mathematical models of human ventricular myocytes. *Philos Transact A Math Phys Eng Sci* **364,** 1207-1222.

Fiset C., Clark R. B., Larsen T. S. & Giles W. R. (1997). A rapidly activating sustained K^+ current modulates repolarization and excitation-contraction coupling in adult mouse ventricle. *J Physiol* **504** 557-563.

Forbes M. S., Hawkey L. A. & Sperelakis N. (1984). The transverse-axial tubular system (TATS) of mouse myocardium: its morphology in the developing and adult animal. *Am J Anat* **170,** 143-162.

Forbes M. S. & van Neil E. E. (1988). Membrane systems of guinea pig myocardium: ultrastructure and morphometric studies. *Anat Rec* **222,** 362-379.

Fozzard H. A. & Lee C. O. (1976). Influence of changes in external potassium and chloride ions on membrane potential and intracellular potassium ion activity in rabbit ventricular muscle. *J Physiol* **256,** 663-689.

Frankenhaeuser B. (1962). Instantaneous potassium currents in myelinated nerve fibres of Xenopus laevis. *J Physiol* **160,** 46-53.

Frankenhaeuser B. & Hodgkin A. L. (1956). The after-effects of impulses in the giant nerve fibres of *Loligo*. *J Physiol* **131,** 341-376.

Frazier C. J., George E. G. & Jones S. W. (2000). Apparent change in ion selectivity caused by changes in intracellular K^+ during whole-cell recording. *Biophys J* **78,** 1872-1880.

Fujiwara Y. & Kubo Y. (2006). Functional roles of charged amino acid residues on the wall of the cytoplasmic pore of Kir2.1. *J Gen Physiol* **127,** 401-419.

Gaborit N., Le Bouter S., Szuts V., Varro A., Escande D., Nattel S. & Demolombe S. (2007). Regional and tissue specific transcript signatures of ion channel genes in the non-diseased human heart. *J Physiol* **582,** 675-693.

Gao Z., Lau C. P., Wong T. M. & Li G. R. (2004). Protein tyrosine kinase-dependent modulation of voltage-dependent potassium channels by genistein in rat cardiac ventricular myocytes. *Cell Signal* **16,** 333-341.

Gay L. A. & Stanfield P. R. (1977). Cs^+ causes a voltage-dependent block of inward K^+ currents in resting skeletal muscle fibres. *Nature* **267,** 169-170.

Gettes L. S., Surawicz B. & Shiue J. C. (1962). Effect of high K, and low K, quinidine on QRS duration and ventricular action potential. *Am J Physiol* **203,** 1135-1140.

Giles W. R. & Imaizumi Y. (1988). Comparison of potassium currents in rabbit atrial and ventricular cells. *J Physiol* **405,** 123-145.

Girmatsion Z., Biliczki P., Bonauer A., Wimmer-Greinecker G., Scherer M., Moritz A., Bukowska A., Goette A., Nattel S., Hohnloser S. H. & Ehrlich J. R. (2009). Changes in microRNA-1 expression and I_{K1} up-regulation in human atrial fibrillation. *Heart Rhythm* **6,** 1802-1809.

Gjini V., Korth M., Schreieck J., Weyerbrock S., Schömig A. & Schmitt C. (1996). Differential class III antiarrhythmic effects of ambasilide and dofetilide at different extracellular potassium and pacing frequencies. *J Cardiovasc Pharmacol* **28,** 314-320.

Gómez R., Caballero R., Barana A., Amorós I., Calvo E., López J. A., Klein H., Vaquero M., Osuna L., Atienza F., Almendral J., Pinto A., Tamargo J. & Delpón E. (2009). Nitric oxide increases cardiac I_{K1} by nitrosylation of cysteine 76 of Kir2.1 channels. *Circ Res* **105,** 383-392.

Grandy S. A., Trépanier-Boulay V. & Fiset C. (2007). Postnatal development has a marked effect on ventricular repolarization in mice. *Am J Physiol Heart Circ Physiol* **293,** H2168-2177.

Guo D. & Lu Z. (2003). Interaction mechanisms between polyamines and IRK1 inward rectifier K^+ channels. *J Gen Physiol* **122,** 485-500.

Guo D., Ramu Y., Klem A. M. & Lu Z. (2003). Mechanism of rectification in inward-rectifier K^+ channels. *J Gen Physiol* **121,** 261-275.

Hadley R. W. & Hume J. R. (1990). Permeability of time-dependent K^+ channel in guinea pig ventricular myocytes to Cs^+, Na^+, NH^{4+}, and Rb^+. *Am J Physiol* **259,** H1448-1454.

Hagiwara S., Miyazaki S. & Rosenthal N. P. (1976). Potassium current and the effect of cesium on this current during anomalous rectification of the egg cell membrane of a starfish. *J Gen Physiol* **67,** 621-638.

Hagiwara S. & Takahashi K. (1974). The anomalous rectification and cation selectivity of the membrane of a starfish egg cell. *J Membr Biol* **18,** 61-80.

Hagiwara S. & Yoshii M. (1979). Effects of internal potassium and sodium on the anomalous rectification of the starfish egg as examined by internal perfusion. *J Physiol* **292,** 251-265.

Hall A. E., Hutter O. F. & Noble D. (1963). Current-voltage relations of Purkinje fibres in sodium-deficient solutions. *J Physiol* **166,** 225-240.

Hamill O. P., Marty A., Neher E., Sakmann B. & Sigworth F. J. (1981). Improved patch-clamp techniques for high-resolution current recording from cells and cell-free membrane patches. *Pflügers Arch* **391,** 85-100.

Harrell M. D., Harbi S., Hoffman J. F., Zavadil J. & Coetzee W. A. (2007). Large-scale analysis of ion channel gene expression in the mouse heart during perinatal development. *Physiol Genomics* **28,** 273-283.

Harrison C. E., Jr., Cooper G. t., Zujko K. J. & Coleman H. N., 3rd. (1972). Myocardial and mitochondrial function in potassium depletion cardiomyopathy. *J Mol Cell Cardiol* **4,** 633-649.

Harvey R. D. & Ten Eick R. E. (1988). Characterization of the inward-rectifying potassium current in cat ventricular myocytes. *J Gen Physiol* **91,** 593-615.

Harvey R. D. & Ten Eick R. E. (1989). Voltage-dependent block of cardiac inward-rectifying potassium current by monovalent cations. *J Gen Physiol* **94,** 349-361.

He Y., Pan Q., Li J., Chen H., Zhou Q., Hong K., Brugada R., Perez G. J., Brugada P. & Chen Y. H. (2008). Kir2.3 knock-down decreases I_{K1} current in neonatal rat cardiomyocytes. *FEBS Lett* **582,** 2338-2342.

Hestrin S. (1981). The interaction of potassium with the activation of anomalous rectification in frog muscle membrane. *J Physiol* **317,** 497-508.

Hibino H., Inanobe A., Furutani K., Murakami S., Findlay I. & Kurachi Y. (2010). Inwardly rectifying potassium channels: their structure, function, and physiological roles. *Physiol Rev* **90,** 291-366.

Hilgemann D. W., Feng S. & Nasuhoglu C. (2001). The complex and intriguing lives of PIP_2 with ion channels and transporters. *Sci STKE* **2001,** re19.

Hille B. (2001). *Ion Channels of Excitable Membranes*. Sinauer Associates Inc., Sunderland, MA, USA.

Hiraoka M. & Fan Z. (1989). Activation of ATP-sensitive outward K^+ current by nicorandil (2-nicotinamidoethyl nitrate) in isolated ventricular myocytes. *J Pharmacol Exp Ther* **250,** 278-285.

Hume J. R. & Uehara A. (1985). Ionic basis of the different action potential configurations of single guinea-pig atrial and ventricular myocytes. *J Physiol* **368,** 525-544.

Hutter O. F. & Noble D. (1960). Rectifying properties of heart muscle. *Nature* **188,** 495.

Hwang T. C., Horie M., Nairn A. C. & Gadsby D. C. (1992). Role of GTP-binding proteins in the regulation of mammalian cardiac chloride conductance. *J Gen Physiol* **99,** 465-489.

Ibarra J., Morley G. E. & Delmar M. (1991). Dynamics of the inward rectifier K^+ current during the action potential of guinea pig ventricular myocytes. *Biophys J* **60,** 1534-1539.

Ibrahim M., Gorelik J., Yacoub M. H. & Terracciano C. M. (2011). The structure and function of cardiac T-tubules in health and disease. *Proc Biol Sci* **278,** 2714-2723.

Isenberg G. (1993). Nonselective cation channels in cardiac and smooth muscle cells. *EXS* **66,** 247-260.

Isenberg G. & Klöckner U. (1982). Isolated bovine ventricular myocytes. Characterization of the action potential. *Pflügers Arch* **395,** 19-29.

Ishihara K. & Ehara T. (1998). A repolarization-induced transient increase in the outward current of the inward rectifier K^+ channel in guinea-pig cardiac myocytes. *J Physiol* **510** 755-771.

Ishihara K., Mitsuiye T., Noma A. & Takano M. (1989). The Mg^{2+} block and intrinsic gating underlying inward rectification of the K^+ current in guinea-pig cardiac myocytes. *J Physiol* **419,** 297-320.

Ishihara K., Yan D. H., Yamamoto S. & Ehara T. (2002). Inward rectifier K^+ current under physiological cytoplasmic conditions in guinea-pig cardiac ventricular cells. *J Physiol* **540,** 831-841.

Jan L. Y. & Jan Y. N. (1997). Voltage-gated and inwardly rectifying potassium channels. *J Physiol* **505,** 267-282.

John S. A., Xie L. H. & Weiss J. N. (2004). Mechanism of inward rectification in Kir channels. *J Gen Physiol* **123,** 623-625.

Jones S. E., Ogura T., Shuba L. M. & McDonald T. F. (1998). Inhibition of the rapid component of the delayed-rectifier K^+ current by therapeutic concentrations of the antispasmodic agent terodiline. *Br J Pharmacol* **125,** 1138-1143.

Jow F. & Numann R. (1998). Divalent ion block of inward rectifier current in human capillary endothelial cells and effects on resting membrane potential. *J Physiol* **512** 119-128.

Kääb S., Dixon J., Duc J., Ashen D., Näbauer M., Beuckelmann D. J., Steinbeck G., McKinnon D. & Tomaselli G. F. (1998). Molecular basis of transient outward potassium current downregulation in human heart failure: a decrease in Kv4.3 mRNA correlates with a reduction in current density. *Circulation* **98,** 1383-1393.

Kameyama M., Kiyosue T. & Soejima M. (1983). Single channel analysis of the inward rectifier K^+ current in the rabbit ventricular cells. *Jpn J Physiol* **33,** 1039-1056.

Karle C. A., Zitron E., Zhang W., Wendt-Nordahl G., Kathöfer S., Thomas D., Gut B., Scholz E., Vahl C. F., Katus H. A. & Kiehn J. (2002). Human cardiac inwardly-rectifying K^+ channel $Kir_{2.1b}$ is inhibited by direct protein kinase C-dependent regulation in human isolated cardiomyocytes and in an expression system. *Circulation* **106,** 1493-1499.

Katzung B. G. (1975). Effects of extracellular calcium and sodium on depolarization-induced automaticity in guinea pig papillary muscle. *Circ Res* **37,** 118-127.

Kelly M. E., Dixon S. J. & Sims S. M. (1992). Inwardly rectifying potassium current in rabbit osteoclasts: a whole-cell and single-channel study. *J Membr Biol* **126,** 171-181.

Kharche S., Garratt C. J., Boyett M. R., Inada S., Holden A. V., Hancox J. C. & Zhang H. (2008). Atrial proarrhythmia due to increased inward rectifier current (I_{K1}) arising from KCNJ2 mutation - A simulation study. *Prog Biophys Mol Biol* **98,** 186-197.

Kiss L., LoTurco J. & Korn S. J. (1999). Contribution of the selectivity filter to inactivation in potassium channels. *Biophys J* **76,** 253-263.

Kiyosue T., Spindler A. J., Noble S. J. & Noble D. (1993). Background inward current in ventricular and atrial cells of the guinea-pig. *Proc Biol Sci* **252,** 65-74.

Kléber A. G. (1983). Resting membrane potential, extracellular potassium activity, and intracellular sodium activity during acute global ischemia in isolated perfused guinea pig hearts. *Circ Res* **52,** 442-450.

Kléber A. G. (1984). Extracellular potassium accumulation in acute myocardial ischemia. *J Mol Cell Cardiol* **16,** 389-394.

Klein H., Garneau L., Coady M., Lemay G., Lapointe J. Y. & Sauvé R. (1999). Molecular characterization of an inwardly rectifying K^+ channel from HeLa cells. *J Membr Biol* **167,** 43-52.

Kline R. P., Cohen I., Falk R. & Kupersmith J. (1980). Activity-dependent extracellular K^+ fluctuations in canine Purkinje fibres. *Nature* **286,** 68-71.

Knopp A., Thierfelder S., Koopmann R., Biskup C., Böhle T. & Benndorf K. (1999). Anoxia generates rapid and massive opening of K_{ATP} channels in ventricular cardiac myocytes. *Cardiovasc Res* **41,** 629-640.

Komukai K., Brette F., Yamanushi T. T. & Orchard C. H. (2002). K^+ current distribution in rat sub-epicardial ventricular myocytes. *Pflügers Arch* **444,** 532-538.

Kondo R. P., Dederko D. A., Teutsch C., Chrast J., Catalucci D., Chien K. R. & Giles W. R. (2006). Comparison of contraction and calcium handling between right and left ventricular myocytes from adult mouse heart: a role for repolarization waveform. *J Physiol* **571,** 131-146.

Koumi S., Wasserstrom J. A. & Ten Eick R. E. (1995). β-Adrenergic and cholinergic modulation of the inwardly rectifying K^+ current in guinea-pig ventricular myocytes. *J Physiol* **486,** 647-659.

Krapivinsky G., Medina I., Eng L., Krapivinsky L., Yang Y. & Clapham D. E. (1998). A novel inward rectifier K^+ channel with unique pore properties. *Neuron* **20,** 995-1005.

Kubo Y. (1996). Effects of extracellular cations and mutations in the pore region on the inward rectifier K^+ channel IRK1. *Receptors Channels* **4,** 73-83.

Kubo Y., Baldwin T. J., Jan Y. N. & Jan L. Y. (1993). Primary structure and functional expression of a mouse inward rectifier potassium channel. *Nature* **362,** 127-133.

Kubo Y. & Murata Y. (2001). Control of rectification and permeation by two distinct sites after the second transmembrane region in Kir2.1 K^+ channel. *J Physiol* **531,** 645-660.

Kuo A., Gulbis J. M., Antcliff J. F., Rahman T., Lowe E. D., Zimmer J., Cuthbertson J., Ashcroft F. M., Ezaki T. & Doyle D. A. (2003). Crystal structure of the potassium channel KirBac1.1 in the closed state. *Science* **300,** 1922-1926.

Kurata H. T., Marton L. J. & Nichols C. G. (2006). The polyamine binding site in inward rectifier K^+ channels. *J Gen Physiol* **127,** 467-480.

Kurata H. T., Zhu E. A. & Nichols C. G. (2010). Locale and chemistry of spermine binding in the archetypal inward rectifier Kir2.1. *J Gen Physiol* **135,** 495-508.

Lado M. G., Sheu S. S. & Fozzard H. A. (1984). Effects of tonicity on tension and intracellular sodium and calcium activities in sheep heart. *Circ Res* **54,** 576-585.

Lawrence C. L., Rainbow R. D., Davies N. W. & Standen N. B. (2002). Effect of metabolic inhibition on glimepiride block of native and cloned cardiac sarcolemmal K_{ATP} channels. *Br J Pharmacol* **136,** 746-752.

Lederer W. J., Niggli E. & Hadley R. W. (1990). Sodium-calcium exchange in excitable cells: fuzzy space. *Science* **248,** 283.

Leech C. A. & Stanfield P. R. (1981). Inward rectification in frog skeletal muscle fibres and its dependence on membrane potential and external potassium. *J Physiol* **319,** 295-309.

Leonoudakis D., Mailliard W., Wingerd K., Clegg D. & Vandenberg C. (2001). Inward rectifier potassium channel Kir2.2 is associated with synapse-associated protein SAP97. *J Cell Sci* **114,** 987-998.

Li J., McLerie M. & Lopatin A. N. (2004). Transgenic upregulation of I_{K1} in the mouse heart leads to multiple abnormalities of cardiac excitability. *Am J Physiol* **287,** H2790-2802.

Lipp P., Hüser J., Pott L. & Niggli E. (1996). Spatially non-uniform Ca^{2+} signals induced by the reduction of transverse tubules in citrate-loaded guinea-pig ventricular myocytes in culture. *J Physiol* **497 (Pt 3),** 589-597.

Liu A., Tang M., Xi J., Gao L., Zheng Y., Luo H., Hu X., Zhao F., Reppel M., Hescheler J. & Liang H. (2010). Functional characterization of inward rectifier potassium ion channel in murine fetal ventricular cardiomyocytes. *Cell Physiol Biochem* **26,** 413-420.

Liu G. X., Derst C., Schlichthörl G., Heinen S., Seebohm G., Brüggemann A., Kummer W., Veh R. W., Daut J. & Preisig-Müller R. (2001). Comparison of cloned Kir2 channels with native inward rectifier K^+ channels from guinea-pig cardiomyocytes. *J Physiol* **532,** 115-126.

Liu T. A., Chang H. K. & Shieh R. C. (2011). Extracellular K^+ elevates outward currents through Kir2.1 channels by increasing single-channel conductance. *Biochim Biophys Acta* **1808,** 1772-1778.

Loboda A., Melishchuk A. & Armstrong C. (2001). Dilated and defunct K channels in the absence of K^+. *Biophys J* **80,** 2704-2714.

Logothetis D. E., Jin T., Lupyan D. & Rosenhouse-Dantsker A. (2007). Phosphoinositide-mediated gating of inwardly rectifying K^+ channels. *Pflügers Arch* **455,** 83-95.

Lopatin A. N., Makhina E. N. & Nichols C. G. (1994). Potassium channel block by cytoplasmic polyamines as the mechanism of intrinsic rectification. *Nature* **372,** 366-369.

Lopatin A. N., Makhina E. N. & Nichols C. G. (1995). The mechanism of inward rectification of potassium channels: "long-pore plugging" by cytoplasmic polyamines. *J Gen Physiol* **106,** 923-955.

Lopatin A. N. & Nichols C. G. (1996). [K^+] dependence of polyamine-induced rectification in inward rectifier potassium channels (IRK1, Kir2.1). *J Gen Physiol* **108,** 105-113.

Lopatin A. N. & Nichols C. G. (2001). Inward rectifiers in the heart: an update on I_{K1}. *J Mol Cell Cardiol* **33,** 625-638.

Lopatin A. N., Shantz L. M., Mackintosh C. A., Nichols C. G. & Pegg A. E. (2000). Modulation of potassium channels in the hearts of transgenic and mutant mice with altered polyamine biosynthesis. *J Mol Cell Cardiol* **32,** 2007-2024.

Lopes C. M., Zhang H., Rohacs T., Jin T., Yang J. & Logothetis D. E. (2002). Alterations in conserved Kir channel-PIP_2 interactions underlie channelopathies. *Neuron* **34,** 933-944.

López-Izquierdo A., Ponce-Balbuena D., Moreno-Galindo E. G., Aréchiga-Figueroa I. A., Rodríguez-Martínez M., Ferrer T., Rodríguez-Menchaca A. A. & Sánchez-Chapula J. A. (2011). The antimalarial drug mefloquine inhibits cardiac inward rectifier K^+ channels: evidence for interference in PIP_2-channel interaction. *J Cardiovasc Pharmacol* **57,** 407-415.

Louch W. E., Sejersted O. M. & Swift F. (2010). There goes the neighborhood: pathological alterations in T-tubule morphology and consequences for cardiomyocyte Ca^{2+} handling. *J Biomed Biotechnol* **2010,** 503906.

Lu C. W., Lin J. H., Rajawat Y. S., Jerng H., Rami T. G., Sanchez X., DeFreitas G., Carabello B., DeMayo F., Kearney D. L., Miller G., Li H., Pfaffinger P. J., Bowles N. E., Khoury D. S. & Towbin J. A. (2006). Functional and clinical characterization of a mutation in KCNJ2 associated with Andersen-Tawil syndrome. *J Med Genet* **43,** 653-659.

Lu Z. (2004). Mechanism of rectification in inward-rectifier K^+ channels. *Annu Rev Physiol* **66,** 103-129.

Luo C. H. & Rudy Y. (1994). A dynamic model of the cardiac ventricular action potential. I. Simulations of ionic currents and concentration changes. *Circ Res* **74,** 1071-1096.

Main M. J., Grantham C. J. & Cannell M. B. (1997). Changes in subsarcolemmal sodium concentration measured by Na-Ca exchanger activity during Na-pump inhibition and beta-adrenergic stimulation in guinea-pig ventricular myocytes. *Pflügers Arch* **435,** 112-118.

Martin R. L., Koumi S. & Ten Eick R. E. (1995). Comparison of the effects of internal Mg^{2+} on I_{K1} in cat and guinea-pig cardiac ventricular myocytes. *J Mol Cell Cardiol* **27,** 673-691.

Mascher D. & Peper K. (1969). Two components of inward current in myocardial muscle fibers. *Pflügers Arch* **307,** 190-203.

Mathias R. T., Cohen I. S. & Oliva C. (1990). Limitations of the whole cell patch clamp technique in the control of intracellular concentrations. *Biophys J* **58,** 759-770.

Matsuda H. (1991). Effects of external and internal K^+ ions on magnesium block of inwardly rectifying K^+ channels in guinea-pig heart cells. *J Physiol* **435,** 83-99.

Matsuda H. (1996). Rb^+, Cs^+ ions and the inwardly rectifying K^+ channels in guinea-pig ventricular cells. *Pflügers Arch* **432,** 26-33.

Matsuda H., Hayashi M. & Okada M. (2010). Voltage-dependent block by internal spermine of the murine inwardly rectifying K^+ channel, Kir2.1, with asymmetrical K^+ concentrations. *J Physiol* **588,** 4673-4681.

Matsuda H. & Noma A. (1984). Isolation of calcium current and its sensitivity to monovalent cations in dialysed ventricular cells of guinea-pig. *J Physiol* **357,** 553-573.

Matsuda H., Saigusa A. & Irisawa H. (1987). Ohmic conductance through the inwardly rectifying K^+ channel and blocking by internal Mg^{2+}. *Nature* **325,** 156-159.

Matsuura H., Ehara T. & Imoto Y. (1987). An analysis of the delayed outward current in single ventricular cells of the guinea-pig. *Pflügers Arch* **410,** 596-603.

Maughan D. W., McGuigan J. A., Bassingthwaighte J. & Reuter H. (1973). Extracellular K^+ depletion in mammalian ventricular muscle. *Experientia* **29,** 746.

McAllister R. E. & Noble D. (1966). The time and voltage dependence of the slow outward current in cardiac Purkinje fibres. *J Physiol* **186,** 632-662.

McDonald T. F., Kholopov A., Terada H. & Asai T. (1989). Experimental and theoretical aspects of excitation, impulse conduction, and block in the heart. In *Electrocardiology 1988*, ed. Abel H, pp. 21-26. Excerpta Medica, Wiesbaden, Germany.

McDonald T. F., Pelzer S., Trautwein W. & Pelzer D. J. (1994). Regulation and modulation of calcium channels in cardiac, skeletal, and smooth muscle cells. *Physiol Rev* **74,** 365-507.

McDonald T. F. & Trautwein W. (1978). The potassium current underlying delayed rectification in cat ventricular muscle. *J Physiol* **274,** 217-246.

McKinney L. C. & Gallin E. K. (1988). Inwardly rectifying whole-cell and single-channel K currents in the murine macrophage cell line J774.1. *J Membr Biol* **103,** 41-53.

McLerie M. & Lopatin A. N. (2003). Dominant-negative suppression of I_{K1} in the mouse heart leads to altered cardiac excitability. *J Mol Cell Cardiol* **35,** 367-378.

Melishchuk A., Loboda A. & Armstrong C. M. (1998). Loss of shaker K channel conductance in 0 K^+ solutions: role of the voltage sensor. *Biophys J* **75,** 1828-1835.

Melnyk P., Zhang L., Shrier A. & Nattel S. (2002). Differential distribution of Kir2.1 and Kir2.3 subunits in canine atrium and ventricle. *Am J Physiol* **283,** H1123-1133.

Miake J., Marbán E. & Nuss H. B. (2003). Functional role of inward rectifier current in heart probed by Kir2.1 overexpression and dominant-negative suppression. *J Clin Invest* **111,** 1529-1536.

Missan S., Zhabyeyev P., Dyachok O., Ogura T. & McDonald T. F. (2004). Inward-rectifier K^+ current in guinea-pig ventricular myocytes exposed to hyperosmotic solutions. *J Membr Biol* **202,** 151-160.

Mitcheson J. S., Hancox J. C. & Levi A. J. (1996). Action potentials, ion channel currents and transverse tubule density in adult rabbit ventricular myocytes maintained for 6 days in cell culture. *Pflügers Arch* **431,** 814-827.

Mitsuiye T. & Noma A. (1987). A new oil-gap method for internal perfusion and voltage clamp of single cardiac cells. *Pflügers Arch* **410,** 7-14.

Morais-Cabral J. H., Zhou Y. & MacKinnon R. (2001). Energetic optimization of ion conduction rate by the K^+ selectivity filter. *Nature* **414,** 37-42.

Murata Y., Fujiwara Y. & Kubo Y. (2002). Identification of a site involved in the block by extracellular Mg^{2+} and Ba^{2+} as well as permeation of K^+ in the Kir2.1 K^+ channel. *J Physiol* **544,** 665-677.

Nakajima S. & Onodera K. (1969). Membrane properties of the stretch receptor neurones of crayfish with particular reference to mechanisms of sensory adaptation. *J Physiol* **200,** 161-185.

Nakamura T. Y., Artman M., Rudy B. & Coetzee W. A. (1998). Inhibition of rat ventricular I_{K1} with antisense oligonucleotides targeted to Kir2.1 mRNA. *Am J Physiol* **274,** H892-900.

Nattel S. (2003). Remodeling of cardiac inward-rectifier currents: an often-overlooked contributor to arrhythmogenic states. *J Mol Cell Cardiol* **35,** 1395-1398.

Nerbonne J. M. & Kass R. S. (2005). Molecular physiology of cardiac repolarization. *Physiol Rev* **85,** 1205-1253.

Noble D. (1965). Electrical properties of cardiac muscle attributable to inward-going (anomalous) rectification. *J Cell Comp Physiol* **66,** 127-136.

Noble D. (1975). *The Initiation of the Heartbeat*. Oxford University Press, Oxford.

Noble D. (1986). Ionic mechanisms controlling the action potential duration and the timing of repolarization. *Jpn Heart J* **27 Suppl 1,** 3-19.

Noble S. J. (1976). Potassium accumulation and depletion in frog atrial muscle. *J Physiol* **258,** 579-613.

Noujaim S. F., Pandit S. V., Berenfeld O., Vikstrom K., Cerrone M., Mironov S., Zugermayr M., Lopatin A. N. & Jalife J. (2007). Up-regulation of the inward rectifier K^+ current (I_{K1}) in the mouse heart accelerates and stabilizes rotors. *J Physiol* **578,** 315-326.

Orkand R. K. (1980). Extracellular potassium accumulation in the nervous system. *Fed Proc* **39,** 1515-1518.

Panama B. K., McLerie M. & Lopatin A. N. (2007). Heterogeneity of I_{K1} in the mouse heart. *Am J Physiol* **293,** H3558-3567.

Park W. S., Han J. & Earm Y. E. (2008). Physiological role of inward rectifier K^+ channels in vascular smooth muscle cells. *Pflügers Arch* **457,** 137-147.

Pásek M., Christé G. & Simurda J. (2003). A quantitative model of the cardiac ventricular cell incorporating the transverse-axial tubular system. *Gen Physiol Biophys* **22,** 355-368.

Pásek M., Simurda J., Orchard C. H. & Christé G. (2008). A model of the guinea-pig ventricular cardiac myocyte incorporating a transverse-axial tubular system. *Prog Biophys Mol Biol* **96,** 258-280.

Paynter J. J., Andres-Enguix I., Fowler P. W., Tottey S., Cheng W., Enkvetchakul D., Bavro V. N., Kusakabe Y., Sansom M. S., Robinson N. J., Nichols C. G. & Tucker S. J.

(2010). Functional complementation and genetic deletion studies of KirBac channels: activatory mutations highlight gating-sensitive domains. *J Biol Chem* **285,** 40754-40761.

Pegan S., Arrabit C., Zhou W., Kwiatkowski W., Collins A., Slesinger P. A. & Choe S. (2005). Cytoplasmic domain structures of Kir2.1 and Kir3.1 show sites for modulating gating and rectification. *Nat Neurosci* **8,** 279-287.

Pennefather P., Oliva C. & Mulrine N. (1992). Origin of the potassium and voltage dependence of the cardiac inwardly rectifying K-current (I_{K1}). *Biophys J* **61,** 448-462.

Plaster N. M., Tawil R., Tristani-Firouzi M., Canún S., Bendahhou S., Tsunoda A., Donaldson M. R., Iannaccone S. T., Brunt E., Barohn R., Clark J., Deymeer F., George A. L., Jr., Fish F. A., Hahn A., Nitu A., Ozdemir C., Serdaroglu P., Subramony S. H., Wolfe G., Fu Y. H. & Ptacek L. J. (2001). Mutations in Kir2.1 cause the developmental and episodic electrical phenotypes of Andersen's syndrome. *Cell* **105,** 511-519.

Pogwizd S. M., Schlotthauer K., Li L., Yuan W. & Bers D. M. (2001). Arrhythmogenesis and contractile dysfunction in heart failure: Roles of sodium-calcium exchange, inward rectifier potassium current, and residual beta-adrenergic responsiveness. *Circ Res* **88,** 1159-1167.

Ponce-Balbuena D., López-Izquierdo A., Ferrer T., Rodríguez-Menchaca A. A., Aréchiga-Figueroa I. A. & Sánchez-Chapula J. A. (2009). Tamoxifen inhibits inward rectifier K^+ 2.x family of inward rectifier channels by interfering with phosphatidylinositol 4,5-bisphosphate-channel interactions. *J Pharmacol Exp Ther* **331,** 563-573.

Postema P. G., Ritsema van Eck H. J., Opthof T., van Herpen G., van Dessel P. F., Priori S. G., Wolpert C., Borggrefe M., Kors J. A. & Wilde A. A. (2009). I_{K1} modulates the U-wave: insights in a 100-year-old enigma. *Heart Rhythm* **6,** 393-400.

Priori S. G., Pandit S. V., Rivolta I., Berenfeld O., Ronchetti E., Dhamoon A., Napolitano C., Anumonwo J., di Barletta M. R., Gudapakkam S., Bosi G., Stramba-Badiale M. & Jalife J. (2005). A novel form of short QT syndrome (SQT3) is caused by a mutation in the KCNJ2 gene. *Circ Res* **96,** 800-807.

Puglisi J. L., Yuan W., Timofeyev V., Myers R. E., Chiamvimonvat N., Samarel A. M. & Bers D. M. (2011). Phorbol ester and endothelin-1 alter functional expression of Na^+/Ca^{2+} exchange, K^+, and Ca^{2+} currents in cultured neonatal rat myocytes. *Am J Physiol Heart Circ Physiol* **300,** H617-626.

Raab-Graham K. F. & Vandenberg C. A. (1998). Tetrameric subunit structure of the native brain inwardly rectifying potassium channel Kir 2.2. *J Biol Chem* **273,** 19699-19707.

Rajakulendran S., Tan S. V. & Hanna M. G. (2010). Muscle weakness, palpitations and a small chin: the Andersen-Tawil syndrome. *Pract Neurol* **10,** 227-231.

Ranjan R., Chiamvimonvat N., Thakor N. V., Tomaselli G. F. & Marban E. (1998). Mechanism of anode break stimulation in the heart. *Biophys J* **74,** 1850-1863.

Robertson J. L., Palmer L. G. & Roux B. (2008). Long-pore electrostatics in inward-rectifier potassium channels. *J Gen Physiol* **132,** 613-632.

Roden D. M., Balser J. R., George A. L., Jr. & Anderson M. E. (2002). Cardiac ion channels. *Annu Rev Physiol* **64,** 431-475.

Rodríguez-Menchaca A. A., Navarro-Polanco R. A., Ferrer-Villada T., Rupp J., Sachse F. B., Tristani-Firouzi M. & Sánchez-Chapula J. A. (2008). The molecular basis of chloroquine block of the inward rectifier Kir2.1 channel. *Proc Natl Acad Sci U S A* **105,** 1364-1368.

Romanenko V. G., Rothblat G. H. & Levitan I. (2002). Modulation of endothelial inward-rectifier K^+ current by optical isomers of cholesterol. *Biophys J* **83,** 3211-3222.

Romero L., Pueyo E., Fink M. & Rodríguez B. (2009). Impact of ionic current variability on human ventricular cellular electrophysiology. *Am J Physiol Heart Circ Physiol* **297,** H1436-1445.

Rosenhouse-Dantsker A., Logothetis D. E. & Levitan I. (2011). Cholesterol sensitivity of KIR2.1 is controlled by a belt of residues around the cytosolic pore. *Biophys J* **100,** 381-389.

Rougier O., Vassort G. & Stämpfli R. (1968). Voltage clamp experiments on frog atrial heart muscle fibres with the sucrose gap technique. *Pflügers Arch Gesamte Physiol Menschen Tiere* **301,** 91-108.

Ryan D. P., da Silva M. R., Soong T. W., Fontaine B., Donaldson M. R., Kung A. W., Jongjaroenprasert W., Liang M. C., Khoo D. H., Cheah J. S., Ho S. C., Bernstein H. S., Maciel R. M., Brown R. H., Jr. & Ptácek L. J. (2010). Mutations in potassium channel Kir2.6 cause susceptibility to thyrotoxic hypokalemic periodic paralysis. *Cell* **140,** 88-98.

Ryu S. Y., Lee S. H. & Ho W. K. (2005). Generation of metabolic oscillations by mitoK_{ATP} and ATP synthase during simulated ischemia in ventricular myocytes. *J Mol Cell Cardiol* **39,** 874-881.

Saigusa A. & Matsuda H. (1988). Outward currents through the inwardly rectifying potassium channel of guinea-pig ventricular cells. *Jpn J Physiol* **38,** 77-91.

Sakmann B. & Trube G. (1984). Conductance properties of single inwardly rectifying potassium channels in ventricular cells from guinea-pig heart. *J Physiol* **347,** 641-657.

Sanguinetti M. C. & Jurkiewicz N. K. (1990). Two components of cardiac delayed rectifier K^+ current. Differential sensitivity to block by class III antiarrhythmic agents. *J Gen Physiol* **96,** 195-215.

Sanguinetti M. C. & Jurkiewicz N. K. (1992). Role of external Ca^{2+} and K^+ in gating of cardiac delayed rectifier K^+ currents. *Pflugers Arch* **420,** 180-186.

Sato R. & Koumi S. (1995). Modulation of the inwardly rectifying K^+ channel in isolated human atrial myocytes by alpha 1-adrenergic stimulation. *J Membr Biol* **148,** 185-191.

Satoh H., Delbridge L. M., Blatter L. A. & Bers D. M. (1996). Surface:volume relationship in cardiac myocytes studied with confocal microscopy and membrane capacitance measurements: species-dependence and developmental effects. *Biophys J* **70,** 1494-1504.

Scherer D., Kiesecker C., Kulzer M., Günth M., Scholz E. P., Kathöfer S., Thomas D., Maurer M., Kreuzer J., Bauer A., Katus H. A., Karle C. A. & Zitron E. (2007). Activation of inwardly rectifying Kir2.x potassium channels by beta 3-adrenoceptors is mediated via different signaling pathways with a predominant role of PKC for Kir2.1 and of PKA for Kir2.2. *Naunyn Schmiedebergs Arch Pharmacol* **375,** 311-322.

Schram G., Pourrier M., Melnyk P. & Nattel S. (2002). Differential distribution of cardiac ion channel expression as a basis for regional specialization in electrical function. *Circ Res* **90,** 939-950.

Sejersted O. M. & Sjøgaard G. (2000). Dynamics and consequences of potassium shifts in skeletal muscle and heart during exercise. *Physiol Rev* **80,** 1411-1481.

Shah A. K., Cohen I. S. & Datyner N. B. (1987). Background K^+ current in isolated canine cardiac Purkinje myocytes. *Biophys J* **52,** 519-525.

Shepherd N. & McDonough H. B. (1998). Ionic diffusion in transverse tubules of cardiac ventricular myocytes. *Am J Physiol* **275,** H852-860.

Shimoni Y., Clark R. B. & Giles W. R. (1992). Role of an inwardly rectifying potassium current in rabbit ventricular action potential. *J Physiol* **448,** 709-727.

Shin H. G. & Lu Z. (2005). Mechanism of the voltage sensitivity of IRK1 inward-rectifier K^+ channel block by the polyamine spermine. *J Gen Physiol* **125,** 413-426.

Silver M. R., Shapiro M. S. & DeCoursey T. E. (1994). Effects of external Rb^+ on inward rectifier K^+ channels of bovine pulmonary artery endothelial cells. *J Gen Physiol* **103,** 519-548.

Silverman B. Z., Warley A., Miller J. I., James A. F. & Shattock M. J. (2003). Is there a transient rise in sub-sarcolemmal Na and activation of Na/K pump current following activation of I_{Na} in ventricular myocardium? *Cardiovasc Res* **57,** 1025-1034.

Singer J. J. & Walsh J. V., Jr. (1980). Rectifying properties of the membrane of single freshly isolated smooth muscle cells. *Am J Physiol* **239,** C175-181.

So I., Ashmole I., Davies N. W., Sutcliffe M. J. & Stanfield P. R. (2001). The K^+ channel signature sequence of murine Kir2.1: mutations that affect microscopic gating but not ionic selectivity. *J Physiol* **531,** 37-50.

Soeller C. & Cannell M. B. (1999). Examination of the transverse tubular system in living cardiac rat myocytes by 2-photon microscopy and digital image-processing techniques. *Circ Res* **84,** 266-275.

Sommer J. R. (1982). Ultrastructural considerations concerning cardiac muscle. *J Mol Cell Cardiol* **14** 77-83.

Sommer J. R. & Johnson E. A. (1968). Cardiac muscle. A comparative study of Purkinje fibers and ventricular fibers. *J Cell Biol* **36,** 497-526.

Song Y. M. & Ochi R. (2002). Hyperpolarization and lysophosphatidylcholine induce inward currents and ethidium fluorescence in rabbit ventricular myocytes. *J Physiol* **545,** 463-473.

Sonoyama K., Ninomiya H., Igawa O., Kaetsu Y., Furuse Y., Hamada T., Miake J., Li P., Yamamoto Y., Ogino K., Yoshida A., Taniguchi S., Kurata Y., Matsuoka S., Narahashi T., Shiota G., Nozawa Y., Matsubara H., Horiuchi M., Shirayoshi Y. & Hisatome I. (2006). Inhibition of inward rectifier K^+ currents by angiotensin II in rat atrial myocytes: lack of effects in cells from spontaneously hypertensive rats. *Hypertens Res* **29,** 923-934.

Spindler A. J., Noble S. J., Noble D. & LeGuennec J. Y. (1998). The effects of sodium substitution on currents determining the resting potential in guinea-pig ventricular cells. *Exp Physiol* **83,** 121-136.

Stadnicka A., Bosnjak Z. J., Kampine J. P. & Kwok W. M. (1997). Effects of sevoflurane on inward rectifier K^+ current in guinea pig ventricular cardiomyocytes. *Am J Physiol* **273,** H324-332.

Stanfield P. R., Davies N. W., Shelton P. A., Khan I. A., Brammar W. J., Standen N. B. & Conley E. C. (1994). The intrinsic gating of inward rectifier K^+ channels expressed from the murine IRK1 gene depends on voltage, K^+ and Mg^{2+}. *J Physiol* **475,** 1-7.

Stanfield P. R., Nakajima S. & Nakajima Y. (2002). Constitutively active and G-protein coupled inward rectifier K^+ channels: Kir2.0 and Kir3.0. *Rev Physiol Biochem Pharmacol* **145,** 47-179.

Stelling J. W. & Jacob T. J. (1992). The inward rectifier K^+ current underlies oscillatory membrane potential behaviour in bovine pigmented ciliary epithelial cells. *J Physiol* **458,** 439-456.

Sung R. J., Wu S. N., Wu J. S., Chang H. D. & Luo C. H. (2006). Electrophysiological mechanisms of ventricular arrhythmias in relation to Andersen-Tawil syndrome under conditions of reduced I_{K1}: a simulation study. *Am J Physiol Heart Circ Physiol* **291,** H2597-2605.

Surawicz B. & Lepeschkin E. (1953). The electrocardiographic pattern of hypopotassemia with and without hypocalcemia. *Circulation* **8,** 801-828.

Swift F., Strømme T. A., Amundsen B., Sejersted O. M. & Sjaastad I. (2006). Slow diffusion of K^+ in the T tubules of rat cardiomyocytes. *J Appl Physiol* **101,** 1170-1176.

Szabó G., Szentandrássy N., Bíró T., Tóth B. I., Czifra G., Magyar J., Bányász T., Varró A., Kovács L. & Nánási P. P. (2005). Asymmetrical distribution of ion channels in canine and human left-ventricular wall: epicardium versus midmyocardium. *Pflügers Arch* **450,** 307-316.

Tamargo J., Caballero R., Gómez R., Valenzuela C. & Delpón E. (2004). Pharmacology of cardiac potassium channels. *Cardiovasc Res* **62,** 9-33.

Tohse N., Kameyama M., Sekiguchi K., Shearman M. S. & Kanno M. (1990). Protein kinase C activation enhances the delayed rectifier potassium current in guinea-pig heart cells. *J Mol Cell Cardiol* **22,** 725-734.

Török T. L. (2007). Electrogenic Na^+/Ca^{2+}-exchange of nerve and muscle cells. *Prog Neurobiol* **82,** 287-347.

Tourneur Y., Marion A. & Gautier P. (1994). SR47063, a potent channel opener, activates K_{ATP} and a time-dependent current likely due to potassium accumulation. *J Membr Biol* **142,** 337-347.

Tourneur Y., Mitra R., Morad M. & Rougier O. (1987). Activation properties of the inward-rectifying potassium channel on mammalian heart cells. *J Membr Biol* **97,** 127-135.

Trautwein W. & McDonald T. F. (1978). Current-voltage relations in ventricular muscle preparations from different species. *Pflügers Arch* **374,** 79-89.

Tristani-Firouzi M. & Etheridge S. P. (2010). Kir 2.1 channelopathies: the Andersen-Tawil syndrome. *Pflügers Arch* **460,** 289-294.

Tseng G. N., Robinson R. B. & Hoffman B. F. (1987). Passive properties and membrane currents of canine ventricular myocytes. *J Gen Physiol* **90,** 671-701.

Vaidyanathan R., Taffet S. M., Vikstrom K. L. & Anumonwo J. M. (2010). Regulation of cardiac inward rectifier potassium current (I_{K1}) by synapse-associated protein-97. *J Biol Chem* **285,** 28000-28009.

Vandenberg C. A. (1987). Inward rectification of a potassium channel in cardiac ventricular cells depends on internal magnesium ions. *Proc Natl Acad Sci U S A* **84,** 2560-2564.

Veeraraghavan R. & Poelzing S. (2008). Mechanisms underlying increased right ventricular conduction sensitivity to flecainide challenge. *Cardiovasc Res* **77,** 749-756.

Vega A. L., Tester D. J., Ackerman M. J. & Makielski J. C. (2009). Protein kinase A-dependent biophysical phenotype for V227F-KCNJ2 mutation in catecholaminergic polymorphic ventricular tachycardia. *Circ Arrhythm Electrophysiol* **2,** 540-547.

Visentin S., Zaza A., Ferroni A., Tromba C. & DiFrancesco C. (1990). Sodium current block caused by group IIb cations in calf Purkinje fibres and in guinea-pig ventricular myocytes. *Pflügers Arch* **417,** 213-222.

Voets T., Droogmans G. & Nilius B. (1996). Membrane currents and the resting membrane potential in cultured bovine pulmonary artery endothelial cells. *J Physiol* **497** 95-107.

Wang Z., Wong N. C., Cheng Y., Kehl S. J. & Fedida D. (2009). Control of voltage-gated K^+ channel permeability to $NMDG^+$ by a residue at the outer pore. *J Gen Physiol* **133,** 361-374.

Warren M., Guha P. K., Berenfeld O., Zaitsev A., Anumonwo J. M., Dhamoon A. S., Bagwe S., Taffet S. M. & Jalife J. (2003). Blockade of the inward rectifying potassium

current terminates ventricular fibrillation in the guinea pig heart. *J Cardiovasc Electrophysiol* **14,** 621-631.

Weaver W. F. & Burchell H. B. (1960). Serum potassium and the electrocardiogram in hypokalemia. *Circulation* **21,** 505-521.

Wendt-Gallitelli M. F., Voigt T. & Isenberg G. (1993). Microheterogeneity of subsarcolemmal sodium gradients. Electron probe microanalysis in guinea-pig ventricular myocytes. *J Physiol* **472,** 33-44.

Whalley D. W., Wendt D. J., Starmer C. F., Rudy Y. & Grant A. O. (1994). Voltage-independent effects of extracellular K^+ on the Na^+ current and phase 0 of the action potential in isolated cardiac myocytes. *Circ Res* **75,** 491-502.

Wible B. A., Taglialatela M., Ficker E. & Brown A. M. (1994). Gating of inwardly rectifying K^+ channels localized to a single negatively charged residue. *Nature* **371,** 246-249.

Wilde A. A., Escande D., Schumacher C. A., Thuringer D., Mestre M., Fiolet J. W. & Janse M. J. (1990). Potassium accumulation in the globally ischemic mammalian heart. A role for the ATP-sensitive potassium channel. *Circ Res* **67,** 835-843.

Wischmeyer E., Lentes K. U. & Karschin A. (1995). Physiological and molecular characterization of an IRK-type inward rectifier K^+ channel in a tumour mast cell line. *Pflügers Arch* **429,** 809-819.

Xia M., Jin Q., Bendahhou S., He Y., Larroque M. M., Chen Y., Zhou Q., Yang Y., Liu Y., Liu B., Zhu Q., Zhou Y., Lin J., Liang B., Li L., Dong X., Pan Z., Wang R., Wan H., Qiu W., Xu W., Eurlings P., Barhanin J. & Chen Y. (2005). A Kir2.1 gain-of-function mutation underlies familial atrial fibrillation. *Biochem Biophys Res Commun* **332,** 1012-1019.

Xie L. H., John S. A., Ribalet B. & Weiss J. N. (2007). Activation of inwardly rectifying potassium (Kir) channels by phosphatidylinosital-4,5-bisphosphate (PIP_2): interaction with other regulatory ligands. *Prog Biophys Mol Biol* **94,** 320-335.

Xie L. H., John S. A., Ribalet B. & Weiss J. N. (2008). Phosphatidylinositol-4,5-bisphosphate (PIP_2) regulation of strong inward rectifier Kir2.1 channels: multilevel positive cooperativity. *J Physiol* **586,** 1833-1848.

Yan D. H., Nishimura K., Yoshida K., Nakahira K., Ehara T., Igarashi K. & Ishihara K. (2005). Different intracellular polyamine concentrations underlie the difference in the

inward rectifier K^+ currents in atria and ventricles of the guinea-pig heart. *J Physiol* **563,** 713-724.

Yang J., Jan Y. N. & Jan L. Y. (1995). Control of rectification and permeation by residues in two distinct domains in an inward rectifier K^+ channel. *Neuron* **14,** 1047-1054.

Yao A., Spitzer K. W., Ito N., Zaniboni M., Lorell B. H. & Barry W. H. (1997). The restriction of diffusion of cations at the external surface of cardiac myocytes varies between species. *Cell Calcium* **22,** 431-438.

Yao J. A., Jiang M., Fan J. S., Zhou Y. Y. & Tseng G. N. (1999). Heterogeneous changes in K currents in rat ventricles three days after myocardial infarction. *Cardiovasc Res* **44,** 132-145.

Yasui K., Anno T., Kamiya K., Boyett M. R., Kodama I. & Toyama J. (1993). Contribution of potassium accumulation in narrow extracellular spaces to the genesis of nicorandil-induced large inward tail current in guinea-pig ventricular cells. *Pflügers Arch* **422,** 371-379.

Yeh S. H., Chang H. K. & Shieh R. C. (2005). Electrostatics in the cytoplasmic pore produce intrinsic inward rectification in Kir2.1 channels. *J Gen Physiol* **126,** 551-562.

Yellen G. (1984). Ionic permeation and blockade in Ca^{2+}-activated K^+ channels of bovine chromaffin cells. *J Gen Physiol* **84,** 157-186.

Zaza A., Rocchetti M., Brioschi A., Cantadori A. & Ferroni A. (1998). Dynamic Ca^{2+}-induced inward rectification of K^+ current during the ventricular action potential. *Circ Res* **82,** 947-956.

Zhabyeyev P., Asai T., Missan S. & McDonald T. F. (2004). Transient outward current carried by inwardly rectifying K^+ channels in guinea pig ventricular myocytes dialyzed with low-K^+ solution. *Am J Physiol* **287,** C1396-1403.

Zhang D. Y., Lau C. P. & Li G. R. (2009). Human Kir2.1 channel carries a transient outward potassium current with inward rectification. *Pflügers Arch* **457,** 1275-1285.

Zhang D. Y., Wu W., Deng X. L., Lau C. P. & Li G. R. (2011). Genistein and tyrphostin AG556 inhibit inwardly-rectifying Kir2.1 channels expressed in HEK 293 cells via protein tyrosine kinase inhibition. *Biochim Biophys Acta* **1808,** 1993-1999.

Zhang H., Garratt C. J., Zhu J. & Holden A. V. (2005). Role of up-regulation of I_{K1} in action potential shortening associated with atrial fibrillation in humans. *Cardiovasc Res* **66,** 493-502.

Zhang H., He C., Yan X., Mirshahi T. & Logothetis D. E. (1999). Activation of inwardly rectifying K^+ channels by distinct PtdIns(4,5)P2 interactions. *Nat Cell Biol* **1,** 183-188.

Zhao Z., Liu B., Zhang G., Jia Z., Jia Q., Geng X. & Zhang H. (2008). Molecular basis for genistein-induced inhibition of Kir2.3 currents. *Pflügers Arch* **456,** 413-423.

Zhou W. & Jan L. (2010). A twist on potassium channel gating. *Cell* **141,** 920-922.

Zhu G., Qu Z., Cui N. & Jiang C. (1999). Suppression of Kir2.3 activity by protein kinase C phosphorylation of the channel protein at threonine 53. *J Biol Chem* **274,** 11643-11646.

Zilberter Y. I., Starmer C. F., Starobin J. & Grant A. O. (1994). Late Na channels in cardiac cells: the physiological role of background Na channels. *Biophys J* **67,** 153-160.

Zobel C., Cho H. C., Nguyen T. T., Pekhletski R., Diaz R. J., Wilson G. J. & Backx P. H. (2003). Molecular dissection of the inward rectifier potassium current (I_{K1}) in rabbit cardiomyocytes: evidence for heteromeric co-assembly of Kir2.1 and Kir2.2. *J Physiol* **550,** 365-372.